POLITECNICO DI MILANO
ENERGY DEPARTMENT
DOCTORAL PROGRAMME IN ELECTRICAL ENGINEERING, XXXI-CYCLE

RENEWABLE ENERGIES INTEGRATION ON DISTRIBUTION GRID

Doctoral Dissertation of:
Sayedeh Mina Mirbagheri

Supervisor:
Prof. Marco Merlo

Tutor:
Prof. Alberto Berizzi

The Chair of the Doctoral Program:
Prof. Gabriele D'Antona

2018 – XXXI

*To all **strong** women and **supportive** men*

Acknowledgements

I would like to offer my special thanks to my advisor Prof. Marco Merlo for his immense support and patience during my Ph.D study and writing thesis, for his motivation, and comprehensive knowledge. His willingness to give his time so generously has been very much appreciated. I would also like to thank Prof. Alberto Berizzi, for his advice and assistance in keeping my progress on schedule. Also I thank my friends and colleagues at the Electrical Engineering section of Energy Department for their support along the way.

Special thanks to my warm-hearted parents, Zahra and Mahdi, this dissertation would not have been possible without their spiritual support and love.

Abstract

Nowadays, distribution networks are being subjected to an increasing penetration of active users on both low and medium voltage levels, typically based on small size power plants from renewable energy sources (known also as distributed generation). Distribution grids are designed for providing electricity to the customers and could take some advantages from the renewable energy sources production such as sustainability, less maintenance and low carbon emissions. However, upward trends of installing dispersed generators cause some power quality challenges for distribution system operators, such as harmonics, voltage regulation issues, interface protection problems and power quality in general.

Therefore, the focus of the present thesis is on appropriate management of distributed generation. However, as available electrical network data in some power system networks are limited, it is required to estimate the unknown grid parameters using available measurements data such as active power, reactive power and voltage magnitudes. Then, the evaluation of maximum active power injection to the grid by dispersed generator (named Hosting Capacity), its applications and its voltage control are studied.

To do so, a novel procedure to estimate the single bus hosting capacity even in case of uncertainties in grid parameters or lack of data is presented, named Bricks approach. This approach could be used when the possibility of data collection is very low or complex. Then, multi-generator hosting capacity is evaluated using the combination of Bricks approach and a suited Monte Carlo procedure. In addition, electric vehicle integration as the other discussed application in this thesis is looked into by Monte Carlo simulation for different charging processes.

At the end, to increase the hosting capacity a novel procedure based on optimal power flow is proposed. The goal is to avoid over and under voltages violations and preserve the grid efficiency. Actually the procedure is proposed in order to optimally set-up the standard voltage control setting, i.e. to be directly integrated into the already in place voltage regulators. All of the mentioned simulations in this thesis work are coded in MATLAB and then validated for a real-life case studies in Italy and Tanzania.

Estratto

Oggigiorno, le reti di distribuzione sono soggette a una crescente penetrazione di utenti attivi sia in bassa che media tensione, basati in genere su impianti di produzione di piccole dimensioni alimentati da fonti rinnovabili (noti anche come generazione distribuita). Le reti di distribuzione sono progettate per fornire elettricità ai consumatori e potrebbero trarre alcuni vantaggi dalla produzione di energia rinnovabile, per esempio in termini di sostenibilità, minore manutenzione e ridotte emissioni di anidride carbonica. Tuttavia, la tendenza all'aumento di generazione diffusa causa alcuni problemi di power quality per gli operatori del sistema di distribuzione, come presenza di armoniche, difficoltà di regolazione della tensione, problemi di coordinamento delle protezioni e qualità dell'alimentazione in generale.

Pertanto, il focus della presente tesi è la gestione appropriata della generazione diffusa. Tuttavia, poiché i dati disponibili sulla rete elettrica in alcune parti del sistema di generazione sono limitati, è necessario stimare i parametri della rete non noti utilizzando i dati misurati a disposizione come potenza attiva, potenza reattiva e tensione. Viene quindi valutata la massima potenza attiva che può essere immessa in rete dalla generazione distribuita (denominata Hosting Capacity), le sue applicazioni e il relativo controllo di tensione.

Per fare ciò, viene presentata una nuova procedura per stimare l'hosting capacity di un nodo, anche in caso di incertezza dei parametri di rete o mancanza di dati, chiamata approccio Bricks. Questo può essere utilizzato quando la possibilità di raccolta dei dati è molto ridotta o risulta complessa. L'hosting capacity multi-generatore viene valutata utilizzando la combinazione dell'approccio Bricks e di una procedura Monte Carlo appropriata. Inoltre, l'integrazione di veicoli elettrici viene discussa in questa tesi come ulteriore applicazione e diversi processi di ricarica sono esaminati tramite il metodo Monte Carlo.

In conclusione, viene proposta una nuova procedura basata sull'optimal power flow, al fine di aumentare l'hosting capacity. L'obiettivo è evitare violazioni di sovratensione e sottotensione e preservare l'efficienza della rete. La procedura viene di fatto proposta per impostare in modo ottimale il setting di tensione standard, per essere quindi integrata direttamente nei regolatori di tensione già presenti. Tutte le simulazioni citate in questo lavoro di tesi sono codificate in MATLAB e convalidate per casi di studio reali in Italia e Tanzania.

Contents

List of Figures

List of Tables

List of Abbreviation

KPI: Key Performance Indicator
DG: Dispersed Generators
DSO: Distribution System Operator
TSO: Transmission System Operator
HC: Hosting Capacity
NHC: Nodal Hosting Capacity
MGHC: Multi-Generator Hosting Capacity
MV: Medium Voltage
LV: Low Voltage
RES: Renewable Energy Sources
PV: Photovoltaic
DER: Distributed Energy Resources
SSV: Steady State Voltage Variations
RVC: Rapid Voltage Change
OPF: Optimal Power Flow
PS: Primary Substation
CHP: Combined Heat and Power
EV: Electric Vehicle
OLTC: On Load Tap Changer
PFC: Power Factor Control
SE: State Estimation
PF: Power Flow
PE: Parameter Estimation
TANESCO: Tanzania Electrical Supply Company
LF: Load Flow
MC: Monte Carlo
HCVP: Hosting Capacity Violation Probability
PCC: Point of Common Coupling
ORPF: Optimal Reactive Power Flow
LVC: Local Voltage Control

CHAPTER 1

Introduction

1.1 Motivation

The key point of international and European policies (e.g. 20-20-20 EU targets) in order to reduce the greenhouse gas emissions is increasing the usage of Renewable Energy Sources (RES). Renewable energy technologies are divided into dispatchable (e.g. hydro and geothermal power) and non-dispatchable or variable (e.g. solar photovoltaic and wind power). The small size RES which is connected to distribution network and very close to demand side is called distributed power generation. This could be useful to reduce the need of high-voltage transmission network and centralized power generation. However, the massive distributed generation connection and its uncontrolled and nonprogrammable power injections may cause power quality and reliability issues such as voltage profile and conductors ampacity problems, harmonics, unwanted islanding phenomena, due to neglecting the actual distribution grid power needs. Consequently it may require new interventions on the grid to improve its ability to accept local generation without incurring the technical problems.

Hence, integration of such variable renewables to the distribution grid needs some grid transformation such as electric protection logics capable to properly manage bidirectional energy flow (top-down and bottom-up), demand management, energy storage, improve regional, national and international interconnection and introducing technologies and procedures to ensure proper grid operation stability and control (frequency regulation, reactive power regulation, active power reservation, congestion management, optimization of grid losses, network restoration) in the presence of significant share of variable renewables. Therefore, at operational level, efforts are made to turn the distribution grids into smart grids in order to achieve an optimal management of these resources.

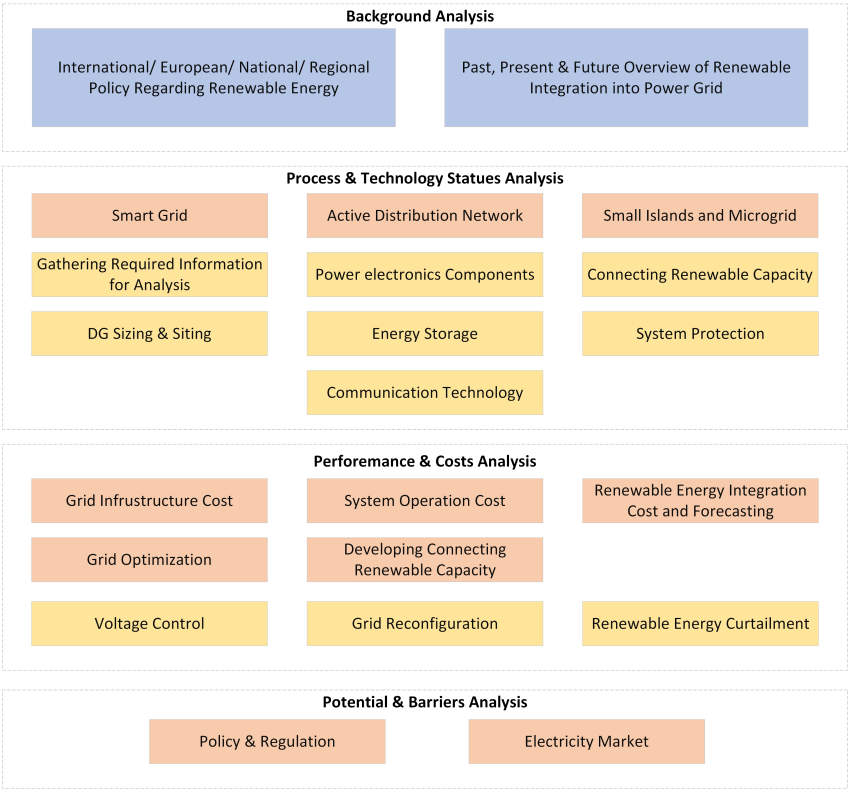

Figure 1.1: *Overall grid renewable integration schematic.*

A wide literature review has been performed in order to properly point out and classify the problem; a schematic of renewable integration into power grids have been reported in Fig. 1.1; process and technology statues, performance and costs, and potential and barriers are the main three frameworks for this subject. Process and technology statues covers the general terms of smart grid, micro grid and in general active distribution grid, therefore studies related to communication technologies, power electronics implementation for frequency control, system protection, energy storage, maximum renewable injection capacity and gathering the required information for these analysis are in this category. While, performance and costs framework in this schematic give people some ideas about the implementation cost and increasing the share of renewable integration. Potential and barriers mainly focus on renewable integration policy and on their liberalized market structures.

Figure 1.2 represents the covered area in this thesis according to the overall schematic. Since a proper management of DGs is vital, strong research activities based on statistical, deterministic and heuristic approaches have been done in order to ensure that, with a given amount of DG connected to the distribution grid, the network is still working within the admitted operational ranges imposed by technical standards and regulatory agencies. Although grid regulations do not allow distribution system operators to refuse any request of DG connection, the goal of many research works is determining the optimal DG sizing and siting. However, these studies have a scarce applicability in real-life. In this regard, evaluation of the maximum generation that can be hosted by the distribution grid without violating the grid constraints is one of the main performance indicators that should be considered for planning and operation of the grid. This indicator is commonly known as Hosting Capacity. In the literature, this

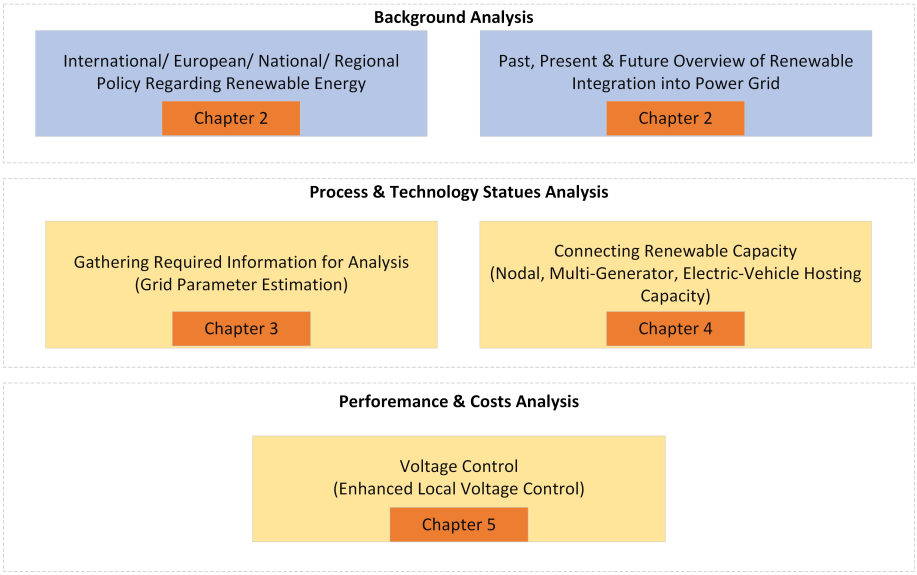

Figure 1.2: *Adopted schematic.*

indicator could be implemented for several applications such as renewable energy sources integration, electric vehicle integration and voltage control; the main focus of this thesis is based on them.

However, one of the main problems in the power system sector in some countries, especially developing and emerging countries for evaluating such an indicator is lack of public data and information about both transmission and distribution grids. Quite often, the only source is limited to the map of the network and general information on the voltage profile and power flows in the lines for a standard working point of the grid. Hence, it is currently hardly impossible to perform further network analysis.

Hence, due to the aforementioned limitation, a procedure is required to be designed in order to estimate the hosting capacity of distribution grids even in case of uncertainties in grid parameters or lack of data. The proposed approach results particularly useful when it is not possible to collect all the necessary data for a classical load flow based analysis, as in the case of studies relevant to emerging countries electrification processes, or when data gathering is difficult, for example when such data are considered sensitive.

As the next step, evaluating the possible ways to increase the hosting capacity without reinforcement is a major concern in both DG and electrical vehicle planning. Therefore, the importance of voltage control as one of the main approach to increase the hosting capacity is highlighted in many research papers. Traditionally, in passive distribution networks the voltage rise has been mitigated by network reinforcement. Nowadays, local voltage control, coordinated voltage control and centralized voltage control have been discussed for active networks in research papers. Although all the approaches have been proven to solve the problem of voltage rise in distribution grids, using plenty of sensors to gather huge number of measurements could cause complexity and cost. Hence, a new procedure to set up a local voltage control law devoted to properly manage the voltage profile to increase the upper limit of total DG injection to the grid is required.

1.2 Research Objectives

1. Available electrical network data in some places especially developing and emerging countries are limited, for technical studies defining unknown parameters through available measurements including power flows and voltage magnitudes is vital. Hence, first objective: To estimate network parameters using some variables using Parameter Estimation.

2. The goal of many research works is determining the optimal DG sizing and siting, although grid regulations do not allow DSO to refuse any request of DG connection. Therefore, the focus should be on the optimal sizing and siting of distribution grid infrastructures rather than the optimal DG unit siting and sizing. Hence, second objective: To evaluate grid hosting capacity even in case of parameters uncertainty.

3. The proposed approaches in the literature are mainly based on iterative calculations, aiming at estimating the maximum DG penetration admitted in each single bus (Nodal Hosting Capacity (NHC)). Hence, third objective: To evaluate Multi-Generator Hosting Capacity (MGHC) in both case of normal condition and parameters uncertainty.

4. In order to properly evaluate the grid hosting capacity, new equipments (e.g. electric cars, battery energy storage system, etc.) have to be properly taken into account. Hence, fourth objective: To Evaluate the impact and hosting capacity of e-mobility charging processes on the electrical distribution grid.

5. Voltage control could be considered in order to increase hosting capacity. For these purpose real time measurements are rarely available through feeders and only are available at primary substation. Moreover, state estimation procedures are affected by uncertainty and errors which may cause wrong decisions. Also, aligning sensors for each node of the distribution system is very costly and unfordable. In addition, the standard local voltage control setting has some limitation such as hosting capacity maximization and energy losses minimization. Hence fifth objective: To Set up a new local voltage control law (Enhanced Local Voltage Control) to define a developed voltage profile to improve entire electrical grid by reducing energy losses and increasing HC.

1.3 Main Contribution

As available electrical network data in some power system networks are limited, for further studies in the first step of this research work, unknown parameters through available measurements including power flows and voltage magnitudes have been estimated. After determining the unknown parameters, the next step which is the evaluation of maximum active power injection to the grid by dispersed generator (Hosting Capacity) and the ways to improve it could be started.

In the second step, hosting capacity evaluation for nodal and multi-generator configurations have been investigated. To do so a new model with less required grid data and processing time has been introduced which is called Bricks approach. This method is based on the assumption that hosting capacity on one feeder is marginally affected by the behavior of other feeders. Moreover, in order to limit the computational effort of the study, the grid is modeled in a simplified way, which means as an aggregation of "bricks", each one representing a portion of the grid which can be added, removed and replaced stochastically to evaluate all the possible configurations of the grid structure.

After that, the combination of Bricks approach and Monte Carlo simulation has been used for evaluating the multi-generator hosting capacity considering various location, DG type and size. From DSO perspective, it is very important to guarantee a reliable management of the distribution grid, consequently proper planning and operational tools are required. Actually, the increasing of electric vehicle utilization may cause overload and undervoltage disturbances on the distribution grid. Hence, Monte Carlo simulation has been used for evaluating their hosting capacity charging process in this thesis. This simulation has been performed considering different number of electric vehicle cars, charging technology, location and time of charging.

At their following, in order to increase the distribution grid hosting capacity a novel set-up procedure based on optimal reactive power flow aimed to define optimized control settings in order to effectively manage the voltage profile, to avoid over and under voltages violations, and at the same time to manage the grid efficiency. The standard local voltage control setting has some limitation in hosting capacity maximization and energy losses minimization. All of the mentioned simulations in this thesis work have been coded in MATLAB and have been validated in a real MV distribution grid including Aosta city in Italy, San Severino Marche in Italy and Tanzania.

1.4 Thesis Structure

In Chapter 2, after this brief introduction, an overview of renewable energies in terms of energy policies, their impact on distribution grid, concept of hosting capacity and its related research works has been discussed.

After that Chapter 3 has been devoted to the parameter estimation procedure for defining the required grid data in case of unavailability of grid parameters for hosting capacity evaluation. In this chapter, different state estimation procedures have been discussed and at the end, the proposed parameter estimation method and its testing on the real-life case study has been reported.

In continue, Chapter 4 covers the most important application of hosting capacity including nodal hosting capacity, multi-generator hosting capacity and electric vehicle hosting capacity by Bricks approach and Monte Carlo simulation. At the end, all of these applications have been implemented on the real-life case studies and the results have been presented.

Chapter 5 is devoted to voltage control as one of the possible way to increase hosting capacity. In this chapter after a brief discussion about different voltage control methods, the proposed set-up law for local voltage control has been introduced. Moreover in order to reduce the processing time, some selection procedures have been suggested to define some nodes and loading hours as representative of the grid. The results of this new set-up control has been compared with some other available methods.

At the end, this thesis work has been summarized in Chapter 6.

1.5 List of Publications

The following is a list of the publications arising from the work presented in this thesis:

[1] S. M. Mirbagheri, J. F. Mushi, V. Ilea, M. Merlo, and A. Berizzi, “Grid parameter estimation procedure for emerging countries scenario,” in *Clean Electrical Power (ICCEP), 2017 6th International Conference on*, IEEE, 2017, pp. 327–333.

[2] S. M. Mirbagheri, M. Moncecchi, D. Falabretti, and M. Merlo, "Hosting capacity evaluation in networks with parameter uncertainties," in *Proceedings of International Conference on Harmonics and Quality of Power, ICHQP*, 2018, ISBN: 9781538605172. DOI: 10.1109/ICHQP.2018.8378891.

[3] S. M. Mirbagheri, F Bovera, D Falabretti, M Moncecchi, M Delfanti, M Fiori, and M Merlo, "Monte Carlo Procedure to Evaluate the E-mobility Impact on the Electric Distribution Grid," in *2018 International Conference of Electrical and Electronic Technologies for Automotive*, IEEE, 2018, pp. 1–6.

[4] S. M. Mirbagheri, V. Ilea, D. Falabretti, and M. Merlo, "Hosting Capacity Analysis: A Review and A New Evaluation Method in Case of Parameters Uncertainty and Multi-Generator," in *18th International Conference on Electricity Distributionth annual conference of the International Conference on Environmental and Electrical Engineering*, 2018, pp. 1–6.

[5] S. M. Mirbagheri, D. Falabretti, and M. Merlo, "Voltage Control in Active Distribution Grids: A Review and a New Set-Up Procedure for Local Control Laws," in *2018 International Symposium on Power Electronics, Electrical Drives, Automation and Motion (SPEEDAM)*, IEEE, 2018, pp. 1203–1208 (cit. on p. 143).

[6] D. Falabretti, M. Moncecchi, M. Mirbagheri, F. Bovera, M. Fiori, M. Merlo, and M. Delfanti, "San Severino Marche Smart Grid Pilot within the InteGRIDy project," *Energy Procedia*, vol. 155, pp. 431–442, 2018.

[7] S. Corgliano, M. Moncecchi, S. M. Mirbagheri, M. Merlo, and M. Molinas, "Microgrid Design: Sensitivity on Models and Parameters," in *13th IEEE PES PowerTech Conference (Submitted)*, 2019.

CHAPTER 2

Renewable Integration Overview

Ratification of the recent international and national environmental policies leads to fast deployment of RES, technology development and economies scale of investment costs. Due to the massive renewable integration some power quality and reliability issues may happen. Hence, considering a Key Performance Indicator (KPI) to evaluate the grid performance is necessary. In this chapter after energy policies and energy planning discussion, distributed generation impact on grid have been presented, and at the end hosting capacity as one of the grid performance KPI has been proposed.

2.1 Energy Planning

The following section is structured in two subsections. The first section presents the current policies and regulatory scenarios in terms of energy planning. It has stressed an overview of the main documents, starting with international relevance and then moving to documents related to local interest. Whereas, in the second subsection, the necessity of energy planning has been explained. In other words, it shows how much the problem of defining an optimal planning is complicated by variety of the context.

2.1.1 Energy Policies

Energy policies have been ratified in order to address energy development issues including its production, distribution and consumption. In the following the importance of renewable integration in terms of energy policy have been discussed.

International Environmental Policies

In the last decades, climate change has become a strong concern on international level. In particular, from center of political attention and public opinion point of view, there is a correlation between global warming and greenhouse gas emissions. Due to these concerns in 1992, at the United Nations conference on the environment and development in Rio de Janeiro, an agreement has been signed under the name of United Nations Framework Convention on Climate Change (UNFCCC) in order to find some solution for global warming problems [8]. The aforementioned document has been signed by 154 nations for reducing greenhouse gas emissions, in order to prevent dangerous human interference with the planet climate system.

In this agreement, the nations agreed to recognize common and specialized responsibilities, more for developed countries which are listed in the UNFCCC Annex I. The agreement entered into force on 21 March 1994 and from that moment, the parties meet annually in the Conference of the Parties (COP) to analyze the climate change tackling progress.

In the third Conference of the Parties (COP 3), held in Kyoto in December 1997, the famous "Kyoto Protocol" was negotiated [9]. The document was adopted to establish legally binding actions for the developed countries in order to reduce their greenhouse gas emissions. In particular a mission reduction of 8% was forecast by 2012 for the industrialized countries.

The COP which took place in December 2015 ended with the Paris Agreement [10], a global agreement for fighting against climate change. This convention has been signed by the representatives of 196 participating parties. The agreement would be legally able to be considered if only being ratified by at least 55 countries which, together, are responsible for at least 55% of global greenhouse gas emissions. Parties after signing the agreement in New York between April 22nd 2016 and April 21st 2017, should adopt it within their own legal systems. The defined agreement stressed that greenhouse gas emission should become zero by the second half of the 21st century. Moreover, the parties have to continue their efforts to limit the increase of Earth average temperature within 1.5 $^{\circ}$ C. The president of USA on June 1, 2017, announced their willingness to withdraw their contribution of this agreement, although their withdrawal could not take place earlier than November 4, 2020.

European Environmental Policies

Historically, EU has been always attended to consumption reduction, energy efficiency and using various sources, due to its energy dependency from abroad. Regardless of the Kyoto protocol, EU has always promoted environmental policies, strategic sustainability and supply security. Some of these policies have been discussed in following.

Climate Energy Package: In 2008, the European Union launched the Climate Energy Package (also called 20-20-20 package [11]) with the following energy and climate objectives until 2020:

- Reducing greenhouse gas emissions with unilateral commitment by at least 20% compare to 1990 levels.
- Obtaining 20% of renewable energy sources contribution on gross final consumption, with a specific target of 10% for biofuels.

- Reducing primary energy consumption by 20% until 2020, through energy efficiency measurements. This objective has been also specified in the efficiency directive energy approved in October 2014 [12].

Directive 2009/28/CE: In the official journal of the Union European in June 2009, Directive of 28 April 2009 on the promotion of renewable energy sources usage has been published [13]. This leads to the establishment of a common European framework for renewable energy sources development. This framework sets mandatory national targets for the share of renewable energy sources on gross final energy consumption and for the share of energy transport from renewable energy sources. The first one is set at 20% (according to the objectives of 2020) which is divided differently between the member states. The second is fixed to 10% and the value remains constant for all the member states.

Table 2.1 represents the general national targets for renewable energy sources shares in final energy consumption by 2020. In addition of these measures, the directive also dictates several rules relating to states joint projects, such as administrative procedures, information, training and access to the electricity grid for renewable energy sources. Moreover, it also sets sustainability criteria for biofuels and bioliquids.

Every two years, the Directive 2009/28/CE for all the state members provides a progress report with a precise outline. These documents are drafted in order to allow the monitoring of the target achievement degree related to renewable energy sources by 2020. Italy has sent the first progress to the European commission report in December 2011 and the second in December 2013, while the third one occurred at the end of 2015.

According to the progress report of 2017 [14], twelve countries thanks to their implemented policies could reach to the target set of 2020. Fig. 2.1 is extracted from the progress report 2017 and shows each country progress, e.g. among 25 member states, only three member states, the Netherlands, France and Luxembourg had 2015 RES estimated shares below their 2016 indicative. Hence, they have to evaluate carefully if the implemented policies and the implemented tools by them are sufficient and effective for the target achievement by 2020, as at present they are not aligned towards this goal.

Horizon 2030 and Roadmap 2050: Once the work on directive package for 2020 has been completed, the EU has moved to set new targets for 2030. The target set have been discussed and approved by the European Council on 23 October 2014 and published as 2030 framework for energy and climate policies [15]. The binding objectives that the Union has set itself in this framework are:

- Reducing greenhouse gas emissions by 40% compared to 1990 levels.
- Achieving at least a 27% of final consumption of renewable energy sources share.
- Reducing at least 27% in energy consumption compared to the "business-as-usual" scenario.

The implemented policies to achieve the 2020 targets have being continued and will influence the following years which lead to decrease the emission by 40% until 2050, even alone thanks to these targets. However, the Europeans objectives for that year are much more ambitious and have been presented in the Roadmap 2050 [16]. The European commission stressed that, following this roadmap the greenhouse gas emission compared to 1990 could be decreased between 80% and 95%. That is why, it is required

Table 2.1: *General national objectives set by Directive 2009/28/CE.*

Country	Renewable energy shares on final energy consumption (2005)	Renewable energy objective shares on final energy consumption (2020)
Belgium	2.2%	13%
Bulgaria	9.4%	16%
Czech Republic	6.1%	13%
Denmark	17%	30%
Germany	5.8%	18%
Estonia	18%	25%
Ireland	3.1%	16%
Greece	6.9%	18%
Spain	8.7%	20%
France	10.3%	23%
Italy	5.2%	17%
Cyprus	2.9%	13%
Lithuania	15%	23%
Latvia	32.6%	40%
Luxembourg	0.9%	11%
Hungary	4.3%	13%
Malta	0%	10%
Netherlands	2.4%	14%
Austria	23.3%	34%
Poland	7.2%	15%
Portugal	20.5%	31%
Romania	17.8%	24%
Slovenia	16%	25%
Finland	28.5%	38%
Switzerland	39.8%	49%
UK	1.3%	15%
Slovakia	16%	25%

to move towards a low-carbon European economy. Hence, several technical and economical feasible operations take place, such as almost total decarbonisation of electrical generation.

National Environmental Policies

All state members in accordance with Directive 2009/28/CE should prepare the National Renewable Energy Action Plan (NREAP). This document follows a specific model established by Article 4 of the aforementioned directive which guarantees the completeness and comparability of the information contained in the different national plans. The complete list of all national action plans is available on the European commission website [17].

Italy has submitted its NREAP to the European commission in July 2010 [18]. In this document some strategies are proposed to identify the renewable energy sources development, and also the main action relies on the design of each intervention area including electricity, heating, cooling and traffic.

The two limiting targets of renewable energy sources consumption by Directive 2009/28/CE for Italy set as 17% and 10% of gross final energy consumption covered by renewable sources respectively on total energy consumption and transport sector consumption. While, NREAP adds two additional non-binding

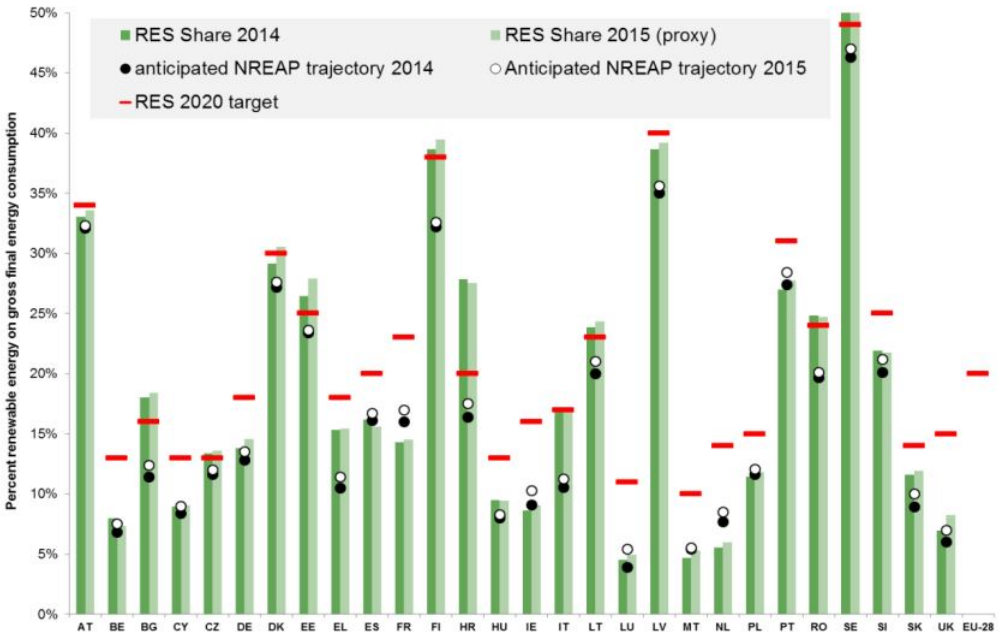

Figure 2.1: *Renewable energy share estimation for member states, progress report 2017 [14].*

factor concerning the electrical and thermal sectors (respectively 26.4% and 17.1% of the consumption covered by RES).

However, these objectives are actually very underestimated, as it is shown by the statistical report of GSE Energy of renewable sources in Fig. 2.2. From Fig. 2.2 (a), it can be seen that the share of gross energy final consumption covered by renewable sources in 2014 is equal to 17.1%, higher than the target assigned to Italy for 2020. Also, the sector of thermal and electrical objectives planned by NREAP for 2020 have been already exceeded, as can be seen in Fig. 2.2(b) and in Fig. 2.2 (c). These excellent results is not only linked to the increase of RES consumption, but also to the continuing effects of economic crisis on gross final consumption. The possibility of maintaining the share of final consumption covered by renewables at these levels will therefore depend on the consumption trend in the coming years, as well as on the trend in consumption of total energy resources from the economic crisis.

On 8th of March 2013, a new document of national energy strategy has been approved [19]. This document is based on the following objectives:

- Competitiveness, it should significantly reduce the energy cost gap between consumers and businesses, with a gradual alignment with European prices.
- Environment, it should overcoming the environmental objectives defined in the 20-20-20 package and should have a leading role in roadmap 2050.
- Security, it should strengthen supply security, especially in the gas sector, and it should reduce foreign countries dependency.
- Growth, it should promoting sustainable economic growth through the development of the energy sector.

(a) Gross final consumption.

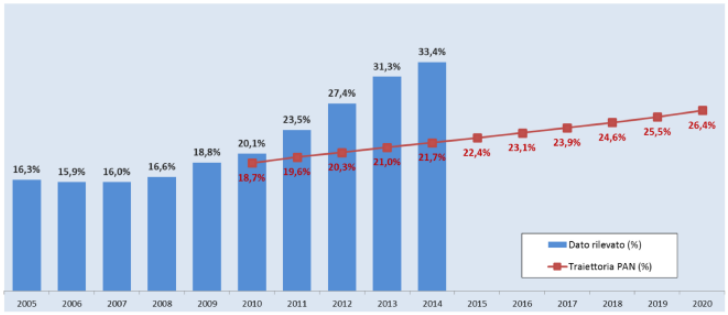

(b) Gross final consumption in the electricity sector.

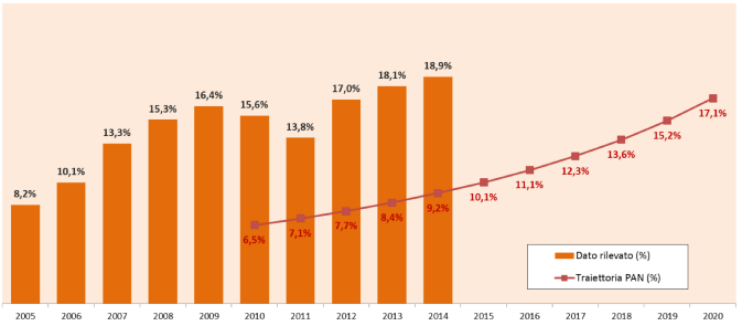

(c) Gross final consumption in the thermal sector.

Figure 2.2: *Share of gross final energy consumption covered by RES [18].*

In particular, with respect to the national action plan (and therefore with respect to the objectives imposed by the European Union directives), the target for the share of final consumption covered by renewable energy sources increased to 19%.

Regional Environmental Policies

The production, transportation and distribution of energy are part of the subjects that Italian law defines as simultaneous legislation. Mainly, the state determines the fundamental principles and the Regions or Provinces have full legislative authority to address the prepared principle by the state.

Regional Energy Plan defined by a law on January 9, 1991, which stressed that the regional energy plan must respect the national one. It is a document of political nature, with technical contents. In other

words, it defines the guidelines and coordination of planning for the promotion of renewable sources and energy savings, implementing the provisions from the Burden Sharing Decree. Any decision regarding legislation regional planning must take into account the need to allow achieving the target for 2020. One of the objectives of the regional energy plan is minimizing the negative impact that can be caused by the usage of some renewable energy sources or some types of systems. In the practical field, energy planning must take into account different dimensions at the same time.

Burden Sharing decree: On 15th of March 2012, the Ministry of economic development have approved a decree which is called Burden Sharing decree [20]. The aforementioned documents defines the contribution of each autonomous region and province which is required to provide the achievement of the national targets up to 2020 in terms of the share of gross final energy consumption covered by renewable sources.

The decree also defines how to manage objectives failure cases by the regions and provinces. In particular, it is specified that starting from 2017, in the event of failure to achieve the objectives, a procedure will be launched to purchase the equivalent renewable energy production from the regional budget. Table 2.2, taken from the Burden Sharing decree, shows the regional targets for 2020 in terms of the share of gross final consumption covered by renewable sources; the trajectories of the objectives for the intermediate years are also defined (2012, 2014, 2016, 2018).

Table 2.2: *Burden Sharing decree trajectory of the regional objectives from initial situation to 2020.*

Regions and Province	Yearly Regional Objective					
	Initial year	2012	2014	2016	2018	2020
Abruzzo	5.8	10.1	11.7	13.6	15.9	19.1
Basilicata	7.9	16.1	19.6	23.4	27.8	33.1
Calabria	8,7	14,7	17,1	19,7	22,9	27,1
Campania	4,2	8,3	9,8	11,6	13,8	16,7
Emilia Romagna	2,0	4,2	5,1	6,0	7,3	8,9
Friuli V. Giuli	5,2	7,6	8,5	9,6	10,9	12,7
Lazio	4,0	6,5	7,4	8,5	9,9	11,9
Liguria	3,4	6,8	8,0	9,5	11,4	14,1
Lombardia	4,9	7,0	7,7	8,5	9,7	11,3
Marche	2,6	6,7	8,3	10,1	12,4	15,4
Molise	10,8	18,7	21,9	25,5	29,7	35,0
Piemonte	9,2	11,1	11,5	12,2	13,4	15,1
Puglia	3,0	6,7	8,3	10,0	11,9	13,7
Sardegna	3,8	8,4	10,4	12,5	14,9	17,8
Sicilia	2,7	7,0	8,8	10,8	13,1	15,9
Bolzano	32,4	33,8	33,9	34,3	35,0	36,5
Trento	28,6	30,9	31,4	32,1	33,4	35,5
Toscana	6,2	8,7	9,5	12,3	14,1	16,5
Umbria	6,2	9,6	10,9	12,3	14,1	16,5
Valle d'Aosta	51,6	51,8	51,0	50,7	51,0	52,1
Veneto	3,4	5,6	6,5	7,4	8,7	10,3
Italia	5,3	8,2	9,3	10,6	12,2	14,3

Share of Renewable on Gross Final Consumption: The decree regional objective is obtained from the report of renewable sources on gross final consumption and total final consumption.

$$ShareRES = \frac{Gross\ final\ consumption\ by\ RES}{Gross\ final\ consumption} \tag{2.1}$$

The gross final energy consumption in this decree for a region or province is given by the sum of the following three terms:

1. Electrical consumption, including consumption of control panel auxiliaries, network losses and electricity consumption for transport.
2. Energy consumption for heating and cooling of all sectors, excluding the contribution of electricity for thermal usage.
3. All transport consumption form, with exception of electric transport and international navigation.

Whereas, the gross renewable sources final consumption for a region is given as followings:

1. Gross electricity from renewable sources produced by the plants located in the region or province;
2. Biomethane and biogas product for thermal or transport purposes;
3. Thermal energy from renewable sources for heating or cooling.

2.1.2 Energy Planning Theory

Despite the global trend points of the electricity market liberalization, there is a large space for the energy planning speech [21]. The energy planning concept starts where the market approach shows its conceptual limits and market failures occurred. It is possible to change the balance of the market in order to increase well-being of some participants without reducing of others, which is called Pareto theorem improvement. To achieve a Pareto improvement, an external regulatory intervention is necessary.

The regulatory intervention can make sure that the possible creation of a dam will bring benefits for everyone, or at least do not bring disadvantages for anyone else. First, theorem Pareto welfare economy defines what are the situations in which the market alone is not able to lead to an efficient allocation of goods and services. According to the theorem, the free market works on the condition that there is not even a failure on some specific market. Then, in the presence of any failure in these markets, the purpose of the policy maker is to compensate them and to make sure that a situation can be achieved of greater well-being for everyone.

Energy Planning Definition

In the technical-scientific literature there are different definitions for energy planning. According to Thery and Zarate the energy planing process is the determination of the optimal combination of the available energy resources in a given territory, to meet a given response [22]. In authors opinion, to define the optimal combination, one must take into account both quantitative and qualitative criteria. In quantitative criteria, the economic and technical aspect is important. Instead, in the qualitative criteria the concern is environmental and social aspects.

Similarly, Hiremath in [23] defines energy planning as a tool looking for a set of energy resources and conversion devices able to meet energy demands in an optimal manner. The definition could be completed by specifying that the optimal condition depends on the prefixed objective, e.g. the minimization

of the energy annual cost, the minimization of the produced energy or maximizing the overall efficiency of the system.

In both cases the energy planning operation is described as the process of looking for a great combination of energy sources to meet a given response. The definition containing different types of planning such as geography scale and time horizon, moreover it contains different definition of the optimal condition.

Energy Planning Technical Dimension

By considering the technical dimension of the energy planning definition, it is clear that the biggest problem of electric power is its storage disability. On one hand, traditional power plants have always been able to modulate the production in a flexible way based on the request of the loads. On the other hand, distributed generation plants that exploit non-programmable sources can not do this adjustment. Sources are random and electrical energy could be produced when the source is available.

To solve the aforementioned problem two approaches can be adopted. For the easier one the geographical and temporal decoupling between generation and load is considered and solutions such as the transport, storage, and intelligent handling of loads are possible ways to tackle this problem. The second approach aims to seek to identify in the energy planning phase which type of generation plant from non-programmable source is able to respond better to the needs of local loads.

Hence, a series of more advanced measures allows to improve the load coupling and non-programmable production profiles. These offer an increasingly significant contribution as it develops effective communication between system users through smart grid. Although the mentioned solution has some advantages, it necessarily needs costs. For this reason, the contemporaneity between production and consumption is also proposed as another solution. According to this approach, when it is desired to exploit non-programmable energy sources, it is a good idea to make sure that the considered source will be usable in places and in times when energy is actually required by end users. The policy maker could therefore make an important contribution in solving the problem, defining the capacity for installing new plants based on how much the source matches the load, taking advantage of the fact that non-programmable sources have daily, weekly and seasonal trends. By comparing these trends with those of the load request it is possible to define which are the most suitable sources.

In principle, the policy maker could give binding indications on the type and positions and optimal size of installed plants. However, in the reality of the Italian national context, the regulator is not in the position to decide the size of the future installed plants and not even their exact position. They can however provide indications on the type of sources to be exploited and on the quantity that can be installed for each of these. In the next chapters the role of energy planning has been defined better.

2.2 Distributed Generation

Dispersed Generators (DG) as a new concept in the electricity industry refers to the presence of electricity generation at any point of the electrical network, particularly on the distribution grid. In the literature, there are many terms and definitions about DG, for instance dispersed generation, embedded generation and decentralized generation are some of these terms. The authors in [24] provided a general explanation for DG as below:

> "DG is an electric power source connected directly to the distribution network or on the customer side of the meter."

This transition from a big centralized power plants to large number of decentralized small plants needs deep and careful studies and investigations. One of the applied planning approach for distribution grid was named fit and forget, it means they build the grid with cable which can host the future increasing of loads. However, this approach is costly as usually not more than 40% of the maximum loading of the cable could be used [25].

Nowadays, increasing penetration of DG by changing the characteristic of the old passive grid to the active grid could cause some issues such as bidirectional power flow and voltage rise. Hence, one of the important and interesting discussion topic related to DG and distribution grid is the amount of DG injection to the grid without violating the technical constraints. However, answering to this question is challenging as the amount of injection could be varied according to some different factors such as the fluctuation of the load and DG generation, the location of the DG and different topologies of the distribution grid. That is why, the new DG connection should be assessed.

2.2.1 Installed Distributed Generation

There are several type of DG technologies such as wind generator, Photovoltaic (PV) generator, hydro generators, microturbine, diesel generators and fuel cells. Among all of them wind and solar generation have the biggest market. In [26], it is expressed that the wind power generation with 433 GW becomes more popular and wide spread in the world. Germany is the country with the highest installation rate of wind turbine by 45 GW followed by Spain with 23 GW, the UK by 14 GW and finally France with 10 GW. Fig.2.3 and 2.4 show the wind power installation share and its cumulative share for the last 15 years of each EU country in 2015 respectively.

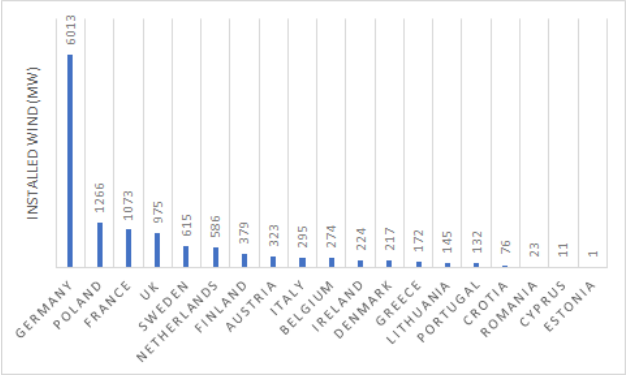

Figure 2.3: *Wind power installation share in European countries during 2015.*

Moreover, Solar generation also shows the increasing trend over that last 15 years [27]. From year 2008 to 2015, for each year there was PV installation rising by 50 to 75% according to their previous year which at the end of 2015, 57.4 GW was added to the installation plants, Fig. 2.5 represents this trend. The same as wind power generator, Germany is the first country with installation increased from 114 MW to 38 GW followed by China with an incredible growth of PV installation from 2011. Italy has the fourth biggest market after the USA with around 18.4 GW of installed capacity. Fig. 2.6 represents the cumulative solar power capacity from 2000 for leading countries [28].

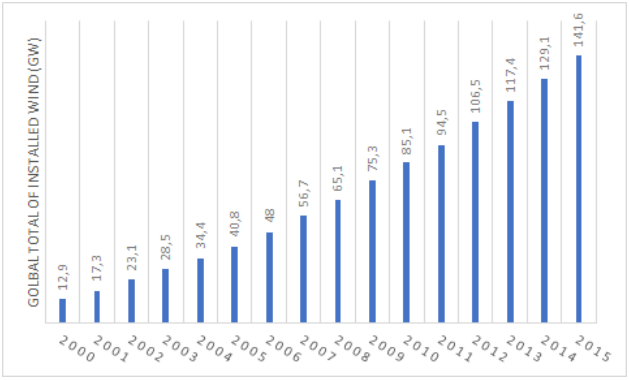

Figure 2.4: *15-year cumulative wind power installation share in European countries.*

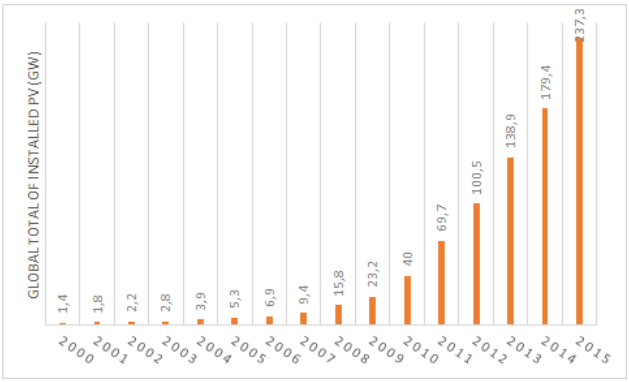

Figure 2.5: *15-year cumulative solar power installation share in European countries.*

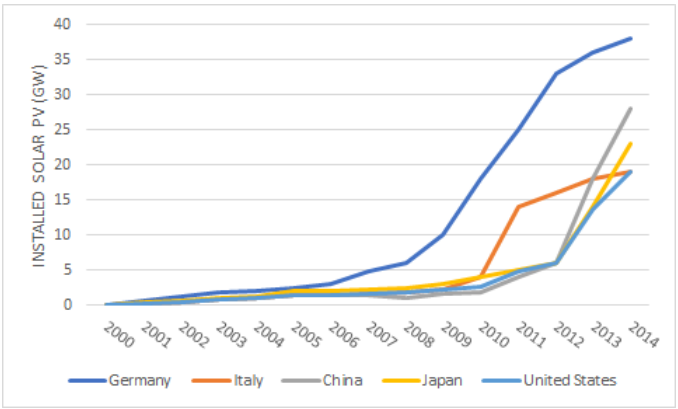

Figure 2.6: *15-year cumulative solar power installation share for leading countries.*

Fig. 2.7, shows the power installation in year 2015. In this year, compare to the previous year the amount of 2.4 GW was added to the total installation. From this pie chart, wind power has the highest installation rate by 12.8 GW whose 44% are new installation. After that, PV power is owning 29% of the total installation by 8.5 GW and the third place belongs to coal by 4.7 GW (16%).

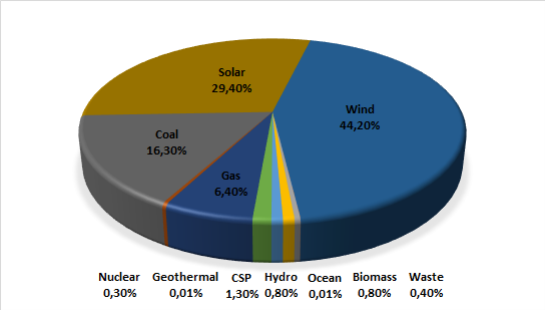

Figure 2.7: *Power installation pie chart, 2015.*

2.2.2 Distributed Generation Impact on Electric Grid

Therefore, in the literature many research works are focusing on the impact of DG both in terms of technical and non-technical factors [29], [30], [31], [32]. If the DG integration is optimal, many benefits are arising by its usage such as following:

- Distribution system loss reduction.
- Electric power system voltage profile improvement.
- Reliability and power quality improvement.
- Feeders overload mitigation.
- Cost reduction due to distribution grid upgrading.
- Rural electrification enhancement due to the high cost of transmission.
- Healthcare improvement due to CO2 reduction.
- Low investment risk due to the short lead time.

Hence, in order to have a sustainable energy sector, according to policy Package 20-20-20 more Distributed Energy Resources (DER) integration has to be connected to the electrical grid [33]. Therefore, there are several approaches to increase these integrations below:

- First approach needs some initial infrastructure such as cables and transformer to be employed in the grid. However, the capacity factor of these new infrastructure could be very low and in this case, could not be the cost-effective approach. The other issue is related to the long lead times before putting in place the new infrastructure. This solution is one of the first considered approach by many grid operators.
- Curtailment happens when it is necessary to reduce the generation output plant to keep the technical constraints. This reduction could be soft curtailment, when a gradual decreasing is needed, or could be hard curtailment, when the complete removal of the production is required. The soft curtailment needs appropriate infrastructure, communication and grid real-time performance to define the desired reduction [34].

- The operational margin can be reduced by the better real-time estimation of the grid capacity. In this solution the existing infrastructure could be used more frequently with their higher capacity factor [35].

- In order to follow the production in a better way by consumption modification there are two main solutions: load removal by load shedding or demand response, and price elasticity. The energy management working progress and response in different conditions to supply the electricity demand is called demand response [36]. The peak demand increasing could be controlled and reduced by demand response especially in a grid with controllable load, e.g. large number of electric vehicle [37]. The implementation of the demand response needs supply conditions assessment and also communication equipment to send the required action to the users or apparatus. The other solution, Price elasticity, could be accomplished by market through defining variant grid tariff with different grid capacity. For this solution also, infrastructure is vital in order to receive the price form the market and working on it. This solution has some disadvantages such as unpredictable grid users behavior. Thus, Distribution System Operator (DSO) usually has problems to put this uncertain market as part of their planning and operation.

- The next solution which is called virtual storage approach is used when the solution in previous paragraph, demand response, did not lead to the consumption reduction, but only moves the energy usage in a later point.

Voltage Variation Impact

On the other hand, DG integration could cause some problems if it is not compatible with the technical boundaries and properties of the considered grid topology such as overvoltage, power system losses growth, voltage flickers and due to bidirectional power flows the increase of short-circuit currents and protective relays faults. For instance, steady-state voltage variation could be happened in a point where a new DG is connected (voltage rise) or where an electric vehicle is connected for charging the electrical battery (voltage drop), following equations represent the concept of voltage variation.

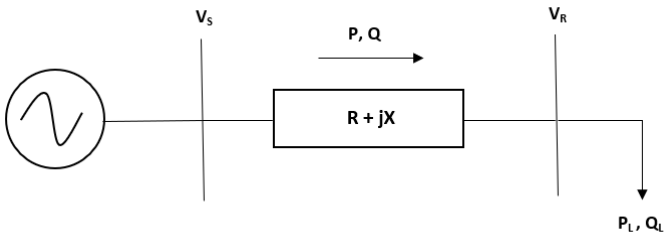

Figure 2.8: *Simplified 2wo-node network model without DG connection.*

The apparent power at $i-th$ bus in a radial distribution grid with N buses which each bus has a connected DG and a load could be defined by equation 2.2. The sign of power in case of absorption by load is negative and in case of injection by DG has been considered positive.

$$S_i = (P_{DG,i} - P_{L,i}) + j(Q_{DG,i} - Q_{L,i}) \tag{2.2}$$

where P_{DG} and P_L represent the active power of DG and loads, while Q_{DG} and Q_L express the reactive power of DG and load. Below the current flow conjugate in each branch has been expressed by equation 2.4, where the voltage relationship between node i and $i-1$ is expressed in equation 2.5.

$$S_i = \bar{V}_i \bar{I}_i^* \tag{2.3}$$

$$\bar{I}_i^* = \sum_{k=1}^{N} \bar{I}_k^* = \sum_{k=1}^{N} \frac{S_k}{\bar{V}_k} \tag{2.4}$$

$$\bar{V}_i = \bar{V_{i-1}} + \bar{I}_i(R_i + jX_i) \tag{2.5}$$

where $\bar{V}_i$ is the voltage vector at node i, and $R_i + jX_i$ is the series impedance (series resistance and reactance) in a branch between i and $i-1$.

The flow in passive radial distribution network is always from the high voltage node to the low voltage node. In order to calculate these voltage drop, Fig. 2.8 represents a two-node distribution network. Hence, the voltage of sending node according to equation 2.5 could be defined as follow.

$$\bar{V_S} = \bar{V_R} + \bar{I}(R + jX) \tag{2.6}$$

where, V_R is the voltage at receiving bus and $\bar{I}$ is the flowing current phasor along the line. Thus, the supplied power by transmission network could be calculated by equation 2.7.

$$P + jQ = \bar{V_S}.\bar{I^*} \tag{2.7}$$

The line current flow using equation 2.4 and the previous equation could be expressed as follow.

$$\bar{I^*} = \frac{P + jQ}{\bar{V_S}} \tag{2.8}$$

Considering the value of $\bar{I}$ in equation 2.5, the voltage at sending bus could be written in equation 2.9.

$$\bar{V_S} = \bar{V_R} + \frac{P - jQ}{\bar{V_S^*}}.(R + jX) = \bar{V_R} + \frac{RP + XQ}{\bar{V_S^*}} + j\frac{XP - RQ}{\bar{V_S^*}} \tag{2.9}$$

Thus, the voltage drop between these two bus could be calculated by:

$$\Delta\bar{V} = \bar{V_S} - \bar{V_R} = \frac{RP + XQ}{\bar{V_S^*}} + j\frac{XP - RQ}{\bar{V_S^*}} \tag{2.10}$$

As the angle of voltage between sending and receiving bus is very low, the imaginary part of this equation could be neglected and only the real part of equation 2.10 is considered as the voltage drop [38]. If an assumption has been made that the sending bus is slack bus then the angle of this node should be considered as zero. Hence, $\bar{V_S^*} = |V_S| = V_S$ and the previous equation has been approximated as follow.

$$\Delta V \approx \frac{RP + XQ}{V_S} \tag{2.11}$$

Moreover, if the sending bus voltage taken as unity, the last equation could be rewritten in equation 2.12

$$\Delta V \approx RP + XQ \tag{2.12}$$

However, due to the connection of DGs to the grid in case of active distribution network, the power flow and also the voltage profile have been affected. In Fig. 2.9 the positive floe of P and Q has been reversed in comparison with Fig. 2.8, thus from now on ΔV means voltage rise, instead of voltage drop and the receiving voltage is approximated to:

$$V_R \approx V_S + RP + XQ \tag{2.13}$$

Figure 2.9 could clarify the bigger voltage in the DG connection node in comparison with sending bus. The DG in this figure is connected to the distribution grid through overhead line with an specific impedance. The voltage rise between these two nodes could be evaluated by equation 2.14.

$$\Delta V = V_{Gen} - V_S \approx \frac{RP + XQ}{V_{Gen}} \tag{2.14}$$

where, active power (P) is equal to difference of DG active power (P_{DG}) and load active power (P_L). While, reactive power is equal to $Q = \pm Q_c - Q_L \pm Q_G$ where Q_C is shunt capacitor reactive power and the other two are related to DG and load. In explanation of the defined sign in the previous equation, DG units always inject the active power, however they may inject or absorb reactive power. Whereas, load consumes both active and reactive power. The compensator could inject or absorb reactive power [39].

If V_{Gen} in the previous equation has been assumed in per unit, equation 2.15 could be rewritten as follow:

$$\Delta V = R.(P_G - P_L) + X.(\pm Q_C - Q_L \pm Q_G) \tag{2.15}$$

where the aforementioned equation is stand if and only if $(\pm Q_C - Q_L \pm Q_G)$ is positive.

The voltage rise worst case scenario could be occurred when there is high generation but low load demand. In addition, high R/X ratio produce more voltage rise which is more complex to reduce this increasing by only reactive power as absorbing reactive power will increase system losses.

Therefore, as it is obvious from these equations by increasing the DG injected power, ΔV is rising also. However, voltage rise has an inverse relationship with load active power. One of the present method to control the voltage rise from these equations is consuming reactive power by DG (inductive mode), Chapter 5 has presented the voltage rise issues and the ways to control it for increasing the hosting capacity. Another method is changing the parameter of R and X which required grid reinforcement leads to cost increasing for the DSO.

Due to aforementioned issues, new interventions may require on the grid to improve its ability to accept local generation without incurring in technical problems. Hence, at operational level, efforts are made to turn the distribution grids into smart grids in order to achieve an optimal real-time management of these resources. Actually, smart grid covers a wide concept and does not have any single definition. According to Electric Power Research Institute [40], smart grid "incorporates information and commu-

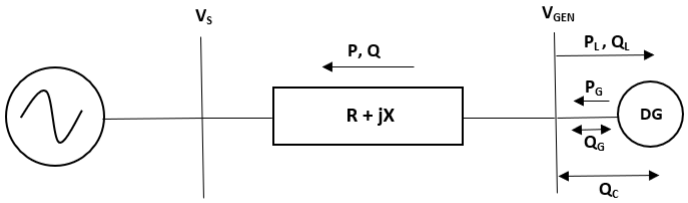

Figure 2.9: *Simplified 2wo-node network model with DG connection.*

nications technology into every aspect of electricity generation, delivery and consumption in order to minimize environmental impact, enhance markets, improve reliability and services, reduce costs and improve efficiency". In the following, one of the main performance indicator (hosting capacity) that should be considered for planning and operation of the smart grid has been discussed.

2.3 Hosting Capacity

The increasing penetration of DG, mainly based on RES on both Low Voltage (LV) and Medium Voltage (MV) levels, gives challenges in the modeling and operation of distribution grids. Low greenhouse gas emissions, better sustainability and less maintenance strongly motivate the installation of DGs, but the massive DG connection and its uncontrolled and nonprogrammable power injections may cause power quality and reliability issues (e.g. voltage profile and conductors ampacity problems, harmonics, unwanted island phenomena, etc.), due to neglecting the actual distribution grid power needs. Consequently it may require new interventions on the grid to improve its ability to accept local generation without incurring in technical problems [41], [42], [43], [44]. Hence, at operational level, efforts are made to turn the distribution grids into smart grids in order to achieve an optimal real-time management of these resources [45], [46], [47]. According to Electric Power Research Institute, smart grid "incorporates information and communications technology into every aspect of electricity generation, delivery and consumption in order to minimize environmental impact, enhance markets, improve reliability and services, reduce costs and improve efficiency".

Since a proper management of DGs is vital, strong research activities based on statistical, deterministic and heuristic approaches have been done in order to ensure that, with a given amount of DG connected to the distribution grid, the network is still working within the admitted operational ranges imposed by technical standards and regulatory agencies [48], [49]. Although grid regulations do not allow distributed system operator to refuse any request of DG connection [50], the goal of many research works is determining the optimal DG sizing and siting [51], [52]. However, these studies have a scarce applicability in real-life. In this regard, evaluation of the maximum generation that can be hosted by the distribution grid without violating the grid constraints is one of the main performance indicators that should be considered for planning and operation of the grid. This indicator is commonly known as Hosting Capacity (HC).

Hosting capacity is the method to determine the electricity grid ability to accept and integrate new production or consumption. The aim is to have better transparency and commensurability between DSO, stakeholders and owners of distributed energy resources. The concept of hosting capacity in order to

assess the electrical grid performance in the future, has been suggested by European grid operators [53] and European energy regulator [54]. The HC concept has been used in an EU research project called EU-DEEP to determine the acceptable amount of DG which could be connect to the grid because on those days unacceptable grid performance due to RES uncertainty was one of the grid operator concern [55]. However, the hosting capacity term has been used by André Evan and later developed by Math Bollen to assess the impact of DG on the quality of the grid voltage [56], [57].

2.3.1 Hosting Capacity Definition

Any change in the value of production or consumption in a distribution grid has some effect on the power flow, short circuit current, voltage profiles and some other grid properties. In general, the grid performance could improve or weaken due to the new changes. The authors in [58] define the hosting capacity as follows: *The maximum amount of new consumption or production that can be connected to the electrical grid without violating the grid quality and reliability for other customers.* The aforementioned HC definition could be clearly shown in Fig. 2.10.

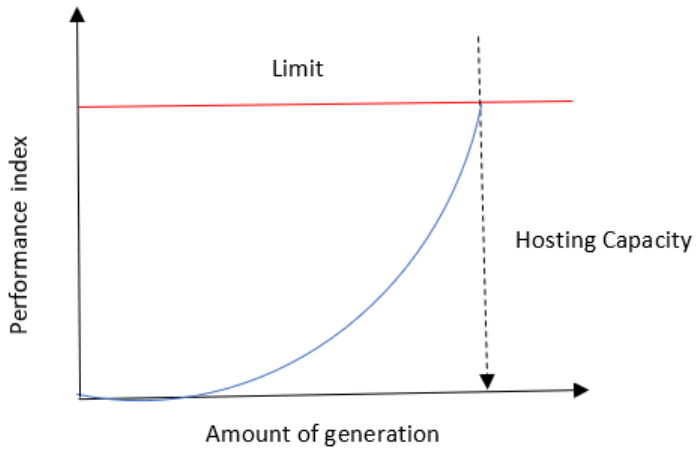

Figure 2.10: *Hosting capacity definition.*

Actually, for evaluating the HC of a connected DER to the distribution grid, many different phenomena which are influenced by various performance indices should be considered such as steady-state voltage variation, transformer and line thermal limit, transformer power rating, rapid voltage change, reverse power flow on the tap changer, protection issues (short circuit problem), power quality (harmonics, islanding). Among all of the mentioned indices, steady-state voltage variation and line thermal limit are the most dominant factors which are usually the limiting factor of the hosting capacity. Moreover, although all of the mentioned factors could be incorporated easily to the framework, power quality and protection issues due to their transient behavior need new field to investigate better.

The performance indices are mainly calculated according to the new amount of production or consumption. As discussed before, the studied phenomena might be intermittent production or consumption such as wind power or electrical vehicle integration to the grid for charging process, that is why based

on each phenomenon, different indices have been considered. Table 2.3 represents several different phenomena and their related performance indexes given by the IEC 50160.

Table 2.3: *Performance indices for different Phenomena.*

Phenomena	**Performance Indices (IEC 50160)**
Frequency Variation	99% interval of 3 second frequency average
Harmonics	10 min voltage and current average
PV rooftop overvoltage	Highest 10 min voltage average
Electric vehicle fast charging undervoltage	Lowest 10 min voltage average
Wind power overloading	Maximum hourly value of transformer current

In evaluation of the hosting capacity, at least one of the phenomenon which could be affected by DER (steady-state voltage variation, line thermal limit, harmonic distortion, rapid voltage change, frequency stability, etc.) is defined by at least one performance indices. As it was already discussed in Table 2.3, for each index an standard change of state is determined [55]. Therefore, when at least one of these performance indicators exceed its limitation, the hosting capacity is reached. Hence, the main limited factor is called "hosting capacity limit". Hence, the hosting capacity is strongly relevant to the acceptable limits [59]. Thus, one of the main challenges in HC studies is defining a set of indices and limits which can cover all the desired power system task. Therefore, a clear understanding of the grid technical needs in order to provide quality and reliability for each costumer is necessary [60]. As an example, in the new defined rules in DACH countries (including Germany, Austria and Switzerland) a DG could be installed if the static voltage variation at the connection point is less than 3% for LV grid and less than 2% for MV grid (static voltage rise is considering the value between zero in-feed and full in-feed) [61]. Consequently, it is the DSO responsibility to make sure that the electric grid is working under the limits of the grid regulation, e.g. in case of a DG connection to the grid, DSO considers the worst-case scenarios such as zero generation with maximum load demand, maximum generation with minimum load demand, maximum generation with maximum demand. Fig. 2.11 gives an example of DG connection hosting capacity and its limits, by increasing the production, the performance index is decreasing. Thus, the hosting capacity is where the performance index turns out to be unacceptable. As the amount of DG injection could be influenced by the defined limits, it is very important which limits are considered in the grid codes and standards.

The authors in [62] indicate that we cannot conclude that the system reaches to its hosting capacity if the number of elements violating the considered limits (especially voltage and loading) are very few, because in reality there is a possibility to replace or enforce easily these elements. Thus, it means considering the frequency distribution of the violating elements is important, e.g. the hosting capacity could be defined when about 2% of the network elements are overloaded. Therefore, for evaluating the hosting capacity is preferred to consider both probabilistic limits and stochastic evaluation, which lead to have different HC for different type and location of DER. That is why the authors in [55] express that in order to have the accurate HC evaluation we need to study each specific case.

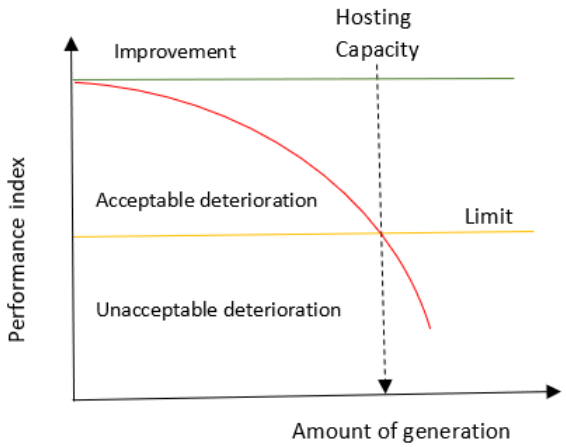

Figure 2.11: *DG injection hosting capacity example.*

2.3.2 Hosting Capacity Evaluation

In order to define the HC, an algorithm needs to be made with the amount of DG injection without violating the technical constraints as its output. One of the method to calculate the hosting capacity is gradually increasing the amount of DG injection until the performance indexes violation. In each incrementation power flow analysis in order to determine the new values of the voltages, currents and powers is necessary to be performed. Equation 2.16 and 2.17 represent the active and reactive load flow equations at each node (k_{th}) during the presence of DG.

$$P_k = P_{DG,k} - P_{D,k} = \sum_{j=1}^{N} |V_k|\,|V_j|\,(G_{kj}\ cos\Theta_{kj} + B_{kj}\ sin\Theta_{kj}) \tag{2.16}$$

$$Q_k = Q_{DG,k} - Q_{D,k} = \sum_{j=1}^{N} |V_k|\,|V_j|\,(G_{kj}\ sin\Theta_{kj} - B_{kj}\ cos\Theta_{kj}) \tag{2.17}$$

where $P_{(DG,k)}$ and $Q_{(DG,k)}$ are the active and reactive power of DG in node k. $P_{(D,k)}$ and $Q_{(D,k)}$ are the active power and reactive power of load in nodes k. N is the total number of the nodes in the feeder. V_k and V_j are the bus voltages in bus k and bus j during the existence of DG. However, this amount in the case of DG absence is converting to V_k and V_j. G_{kj} and B_{kj} are the branch characteristics.

The new state values should be compared with the maximum permissible values in order to evaluate if the grid still has the capacity to host more DG injection. This trend will continue up until one of the maximum value violation. Then, the penetration on that step is considering as the hosting capacity of the grid. After defining the HC in this node, the study will start for the next node until all the nodes of the grid be assessed. Actually the DG source integration in the distribution grid could be simulated in different ways such as PQ flow (loadability) [63], PV flow [64], P representation. If the DG control circuit is based on the controlling of active and reactive power independently, the DG model is simulates as the PQ model and if the control circuit is based on controlling the active power and voltage independently the DG simulates as PV model. The most common DG simulation is the first one as the voltage rise consequence is usually investigated in the studies. Fig. 2.12 shows the HC algorithm flowchart.

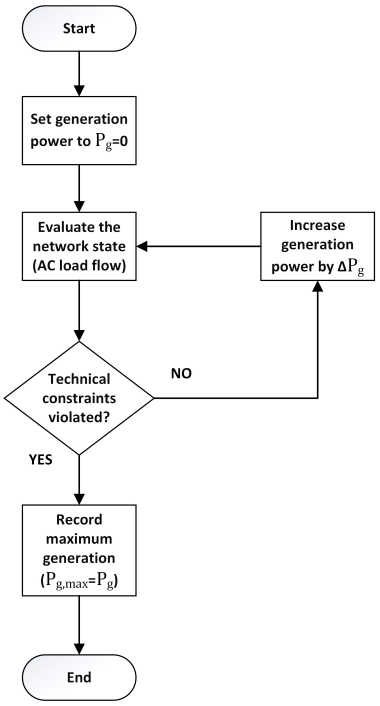

Figure 2.12: *Hosting capacity evaluation flowchart.*

Typically, in literature the HC approach is presented as shown in Fig. 2.10. The amount of HC is defined when the blue curve is going to violate the red line, representing the system limits. In very short words, [65] and [66] outlines the steps to obtain hosting capacity as following:

1. Choosing a phenomena and at least one performance indices.
2. Defining suitable limits.
3. Calculating the performance index according to the new generation.
4. Obtaining the hosting capacity.

2.3.3 Hosting Capacity Research Works

The HC method was originally discussed as part of EU-DEEP project by STRI in 2004 [67], [68], [69], [70]. The histogram of Fig. 2.13 depicts the number of publications per year using the exact term "$Hosting\ Capacity$"; the histogram covers the years from 2004 until 2017 and was plotted using the data available on Google Scholar. According to this figure, the number of publication is growing after 2010. In these literatures the concept of HC has been applied for different voltage regulation methods, evaluating the integration of renewable energies to the grid or the electric vehicle impact on the grid, where this thesis is based on these three pillars. These days the HC concept has been adapted by utilities and regulatory bodies in some countries such as Italy, UK and Australia.

In the literature of the other fields the hosting capacity term has been used in the similar way, e.g. in computer science HC defines the capacity of web server to host as many access calls as possible. In addition, some research papers instead of using HC term have used "network capacity" [71], [72] and "absorption capacity" with same concept of it. Many approaches have been used to determine the

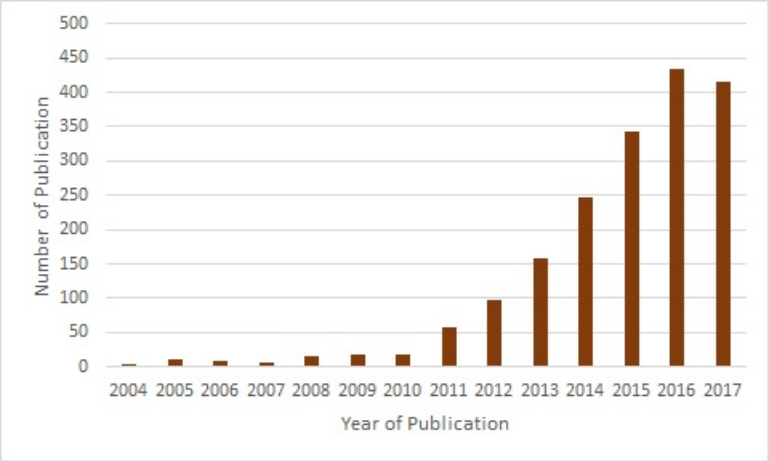

Figure 2.13: *Number of publication using term "Hosting Capacity".*

capacity of the existence grid for hosting new DG [73]. In [48], different estimations for evaluation hosting capacity is expressed. The aim of many statistical approaches are finding the optimal location (siting) and sizing [74]. However, these approaches are not mostly compatible with real life as DSO could not refuse any request of DG connections [74].

Estimating the NHC for LV Italian grid according to the thermal limits of transformer and lines, steady state voltage variation and fast voltage variation with iterative calculations (1 kW step) has been studied in [75]: the NHC is evaluated considering a single constraint at each time and assuming the overall HC as the minimum HC obtained for all the constraints. In this study DGs are representing by a negative load. The paper concludes that the maximum HC is observed near HV/MV substations. Moreover, the rural networks have a limited HC compared to urban networks, due to the limited cross sections and long length of their lines.

Different softwares for performing Power Flow have been used by researchers, e.g. a NHC evaluation has been discussed for 73-node and 19-node Jordanian network grid with high (X/R) ratio in [76] using Newton-raphson in MATPOWER. Paper [77] calculates NHC using the software SimPow for a distribution grid at the center of Sweden. MATPOWER and MADGTPOWER for nonlinear numerical methods have been used in [78] for NHC estimation. Eventually, Swedish regional distribution grid in [79] used commercially available power system simulation software for assessing NHC.

In order to define the possible injection into the grid by DGs, it is very important to choose suitable performance indicators including directly related (such as upper bound and lower bound of RMS voltage) or indirect ones [66]. Typically, researchers consider the main technical constraints such as Steady State Voltage Variations (SSV), thermal limits and Rapid Voltage Change (RVC) [80], [79], [75], [76], [77], [78], [81], [80], [82], [83]. In [79], the most limiting factor for the HC are the overcurrents. The authors in [81] mentioned that the factors limiting the HC depend on the type of network and its voltage level. In weak MV networks (i.e. characterized by long lines), the voltage rise is usually the main limiting factor, while in stronger networks (e.g. urban grids) the feeder and transformer overloading are the main limiting factors.

In [84] author uses an thoroughgoing method to evaluate the NHC considering voltage levels and conductors current flows as technical constraints. For each node at each time a defined maximum value of HC is selected and a PF is performed to check the compliance of voltage and current constraints; in case

of violation, HC is reduced via bisection method until a viable value is found. Since the dynamic behavior of background distortion (e.g. harmonics) may change HC, the harmonic distortion phenomenon has been considered as the technical constraint in [85], in order to have a more efficient distributed generation planning.

Solving optimization problems to obtain HC has been considered in some research papers [83], [86], [87], [88]. A novel Optimal Power Flow (OPF) with the objective of maximizing the nodal loading parameters to evaluate NHC and to define the DG control rules has been proposed in [83], [86]. The authors of these papers conclude that the maximum HC is obtained at the location where the feeder is most loaded. The more distant from the MV Primary Substation (PS), less increase of HC occurs, since the nodes at the end of the feeder experience severe problems of undervoltage. The authors in [87] mentioned that the best location for connecting a DG unit is close to the load center and two optimization models using Primal-dual interior-point method to calculate and optimize the voltage profile and line losses have been proposed. The objective functions in [88] are the energy purchased and the operation and maintenance cost of a wind farm; the problem is solved by NSGA-II algorithm. In this thesis, the network parameters uncertainty has been considered as input and a two-stage stochastic method has been used in order to make decisions under uncertainty.

The stochastic nature of the loads and generation and DG location has been considered in [89] where Monte Carlo simulation was used. Probabilistic PF may be more adequate compared to Deterministic PF, because of the realistic representation of the inputs and the probabilistic margins obtained with respect to the technical constraints violation. In [90], probabilistic load modeling and costumer's hourly power request probability have been considered. Then, the probability density function of each technical constraints for DGs has been estimated by Monte Carlo simulation. The Swedish distribution grid in [91] has been divided into rural, residential and city areas; Monte Carlo has been used in this study to assess the probability of the technical constraints at different voltage levels. A LV Slovenian distribution network has been modeled in [92] using statistical Monte Carlo simulation. In this study, the probability of voltage violation with respect to installed PV capacity is evaluated. A probabilistic method has been proposed in [93] for assessing the impact of Low Carbon Technologies in LV networks considering network parameters uncertainty. This work highlights that the cumulative density functions for each feeder could show to DSO the customers with high probability to cause voltage or thermal problems. The authors of [94] proposed an approach to consider the "equivalent" maximum injection to the generators downstream the bus under examination. This method is useful for considering MGHC where the total injection is equal to the equivalent generator.

As it was mentioned before, the first publication about electrical grid HC was published on 2004 [59], then it continued in 2005 by several research papers [95], [96], [60], [67], [97], [98], [68]. The authors in [41] evaluate the impact of increasing the penetration on the number of voltage dip in the distribution grid for end-customers. The HC consideration is useful in this kind of studies as "no general rule on how the dip frequency for end customers is impacted. It depends strongly on the transmission system, on the location and amount of large generator stations taken out of operation, on the type of distributed generation and on the immunity of the end customers against voltage dips."

In [57] the HC evaluation has been done for assessing the protection performance. In this paper, the dynamic simulation have been performed in order to have more precise assessment of the system protection in case of significant DG injections. From this paper it can be conclude that in this case it is required to add or change some of the component setting such as changing the current setting or using

an extra time delay for the relay with overcurrent, adding extra fuses or circuit breakers or replacing the overcurrent relays by directional components.

The effect of starting the motor on the voltage and current on the weak grid has been studied in [95]. The concept of HC in this study is used to evaluate the biggest size of the motor which could be connected to grid without violating the technical constraints.

On the other hand, the limitation on the hosting capacity due the effect of reducing or emitting the high frequency distortion are studied in [99], wheres HC evaluation could be done in order to define the voltage limit distortion on the same frequency range [100]. The authors of [101] have studied the effect of DG by considering HC on the frequency control both on normal and emergency conditions. The hosting capacity in this paper is considered as the maximum load deviation which the primary frequency control could manage it and could be calculated according to the following equation, where S is related to the governor droop and D to DG constant damp.

$$\Delta P \; = \; P_{rated} \, . \, \left(\frac{\Delta f_{max}}{f_{rated} . S} \; + \; \frac{\Delta f_{max} . D}{f_{rated}} \right) \tag{2.18}$$

The deterministic and statistic approach have been performed in [102] in order to examine the over-voltage risk in the network with injection of the wind power. In [103] the concept of HC has been used to study the advantageous of the Combined Heat and Power (CHP) using the network replacement. The Italian authority of the electric energy and gas (AEEG) in 2008 and 2009 have done a survey on MV and LV [75] distribution grid in order to define the possible maximum injection to the grid for each node without violating the steady state voltage variation of the grid, the thermal limit of the transformer and the lines and also the rapid voltage changes. The results were published on ARG/elt 223/10 for LV and ARG/elt 25/09 for MV grid [104], [94], [80], [105], [106]. In this study, the number of 60,000 buses which is the 6% of the total Italian grid have been studied for evaluating the MV hosting capacity through performing PF [94]. The limiting factor in this study was mostly SSVV and RVC and only half the buses are able to receive more than 6 MW. However, in the study case of [80] 85% of the buses could host at least 3 MW. The authors in this paper has indicated that mostly the limiting factor of the buses close to the primary substation is "thermal limiting factor", wheres this value for the buses at the end of the feeder is "RVC". Moreover, in this study, the term of System Hosting Capacity has been used as the maximum injection of the DG to the grid according to the thermal limits. To do so, using the advance voltage regulation and a communication between protection relays have been suggested by the report.

The comparison between the HC of the single and three phase LV grid have been done by [107]. From this paper, it has been found that with 10 A rated current compare to three phase connection, only half of the load are able to connect to the single phase. Moreover, Power factor correction effect on hosting capacity has been discussed in [74]. As it was explained before, in the literature besides using the HC on the above mentioned areas, it could be implemented for some applications such as DER integration, voltage control and electric vehicle integration, where the main focus of this thesis is based on them.

DER Integration

The concept of hosting capacity in PV systems has been discussed in [108]. The authors of this paper have declared that the smart controlling of PV could increase the HC. They also stressed the use of European Norm EN 50160 for determining the voltage limits in order to translate it into DSO planning levels. The hosting capacity enhancement by use of reactive power control of PV inverters has been

mentioned in [109].

The possible increasing of HC of DER in LV grid has been covered in [110] using voltage controller and several voltage regulation approaches. It is expressed that, by reactive power control the hosting capacity could be double and even it could increase 2.5 times if we control the MV/LV transformer, and if we have the components limiting. However, combining these two methods does not lead to more HC increasing as the extra loading which is caused by reactive power will decrease the capacity of the active power injection. In addition, [79] published the research of the impact of DG on the voltage of LV grid. In [111], [112] the possibilities of improving the LV distribution grid to increase the hosting capacity of the integrated PV have discussed.

In [113] hosting capacity has been used to discuss the role of active distribution grid control for increasing connection and injection of urban-area PV. Also, in [112] the impact of several PV voltage control on increasing the HC has been studied. The decentralized voltage control located in LV grid in [114] caused an HC increasing beyond 3% of voltage threshold until the limitation of the allowable equipments loading. The aforementioned method increase the HC from 3.5 kW to 7.5 KW in LV grid. Moreover, [115] has stressed the help of volt-var control to increase the hosting capacity.

The research works has been presented in [116], [117] indicate the use of HC in National Renewable Energy Laboratory and Electric Power Research Institute in the USA to determine the allowable connected renewable energy to the grid such as PV.

Electric Vehicle Integration

As it was expressed before, the HC studies could be implemented for the plug-in Electric Vehicles (EVs). The effect of EVs on distribution grid without violating the technical constraints such as under-voltage and equipment loading have been studied in [62], [62].

Moreover, the impact of EVs along the feeder according to their charging location and their power have been discussed in [62]. In [118], [119], after comparing the load curves from smart meter with the cable rating, the HC is used to analyses the effect of EVs on LV grid. Moreover, in these papers the possibility of MV/LV transformer substitution is also made. The research work which is presented in [120] used the same approach of the previous work to study the effect of EVs on the LV grid in the center of Italy with different charging station. According to them, the main limiting factor was overloading compare to voltage drop and total harmonic distortion. In [121] different methodology has been proposed by its authors to evaluate the grid maximum HC in case of EVs charging. In addition, the possibility of increasing hosting capacity by demand response capability has been expressed in [122].

Active Voltage Control

In 2010, electricity of France through the published papers in [123], [124] expressed the role of DG voltage control to increase the hosting capacity of the French MV grid. In [125] after providing a detailed HC evaluation for the MV grid, the effect of different voltage regulators especially based on local ones are investigated. The HC enhancement by the real-time reactive power producer, such as DG, has been assessed in [126]. In [127], [127], [128] the role of active voltage control in low voltage level in an active grid including DER and e-mobility to increase the hosting capacity has been discussed. Moreover, in [129] hosting capacity approach has been performs in order to evaluate the active distribution grid. The

results shown in [130] proves the increasing of HC by 27% using local voltage control in MV distribution grid of Italy.

The hosting capacity evaluation in Ireland by its Transmission System Operator (TSO) has been done in [131]. In order to maximize the penetration of the wind turbine, active voltage control has been used in this study. Whereas, increasing HC by this kind of control for a LV grid in Austria has been discussed in [127]. On the other hand, coordinated voltage control and its impact on maximizing hosting capacity in Finland has been done in [132], [133]. The author in [134] expressed the impact of DG inverter and transformer tap changer developed-voltage-control to increase the hosting capacity.

An investigation related to type voltage regulation and line length in distribution grid was done in [135]. According to this research work, DG could be used at the end of the feeder as by going further from transformer voltage is decreasing. However, for the nodes close to transformer, its tap changer makes the voltage almost constant. Therefore, the connected DGs to primary substation or close to it usually have the reactive power balance problem.

2.3.4 Hosting Capacity Increasing

For planning issues it is a major concern to evaluate the upper limit of total RES injection to the grid and the ways to increase it without reinforcement. In the following, HC increasing approaches are detailed.

Network Reconfiguration

In [136] network reconfiguration is used for HC increasing by multi period optimal power flow. The proposed method in this paper, first solves the problem for periods with worst case scenarios, the resulting configuration is then assessed for the remaining time periods to check if it complies with the given constraints. The authors in [137], [138] purposed Genetic Algorithm based network reconfiguration to maximize HC at selected nodes. In this paper objective function is built to penalize network configurations leading to overloads of distribution lines and over or under voltages at buses. For a given network configuration, the fitness function is obtained by considering both the maximum allowed power supplied by DG sources and the exploitation of the lines together with the bus voltage profiles. uniform voltage distribution algorithm based constructive reconfiguration is used as heuristic in [139], [140]. Objective of the problem is to reconfigure the network and DG sizing to maximize network power loss reduction and HC. Particle swarm optimization technique is used to find the best solution of the proposed multi-objective problem.

RES Curtailment

Active power curtailment was studied in some papers and is also finding its ways into national regulatory framework. RES curtailment includes decreasing the output power of specific resources which exceed the HC limitations [79]. Another major advantage of RES curtailment is preventing inverters disconnection due to overvoltage tripping. In [141] two methods are compared for active power limitation: fixed percentage of the nominal power and VoltWatt control where the active power depends on voltage. The results show that fixed curtailment has better performance compare to that VoltWatt control. In [142], optimal setting of DG curtailment based on multi-period OPF has been investigated for economic benefits.

Voltage Control

Local voltage control by using local information allows to increase HC; it is also called decentralized method. The local voltage control may be performed by the regulatory of On Load Tap Changer (OLTC) in primary substation and the Power Factor Control (PFC) of DG.

The voltage set-point of MV bus-bar at PS could be controlled by OLTC through offline OPF [143]. The authors in [144] have compared a real network case study with no OLTC, five tap position on OLTC and nine tap position on OLTC. The results show that HC could be increased more than 50% in 16% of the analyzed scenarios and more than 100% in about 3%. Moreover, no significant difference between 5 and 9 tap position has been reported, meaning that the OLTC HC impact neither depends on the size of network, nor the level of loading. In [145] different modern control schemes are discussed including Enhanced transformer automatic paralleling package and super TAPP n+ relay, to reduce the circulating current between transformers and to estimate the RES output current respectively. In [146] state estimation approach is suggested for OLTC controlling.

DG injections cause voltage rise in the MV feeders and PFC could control the systems voltage by increasing the HC of the distribution grid. In [147], [148], [149], [150], Static compensators (STATCOM), D-STATCOM, static VAR compensators, fixed capacitor banks and shunt capacitor banks have been investigated as generator compensators to regulate the voltage. Four different local control schemes are discussed in [151], [152], [46]. These schemes have been modified according to European technical standards, as listed in the following:

- $LawA$) control of tangent of ϕ according to the PCC voltage ($\tan\phi = f(u)$);
- $LawB$) control of reactive power according to the PCC voltage ($q = f(u)$);
- $LawC$) control of tangent of ϕ according to the real power injected ($\tan\phi = f(p)$);
- $LawD$) control of reactive power according to the real power injected ($q = f(p)$).

2.3.5 Regulatory Framework

In the mid of 2000s, one of the hosting capacity main objective in the project EU-DEEP was market mechanism identification to bring out the DER value to nominate a suitable regulatory framework [56]. Moreover, in the previous research work different hosting capacity approaches have been proposed in order to define a most appropriate market architecture in different aspects such as cost, regulation, structure, ownership and competent allocation. Hence, it is important to have a very depth analysis for implementation cost as they should remain lower than anticipated gain. In order to make some advantage of DER benefits and determine their appropriate type, apart from management and control some technical question regarding the connection of DG to the distribution grid needs to be considered. Therefore, integration process must compatible with system and other words must be system-oriented.

The allowable DER injection for power quality and reliability evaluation is needed for other customers, hence HC simplifies the actor's communications [41]. Moreover, HC is used to estimate the extra cost of the system for providing reliability in case of high DER penetration in comparison with the system without DER. After this step, there is a possibility to provide a full picture of the grid consisting market and also regulatory scene.

To make sure that the grid operators do not need an extravagant investments, a right view could be accomplished by comparison between the cost-effectiveness of several defined solution by by performing HC in order to connect more DG. Therefore, the investment cost of replacing transformer or line branches could be compared with other solution such as advanced voltage control, curtailment, energy storage or demand-response.

As it was explained before, using HC is advised by European energy regulators and European grid operators [54], [53] in order to determine the future electrical grid performance. The HC in Italy, Ireland, Austria and Poland is considered as a revenue driver. Whereas, Czech Republic, Latvia and Lithuania usually have been used for monitoring, while the HC obligations in Norway and Great Britain are very few. According to the European Regulators Group for electricity and gas, the regulatory framework should be determined according to performance improvements of the grid which are defined by the suitable indicators [54]. Moreover, the Council of European Energy Regulators are stressed HC as the key inductor for the capacity assessment of the distribution and transmission grid for providing electricity to the consumers by collecting and bringing to them [153]. In addition, the other HC approach benefits is indicators value possibility to be affected by the network or system operators [54].

In order to express the hosting capacity role as a regulatory framework, the following definition by authors in [109] has been proposed:

> "The hosting capacity is estimated as the maximum penetration of DG where the distribution network yet operates based on its design criteria and network planning according to the European standard EN50160."

In Italy, many regulatory efforts have been done to have a more transparent and efficient connection. In this regard, to find the regulation framework for the DER integration, current system robust technical information and system potential HC is necessary. As it was expressed before, a study for evaluating HC of Italy distribution grid by AEEG has been started in 2009 [106], [154]. Later,the Italian transmission operators identified the HV lines and some grid areas where connecting DG is vital. Moreover, AEEG uses HC evaluation and the ways to increase it as the smart grid solution implementation.

Therefore, AEEG mainly gives the priority to the smart grid projects with hosting capacity development. Therefore it could commences a valued benefits indicator from smart grid technology investments for the grid. The following equation shows the acceptable growth of DG power injection to the grid without any grid reinforcement and violating technical constraint:

$$P_{smart} = \frac{EI_{post} - EI_{pre}}{8760} \tag{2.19}$$

where EI_{post} is the yearly amount of DG injection to the grid without violating the technical constraint after the grid smartening in MWh, EI_{pre} is the yearly amount of DG that can be injected to the grid without any risk of reverse power flow before the grid smartening in MWh. Both values are calculated based on the grid structure and HC approach.

In general, the aim is to obtain an indicator based on the DSO assessment. Therefore, the number of HC level could be defined as the type of DG to define the exact HC is important.

In Australia the HC approach to define the limit of DG injection to its grid has been explained in [155]. The criteria which have been considered in this project is consisting transformer and network capacity, generating units minimum load, voltage rise, and reverse power flow. Then, by using a mathematical model the hosting capacity will be evaluated according to all aforementioned criteria. Moreover,

all costumers could be informed monthly about the permissible amount of PV injection in each specific city [156]. As an example, a map of possible RES connection for all MV, HV and extra high voltage grid of France has been published by considering a some amount of curtailment on the connection rules.

2.4 Summary

In this chapter, current regulatory scenarios of energy planning including international and European environmental polices and regional roles had been explained. These policies motivated European Union for a fast renewable energy sources deployment in the last years (e.g. 20-20-20 package has been marked a turning point in the EU electricity sector pushing to develop renewable energy sources). However, due to massive renewable energy integration around the world and specially Europe the importance of considering and evaluating hosting capacity for the grid network was highlighted in this chapter. Generally, power system performance is affected by changes in the generation and load patterns. Hence, the HC is defined by an algorithm which determines the amount of acceptable DG without endangering the grid power quality and reliability with respect to some limits, i.e. steady-state voltage limits, transformer and lines thermal limits and fast voltage variations.

The proposed approaches in the literature are mainly based on iterative calculations, aiming at estimating the maximum DG penetration admitted in every bus according to the considered technical limits; the HC is evaluated for a single constraint at each time and the overall HC is defined as the minimum HC over all the constraints. However, in some specific networks the required data for hosting evaluation are missing, thus in the next chapter parameter estimation has been proposed to define all the required grid parameters.

CHAPTER 3

Power System Parameter Estimation

3.1 Introduction

Power system State Estimation (SE) has been considered as a critical part of the transmission systems management and operation due to the concept development in early 1970 [157]. SE is a fundamental tool to show the real-time behavior of power systems. This process defines the system state including voltage and angle of each bus based on the grid parameters [158]. For that matter, at the present time state estimators are used to make power system more secure and economic, hence SE is the main part of Energy Management System (EMS). The SE procedure is assigning a value to an unknown system state variable based on imperfect measurements and statistical criterion for maximizing or minimizing.

In this thesis, on the contrary, starting from information on states (voltages, Power Flow (PF), etc.) the goal is to find parameter values as much accurate as possible: as decisions making depends on current parameters and on states, accurate system parameter estimation is a critical problem. Hence, their values are to be defined indirectly through an inverse state estimation procedure [157]. The reverse problem (Parameter Estimation (PE)) is set up using some variables (voltage magnitudes, PF, etc.) to estimate the network parameters, assuming a π-equivalent model for each branch of the network (series reactance and resistance, line charging). In the inverse state estimation procedure, measurements or available information are fit into the proposed model, and parameters are adjusted to minimize mismatches between given values and estimated values [159]. This approach is based on the theory developed for state estimating the values of parameters based on available measured data and taking into account the probabilistic modeling of the error and also truncation errors that can significantly affect results [160].

A PE model is proposed, where:

- Available information (either measurements or results of a PF computation made available) is assumed to represent the real state of the system and hence are modeled like available measurements.
- Network parameters are modeled as the independent control variables of a minimization problem.

In this chapter, after talking about different state estimation procedures, the proposed methodology in this thesis have been discussed. After that the real-life case study (Tanzania transmission grid) has been introduced deeply and at the end results and discussion have been presented.

3.2 State Estimation Procedures

The theory of estimation is a part of signal processing and statistics that using available measurement sets, can estimate the immeasurable states. There are physical relationships between the parameters that their values influence the distribution of the measured data.

The idea of SE had been proposed by Gauss and Legendre in early 19 century [161]. Then, in 1970, power system SE as a mathematical curiosity was proposed by Fred Schweppe to define the voltage and angle of the network [162], [157], [163]. The SE output data consists of phase and voltage of the nodes, while the input data is including lines resistance, reactance and susceptance and a set of measurements that contains power flow in each bus and through each line, though all the measurements across the network have some faults and uncertainty. The power system model could have two different type of errors consisting parametric error and non-parametric errors [164]. The first group could happen due to usage of incorrect parameters value such as resistance or susceptance, while the non-parametric error could occur when the approximate model of the power system was used instead of the real one [165], [166].

Although phasor measurement unites could be installed in each point of the network to measure the aforementioned parameters, it is not applicable in terms of economical overview. Hence, the existence of SE application in power system is vital and could be defined as “boarding pass” of the system monitoring and control application. Applying SE according to Supervisory Control And Data Acquisition (SCADA) measurements and power system model could give us the best estimation of the current voltage phasors, the position and statues of the tap changers and circuit breakers.

Fig. 3.1 demonstrates the role of state estimation in Energy Management System (EMS). The following real examples make the importance role of SE clearer: the inappropriate information regarding the conditions of the systems circuit caused the big blackout in New York state in 1977 [167]. Hence, the real time electricity market control and operation is highly dependent on the information of power system states. In shorter words, certainly state estimation procedure in the modern power system is crucial as it is the connector of real time information and power system control and operation.

The state estimation procedure could be summarized as follows:

1. Converting the model of switching device/bus section to bus/branch model.
2. Confirming if the system could be observed or not.
3. Obtaining the states and measurement estimates.
4. Performing the residual analysis to check the consistency of SE.

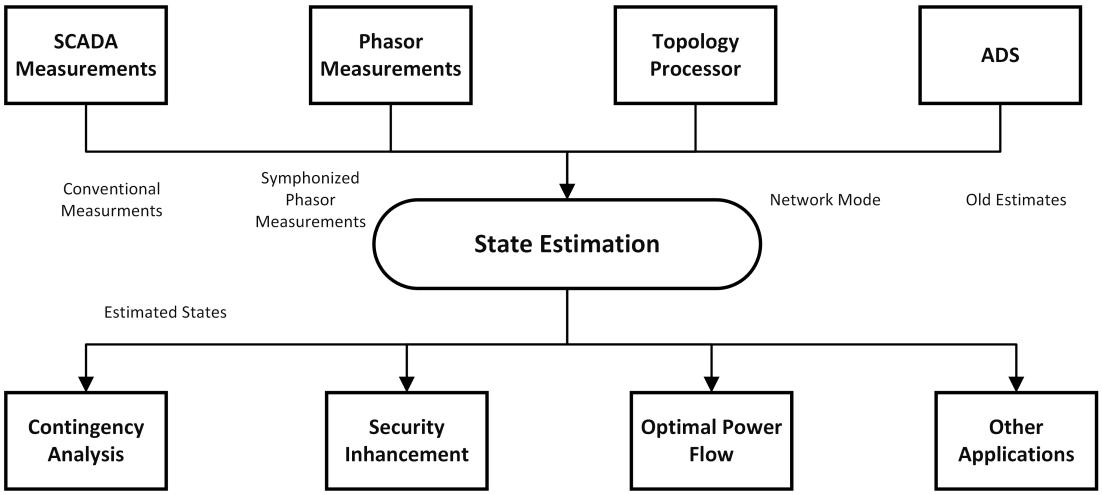

Figure 3.1: *The role of state estimation in EMS*

The decades of research in the area of SE leads to a diversity in the algorithms and approaches for it. The authors in [168], [169], [170], [171] reviewed these methods completely. Moreover as SE has different applications, different approaches are needed to be used such as conventional SE [169] and distributed SE (Multi Area State Estimation) [172]. Although state estimation could be categorized into many groups, however in this thesis it is classified in to three different groups: static state estimation, dynamic state estimation and distributed state estimation. A brief overview of them are provided in the following.

3.2.1 Static State Estimation

Since the energy demand has been increasing these days, the real time monitoring, and controlling of power system using EMS are becoming more complex and vital [173]. Therefore, to improve the grid real-time monitoring, shorter intervals are needed for updates. Thus, SE for calculating state vector with high accuracy after collecting measurement set from SCADA or phasor measurement unit is inevitable [174]. If a state vector was estimated at the instant time using the measurement set at the exact instant time, then it will be called as the Static State Estimation (SSE). Most commonly used criterion for SSE in power system relies on Weighted Least Square (WLS) approach to minimize the norm of residues of measurement which is based on the linearization power system equations, this procedure is completely explained in [175], [162], [157], [163], [161]. In the following a brief introduction of WLS is presented.

Weighted Least Square State Estimation

In a N bus system, there are $2N-1$ system states which includes the bus voltages and bus angels except the slack bus (reference bus) angle which is considered zero. The structure of the state vector is organized in the way to show the voltage magnitude first, and then voltage phase angles are shown in continue, equation 3.1 shows this vector.

$$x = (|V_1|\ |V_2|\ \ldots\ |V_N|\ \theta_2\ \theta_3\ \ldots\ \theta_N) \tag{3.1}$$

The state estimator using the measured data set (Z) from the power system (SCADA), as an input including power flows through line (S_{flow}), power injection of nodes (S_{inj}) and voltage magnitudes (V_{mag}), could estimate the system states. However as it is obvious in any estimation there are some nominal errors inevitably, 3.2 and equation 3.3 shows the aforementioned vector in following.

$$Z = h(x) + e \tag{3.2}$$

$$\begin{bmatrix} Z_1 \\ Z_2 \\ . \\ . \\ . \\ Z_m \end{bmatrix} = \begin{bmatrix} h_1(x_1, x_2, ..., x_n) \\ h_2(x_1, x_2, ..., x_n) \\ . \\ . \\ . \\ h_n(x_1, x_2, ..., x_n) \end{bmatrix} + \begin{bmatrix} e_1 \\ e_2 \\ . \\ . \\ . \\ e_m \end{bmatrix} \tag{3.3}$$

where $h(x)$ is the nonlinear function of system states (x) and e is the normally distributed measurement error. Equation 3.4 represents the measurement vector, equation 3.5 as a non-linear function to relate the states to the measurement and equation 3.6 as the measurement vector error.

$$Z^T = [Z_1,\ Z_2,\ \dots Z_m] \tag{3.4}$$

$$h^T = [h_1(x),\ h_2(x),\ \dots h_m(x)] \tag{3.5}$$

$$e^T = [e_1,\ e_2,\ \dots e_m] \tag{3.6}$$

The covariance of noise vector with the gaussian (normal) distribution composes the covariance diagonal matrix R with the measurement inputs. Actually, considering the error vector with mean value equal to zero and assuming that they are uncorrelated and independent from each other, make WLS algorithm tries to minimize the weighed sum of the measurement errors squared.

$$E\{e_i\} \qquad i = 1, 2, ..., m \tag{3.7}$$

$$E\{e_i e_j\} \qquad i = 1, 2, ..., m \ \ j = 1, 2, ..., m \ \ i \neq j \tag{3.8}$$

$$cov(e) = E\left\{e.e^T\right\} = R = diag\left\{\sigma_1^2,\ \sigma_2^2 \dots \sigma_m^2\right\} \tag{3.9}$$

where m characterizes measurements number and (σ_i) is the standard deviation of the SCADA measurements errors which is mostly related to the accuracy of the corresponding used meters. Equation 3.10 in following represents the measurement Jacobian matrix H as a partial derivatives of $h(x)$ respect to x.

$$H = \left[\frac{\partial h(x)}{\partial x}\right] = \begin{bmatrix} \frac{\partial P_{inj}}{\partial V_{mag}} & \frac{\partial P_{inj}}{\partial V_{ang}} \\ \frac{\partial P_{flow}}{\partial V_{mag}} & \frac{\partial P_{inj}}{\partial V_{ang}} \\ \frac{\partial Q_{inj}}{\partial V_{mag}} & \frac{\partial Q_{inj}}{\partial V_{ang}} \\ \frac{\partial Q_{flow}}{\partial V_{mag}} & \frac{\partial Q_{inj}}{\partial V_{ang}} \\ \frac{\partial V}{\partial V_{mag}} & 0 \end{bmatrix} \tag{3.10}$$

The goal of WLS algorithm will be accomplished when the following objective function is minimized.

$$J(x) = \frac{\sum_{i=1}^{m}(z_i - h(x)_i)^2}{R_{ii}} \; = \; [z - h(x)]^2 \; R^{-1} \, [z - h(x)] \tag{3.11}$$

The weighting process in this algorithm is giving more weight to the more accurate measurement and less weight to the less accurate one; the weighting factor is the measurement standard deviation inversed square. Thus, to minimize equation 3.11 the first derivative respect to x has to be satisfied:

$$g(x) = \frac{\partial J(x)}{\partial x} = -\left[H(x))\right]^T \; R^{-1} \, [z - h(x)] = 0 \tag{3.12}$$

The mentioned equation could be solved by Gauss-Newton method.

$$x_{k+1} \; = \; x_k \; - \; [G(x_k)]^{-1} . g(x_k) \tag{3.13}$$

where the number of iteration is shown by k and the state vector in this iteration is represented by x_k. The gain matrix ($G(x)$) which is signified in the following is usually sparse and could break apart to its triangular factors.

$$G(x_k) \; = \; \frac{\partial g(x_k)}{\partial x} \; = \; [H(x_k)]^{-T} . R^{-1} . H(x_k) \tag{3.14}$$

$$g(x_k) \; = -\left[H(x_k)\right]^T . R^{-1} . \, [z - h(x_k)] \tag{3.15}$$

Backward and forward substitution are used to solve the linear equation 3.16.

$$x_{k+1} = x_k - [H(x_k)^T . R^{-1} H(x_k)]^{-1} [-H(x_k)^T . R^{-1} (z - h(x_k))] \tag{3.16}$$

In the following equations, the convergence criterion has been stated as the exceeding of the defined maximum number of iterations or going beyond the defined acceptable range of state variables. However, the constraints in equation 3.18 which is the objective of WLS is rarely considered in real time operation because of implementation time [176].

$$max(\Delta x_k) \; \leq \; \varepsilon_1 \tag{3.17}$$

$$J_{k+1} - J_k \; \leq \varepsilon_2 \tag{3.18}$$

The computational steps for applying WLS algorithm are briefly mentioned as follows [177]:

1. Start iteration by number i=1.
2. Initialization of state vector.
3. Reading the input of measurements.
4. Building measurement Jacobian ($H(x)$).
5. Calculating gain matrix ($G(x)$).
6. Solving Δx.
7. Checking convergence limit.
8. If the convergence criteria are not accomplished yet, go to step 4 and increase iteration.

In the literature there are many works proposing new procedures to improve WLS in specific aspect. In [178], [179] the voltage magnitude and the voltage angles are estimated singly by the fast-decoupled SE. In this approach the voltage values are related to the reactive power injection, whereas voltage angels are concerned by active power. The proposed method in this paper could be performed in parallel so it could improve the assessment time. The power system regularized least square in [180] assessed the observability issues in different WLS and proposed a method which could be performed in case of partial observability. In [181] Levenberg MarquardtLM algorithm was used instead of typical Newton Raphson approach to solve the WLS objective. This paper proved that this algorithm is useful in case of partial observability and ill conditions.

The aim of WLS state estimation is overwhelming the normal distributed measurement errors inherently. However, in real life due to the contaminated measurement with error, the estimation will be deviated. Thus, the introduction of a new approach to identify, modify or eliminate the inaccurate data is necessary here. In this regard, in [182] and [183] a straightforward method according to the comparison of the expected value with defined threshold has been proposed.

One of the main disadvantage of WLS algorithm is the execution time which is high as in each iteration gain matrix needs to be built and factorized. In order to reduce the operational time, an assumption could be made that the elements of this matrix have very little changes during each iteration as power equations are insensitive to voltage angles. Hence using a constant gain matrix is recommended by these assumptions [177].

As it was mentioned at the beginning of this section, the WLS assumption has been discussed, considering the zero mean value for measurement which makes some challenges for large scale application such as “sensor-less” technologies (e.g. A/D converters). To tackle this problem as the calibration error are constant compare to normal distributed measurement error, one of the suggestion would be considering parallel state estimation with measurement calibration [184]. The other perquisite of WLS is the observability of the system. Hence, authors in [185] and [186], have proposed some approaches for observability analysis.

3.2.2 Dynamic State Estimation

Due to the quasi-static behavior of nature, the power system states change slowly with time. Moreover, if the changes are in the load or in some special occasion such as contingency, the system must be monitored very thoroughly. Hence, it is compulsory to do the estimation of the state in high frequency rate. For this reason, SSE could not be a good option as the duration between two estimates is more than what is expected here which leads to a weak-state-correlation. To do so, Dynamic State Estimation (DSE) in the modern power system with the new EMS system becomes very important. In this regard, by using the present states of the power system and the system physical model information, DSE could forecast the state vector of next instant time [187], [188], [189]. After the arrival of the new measurements of the next instant time, the forecasted values are filtered in order to obtain a more accurate state estimation procedure. Hence, DSE compared to traditional SE has several advantages such as:

- As security analysis may be done in advance, there will be more time for controlling in the emergency situation.
- It could identify and reject the bad data.
- It replaces pseudo measurement with high quality value leading to avoid harsh conditioning.

In [190] a computational algorithm using a new weight function for robustness of DSE has been discussed. In 1973, Masiello introduced the concept of state estimation tracking. After that, Leite da Silva improved this method and described the state transition equations [191].

In DSE there are two equations giving us the system description; equation 3.2 in the previous section and equation 3.19 as follows:

$$\bar{x}_{t+1} = \Phi_{t\rightarrow(t+1)}(x_t) + v_t \tag{3.19}$$

where, x is showing the system states in time instant t and forecasted $t+1$, Φ_t evolution function of the system and v_t is the evolution time error including white noise.

In overall, DSE has two important phases: prediction and filtering [168], which have been discussed in following.

Prediction : The state variable forecasting contains the model and behavior of the power system. The forecasting procedure in this system is based on the last estimation and dynamic state of the system. In order to make an advance dynamic state estimator, defining the correct mathematical equation of the state time evolution is vital. Whereas, due to the importance of having the precise and correct knowledge of the future behavior of the system such as load and generator, it is not an easy task to obtain that mathematical equations. Hence some methods are used in order to complete this prediction step including load forecasting and generator dynamic model. Opposite of SSE that considers linear mathematical model for the ease of calculation [192], DSE uses nonlinear model. Even the typically used algorithms in DSE prediction part (fuzzy logic [193] and Artificial Neural Network (ANN) [194]) are also complex and have time-consuming process. Hence, DSE is not widely used in real life [189].

Filtering: It filters out the bad data using the combination of forecast information in the previous section and actual on arrival measurements. For this step the Kalman Filter (KF) is widely used which is

discussed briefly in the next part. Moreover, the extended Kalman Filter could be used in DSE because of the non-linear relationship of power and voltage. In the following table, some of combinations of these two phases from the literature are summarized.

Table 3.1: *Combination methods for DSE*

Prediction	Estimation
Noise Model	Kalman Filter [195] Extended Kalman filter [196] Kalman-Bucy filter [197]
Linear Exponential Smoothing	Extended Kalman filter with anomaly suppression [190] WLS algorithm [198]
Dynamic Generator Equations	Kalman filter variant [199]
ANN based busload prediction	Extended Kalman filter [194]
Current State and Change at Neighbors	M-estimation [200]

Kalman Filter

In 1960, for the first time the Kalman filter theory was presented, the full formulation and its theory could be found in [201]. After the introduction of Kalman filter, many power system applications have been performed using it such as [202], [203] and [204] which the authors used Kalman filter for distance relaying scheme, relaying power system measurements and harmonic analysis respectively. As the power system equations has nonlinear trend, extended Kalman filter has been proposed [205]. In [206] and [207] a dynamic model of power system for calculation of the active and reactive power injection using Jacobian is discussed.

Kalman filter which is also called optimal estimator could calculate the parameters state in an uncertain and noisy condition in online mode. The mathematical model of Kalman filter is presented in the following:

$$x_{k+1} = Ax_k + Bu_k + w_k \tag{3.20}$$

Where, x is showing the system states at discrete time instant of k and $k+1$, u_k represents a set of control variables and finally matrix A and B are linking the state variables at time k to time $k+1$.

Like WLS algorithm this method also needs some assumption which are written in the following:

$$E\left[x_0\right] = x_0 \tag{3.21}$$

$$E\left[w_k\right] = 0 \; \forall \; k \tag{3.22}$$

$$E\left[x_0, w_k\right] = 0 \; \forall \; k \tag{3.23}$$

$$E\left[v_k\right] = 0 \; \forall \; k \tag{3.24}$$

$$E\left[x_0, v_k\right] = 0 \; \forall \; k \tag{3.25}$$

$$E\left[v_j, v_k\right] = 0 \,\forall\, k \neq j \tag{3.26}$$

$$E\left[w_j, w\right] = 0 \,\forall\, k \neq j \tag{3.27}$$

It is also assumed that the initial estimates (x_0) and its covariance matrix (p_x^0) at any time instant are known. Therefore, the computational steps of Kaman filter can be expressed shortly in following:

1. Initialization of the initial estimate and its covariance matrix.
2. Reading the measurements input.
3. Calculating Δz_k.
4. Calculating Jacobian matrix H_k.
5. Calculating Kalman gain G_k according to equation 3.28.
6. Solving Δx according to equation 3.29.
7. Updating error covariance matrix according to equation 3.30 and equation 3.31.
8. The aforementioned steps will be repeated for defined tolerance Δx limit.

As it was discussed in the previous chapter, the initial estimate errors have zero mean value and they are uncorrelated with each other which means they have only diagonal inputs in their covariance matrix.

$$G_k = P_0 H_k^T (H_k P_k^0 H_k^T + R)^{-1} \tag{3.28}$$

$$\Delta x = G_k(\Delta z_k - h(x_k)) \tag{3.29}$$

$$P_k = (I - G_k H_k) P_k^0 \tag{3.30}$$

$$P_{k+1}^0 = P_k + Q_k \tag{3.31}$$

Using Kalman filter adopting two different methods considering equality and inequality constraints were discussed in paper [208]. One of the method is restricting the optimal Kalman gain and the other one is projecting the unconstrained estimate. Extended Kalman Filter for DSE using fuzzy control theory is discussed in [189].

3.2.3 Distributed State Estimation

Estimating the system state in single state estimator results optimal estimate which is called integrated. However, according to computational efficiency the integrated state estimation cannot perform well. That is why the usage of Distributed State Estimator (DSSE) results to state estimation computational time reduction. DSSE can be categorized into some groups according to some criteria such as follows [172]:

- Overlapping areas
  - Non-overlapping
  - Border-bus overlapping
  - Tie-line overlapping
  - Deep overlapping
- Computing architecture
  - Hierarchical architecture
  - Decentralized architecture
- Coordination methods
  - State estimation level
  - Iteration level
  - Hybrid condition
- Measurement synchronization
- Process synchronization
  - Classical distributed state estimation
  - Agent-based distribution state estimation

In the literature, there are mainly two approaches for solving DSSE including weighted least square approaches and power flow approaches.

Weighted Least Square

The author in [209] proposed a DSSE using WLS and three phase modeling approach. In this paper, the estimated quantities uncertainties were defined by calculating the bus voltage and power flow deviations. Also, a three-phase current estimator was proposed in [210] to minimize the WLS objective function. In this paper, the measurement values of power, voltage and current are transformed to their corresponding current. In addition, the Jacobian matrix are considered constant with the value of admittance elements. Then in [211] Lin and Tang improved the convergence speed of this method by decoupled formulation and measurement pairing. In this article the SE has equality constraints based on the measurement of corresponding current in rectangular coordinates.

In [212] a new method was introduced in order to define the branch currents as state variables. The main target of this algorithm is radial and weakly meshed system which helps to make the computational effort very efficient. Wang and Schulz in [213] developed this method by revision of DSSE branch current in terms of parametric variation and they could estimate the load through automated meter reading. Moreover, in this work the impact of measurement location and types on the estimation procedure have been discussed.

Power Flow

Real measurements are considered in [214] as solution constraints using a probabilistic extension of radial load flow algorithm for DSSE. In this paper, the aforementioned algorithm which could use for the non-normally distributed loads also could use for the load diversity and can interact with a load allocation routine. This method has been explained by the radial nature of distribution grid and state variables are considered as random variables; the experimental results of this algorithm is presented in [215].

Gauss-Seidel algorithm for performing load flow SE in radial distribution network was used in [216]. In this work, the load profiles were taken from the historical data and they scaled according to the actual measurement. Similar method was performed in [217] by Roytelman and Shahidpour using Kirchhoff law based on current balancing.

3.3 Proposed Parameter Estimation Methodology

The study in this chapter has been done in order to obtain the reliable network data starting from information that can readily be found. Currently, in emerging countries the available information regarding the electrical network is typically in the form of paper network diagram where simple power flow (PF) results are graphically reported: nodal voltage magnitude and power flows in the branches of the network (published for specific operating conditions, e.g. yearly peak load, sometime related just to a fraction of the main grid). Usually, this information does not cover the minimum necessary set of network data for further planning or operation analysis (power flows, optimal power flow, security analysis, etc.). Here a procedure for reformulation of the traditional state estimation problem is proposed to find out network parameters using the available data that can be retrieved from public reports (in most cases, just paper diagram). This problem is very important from the practical point of view when trying to set up a project in countries where complete information is not available.

Accurate parameter estimation is crucial as decisions making depends on current parameters and on states. Hence, in this thesis the goal is to find the parameters as much accurate and precise as possible. To do so, these values will be defined indirectly through an inverse state estimation procedure. This parameter estimation by some variables could estimate the network parameters. This approach is based on the developed theory for state estimating the values of parameters based on available measured data and taking into account the probabilistic modeling of the error and also truncation errors that can significantly affect results.

3.3.1 Available Information

The developed model in this thesis relies on the knowledge of the following:

- Network topology in terms of network buses, branches, location of generators and loads and their interconnections.
- Typical information commonly available on network diagrams (they could be the output of either a state estimation procedure or a PF computation) which includes some set of variables: voltage magnitudes, and/or real and reactive branch power flows, and/or real and reactive power injected by the generators and withdrawn by loads. Such variables could be available for the whole grid or just for some selected busses or areas.

3.3.2 Problem Definition

The main concern with the available information (namely, public data) is the numerical accuracy due to truncation of values: the accuracy can range from ± 1 kV to ± 0.01 kV for voltages and from ± 1 MVA to ± 0.01 MVA for power flows. This leads to an accuracy generally much lower than the standard tolerances of the PF; hence, this is a first source of inaccuracy in the calculation of the network parameters starting from available data. In this thesis, the above-mentioned issue is mitigated by solving an optimization problem derived from the traditional state-estimation, which makes it possible to exploit redundancy of information. The available input data is collected into a vector x^m, and the distance to the estimated values of x^m, x^{est} is minimized by solving the following optimization problem:

$$min \left[x^m - x^{est}\right]^T .W. \left[x^m - x^{est}\right] \tag{3.32}$$

where x^m is the column vector of the input values, e.g., voltage magnitudes, power flows through branches etc. x^{est} is the column vector of the corresponding estimated values, linked by means of the non-linear PF equations as constraints. These constraints are functions of the network parameters to be determined. W is the diagonal matrix of weight coefficients, which consider the accuracy of each input.

In the following subsections, the proposed model is described in detail.

3.3.3 Electrical Branch Model

The network parameters of interest are series and shunt impedances describing the electric branches of the network. In this thesis, the well-known π-equivalent branch model is adopted [218]. The model is depicted in Fig. 3.2.

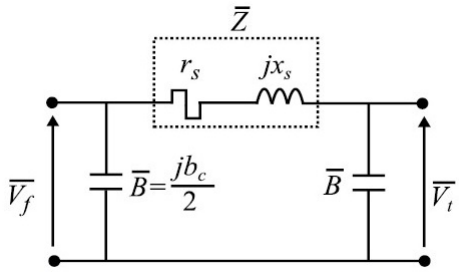

Figure 3.2: *The π-equivalent branch model.*

In Fig. 3.2, V_f stands for the voltage phasor of the "from" bus of the branch while V_t stands for the voltage phasor of the "to" bus of the branch. These are described by equations 3.33 and equation 3.34.

$$\bar{V_f} = V_f.e^{j\delta_f} \tag{3.33}$$

$$\bar{V_t} = V_t.e^{j\delta_t} \tag{3.34}$$

According to Fig. 3.2, three parameters need to be determined: the branch series impedance (magnitude Z and angle θ) and the line charging B:

$$\bar{Z} = Z.e^{j\Theta} = r_s + j.x_s \tag{3.35}$$

$$\bar{B} = jB = j\frac{b_c}{2} \tag{3.36}$$

In the defined optimization problem variables Z, Θ and B are determined such that the estimated power flows in the branches are converging towards the known, measured values. These power flows are computed according to [219], [201]:

$$P_{ft} = \frac{V_f^2}{Z}cos\Theta - \frac{V_f V_t}{Z}cos(\delta_f - \delta_t + \Theta) \tag{3.37}$$

$$Q_{ft} = \frac{V_f^2}{Z}sin\Theta - \frac{V_f V_t}{Z}sin(\delta_t - \delta_f + \Theta) + BV_f^2 \tag{3.38}$$

$$P_{tf} = \frac{V_t^2}{Z}cos\Theta - \frac{V_t V_f}{Z}cos(\delta_t - \delta_f + \Theta) \tag{3.39}$$

$$Q_{tf} = \frac{V_t^2}{Z}sin\Theta - \frac{V_t V_f}{Z}sin(\delta_t - \delta_f + \Theta) + BV_t^2 \tag{3.40}$$

3.3.4 Optimization Model

According to equation 3.32 and the previously defined electric branch model, the vectors x^m , x^{est} and W, describing the proposed optimization model can now be defined as:

$$x^m = \left[P_{ft,1}^m \ldots P_{ft,l}^m\, P_{tf,1}^m \ldots P_{tf,l}^m\, Q_{ft,1}^m \ldots Q_{ft,l}^m\, Q_{tf,1}^m \ldots Q_{tf,l}^m\, V_1^m \ldots V_n^m\right]^T \tag{3.41}$$

$$x^{est} = \left[P_{ft,1}^{est} \ldots P_{ft,l}^{est}\, P_{tf,1}^{est} \ldots P_{tf,l}^{est}\, Q_{ft,1}^{est} \ldots Q_{ft,l}^{est}\, Q_{tf,1}^{est} \ldots Q_{tf,l}^{est}\, V_1^{est} \ldots V_n^{est}\right]^T \tag{3.42}$$

$$W = diag\left(\left[W_{Pft,1} \ldots W_{Pft,l}\, W_{Ptf,1} \ldots W_{tf,l}\, W_{Qft,1} \ldots W_{Qft,l}\, W_{Qtf,1} \ldots W_{Qtf,l}\, W_{V1} \ldots W_{Vn}\right]^T\right) \tag{3.43}$$

In equation 3.41, $P_{ft,1}^m$, $P_{tf,1}^m$, $Q_{ft,1}^m$, and $Q_{tf,1}^m$ are the known real and reactive power flows in the branches of the network, while V_m are the known nodal voltage magnitudes, and l and n are the number of branches and buses respectively. Moreover in equation 3.42, $P_{ft,1}^{est}$, $P_{tf,1}^{est}$, $Q_{ft,1}^{est}$, and $Q_{tf,1}^{est}$ are calculated using equation 3.37 – 3.40 while V^{est} stands for the estimated nodal voltage magnitudes.

According to 3.44 there is an error with input measurements. Thus, for the evaluation of W coefficients, uniform distribution of data's error is assumed. Measurement error could be distributed to the interval from $-A$ to $+A$ which is related to the procedure of rounding. Fig. 3.3 represents the rounding error according to probability density function.

$$x^{est} = x^m \pm \Delta x \tag{3.44}$$

The amount of W coefficients is calculated as [220]:

$$W = \frac{1}{\sigma^2} \tag{3.45}$$

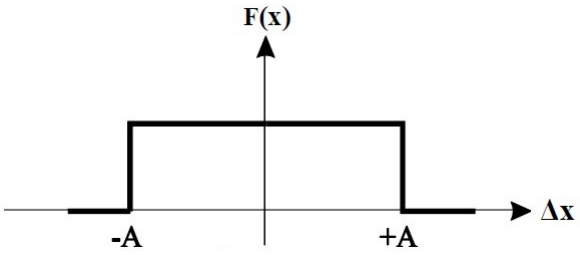

Figure 3.3: *Uniform distribution of error.*

where:

$$\sigma = \frac{A}{\sqrt{3}} \tag{3.46}$$

Hence, different variables have different weights; very accurate input data have higher weights, as they are more trustable [220]. The mentioned model could be solved with one of the nonlinear solver in MATLAB, such as fmincon, fminunc.

3.4 Validation of the Proposed Approach

The energy sector in emerging countries is currently under strong development and hence it is a very attractive area for business and industry. Due to the peculiarities of these countries, micro-grid solutions are of interest. However, private companies interested in micro-grid opportunities often have difficulties in finding information required for the evaluation and development of their projects; this includes pertinent laws and regulations, benchmark project-development costs in off-grid areas, local socio-economic indicators and the current state of energy access, data regarding the existing grid and so on. To bridge this gap, the energy sector encourages more and more actors to enter the market. In this regard, public institutions such as rural electrification agencies, are playing an important role by giving consultation for suitable micro-grid sites and grid extension [221].

In order to properly approach the problem, a real-life case study has been selected: Tanzania. The National Energy Policy is implementing new policy to ask for availability of updated information, especially grids models/data and renewable energy sources database from Tanzania Electrical Supply Company (TANESCO) and Rural Energy Agency. The data should be available and freely downloadable from the website of Ministry of Energy and Minerals [222]. Although information can be made available very simply through media, the preparation of this information requires trained professionals who can use suitable engineering tools for data collection. Actually, notwithstanding the above-mentioned statements, it is often very difficult to get reliable and certified grid data.

As it was mentioned before, currently in Tanzania, the available electrical network information is typically in the form of paper network diagram where simple power flow results are graphically reported: nodal voltage magnitude and power flows in the branches of the network (published for specific operating conditions, e.g. yearly peak load, sometime related just to a fraction of the main grid) which do not provide us a set of full data for advance planning and operation. Hence, by using the traditional state estimation reformulation discussed in the previous subsection and the available data, the network parameters will be determined.

3.4.1 Tanzania in Brief

In 1964, the United Republic of Tanzania was organized by the Tanganyika union (Tanzania mainland) and Zanzibar. This country is located in East Africa and has border with Rwanda, Burundi and Democratic Republic of Congo in the west, Kenya and Uganda in the north and Mozambique, Malawi and Zambia in the south, while it is bordered with Indian Ocean to the east. In terms of land, 93.4 % (883,000 sq. km.) of this country is land area and the percentage of 6.6% (62,000 sq. km.) are covered by water. Tanzania has 29 administrative regions in the mainland and 5 regions in Zanzibar. Fig. 3.4 shows the geographical overview of this country.

Figure 3.4: *Tanzania geographical overview.*

Although the official capital city of Tanzania is Dodoma where the government offices and political places is located, the most important seaport and commercial places are located in Dar es Salaam. The total population of this country in 2012 was about 45 million people that 80% of this population are living in the rural area.

Tanzania Energy Sector

There are many natural energy resources in Tanzania such as solar, wind, hydro, uranium, natural gas, coal, biomass and geothermal which still most of them are untapped. Fig. 3.5 represents Tanzania energy sector; it defines 90% of main energy is supplied by biomass for cooking and heating in rural areas, 8% by petroleum for rural and urban transportation, 1.5% by electricity mainly in urban areas for industry and commercial activity and the rest by coal for residential heating and lighting [223].

Some specific information about these RES specifically in Tanzania are described in following:

- Solar energy: As Tanzania lies across the equator has plentiful solar insolation (200Wp/m^2). Hence, there are several off-grid projects by solar power for households especially rural area.
- Wind energy: There are several wind sites (Singida, central part of Tanzania and Makambako in south west) for commercial electricity generation which are typically working with average speed of 5 to 9 m/s annually.
- Biomass energy: Several sugar factories and wood industries are generating electricity for their use by cogeneration generator, moreover they could inject the excess to the national grid.

- Hydro energy (small scale): All or part of the production of 141 hydro sites with the capacity of 10 MW in Tanzania could be sold to national grid with the defined feed in tariff.
- Geothermal energy: Tanzania is transacted by East African Rift Valley basin with high geothermal potential. However, there are some constraints for it development such as investment cost and insufficient data and human.

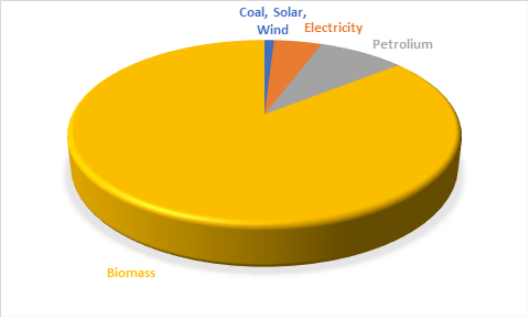

Figure 3.5: *Tanzania energy sector.*

Tanzania Power Sector

In 1908, the colonial authority introduced the electricity to Tanzania. Then, in 1931, two electric company with names of DARESCO and TANESCO were established. After the independence happened, in 1961, the government asked for some shares from each company. The two utilities were joined in 1975, when the government acquired their all shares and called it TANESCO.

The energy policy is formulated through the Ministry of energy and Minerals (MEM) in Tanzania. The aim of electricity acts in MEM is attracting more private sectors to ending up TANESCO monopoly. Moreover, MEM established the electricity import and export in Tanzania. In addition, the responsibility of technical and economic regulation of electricity, water, natural gas and petroleum is with Energy and Water Utility Regulatory Authority in this country as Rural Energy Agency is responsible for enhancing energy services in rural areas. The role of government in this framework is facilitates the activities and investments by private sectors. Fig. 3.6 and Fig. 3.7 show the existing (2015) and planned (2016-2025) TANESCO grid power network.

Current Power Situation

The electricity peak demand in Tanzania was reported by 1026.02MW in 2015 (On-grid), while the total generated energy in this year by TANESCO was 6227 GWh and imported neighboring countries was 1,621MWh; Fig. 3.8 illustrates the current and projected situation of it. Moreover, in each year according to the government report the electricity demand will be grown by 10 to 15%. In the same year, the official access to electricity was stated by 30% which the majority of this number of people are in urban area. Hence, the aim of Tanzania's government is to increase the connections to 30% by 2015, 50% by 2025 and more than 75% by 2033. However, extending the National Grid to many parts of the country including rural areas is not financially and economically feasible [223].

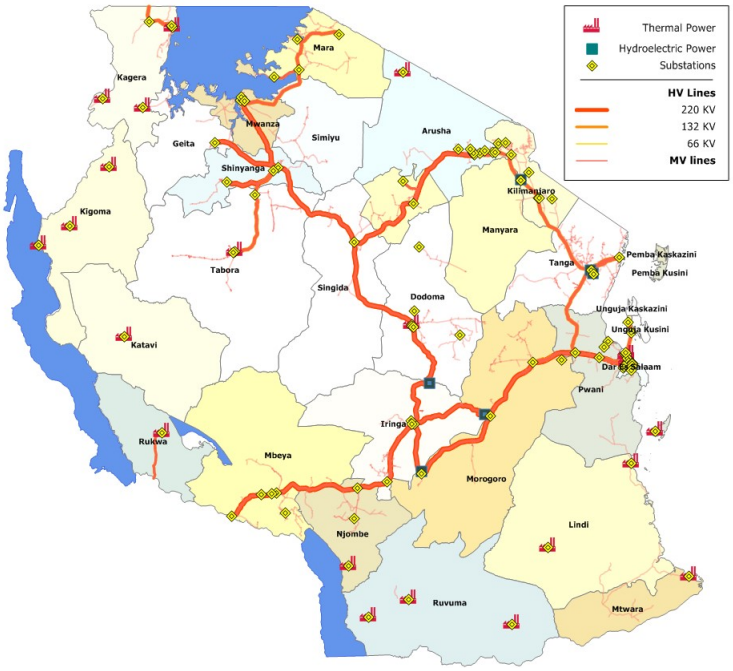

Figure 3.6: *Tanzania existing grid power network.*

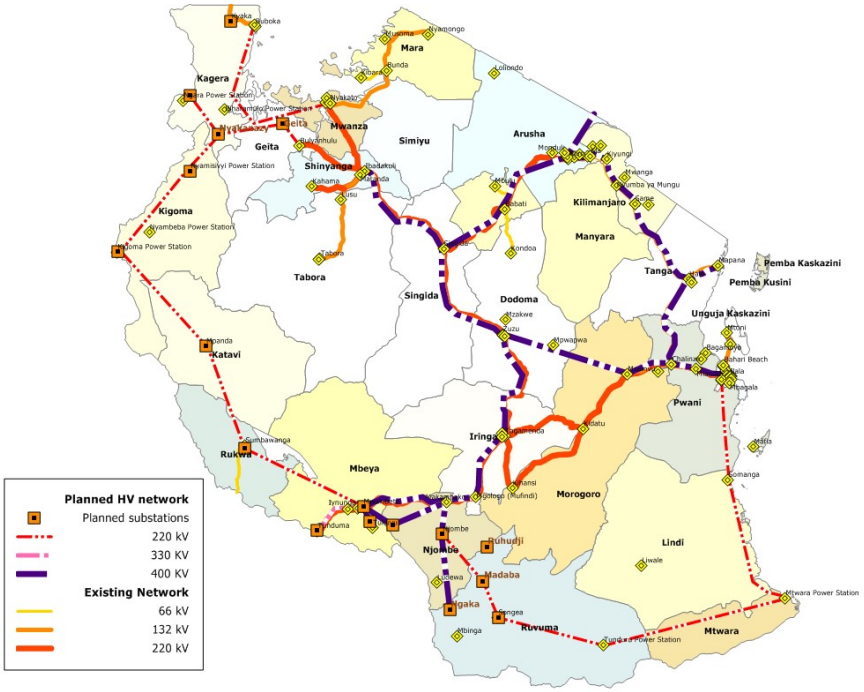

Figure 3.7: *Tanzania planned grid power network.*

The average tariff for 1 kWh is priced 0.126 US$, while there are four different price rates is defined in Tanzania:

- Domestic low usage (D1): the consumption less than 50 kWh per month with 230 V is subjected to subsidy.

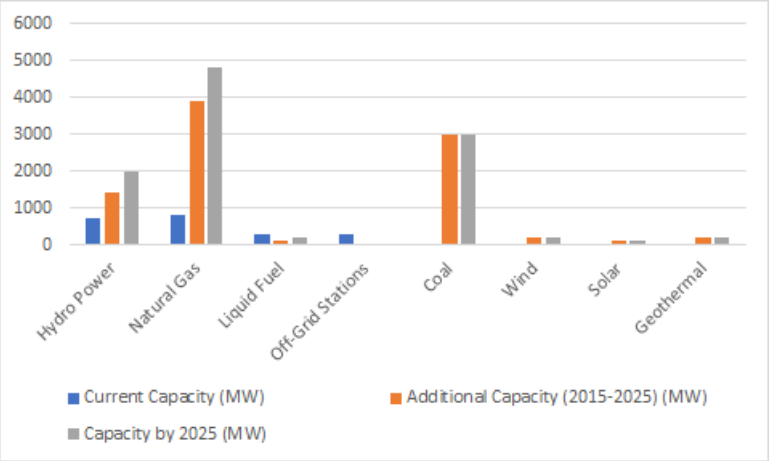

Figure 3.8: *Tanzania projected power situation.*

- General usage (T1): the consumption below 283 kWh and upper than 50 kWh per month with 230 V or 400 V.
- Low voltage usage (T2): the consumption above 7500 kWh per month with 400 V.
- High voltage usage (T3): the consumption with 11 kV and above.

As it was already mentioned, TANESCO owns the whole transmission and mainly the distribution network in Tanzania. The transmission network in Tanzania has four different voltage levels: 440 kV, 220 kV, 132 kV and 66 kV which have 4 lines (670 km), 18 lines (3,610 km), 16 lines (1,662 km) and 5 lines (543 km) respectively. The number of 38 primary substations (2,189 MVA) are located in this network. While, the distribution system in Tanzania includes 33 kV, 11 kV and 400 V lines with the length of 17,079 km, 5,384 km and 40,094 km respectively.

The total installed power capacity in Tanzania was reported 1509.85 MW. Also, TANESCO imports 8 MW and 5 MW from Uganda trough 132 kV and Zambia via 66 kV. Fig. 3.9 and Table 3.2 show the installed capacity and total production in 2015 [223]. The total number of customers was informed around 1 million, and in each year there will be 90 thousand new connections. Thus, the amount of generation needs to be increased. Fig. 3.10 illustrates this increasing.

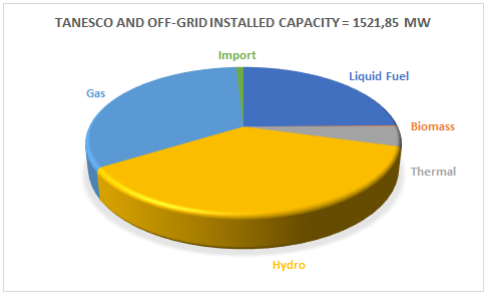

(a) Grid and off-grid intalled capacity.

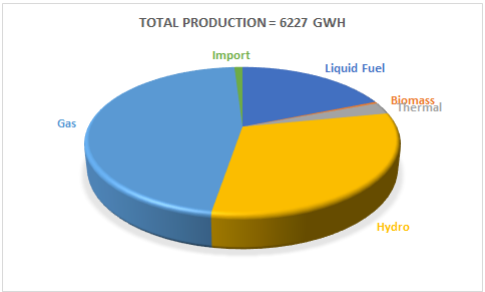

(b) Grid and off-grid Production.

Figure 3.9: *Power installed capacity and production in Tanzania.*

Table 3.2: *Tanzania energy mix and their potential*

No.	Energy Sources	Installed Capacity	Potentioal	Capacity by 2025
1	Hydro Power	566.79 MW	4.7 GW	2,090.84 MW
2	Natural Gas	711 MW	55 Tcf	4,469 MW
3	Liquid Fuel	183.9 MW	-	183.9 MW
4	Off-grid Stations	201.44 MW	-	-
5	Coal	-	1.9 T billions	2,900 MW
6	Wind (5 - 8 m/s)	-	200 MW	100 MW
7	Solar (4.6 / kWh /m^2)	4 MW	-	100 MW
8	Geothermal	-	5 GW	200 MW
9	Biomass	35 MW	500 MW	-
10	Improved Power	16 MW	-	-

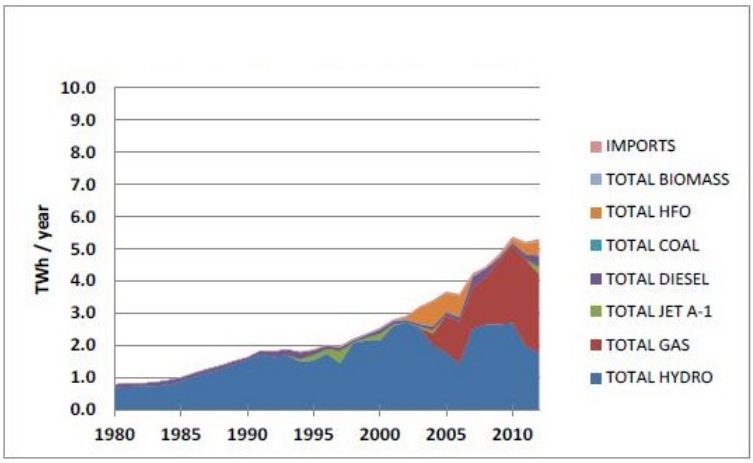

Figure 3.10: *Tanzania planned grid power network.*

Tanzania Power Sector Challenges

Since the electricity sector in Tanzania is heavily relies on hydropower energy, in the time of drought it cannot be assured. Hence, drought has some impacts on the power such as Loads curtailment, reserve capacity reduction, frequent black out and high generation cost. The next challenges in Tanzania could be undistributed generation; overloaded transformer in transmission and distribution grids cause high technical losses. Moreover, due to the high expense of national grid extension the electricity access and also electricity penetration is very low. In other words, unreliable energy supplies, distance from the utility grid, same entity for TSO and DSO and no public data availability for transmission and distribution grid (the only source are limited to “Map of the main lines”, “general information on the voltage profiles”) are some of the issues.

Therefore, in Tanzania a reformation for Electricity Supply Industry (ESI) starts to happen. The aim of this reformation is growing access and connection level, also providing a better environment in distribution and generation part for private investment. The flowchart in Fig. 3.11 shows these specific objectives of ESI primary reform. By ESI reform, TANESCO plans to increase the number of customers with reducing connection fee by 60% in urban area and 75% in the rural area.

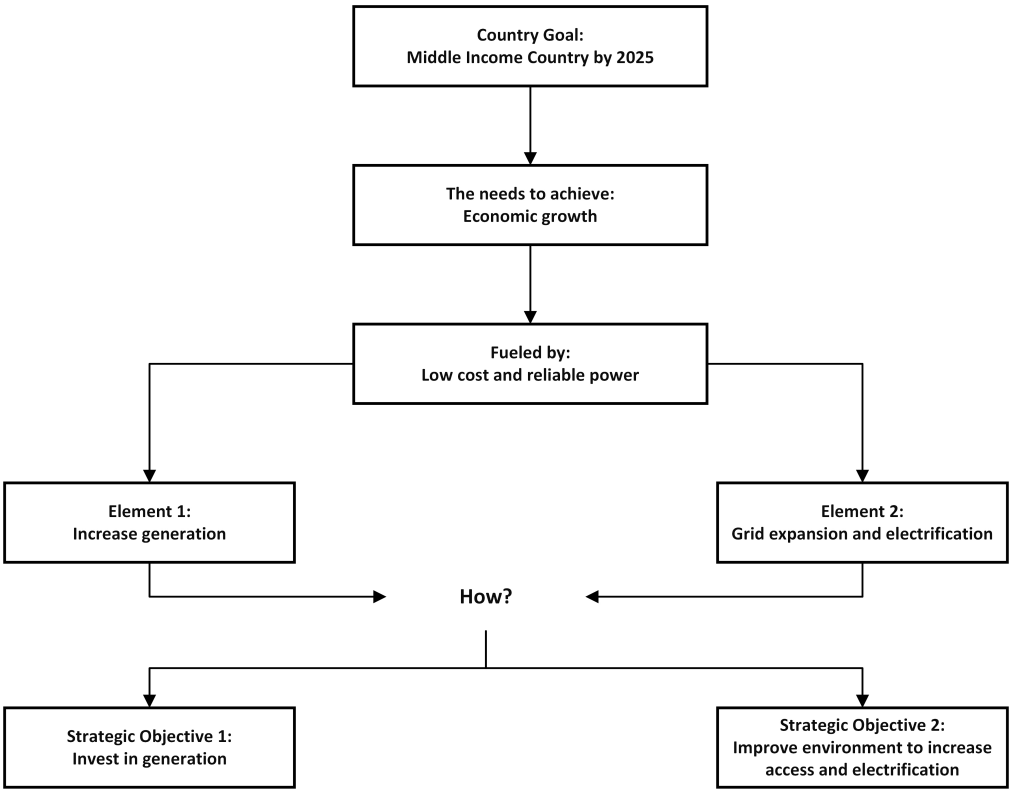

Figure 3.11: *Reform flowchart of ESI.*

3.4.2 Test Case Model

To test the methodology, the Tanzania transmission grid, with total 1081 MW real load and 327 Mvar reactive load, was adopted. This power system is made of 38 buses and 41 branches, while the available data consists of the diagram reported in Fig. 3.13, where nodal voltage magnitudes at each bus and the real and reactive power flows in each branch of the network are shown. The voltage magnitudes are known with an accuracy of ± 0.0005 p.u., while branch power flows are rounded to integer numbers; hence, the accuracy is of ± 0.5 MVA. The data and the network topology have been obtained from [224].

To simplify the network and reduce the number of variables, the radial branches representing a transformer and ending with a generator were represented as an equivalent generator with active and reactive power injections. Fig. 3.12 shows this simplification. In this way, the number of buses was reduced to 24 and the number of branches to 27. Moreover, the assumption proposed simplifies the needs to define a model for each transformer; this task could be complex due to the lack of information about these machines, e.g., no data are available about the winding connections, the nominal power, and on-load tap changer.

Table 3.3 illustrates the nominal voltage of each branch and its length obtained from geographical overview, as detailed in [225]. Then, a rough estimation of the required network parameters, i.e. series resistance (R_{Ge}), series reactance (X_{Ge}), line charging (B_{Ge}), is obtained considering standard and homogeneous per length parameters over the entire length of the lines according to Table 3.4. The obtained values are reported in Table 3.5 in p.u.

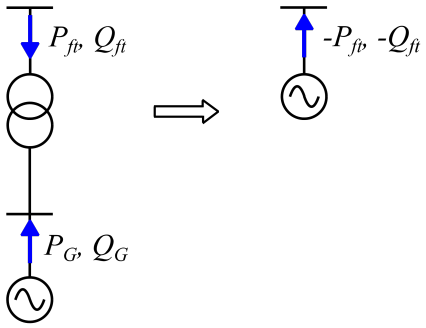

Figure 3.12: *Radial branches simplification in the studied network.*

Table 3.3: *Length and nominal voltage of branches*

Branch S/No.	From bus	To bus	V (kV)	L (km)	Type of Conductore
1	1	3	220	15	Bluejay
2	2	3	220	172	Bluejay
3	2	3	220	179	Bluejay
4	2	6	220	130	Bluejay
5	3	4	220/132	0.1	Bluesjay
6	4	5	132/33	0.1	Bluejay
7	6	7	220/33	0.1	Bluejay
8	6	8	220	180	Bluejay
9	6	9	220	160	Bison
10	8	9	220	95.23	Bluejay
11	9	13	400/220	10	Bluejay
12	9	14	220	107	Bison
13	9	10	220	130	Bison
14	10	11	220	73	Bison
15	11	12	220	180	Bison
16	13	15	400	175	Bison
17	14	16	220	130	Bison
18	15	16	400/220	10	Bison
19	15	17	400	245	Bison
20	16	18	220	210	Bison
21	17	18	400/220	10	Bison
22	18	19	220	150	Rail
23	18	21	220	200	Bison
24	19	20	220	162	Rail
25	21	22	220	100	Bison
26	21	23	220	129.5	Bison
27	21	24	220	140	Bison

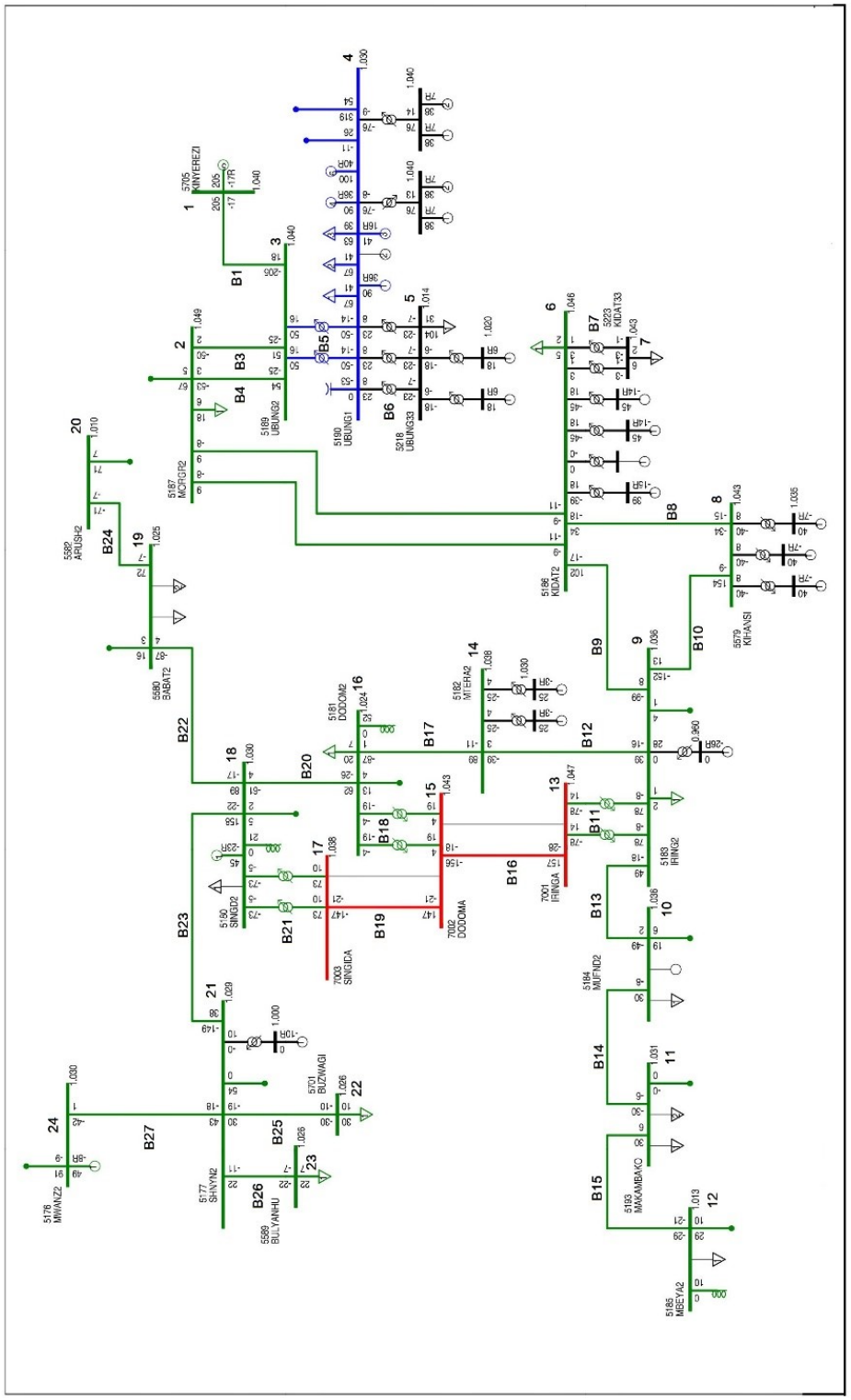

Figure 3.13: *Tanzania transmission network map.*

Table 3.4: *Tanzania transmission line parameters*

Parameter	400 kV	220 kV	Comments
Conductor	ACCC: Flint	ACSR: Drake	
Size (MCM/MM^2)	714/345.4	795/468.6	
No. of Conductor per Phase	4	2	
Current (A)	775	890	
R	0.001718	0.007360	Per unit on 100 MVA base for 100km line
X	0.017723	0.072730	
B	0.542608	0.022544	
Normal Rating (MVA)	1720	540	80% of current rating
Emergency Rating	2064	650	120% of normal rating

Table 3.5: *Adopted parameters from geographical overview*

Branch S/No.	From bus	To bus	$\mathbf{R}_{Ge}$ (pu.)	$\mathbf{X}_{Ge}$ (pu.)	$\mathbf{B}_{Ge}$ (pu.)
1	1	3	0.0011	0.0109	0.0034
2	2	3	0.0127	0.1251	0.0388
3	2	3	0.0132	0.1302	0.0404
4	2	6	0.0096	0.0945	0.0293
5	3	4	0	0.02	0
6	4	5	0	0.0333	0
7	6	7	0	0.0333	0
8	6	8	0.01325	0.1309	0
9	6	9	0.0118	0.1164	0.0361
10	8	9	0.007	0.0693	0.0215
11	9	13	0	0.0333	0
12	9	14	0.0079	0.0778	0.0241
13	9	10	0.009	0.0945	0.0293
14	10	11	0.0054	0.0531	0.0165
15	11	12	0.01325	0.1309	0.0406
16	13	15	0.003	0.031	0.9496
17	14	16	0.009	0.0945	0.0293
18	15	16	0	0.0333	0
19	15	17	0.0042	0.0434	0.3294
20	16	18	0.0155	0.1527	0.0473
21	17	18	0	0.0333	0
22	18	19	0.011	0.1091	0.0338
23	18	21	0.0147	0.1455	0.0451
24	19	20	0.0119	0.1178	0.0365
25	21	22	0.0074	0.0727	0.0225
26	21	23	0.0095	0.0942	0.0292
27	21	24	0.0103	0.1018	0.0316

3.5 Results and Discussion

The proposed optimization model in Section 3.3 has been implemented and solved in MATLAB. Therefore, the estimated parameters (R_{est}, X_{est},B_{est}) of this case study is presented in Table 3.6. In order to do a mathematical check based on public model of data reported in Table 3.4 and the obtained data by the proposed model, Fig. 3.14 illustrates the difference between the line parameters.

Table 3.6: *Adopted parameters from parameter estimation approach*

Branch S/No.	From bus	To bus	$\mathbf{R}_{est}$ (pu.)	$\mathbf{X}_{est}$ (pu.)	$\mathbf{B}_{est}$ (pu.)
1	1	3	0.0001	0.0016	0.001
2	2	3	0.0064	0.0909	0.225
3	2	3	0.0073	0.096	0.233
4	2	6	0.004	0.0793	0.3486
5	3	4	0	0.0345 0	0
6	4	5	0.0059	0.0547	0
7	6	7	0.009	0.1273	0.0006
8	6	8	0.0114	0.0489	0.307
9	6	9	0.0269	0.1336	0.2002
10	8	9	0.0103	0.0781	0.1208
11	9	13	0	0.0522	0.0002
12	9	14	0.0276	0.1352	0.1398
13	9	10	0.0084	0.0412	0.158
14	10	11	0.0173	0.0007	0.1308
15	11	12	0.0494	0.0281	0.1462
16	13	15	0.0034	0.0229	0.4686
17	14	16	0.02	0.053	0.1304
18	15	16	0.0417	0.0429	0.0056
19	15	17	0.0035	0.0267	0.4372
20	16	18	0.0362	0.1886	0.277
21	17	18	0.0006	0.0494	0
22	18	19	0.0165	0.0892	0.186
23	18	21	0.0386	0.1944	0.282
24	19	20	0.0211	0.1123	0.189
25	21	22	0.0169	0.0443	0.2784
26	21	23	0.0195	0.0608	0.173
27	21	24	0.0244	0.1198	0.1808

In addition, to evaluate the accuracy of the proposed approach, a PF computation was done for both estimated parameters (R_{est}, X_{est} and B_{est}) obtained by the proposed method and parameters obtained from geographical overview (R_{Ge}, X_{Ge} and B_{Ge}). Afterwards, a comparison between these two PF results and the input data was accomplished. Table 3.7 shows these results in terms of the real and reactive power flows in the branches of the network at the "from" and "to" buses, respectively, for the input data (superscript m), for the proposed method (superscript est) and for the geographical overview estimation (superscript ge) in MW and Mvar. In order to make the difference more clear, Fig. 3.15 and 3.16 in the following have stressed the difference between these values.

Table 3.7: *Power flow computation by two different methods*

From	to	P^{m}_{ft}	P^{est}_{ft}	P^{ge}_{ft}	P^{m}_{tf}	P^{est}_{tf}	P^{ge}_{tf}	Q^{m}_{ft}	Q^{est}_{ft}	Q^{ge}_{ft}	Q^{m}_{tf}	Q^{est}_{tf}	Q^{ge}_{tf}
		(MW)						**(Mvar)**					
1	3	205	202.97	190.35	-205	-202.93	-189.98	-17	-15.15	26.16	18	15.64	-22.80
2	3	-53	-52.59	-45.64	54	52.76	45.89	3	1.65	1.37	-25	-23.72	-3.06
2	3	-50	-49.70	-43.85	51	49.88	44.09	2	0.74	1.14	-25	-23.81	-3.10
2	6	18	17.29	4.49	-18	-17.28	-4.47	-16	-13.39	-13.51	-22	-24.48	10.50
3	4	100	100.29	100.00	-100	-100.29	-100	32	31.89	28.96	-28	-28.36	-26.94
4	5	69	68.29	68.00	-69	-68.00	-68	24	23.89	50.18	-21	-21.19	-47.93
6	7	6	6.00	6.00	-6	-6.00	-6	2	1.98	2.01	-2	-2.00	-2.00
6	8	34	33.87	18.50	-34	-33.74	-18.46	-18	-7.30	4.70	-15	-25.28	-4.26
6	9	102	101.40	103.97	-99	-98.84	-102.80	-17	-19.25	-0.41	8	10.33	8.08
8	9	154	153.74	138.46	-152	-151.45	-137.20	-9	-12.25	-10.34	13	23.64	20.49
9	13	156	156.35	154.30	-156	-156.35	-154.30	-16	-16.64	-72.75	28	28.64	81.79
9	14	39	39.12	31.22	-39	-38.71	-31.14	-16	-15.97	-6.76	3	2.96	4.90
9	10	49	48.83	48.48	-49	-48.63	-48.23	-18	-17.97	23.26	2	1.96	-23.71
10	11	30	29.63	29.23	-30	-29.49	-29.17	-8	-19.96	17.72	-6	-6.01	-18.75
11	12	30	29.49	29.17	-29	-29.00	-29	6	6.01	18.75	-21	-21.00	-21
13	15	157	156.35	154.30	-156	-155.59	-153.64	-28	-28.64	-81.79	-18	-17.47	-18.74
14	16	89	88.71	81.14	-87	-87.25	-80.59	-11	-11.38	-9.62	1	1.39	12.28
15	16	8	8.56	15.86	-8	-7.95	-15.86	38	38.50	78.47	-38	-38.48	-76.58
15	17	147	147.03	137.79	-147	-146.34	-137.08	-21	-21.03	-59.73	-21	-21.05	-82.38
16	18	62	62.20	63.44	-61	-60.82	-62.87	-26	-25.92	1.30	4	3.88	-0.68
17	18	146	146.34	137.09	-146	-146.21	-137.08	20	21.05	82.38	-10	-11.03	-74.72
18	19	89	89.29	88.47	-87	-88.05	-87.62	-17	-16.89	17.46	4	4.00	-12.53
18	21	158	157.74	151.47	-149	-148.67	-148.29	-22	-22.01	-1.09	38	37.80	27.78
19	20	72	72.05	71.62	-71	-71.00	-71	-7	-7.00	9.53	-7	-7.00	-7
21	22	30	30.15	30.07	-30	-30.00	-30	-19	-19.00	8.32	-10	-10.00	-10
21	23	22	22.09	22.05	-22	-22.00	-22	-11	-10.98	4.39	-7	-7.00	-7
21	24	43	42.43	42.18	-42	-42.00	-42	-18	-17.97	-6.08	1	0.93	4.46

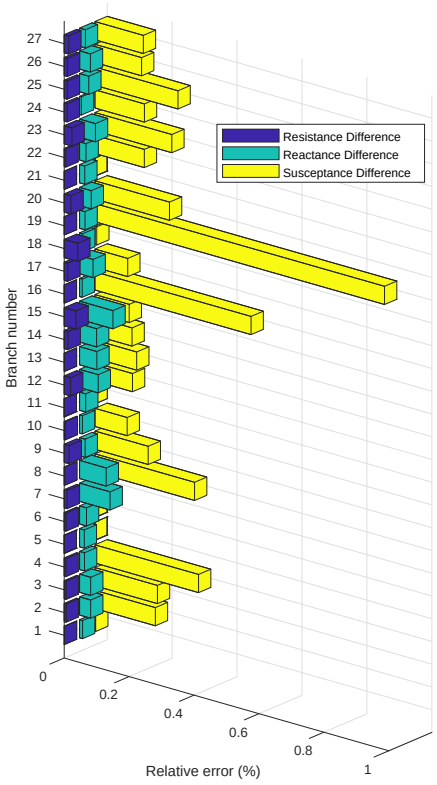

Figure 3.14: *Parameters relative error (%) between geographical and PE approach.*

From these Tables and Figures, it is obvious that the proposed method gives very good results when compared with both the input data and with the geographical-based model. The largest difference for the real power between the proposed method and the input data is 2.07 MW which is related to slack bus. However, for the geographical based estimation this difference is 15.54 MW. In addition, for reactive power the numbers show the benefit of the proposed method. As an example, the numbers for Branch 16-18 with proposed method and geographical estimation are -25.92 and 1.30 Mvar respectively, whereas the input reactive power for this branch is -26 Mvar. This huge difference is due to the big susceptance and reactance difference which could affect reactive power flow. Actually, defining the reactance value needs more geographical details such as the type of cable in terms of underground or overhead form.

Therefore, Fig. 3.17 shows the percentage of generated error by each model in the format of box plot with median, upper and lower bound, where Fig. 3.17 (a), 3.17 (b), 3.17 (c) and 3.17 (d) demonstrate real power (direction from bus- to bus), real power (direction to bus- from bus), reactive power (direction from bus- to bus), reactive power (direction to bus- from bus) respectively. As it can be seen from this figure, the median error of the proposed method is close to zero and the upper bound is around 3%. For the geographical overview approach the median for the real power is near 2% and for reactive power are 10% and 20%, respectively.

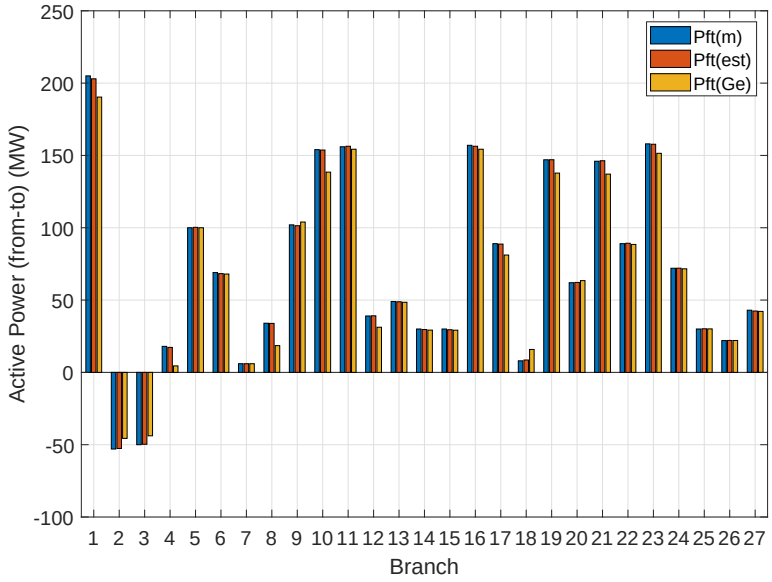

(a) Active Power (from-to), MW.

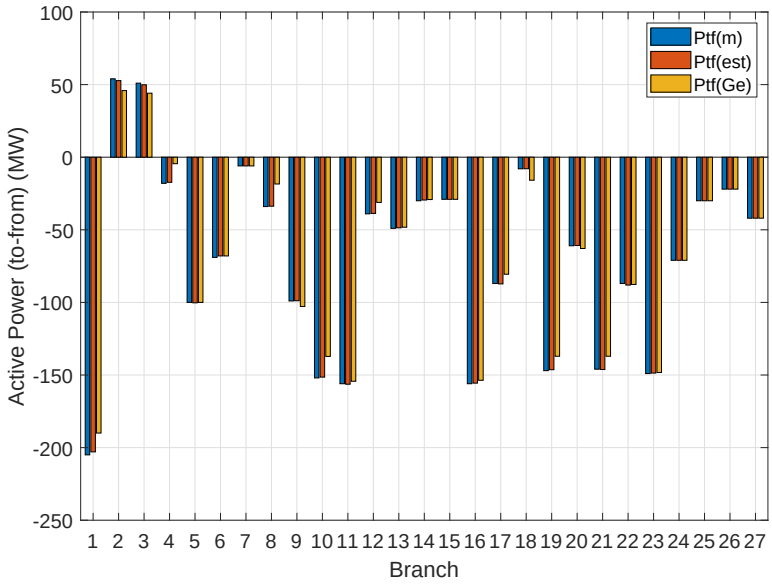

(b) Active Power (to-from), MW.

Figure 3.15: *Active power flow for different approaches.*

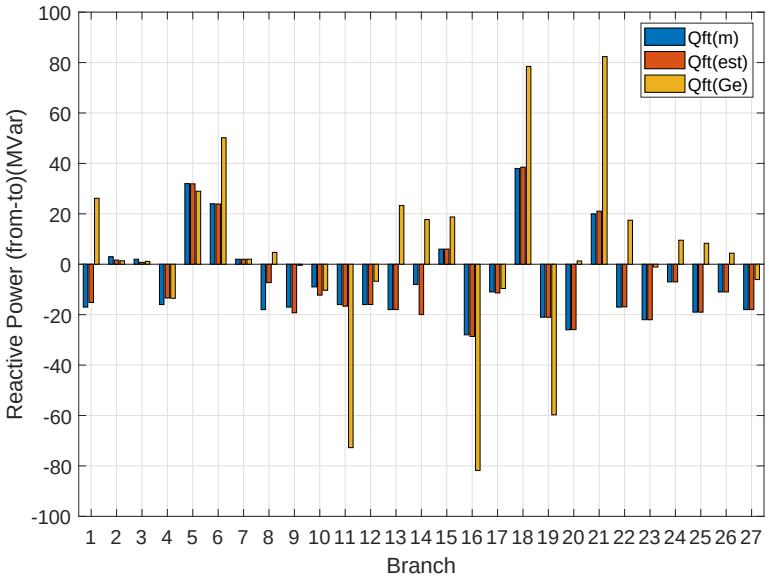

(a) Rective Power (from-to), Mvar.

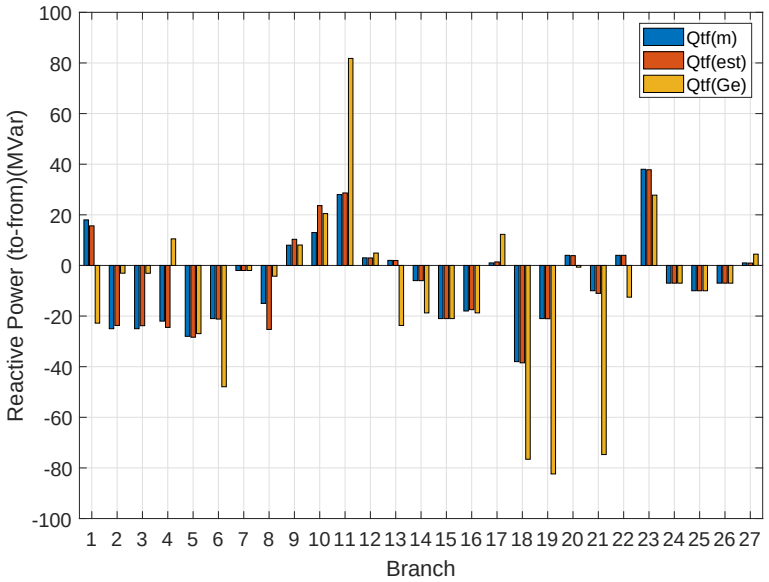

(b) Rective Power (to-from), Mvar.

Figure 3.16: *Reactive power flow for different approaches.*

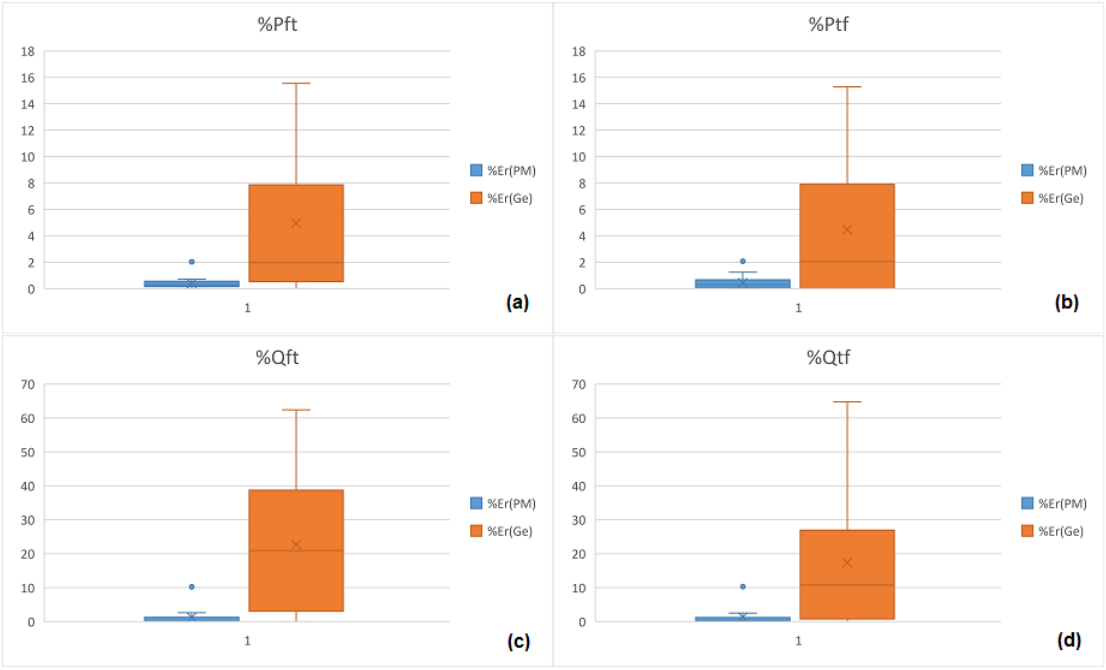

Figure 3.17: *Percentage Error comparison between proposed method and geographical approach.*

Table 3.8: *Voltage and voltage angle by two different methods*

Bus Index	V^m **(V)**	V^{est} **(V)**	δ^{est} **(Rad)**	V^{ge} **(V)**	δ^{ge} **(Radian)**
1	1.040	1.040	0	1.040	0
2	1.049	1.048	-0.048	1.032	-0.072
3	1.040	1.040	-0.003	1.035	-0.019
4	1.030	1.030	-0.035	1.030	-0.037
5	1.014	1.014	-0.070	1.014	-0.058
6	1.046	1.043	-0.060	1.043	-0.078
7	1.043	1.040	-0.067	1.042	-0.080
8	1.043	1.035	-0.074	1.035	-0.099
9	1.036	1.036	-0.188	1.036	-0.186
10	1.036	1.036	-0.207	1.010	-0.219
11	1.031	1.031	-0.208	0.999	-0.230
12	1.013	1.013	-0.209	0.968	-0.254
13	1.047	1.047	-0.263	1.061	-0.235
14	1.038	1.038	-0.239	1.038	-0.208
15	1.043	1.043	-0.296	1.065	-0.276
16	1.024	1.024	-0.284	1.041	-0.274
17	1.038	1.039	-0.332	1.055	-0.320
18	1.030	1.030	-0.400	1.030	-0.348
19	1.025	1.025	-0.476	1.004	-0.409
20	1.010	1.010	-0.554	0.986	-0.460
21	1.029	1.029	-0.696	1.029	-0.500
22	1.026	1.026	-0.709	1.020	-0.509
23	1.026	1.026	-0.709	1.021	-0.508
24	1.030	1.030	-0.746	1.030	-0.525

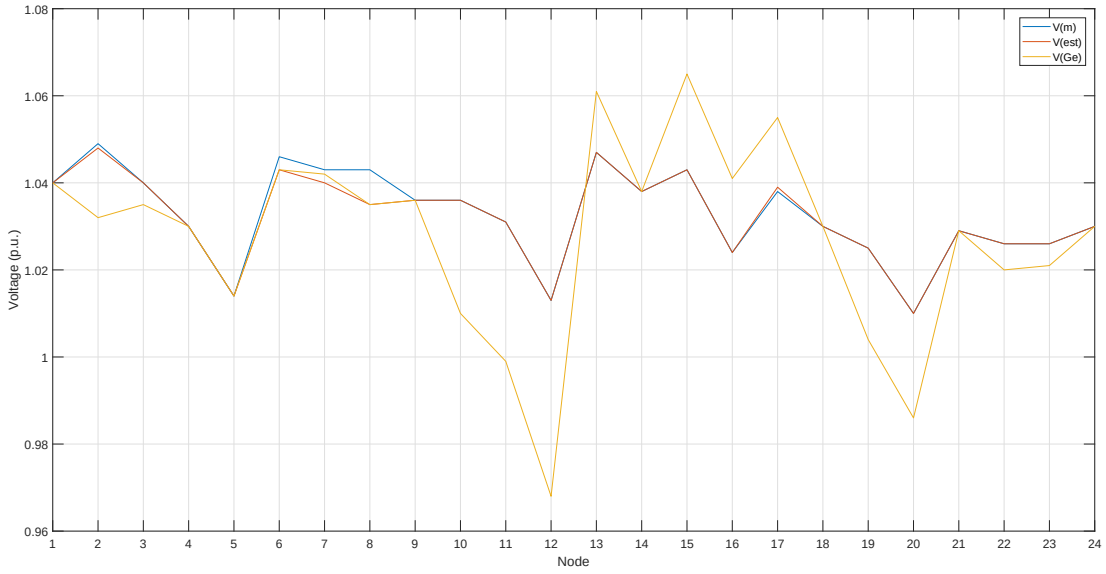

Figure 3.18: *Network voltage profile for different approaches.*

Moreover, Table 3.8 represents voltage in each bus for the input data, the proposed method and for the geographical overview estimation in V. Again, the calculated voltage in both methods shows the advantage of the proposed method; bus number 11 is one of the example, Fig 3.18 shows these values.

From Fig. 3.18 it can be found that there is a voltage drop at node 5, 12, 16 and 20, where according to Fig. 3.19 which presents the power of the generators already in-place, and 3.20 which shows the load profile of this grid, there is more amount of load compare to the injected power by generators. However, this voltage drop is still between the voltage boundaries. On the other hand, the high injection of the generator in the node 4 prevents the big voltage drop due to the big load in this node. In order to have a more clear idea regarding the performance of the grid, the loading percentage of each branch has been indicated in Fig. 3.21. According to this Figure, branch number of 1, 9, 10 and 23 are loaded more than 40% of the maximum amount, where there is generator connection in the nodes of these branches, which is still under the acceptable amount. However, if generator injection increasing and decreasing could affect the whole electrical grid. Hence, generator connection as one of the very important factor on the electrical grid has been studied in Chapter 4 of this thesis.

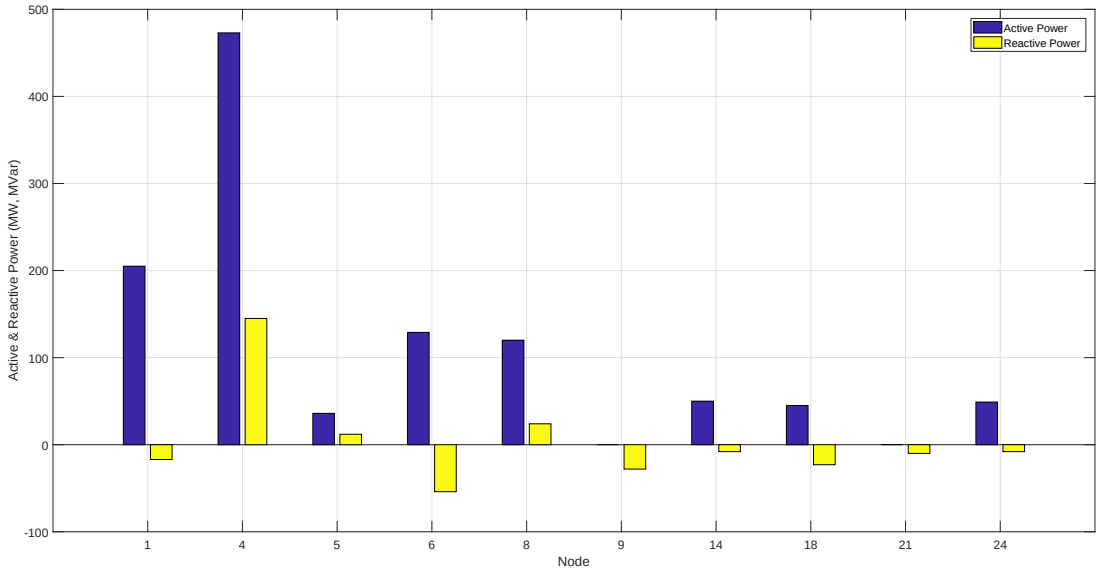

Figure 3.19: *Studied transmission network generator power profile.*

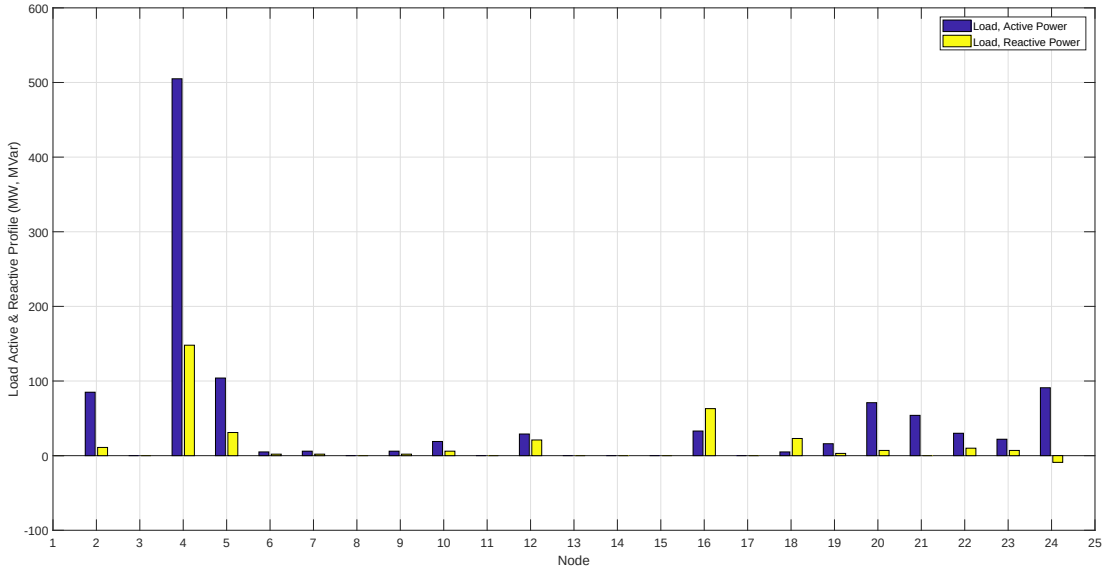

Figure 3.20: *Studied transmission network load profile.*

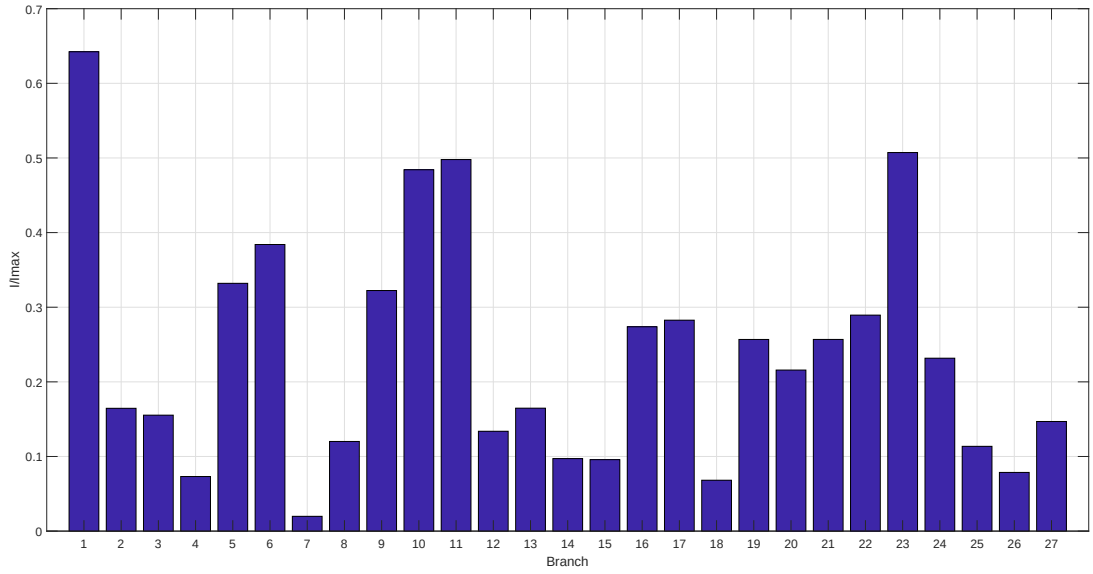

Figure 3.21: *Studied transmission network current flow percentage.*

3.6 Summary

One of the important practical problems to carry out a study on a transmission and distribution grid in some countries (especially emerging countries) is lack of available data. This motivates the need of a reverse engineering procedure (Parameter Estimation) to estimate branch parameters starting from typical available data, i.e., approximated values of bus voltages, active and reactive power flows of each branch. The parameter estimation model that can be applied to large systems makes it possible to derive estimations for the series resistance, the series reactance and the line charging of each branch. Once system parameters are known, further studies (such as hosting capacity, detailed in the next chapter) on the system can be carried out adopting typical planning and operation procedures. The procedure was tested on the Tanzanian network and the results compared with the result obtained from a rough geographical feature of the grid including line lengths. This comparison shows the proposed method in this study is, as expected, more reliable and accurate, especially for reactive power estimations.

CHAPTER 4

Hosting Capacity Application

4.1 Introduction

Nowadays, distribution networks are being subjected to an increasing of active users in both low and medium voltage grid, i.e. installing small size generation, mainly based on renewable energy sources (Distributed Generation). Distribution grids are designed for providing electricity to the customers and could take some advantages from the RES production: sustainability, less maintenance and low carbon emission. However, upward trends of installing dispersed generators makes some issues for distributed system operators, such injected power to the grid is leading to several operational problems which is affecting the distribution grids power quality and reliability [41], [42], in particular power quality challenges such as harmonics, voltage regulation and interface protection problem could arise [226], [43].

Despite the fact that DG itself has some merits, the impact of DG on the operation of electrical grid motivates a strong research activity based on statistical, deterministic and heuristic approaches [226], [48], [49]. The goal of some research studies is defining the optimal DG location and sizing [87]; though, grid regulation typically, e.g. in Italy, does not allow DSOs to refuse any request of DG connection in any location [50]. Therefore, DG optimization studies have a scarce applicability in real-life. In this regard, the estimation of the maximum amount of dispersed generation that can be connected to the distribution grid without violating its operating criteria is one of the main performance indicator which should have been considered for planning and operation of the grid. As detailed in Chapter 2, this capacity of the electrical network is called Hosting Capacity.

The interest in numerical methods for the HC evaluation is based on the fact that power system

performance is affected by every change in the generation and the load pattern. Hence, the HC is defined as the amount of acceptable DG without endangering the grid power quality and reliability with respect to some limits, i.e. steady-state voltage limits, transformer and lines thermal limits, fast voltage variation [41], [79], [94], [55]. The proposed approaches in the literature are mainly based on iterative calculations, aiming at estimating the maximum DG penetration admitted in every bus according to the considered technical limits; the HC is evaluated for a single constraint at each time and the overall HC is defined as the minimum HC over all the constraints. Hereinafter, this index will be referred as " Nodal HC (NHC)". Although NHC gives us a right view of the power injection admitted in each node of the grid, it does not assess the impact of installed DG units in different nodes of the network on its operational parameters, as usually occurs in real life scenarios [227]. Thus, evaluating "Multi Generator HC (MGHC)" is inevitable in distribution grids. This is an up-to-date approach and very few works could be found in literature in such a direction. Moreover, in order to manage the hosting capacity evaluation in the best way, electric networks infrastructure and the relevant regulatory and market frameworks need to be properly investigated and update, thus electric vehicle integration hosting capacity will be considered.

Therefore, DER integration, electric vehicle integration and voltage control have been studied in this thesis as the three most important HC application according to the literature. In this chapter, the HC evaluation of DER for nodal, multi-generator and e-mobility have been discussed respectively in this chapter, while the voltage control have been explained in Chapter 5.

The novelty of this chapter of thesis is summarized in the ability to find a model which is easy to manage and applies to the generality of network structures which is used in order to perform a Load Flow (LF) to define HC with respect to three operation constraint: steady-state voltage limits, rapid voltage changes and thermal limits of transformer and line.

4.2 Nodal Hosting Capacity

Typically, as it was explained before, the proposed approaches in the literature (in Section 2.3.3) are based on increasing DG penetration step by step for each single bus, until the limits are violated. In this method only one constraint in each time is considered and HC assumed to be the amount of injection in worst case scenario, such an index will be named nodal HC (NHC). In Italy the Energy Authority commissioned a study to evaluate the NHC in LV [228] and MV grid [105]. The study has been based on an extended sample of the Italian distribution grid (the database was detailed in about 5% of the Italian MV distribution grid, and 1% of the LV one); details, both on the model adopted and on the results, are provided in [75] for the LV grid and in [80], [82] for the MV grid.

4.2.1 Proposed Bricks Approach

Hosting capacity of each node could be formulated as an objective function of maximizing the nodal active power of dispersed generator in a specific bus.

$$HC = Max(Nodal\ Loading\ Parameters) \tag{4.1}$$

In order to perform the HC analysis, a complete model of the distribution grid is required. Actually, HC is impacted by the topology of the grid, by the grid parameters and also by the power profiles of the loads and generators, resulting in a quite heavy data set to be properly managed. Practically speaking,

only DSOs could have all the data required and in some cases, e.g. in emerging countries scenarios, besides in some cases DSOs could be unable to gather all the required information. Consequently, in this thesis a novel approach is proposed for the distribution grid modeling, named Bricks approach.

Actually, the standard structure of distribution grid is shown in Fig. 4.12, this structure is including the main feeder and connected branches to the main line which is typically named collaterals. The standard model has been developed in order to represent the grid network for evaluating HC in a shorter time and practical way, without affecting results accuracy.

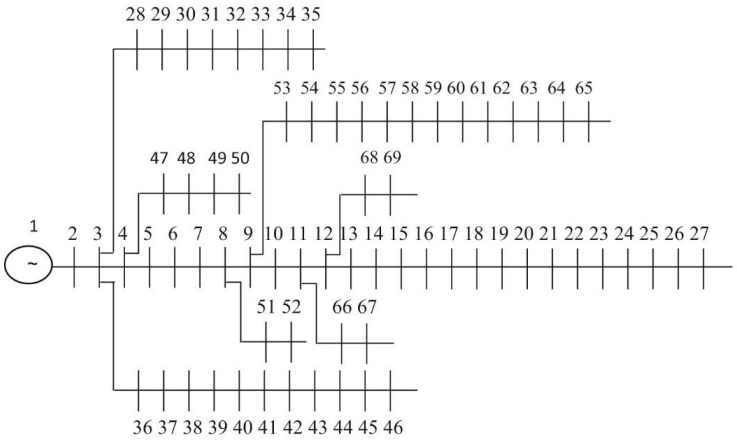

Figure 4.1: *Standard structure of 67-bus distribution grid.*

The new method is based on the assumption that HC in one feeder is marginally affected by the other feeders. Moreover, in order to limit the computational effort of the study, the grid is modeled in a simplified way, i.e. it is modeled as an aggregation of "bricks", each one representing a portion of the grid which can be added, removing and replacing easily to evaluate all the possibility of the grid structure in shorter time. In addition, only critical nodes of the grid are being assessed by the Bricks approach. In following the Bricks approach components is discussing in details.

Feeders: In the bricks approach, all the feeders are categorized into three groups; Short Feeder ($F1$), Medium Feeder ($F2$) and Long Feeder ($F3$). Main feeders are the backbones of the distribution networks, in rural area the main feeders are too long with overhead conductors and small sections which have the inverse relationship with the distance from the HV/MV transformer; the cable section at the end of the feeder is smaller than the beginning [75]. In order to implement the proposed method, feeders are categorized according to their characteristic. The feeders characteristic mean value in each category is considered as the main characteristic of the Bricks approach feeders.

Collaterals: Besides, collaterals are such as body capillary for distribution networks, and they are connected to the main feeders. Since industrialized countries and developing ones have different distribution grid (i.e. topology, equipment, etc.), the length of the collateral is longer and its cable section is smaller in rural area, developing and emerging countries rather than the developed one. In the proposed method, collaterals are also divided into two groups; Short Collateral ($C1$) and Long Collateral ($C2$). In this method, short feeders are allowed to have only short collateral.

Nodes: Basically, hosting capacity is higher at the beginning of the feeder; then, it decreases moving far from the primary substation toward the end of the line. Hence, hosting capacity changing trend along all feeders in case of no DG connection could be considered approximately the same along feeders having similar electric parameters. In addition, HC in collaterals is in lower amount compare to the connected nodes of the feeders and collaterals. Thus, it is necessary to consider all significant nodes in the Bricks approach. Therefore, three critical nodes in each feeder, which are representing the whole feeder, and two significant nodes in each collateral based on their impedance (Z) being considered to calculate the load flow which is a trade-off assumption in order to limit the computational effort. The first node of feeder is located in the 10% of total amount of feeder impedance ($N1$) which is the representer of the nodes near primary substation, the second one is defined at the middle ($N2$) which is representing nodes at the middle of the feeder and the last one is at the 90% of total amount of feeder Z ($N3$) which is evaluating on behalf of all nodes near the end of the feeder. For collaterals, the first one is at its middle ($N4$) and the second one is at the end ($N5$). Fig. 4.2 shows a long feeder with three long collaterals and its 9 nodes for implementing the power flow calculation.

Loads: According to Italian DSO practice, in primary substations each transformer can be loaded up to 65% of its rated power to ensure an adequate degree of redundancy [229]. In the Bricks approach, such a limit has been assumed as the peak load the grid is asked to feed. In particular, the loads are divided into three groups, the yearly minimum value ($L1$), the mean value ($L2$) and the pick value ($L3$) with lowest reactive charges in Italy, power factor of 0.9.

Generators: In the bricks approach, a generator is added to each defined-node of each combination of the feeder and the collaterals, in case of Fig. 4.2, there is nine nodes for DG connection. The injected power to the grid by generator will change in the simulation to define HC. Fig. 4.3 shows the Bricks approach flowchart and Table 4.1 are showing all the possible combination for performing flowchart.

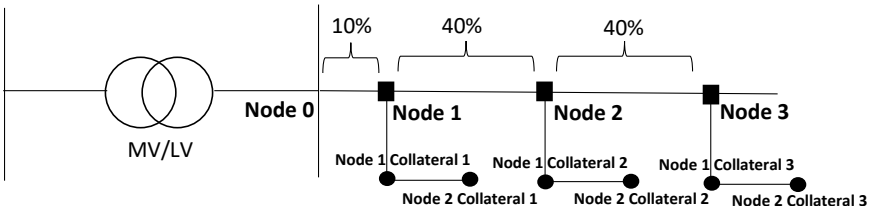

Figure 4.2: *Long feeder with 3 long collaterals and relevant nodes.*

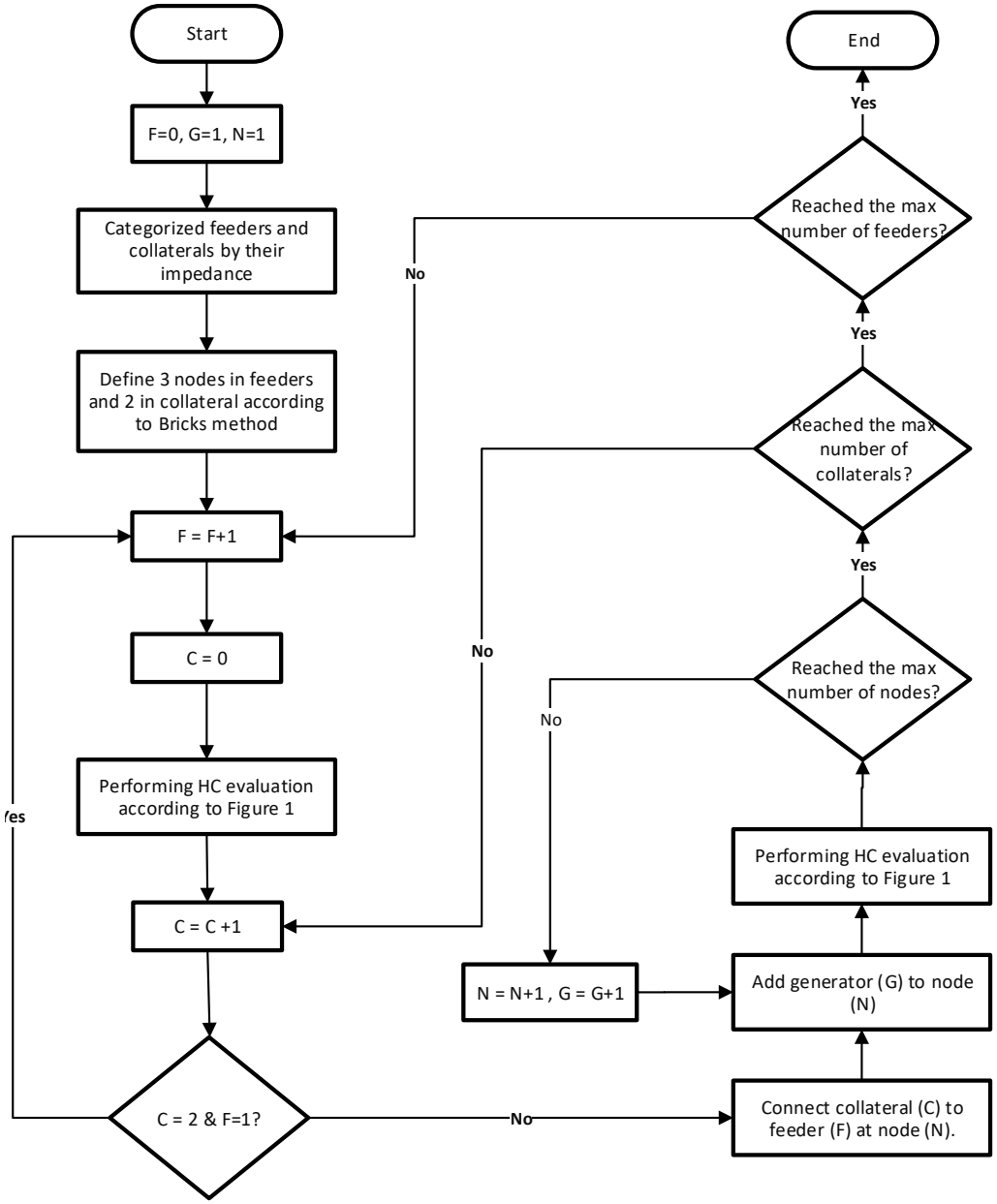

Figure 4.3: *Bricks approach flowchart.*

Table 4.1: *Possible combination for power flow calculation*

Feeder	Collaterals			Load (L1,L2,L3)									DG (G1,...,G9)	No. of Combination
	N1	N2	N3	N1	N2	N3	N4	N5	N6	N7	N8	N9	No. of Positions	
F1	-	-	-	3	3	3	0	0	0	0	0	0	3	81
	C1	-	-	3	3	3	3	0	0	0	0	0	4	324
	-	C1	-	3	3	3	0	0	3	0	0	0	4	324
	C1	C1	-	3	3	3	3	0	3	0	0	0	5	1215
	-	-	C1	3	3	3	0	0	0	0	3	0	4	324
	C1	-	C1	3	3	3	3	0	0	0	3	0	5	1215
	-	C1	C1	3	3	3	0	0	3	0	3	0	5	1215
	C1	C1	C1	3	3	3	3	0	3	0	3	0	6	4374
F2	-	-	-	3	3	3	0	0	0	0	0	0	3	81
	C1	-	-	3	3	3	3	0	0	0	0	0	4	324
	C2	-	-	3	3	3	3	3	0	0	0	0	5	1215
	-	C1	-	3	3	3	0	0	3	0	0	0	4	324
	C1	C1	-	3	3	3	3	0	3	0	0	0	5	1215
	C2	C1	-	3	3	3	3	3	3	0	0	0	6	4374
	-	C2	-	3	3	3	0	0	3	03	0	0	5	1215
	C1	C2	-	3	3	3	3	0	3	3	0	0	6	4374
	C2	C2	-	3	3	3	3	3	3	3	0	0	7	15309
	-	-	C1	3	3	3	0	0	0	0	3	0	4	324
	C1	-	C1	3	3	3	3	0	0	0	3	0	5	1215
	C1	-	C2	3	3	3	3	0	0	0	3	3	6	4374
	C2	-	C2	3	3	3	3	3	0	0	3	3	7	15309
	-	C1	C2	3	3	3	0	0	3	0	3	3	6	4373
	C1	C1	C2	3	3	3	3	0	3	0	3	3	7	15309
	C2	C1	C2	3	3	3	3	3	3	0	3	3	8	52488
	-	C2	C2	3	3	3	0	0	3	3	3	3	7	15309
	C1	C2	C2	3	3	3	3	0	3	3	3	3	8	52488
	C2	C2	C2	3	3	3	3	3	3	3	3	3	9	59049
F3	The same as F2.													

Figure 4.3 and Table 4.1 show the bricks method implementation for a general case. First, short feeder ($F1$) without any connected collateral and low value of load ($L1$) in all nodes is considered, the DG for the first scenario is in the first node of the feeder, the second combination is with the same structure but different position of DG to the second node. This trend continues until considering all the three possibility of the loads in each node with this structure. In Table 1, the maximum amount of 3 in the column related to load means all the possibility of loads ($L1$, $L2$, $L3$) and in the column of DG the maximum amount of 9 means all the possibility of connecting DG to all nodes ($G1$, $G2$, $G3$, $G4$, $G5$, $G6$, $G7$, $G8$, $G9$).

The next structure is the short feeder ($F1$) with a short collateral ($C1$) in the first node ($N1$). All the possible scenarios in the previous structure are repeating, the only difference is the number of nodes which here are four nodes (three nodes for main feeder and one node for collateral.)

The last structure which has been mentioned in the last row of the Table 4.1 is a long feeder ($F3$) with a long collateral ($C2$) at node 1,2 and 3 ($N1$, $N2$, $N3$) of the feeder and the DG ($G5$) is located in the node 9 ($N5$) the second node of the last collateral. This structure is the same as structure of Figure 4.2 with three long collateral at three defined nodes. By this procedure, the combination number of 506410 are represented which can estimate HC promisingly.

Load Flow Calculation: To make sure that the transferred power through the grid is reliable and secure, Power flow analysis should be employed. A load flow is a mathematical tool that defines the operation conditions of an electrical network by considering the network structure and characteristics of connected users. Then, the results for every possible scenario such as the voltage of each node, the current flow on each line and the system power loss should be evaluated. The classical power flow model has been explained in the following.

The main unknowns of the load flow problem are the voltages (V) and the phases δ of the voltages in each node of the network. Once these quantities are known, it is possible to derive the secondary variables, that is the values of the currents, active powers and reactive powers. Typically, at least two variables are constant for each node; in particular in the classical LF theory three types of nodes are distinguished:

- Load Nodes (PQ): For this topology of nodes the active power P and reactive power Q are known, while nodes voltage V and phase δ are unknown.

- Generator Nodes (PV): In this case the input power P and nodes voltage is constant. Hence, the unknowns are the voltage phase and the reactive power supplied or absorbed by the network.

- Slack (Reference) Node ($V\delta$): There could be only one or even few (in bigger network) slack bus across the network. The voltage and its phase angle are known and kept constant, while the unknowns are the active power and reactive. Actually, this node shows and guarantees the network energy balance.

Once the main variables of the network have been defined by LF, the active and reactive powers for all nodes in the network can be calculated knowing the characteristics of the network. The following equations show the active and reactive load flow equations at each node, where the terms Y_{PQ} are the elements of the network admittance matrix.

$$P_P(V_Q, \delta_Q) = V_P. \sum_{Q=1}^{n} [Y_{PQ}. V_Q. cos(\delta_P - \delta_Q - \Theta_{PQ})] \tag{4.2}$$

$$Q_P(V_Q, \delta_Q) = V_P. \sum_{Q=1}^{n} [Y_{PQ}. V_Q. sin(\delta_P - \delta_Q - \Theta_{PQ})] \tag{4.3}$$

In mathematics the Newton-Raphson method is also called the tangent method as the first derivative of a function is used to search for a solution of a problem.This method is also used to solve the load flow problem, but given its multidimensionality in this case it is necessary to use the Jacobian matrix, that is the matrix of all first derivatives.

Since this is an iterative method, it plans to recalculate the values of the main unknowns at each iteration. Assuming that there is an initial voltage profile, the active and reactive powers exchanged in the nodes can be calculated by equations 4.2 and 4.3. As the real powers are known in the PQ and PV nodes, it is possible to calculate the difference between the actual value and the calculated one which this difference is called "residual". By Knowing the residuals and the network Jacobian matrix, the primary variables variation could be defined in equation 4.4.

$$\begin{bmatrix} \Delta V_{PQ} \\ \Delta \delta_{PQ} \\ \Delta \delta_{PV} \end{bmatrix} = [J]^{-1}. \begin{bmatrix} \Delta P_{PQ} \\ \Delta Q_{PQ} \\ \Delta P_{PV} \end{bmatrix} \tag{4.4}$$

where: ΔP_{PQ} is the active power residual in the PQ nodes, ΔQ_{PQ} reactive power residual in the PQ nodes and ΔP_{PV} is the active power residual in the PV nodes. In addition, the Jacobian matrix is reported in equation 4.5.

$$J = \begin{bmatrix} \frac{\partial P_{PQ}}{\partial V_{PQ}} & \frac{\partial P_{PQ}}{\partial \delta_{PQ}} & \frac{\partial P_{PQ}}{\partial \delta_{PV}} \\ \frac{\partial Q_{PQ}}{\partial V_{PQ}} & \frac{\partial Q_{PQ}}{\partial \delta_{PQ}} & \frac{\partial Q_{PQ}}{\partial \delta_{PV}} \\ \frac{\partial P_{PV}}{\partial V_{PQ}} & \frac{\partial P_{PV}}{\partial \delta_{PQ}} & \frac{\partial P_{PV}}{\partial \delta_{PV}} \end{bmatrix} \tag{4.5}$$

Once the increasing amount of the initial values have been defined,the new values could be calculated according to equation 4.6.

$$\begin{bmatrix} V_{PQ,i} \\ \delta_{PQ,i} \\ \delta_{PV,i} \end{bmatrix} = \begin{bmatrix} V_{PQ,i-1} \\ \delta_{PQ,i-1} \\ \delta_{PV,i-1} \end{bmatrix} + \begin{bmatrix} \Delta V_{PQ} \\ \Delta \delta_{PQ} \\ \Delta \delta_{PV} \end{bmatrix} \tag{4.6}$$

At this point, equation 4.2 and 4.3 should be recalculate according to the update values and continues until the residues become small enough.

However, mainly in MV distribution networks, the performed LF model has several differences compared to the classical theory by two significant changes. Distributed power plants enter a constant P power at constant $cos\phi$, which is why the model also appears as PQ nodes and there are no PV nodes. Furthermore given the presence of the transformer with variable ratio, the voltage is constant both at the HV busbar, and at the MV busbar where the set-point voltage is set.

Hence, a new node category called PVQ is used, to which the representative bars of the MV busbars belong. In these nodes the detachment of the active power P and reactive power Q are known and the

voltage is considered constant. The mathematical model still remains the same except the missing of the free variable, therefore it is necessary to define an additional nodal variable. The HV/MV transformer ratio (k) is considered as a free variable (for all the other nodes k is equal to one). The ratio k and the phase of the voltage δ constitute the pair of unknowns of the PVQ node. Then, the updated equations considering the transformation ratio are expressed in equation 4.7 and 4.8.

$$P_P(V_Q, \delta_Q) = k_P.V_P.\sum_{Q=1}^{n}[Y_{PQ}.\,V_Q.\,cos(\delta_P - \delta_Q - \Theta_{PQ})] \tag{4.7}$$

$$Q_P(V_Q, \delta_Q) = k_P.V_P.\sum_{Q=1}^{n}[Y_{PQ}.\,V_Q.\,sin(\delta_P - \delta_Q - \Theta_{PQ})] \tag{4.8}$$

In order to perform load flow, three main variables and three main constraints have been considered as the input and limiting factors respectively. The first input is the structure of the network, as in this research network reconfiguration has not been analyzed, the branch matrix remains constant for all the load flows. The second variable of the input is the load profile matrix, this matrix shows the power required in each node for each simulation time step. Finally, the third variable is the DG profiles for each simulation time step. From DG profiles the active power supplied by the generators and reactive power which is implicitly obtained from the active one in all the nodes could be obtained. In the following three-used constraints have been explained.

Steady-State Voltage Variation: Adding a DG to the MV feeder causes voltage increase at the hosting bus and generally the hosting feeder. Hence, in order to avoid malfunctions of grid connected equipment, the slow voltage variations according to the EU regulation must remain within $\pm 10\%$ of the rated voltage and must be satisfied during 95% of the time [230].

$$V_{min,k} \leq V_{DG,k} \leq V_{max,k} \tag{4.9}$$

Transformer and Lines Thermal Limits: Since adding DG increase the cause of inverse power flow in MV branches, the thermal limits of each line should be considered. Each branch of the network from bus k to j has an impedance (Z_{kj}) including resistance (R_{kj}) and reactance (X_{kj}). Thus, this limit depends on the characteristics of each component.

$$I_{DG,kj} \leq I_{max,kj} \tag{4.10}$$

Rapid Voltage Change: RVC depends on the short-circuit power in common coupling point [231]. Generally, RVC is evaluated as the difference between when DG is connected and is injecting power to the grid and after its sudden disconnection. There is no restrict constraint for RVC in [230]; only an approximate range of 4% to 6% of rated voltage in MV networks is defined.

$$|V_{DG,k} - V_k| \leq 4\% \div 6\% \tag{4.11}$$

As it was discussed before, in order to evaluate the nodal HC an iterative procedure has been developed, iteratively increasing the DG power injection to the grid from the specific bus until the defined

constraints are violated. The procedure has been continued until all the buses in the network have been analyzed. In order to limit the computational effort of the procedure, a bisection method by root-finding behavior has been adopted up to a resolution of 1 kW. Unlike common load flow calculation which is started the calculation from minimum amount and increase it step by step, in this method calculation is started by the maximum amount. The minimum possible injected power to the grid is considered as 0 and maximum possible injected power to the grid is considered as upper bound and in the first step as HC. If one of the technical constraints is violated by this HC, considered amount should be divided into two and the procedure will be repeated. However, if the considered HC is not violating the constraints, it will increase by half of the difference of previous HC and the considered one. This iteration will continue until the convergence of method. The bisection method is defined by an inverse loop from the high amount to 1kW. Fig. 4.4 shows the flow chart of the aforementioned procedure in Bricks approach.

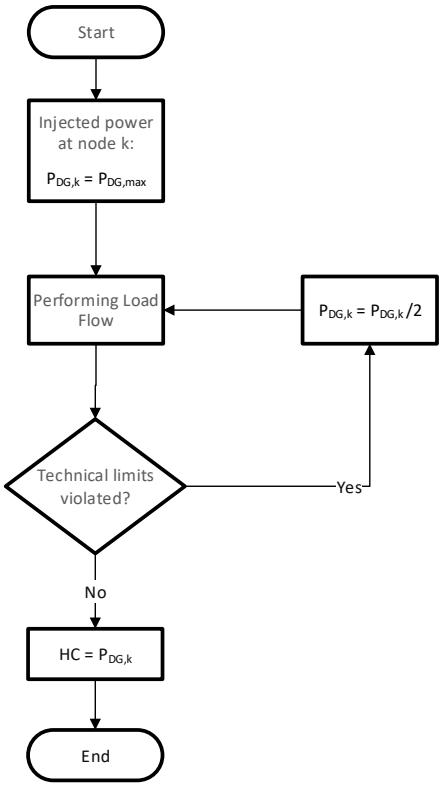

Figure 4.4: *Applied bisection method in HC evaluation.*

4.2.2 Validation of the Proposed Approach

In this section the case study, to whom the proposed hosting capacity procedure in this thesis work has been applied, is introduced. As it was described in the Section 4.2, the procedure is structured to be applied to the MV distribution network connected to the HV/MV transformer as a primary substation. The proposed method has been applied to the regional territory of Valle d'Aosta in north west of Italy.

"Ponte Pietra" is the name of the PS which supplies the electricity grid of Aosta city. This PS has the most energy demand throughout the year among other primary substations on that area. As the

concentration of the users in the urban area is higher, it therefore entails a consistent and reasonably regular overall energy demand. The Ponte Pietra PS has a typical daily domestic load profile, as shown in Fig. 4.5, with a peak demand in the late morning and a second peak in the evening. Moreover in terms of the seasonal trend, in Aosta city the summer transit is less than in winter.

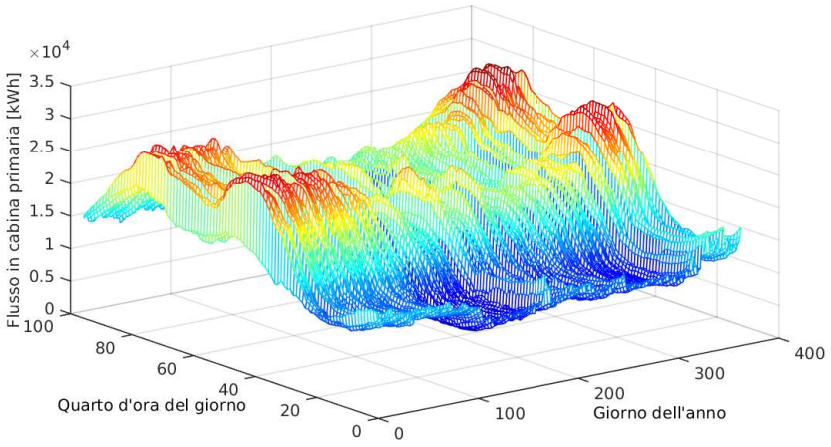

Figure 4.5: *Ponte Pietra primary substation load profile.*

In the Ponte Pietra PS there are two HV/MV transformers, indicated as "Red" transformer and "Green" transformer, each one with a nominal power of 25 MVA. Fig. 4.6 (a) and Fig. 4.6 (b) report the net transits of each transformer. As it can be seen from the pictures, there is not any reverse power flow in any transformer. Moreover, in this figure when one of the transformers shows a drop in sampling, in the other one an increase appears to ensure the supply of the MV distribution network. The profile in Fig. 4.6 (c) represents the sum of the transits in two transformers.

The MV distribution network of Aosta city has about 140 km length and supplies 486 nodes and distributed over 16 feeders. Nodes can represent MV users or secondary substation for LV users. In Fig. 4.7 the distribution network of Aosta where each feeder is represented by a different color is pictured. In this representation the city of Aosta some lines go several kilometers away from city to feed some neighboring centers.

Every node in the network could be numbered to identify easily, and in particular there are three significant nodes in this network:

- Node 1 : HV busbar of PS.
- Node 2 : MV busbar of PS (Red transformer).
- Node 3 : MV busbar of PS (Green transformer).

The technical details of the two active transformers in Ponte Pietra PS are reported in Table 4.2. As it was described before from this PS, 16 lines by the nominal voltage of 15 kV has departed which 9 of them are normally powered by the red transformer, and the remaining are supplied by the green one.

Feeders are almost underground cable, as it is a typical of a city network, but there are also some lines which made by aerial conductors. The PS diagram is also shown in Fig. 4.8. The HV busbar is represented by the central node in the diagram, the MV busbar of the red transformer is represented by

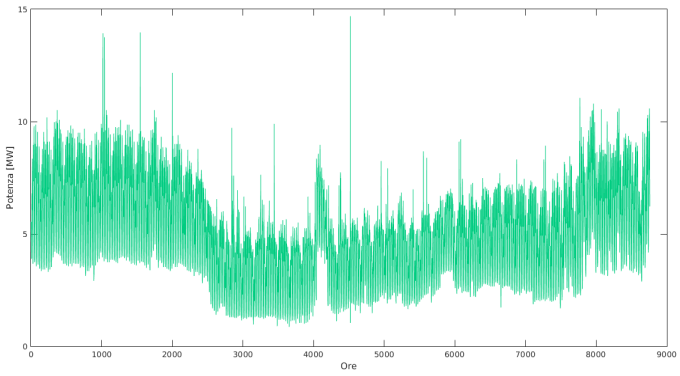

(a) Green transformer power transient.

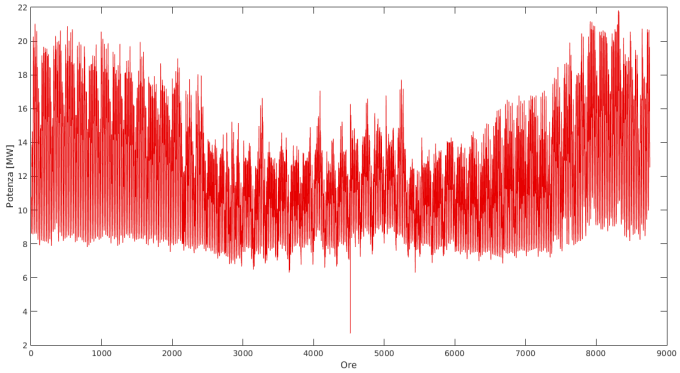

(b) Red transformer power transient.

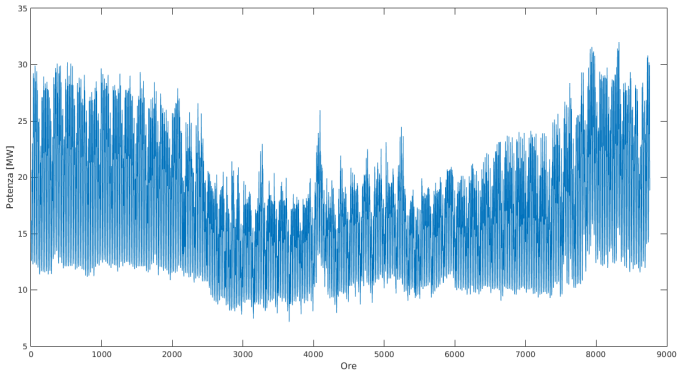

(c) Total power transient.

Figure 4.6: *Total power managed in Ponte Pietra PS, 2013.*

the red node from which lines 2 to 9 have supplied, while the MV busbar of the green transformer is represented by the green node from which the lines 10 to 16 have departed.

According to standard EN 50160 [230], voltage magnitudes are assumed to be acceptable when between 90% and 110% of the nominal value. In addition, thermal limits in this test case are considered according to Table 4.3, as the feeder ampacity (considering an overloading admitted for conductors of

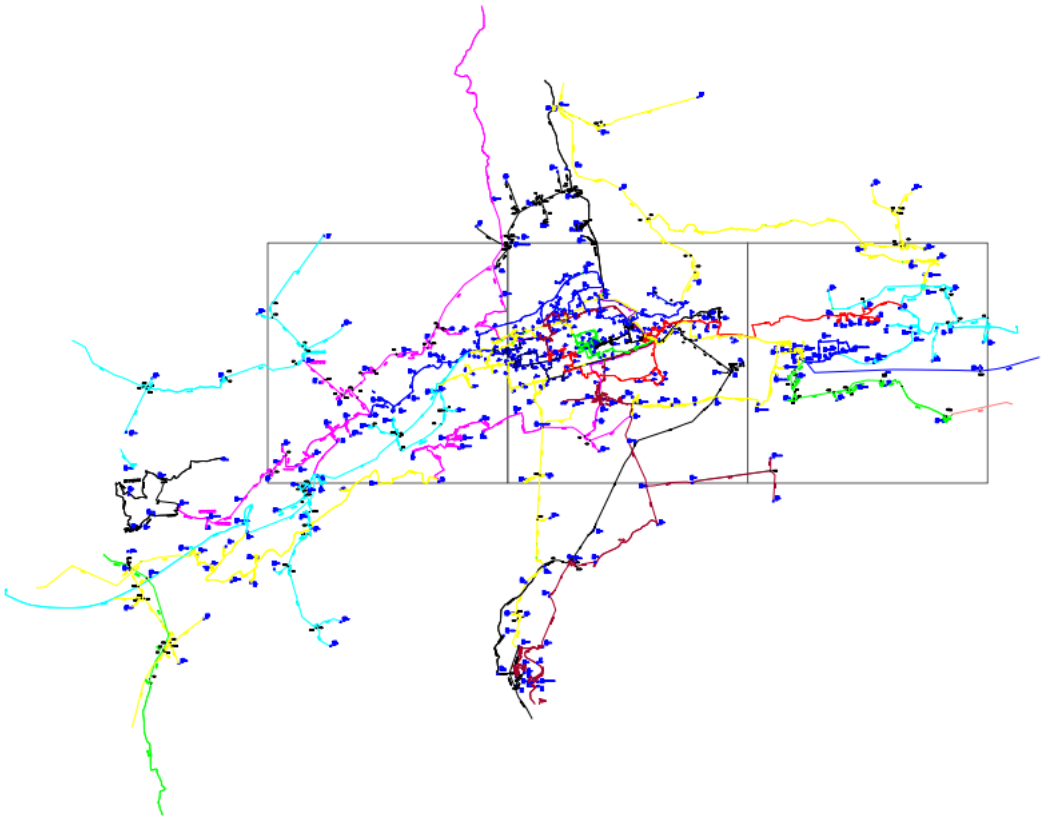

Figure 4.7: *Aosta MV distribution network.*

Table 4.2: *Ponte Pietra transformers characteristic.*

Characteristics	Remarks
Nominal Power	ONAN: 25000 kVA ONAF: 31250 kVA
Nominal Voltage	HV Side: 132 kV $\pm$ 12 1.5% MV Side: 15.6 kV
Nominal Current	HV Side: 109.3 A MV Side: 925 A
Losses	P_{fe} with nominal voltage: 14.33 kW P_{cu} with under load variation in 0 position: 115.7 kW
Short-Circuit Parameters	V_{cc}: 13.85%

20% w.r.t. the nominal value) commonly assumes this amount in Italy [232]. In spite we tested the proposed method on a distribution network supplying a urban area, the Bricks approach has been designed so that it could effectively manage all network grids where data are difficult to collect or reprocess (e.g. emerging countries).

In the following Fig. 4.9 shows the radial structure of the network, while Table 4.4 represents the number of nodes in each feeder and the total number of collateral in it. Moreover, the line characteristic is also shown in this table. Each branch is modeled by a π-equivalent circuit model which has the series impudence of $Z = R + jX$ and line charging of B explained in Section 3.3.3

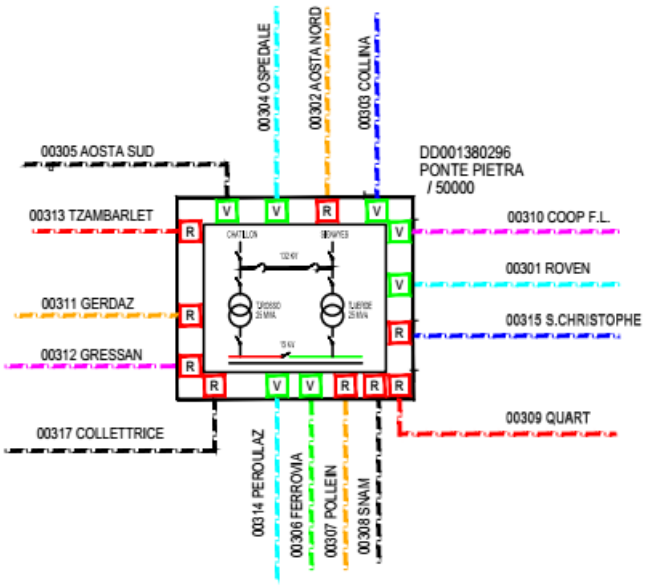

Figure 4.8: *Aosta MV distribution network from Ponte Pietra.*

Table 4.3: *Thermal limits for different cable size*

Cable Section (mm^2)	Thermal Limit (A)	Cable Section (mm^2)	Thermal Limit (A)
16	119	95	345
25	155	120	398
35	188	150	450
50	225	185	517
70	280	240	613

Table 4.4: *Aosta branch representation.*

Feeder	No. of Nodes (including Coll.)	No. of Collateral	Nodes of Collateral	R (pu.)	X (pu.)	B (pu.)(10^{-3})
1	42	3	15	0.0157	0.0084	0.0311
2	47	4	24	0.0368	0.0297	0.0411
3	18	1	3	0.0523	0.0415	0.0912
4	28	2	6	0.0236	0.0136	0.0497
5	28	0	0	0.0274	0.0178	0.0708
6	54	7	21	0.0568	0.0513	0.0220
7	28	1	1	0.0255	0.0163	0.0631
8	6	1	1	0.0224	0.0188	0.0867
9	37	4	13	0.0265	0.0110	0.0348
10	48	4	13	0.0466	0.0357	0.0417
11	24	3	5	0.0212	0.0116	0.0407
12	12	2	3	0.0377	0.0202	0.0540
13	2	0	0	0.0681	0.0390	0.1420
14	60	5	22	0.0269	0.0139	0.0477
15	26	1	2	0.0229	0.0113	0.0374
16	23	1	3	0.0106	0.0060	0.0220

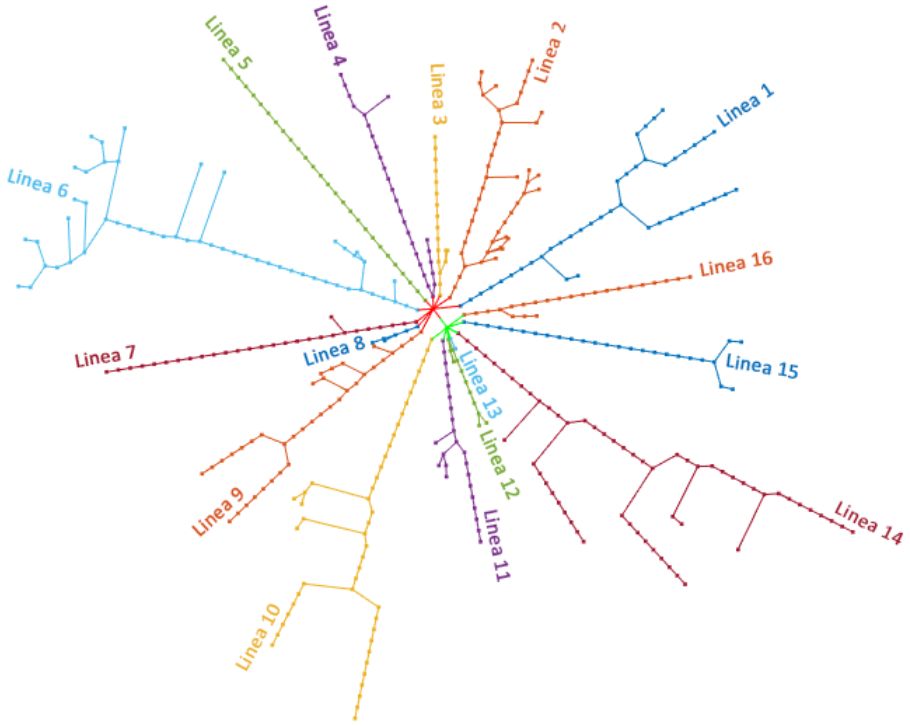

Figure 4.9: *Radial schematic of Aosta MV distribution network from Ponte Pietra.*

Five generators, three cogeneration plants, one hydroelectric plant and one photovoltaic one, are connected directly to the MV distribution network. These generators together could supply a power of approximately 4.6 MW. The active users suppling by Ponte Pietra PS are 264. However, the already-in-place generators for the proposed approach in this chapter have not been considered and the network at the initial point has been considered as the passive one; actually simulations are devoted to clarify the proposed approach. Moreover, in this network loads are modeled as PQ buses with power factor of 0.9 leading, Fig. 4.10 shows the load profile of all nodes of Aosta city for each hour in one year. In each time a DG is installed to each node of the passive network and two cases are simulated: a) DG has a PF equal to 1, b) DG has a PF equal to 0.9. Different PF is considered to make an evaluation if the reactive power control is useful here or not.

4.2.3 Results and Discussion

In order to validate the Bricks approach, a comparison between the proposed approach and the HC evaluation based on the complete model of the Aosta city grid (full grid, without categorizing the feeders) is performed. This section shows in detail the obtained results for the proposed three categories of the feeders and a feeder with collaterals. Briefly, by considering the impedance of each feeder, its length, and the number of the nodes, feeders number 8, 11, 12, 13, 16 are included in the short feeders category, feeders 1, 2, 3, 4, 5, 7, 9 and 15 in the medium feeders category and feeders 6, 10 and 14 in the long feeders category. In order to implement the proposed method, the mean values of the electrical parameters of feeders in each category are considered as electrical parameters of the relevant feeder in

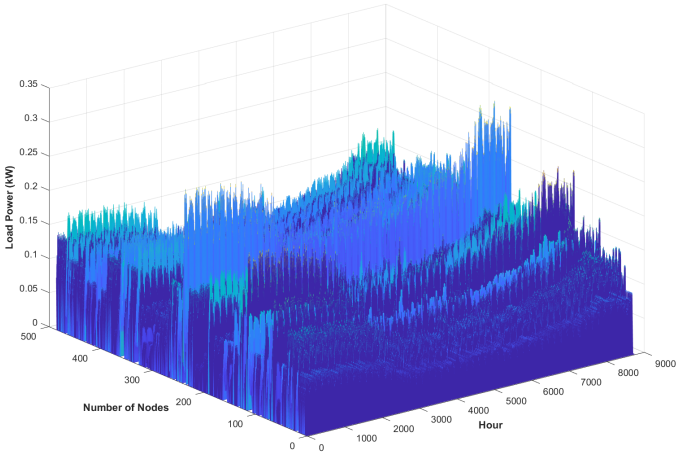

Figure 4.10: *Yearly load profile (kW) in each node.*

the Bricks approach. In the following the results of each category have been explained by details.

Short Feeder

As it was explained in the last paragraph, considering the impedance of each feeder, its length, and the number of the nodes, feeders number 8, 11, 12, 13, 16 are including short feeders categories. In order to implement the proposed method, the feeders characteristic mean value in each category is considered as the main characteristic of the Bricks approach feeders; Table 4.5 details the branch parameter of short feeder in Bricks approach. Table 4.6 represents the HC for short feeder without any collateral with PF equal to 1 and PF equal to 0.9, considering all three constraints. First each constraint is considered separately, then at the end the worst-case scenario is defined as the maximum power injection to the grid.

Table 4.5: *Branch parameters (p.u.) in Bricks approach for the short feeder.*

Bus/from	Bus/to	R	X
0	1	0.0232	0.0134
1	2	0.0939	0.0545
2	3	0.0939	0.0545

Table 4.6: *Hosting capacity evaluation results for short feeder (MW).*

Method		First Node			Second Node			Third Node		
		Min	Mean	Max	Min	Mean	Max	Min	Mean	Max
PF 1	Bricks	10.585	10.828	11.108	10.630	10.793	10.981	10.673	10.756	10.851
	Complete Grid	10.705	11.066	11.624	10.632	10.766	10.974	10.611	10.654	10.720
PF 0.9	Bricks	9.535	9.780	10.063	9.537	9.701	9.890	9.537	9.620	9.7155
	Complete Grid	9.659	10.025	10.593	9.5375	9.672	9.880	9.493	9.536	9.603

In the short feeders the main constraint which defines the HC is thermal limit, whereas the voltage limits including steady-state voltage variation and RVC have not played any role for defining the HC, Fig. 4.11 (a) and 4.11 (b) demonstrate the HC defined by each constrains separately for both PF1 and PF0.9 respectively. As it is obvious, the HC for PF1 is bigger than HC for PF0.9, Fig. 4.11 (c). The reason of this difference is based on the constraint defining the HC which in this structure is thermal limit.

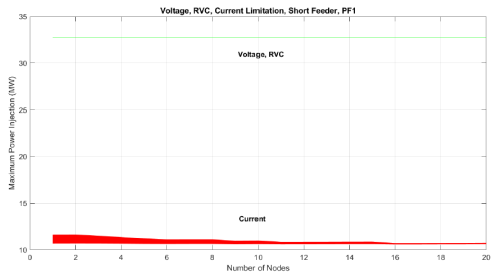

(a) Comparison between defined HC by each constraint for short feeder, PF1.

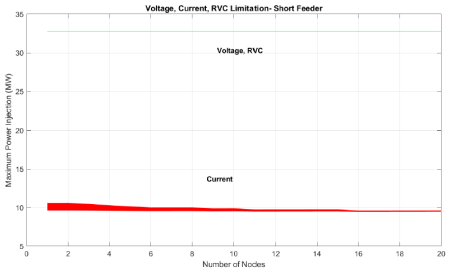

(b) Comparison between defined HC by each constraint for short feeder, PF0.9.

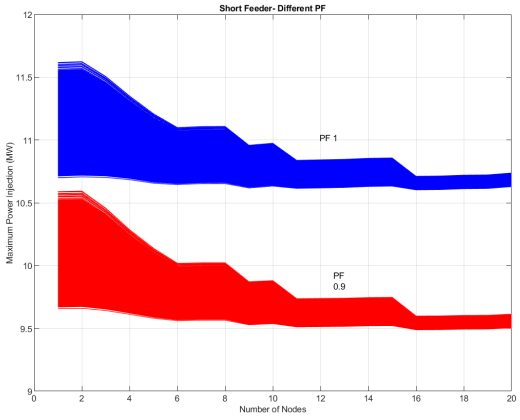

(c) Different PF comparison for short feeder.

Figure 4.11: *Different PF influence on HC of the short feeder.*

Table 4.7 shows the bricks approach error in comparison with complete grid method, as it can be seen by going further from transformer the error is slightly increasing. Moreover, Fig. 4.12 (a) and 4.12 (b) demonstrate the HC for both PF in short feeder. The highlight benefits of Bricks approach are less-required information and very short computation time. The computation time in this case-study for Bricks approach was 5 minutes and 37 seconds, whereas for complete grid approach it was 92 hours and 43 minutes and 86 seconds.

Table 4.7: *Comparison between Bricks approach and complete grid for short feeder.*

Bricks Approach		Error			Probability	
		Min Value	Mean Value	Max Value	Underestimate	Overestimate
PF 1	First Node	0.0112	0.0215	0.0444	0.1658	0
	Second Node	1.8810e-04	0.0025	6.3784e-04	0.0608	0.0413
	Third Node	0.0058	0.0096	0.0122	0.0251	0.3862
PF 0.9	First Node	0.0128	0.0244	0.0500	0.1719	0
	Second Node	0	0.0030	0.0010	0.0583	0.0432
	Third Node	0.0046	0.0088	0.0117	0.0429	0.5899

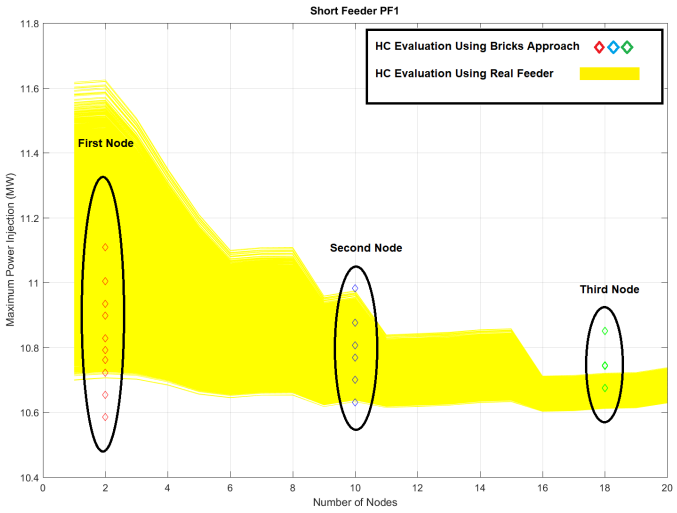

(a) Hosting capacity evaluation for short feeder with PF1.

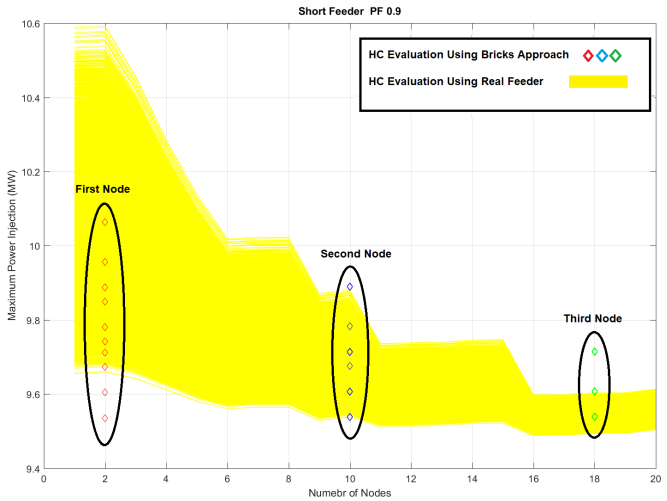

(b) Hosting capacity evaluation for short feeder with PF0.9.

Figure 4.12: *Hosting capacity evaluation for short feeder with different PF.*

Medium Feeder

Considering the impedance of each feeder, its length, and the number of nodes, feeders number 1, 2, 3, 4, 5, 7, 9 and 15 are including medium feeders category and Table 4.8 details the medium feeder category branch parameter in Bricks approach. Table 4.9 represents the maximum possible injection to the grid by DG for medium feeder without any collateral with PF equal to 1 and 0.9 in three defined nodes.

Table 4.8: *Branch parameters (p.u.) in Bricks approach for medium feeder.*

Bus/from	Bus/to	R	X
0	1	0.0621	0.0367
1	2	0.2514	0.1486
2	3	0.2514	0.1486

Table 4.9: *Hosting capacity evaluation result for medium feeder (MW).*

Method		First Node			Second Node			Third Node		
		Min	Mean	Max	Min	Mean	Max	Min	Mean	Max
PF 1	Bricks	10.783	11.253	11.790	11.030	11.347	11.711	9.792	9.843	9.886
	Complete Grid	10.799	11.136	11.655	10.890	11.009	11.655	9.973	10.014	10.041
PF 0.9	Bricks	9.716	10.191	10.739	9.827	10.144	10.509	9.887	10.050	10.237
	Complete Grid	9.705	10.044	10.570	9.692	9.810	9.994	9.808	9.838	9.884

As it can be seen by numbers, the HC for medium feeder category with PF1 is greater than PF0.9 until the end of the feeder, at the end of the feeder, when the PF is equal to 1, the dominant constraint is converted to RVC and the HC is dropped sharply, Fig. 4.13 (a) and (b) shows these trends. From Fig. 4.13 (c) could be seen that the HC for PF0.9 has steady behavior.

Moreover, Table 4.10 highlighted the error of the Bricks approach in comparison with complete grid approach. Fig. 4.14 demonstrates the HC for both PF in Medium feeder.

Table 4.10: *Comparison between Bricks approach and complete grid for medium feeder.*

Method		Error			Probability	
		Min Value	Mean Value	Max Value	Underestimate	Overestimate
PF 1	First Node	0.0015	0.0105	0.0116	0.0315	0.0495
	Second Node	0.0129	0.0307	0.0463	0.0116	0.0631
	Third Node	0.0181	0.0172	0.0154	0.2086	0
PF 0.9	First Node	0.0011	0.0146	0.0160	0.0249	0.0627
	Second Node	0.0139	0.0340	0.0515	0.0126	0.7707
	Third Node	0.0081	0.0216	0.0357	0.0447	0.8782

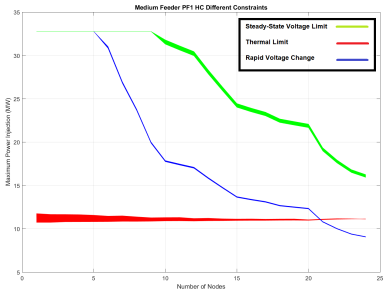

(a) Comparison between defined HC by each constraint for medium feeder, PF1.

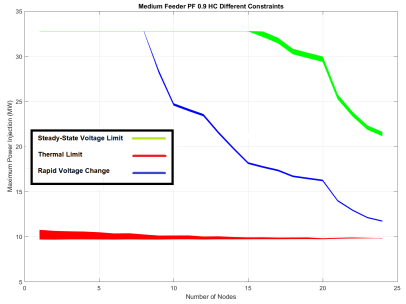

(b) Comparison between defined HC by each constraint for medium feeder, PF0.9.

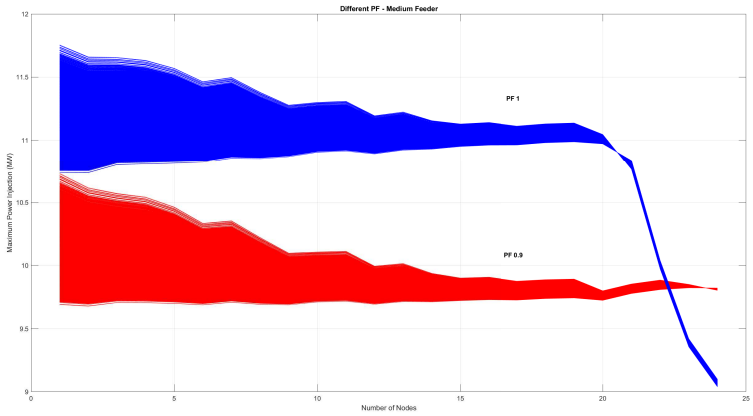

(c) Different PF comparison for medium feeder.

Figure 4.13: *Different PF influence on HC of medium feeder.*

Long Feeder

Considering the impedance of each feeder, its length, and the number of the nodes, feeders number 6, 10 and 14 are including long feeders category and Table 4.11 described the long feeder category branch parameter in Bricks approach. In Table 4.12, the maximum power injection by DG to the grid in long feeders considering three-main technical constraints with two different power factor are shown.

Table 4.11: *Branch parameters (p.u.) in Bricks approach for long feeder.*

Bus/from	Bus/to	R	X
0	1	0.1314	0.1099
1	2	0.5318	0.4449
2	3	0.5318	0.4449

It can be seen that in long feeders the HC with PF1 is bigger than PF0.9 until the middle of the feeder, whereas from the middle of the feeder the HC with reactive power generated by DG has bigger amount compare to the situation when the reactive power is equal to zero, Fig. 4.15 (c). The main reason it can be found from Figure 4.15 (a), as the three main constraints for calculating the HC is plotted. The dominant constraint in long feeder with unity power factor at the beginning is thermal, however from middle of the

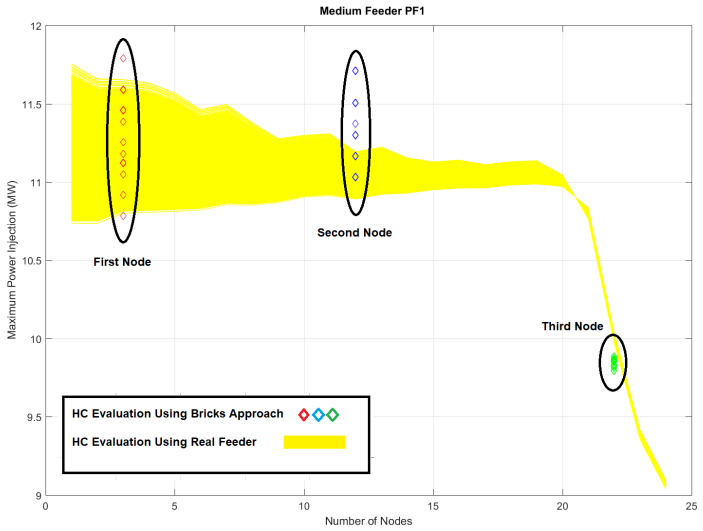

(a) Hosting capacity evaluation for medium feeder with PF1.

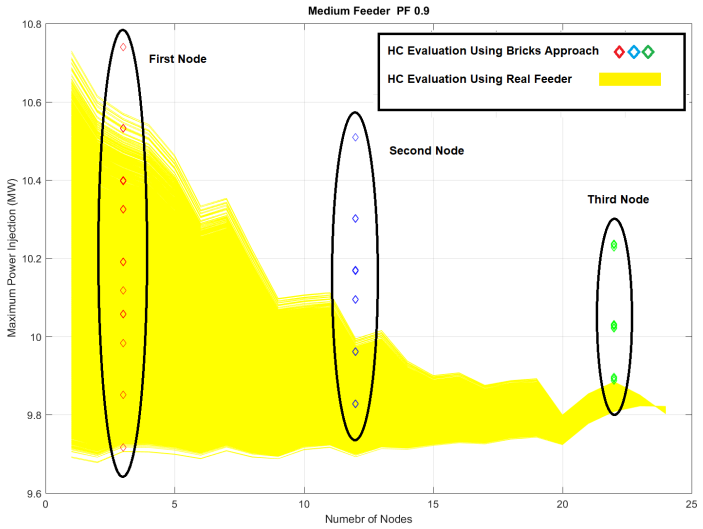

(b) Hosting capacity evaluation for medium feeder with PF0.9.

Figure 4.14: *Hosting capacity evaluation for medium feeder with different PF.*

Table 4.12: *Hosting capacity evaluation results fo long feeder (MW).*

Method		First Node			Second Node			Third Node		
		Min	Mean	Max	Min	Mean	Max	Min	Mean	Max
PF 1	Bricks	11.138	12.011	13.006	9.368	9.552	9.703	5.183	5.292	5.381
	Complete Grid	10.815	11.185	11.759	10.272	10.377	10.459	5.136	5.219	5.271
PF 0.9	Bricks	10.025	10.911	11.936	10.064	10.655	11.337	9.952	10.142	10.315
	Complete	9.713	10.084	10.662	9.860	10.149	10.599	9.879	9.924	9.994

feeder it replaced with RVC. In long feeder with PF equal to 0.9, the main constraints defining the HC is thermal limit until the last nodes, which converted to the RVC at the end of the feeder, Fig. 4.15 (b).

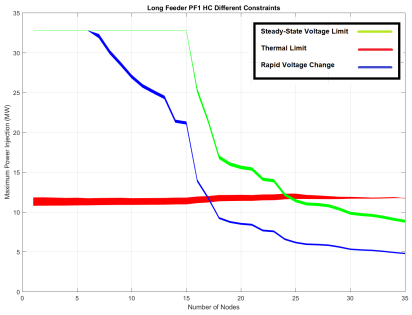

(a) Comparison between defined HC by each constraint for long feeder, PF1.

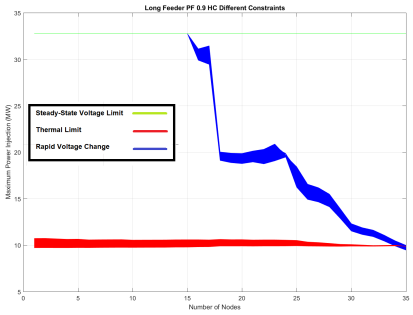

(b) Comparison between defined HC by each constraint for long feeder, PF0.9.

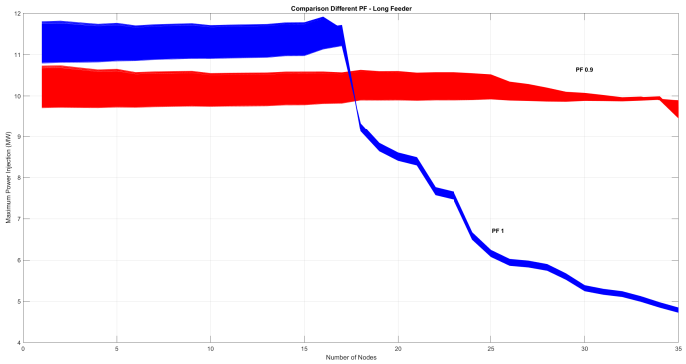

(c) Different PF comparison for long feeder.

Figure 4.15: *Different PF influence on HC of long feeder.*

In Table 4.13, the Bricks approach error and the probability of underestimating and overestimating is shown, as it is obvious the probability of underestimate is very low. Moreover, in the following figure, Fig. 4.16, the maximum power injection by DG to the grid in long feeders considering three-main technical constraints with two different power factor are shown.

Table 4.13: *Comparison between Bricks approach and complete grid for long feeder.*

Bricks Approach		Error			Probability	
		Min Value	Mean Value	Max Value	Underestimate	Overstimate
PF 1	First Node	0.0299	0.0738	0.1061	0.0041	0.7113
	Second Node	0.0880	0.0794	0.0723	0.8634	0
	Third Node	0.0092	0.0139	0.0210	0.005	0.637
PF 0.9	First Node	0.0321	0.0820	0.1195	0.0048	0.7048
	Second Node	0.0207	0.0498	0.0697	0.0173	0.5594
	Third Node	0.0074	0.0220	0.0322	0.0172	0.8834

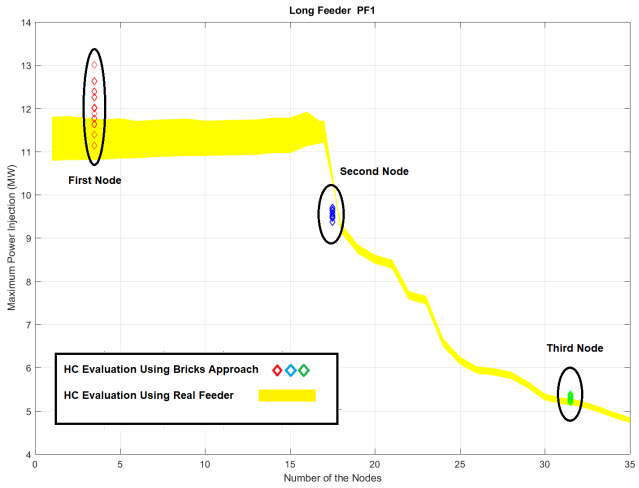

(a) Hosting capacity evaluation for long feeder with PF1.

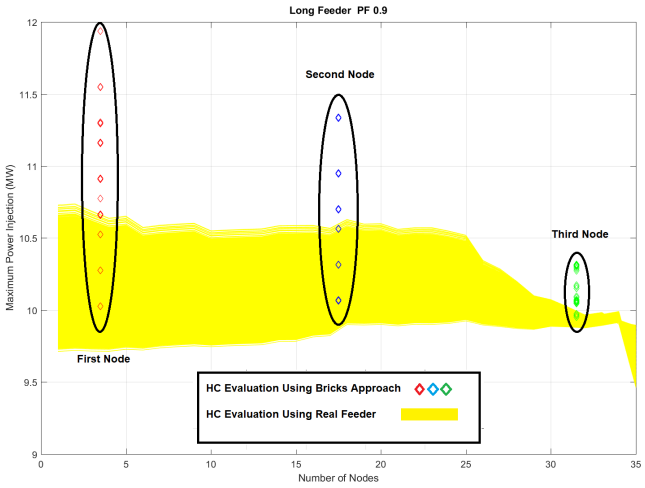

(b) Hosting capacity evaluation for long feeder with PF0.9.

Figure 4.16: *Hosting capacity evaluation for long feeder with different PF.*

Feeder with Collateral

In order to show that the proposed approach is designed properly, a random feeder from Aosta city with the exact structure is considered to adopt to Bricks approach. Feeder 9 has 24 nodes and 4 collaterals with 13 nodes, collaterals are located in nodes number 4, 7, 9 and 16 of main feeder. The first collateral has 1 node, the second one 3 nodes, the third and last one have 2 and 7 respectively, Fig. 4.17 represents the feeder 9 structure.

According to the Bricks approach the first, second and the third collateral are categorizing in short collateral and the last one is in the long category (considering the feeder and collateral characteristic). In addition, the first and the second collateral should be connecting to the first node of the main feeder with 10% of the total impedance, the second collateral should connect to the second node which is at the

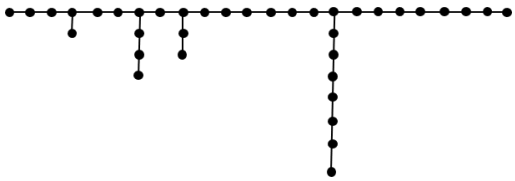

Figure 4.17: *Aosta distribution network Feeder 9 structure.*

middle and the last one should connect to the last node with 90% of the total impedance of the feeder. Table 4.14 and Table 4.15 have represented the branch parameter of short and long collateral in Bricks approach.

Table 4.14: *Short collateral parameter (p.u.).*

Bus/from	Bus/to	R	X
2	5	0.0411	0.0239

Table 4.15: *Long collateral parameter (p.u.).*

Bus/from	Bus/to	R	X
3	7	0.1536	0.1535
7	8	0.1536	0.1535

In following, Table 4.16, Fig. 4.18 and 4.19 show the HC evaluation results for real feeder 9 with both PF1 and PF 0.9. As it can be seen from the numbers and figures, from the beginning of the feeder, the HC for PF 1 is greater than PF 0.9, however near the end of the feeder this trend reverses due to the different technical constraints as it was discussed in previous section for each different category of feeders.

Moreover, HC on collaterals is lower than the main feeder at the DG connection point (e.g. the maximum hosting capacity of first node in collateral 1 is 10.838 MW, while this number in the main feeder connection point is 11.791 MW), and by going toward the end of the collateral it decreases (e.g. the maximum hosting capacity at the first node of the collateral 4 is 10.651 MW, while this amount for the second node of this collateral is 9.448 MW).

Finally Table 4.17 represents the comparison between Bricks and complete grid simulation with error and probability in percentage. From this table we can see that the maximum relative error is around 0.03 which is still showing a good performance of this method, moreover in the case of high underestimate or over estimate probability such as Collateral 4, the amount of error is still low.

At the end, from the detailed Tables and Figures in this section it is concluded that Bricks results are effective in estimating nodal HC. Some limits could be in the definition of the "Bricks" (model of the main feeder, model of the collateral, etc), but at the same time it is much more simple to define such models rather than gather detailed data for the real lines, nodes, load profile, etc. In short words, despite the simple mathematical formulation of the Bricks approach, the Bricks assumptions have to properly defined.

Table 4.16: *Hosting capacity evaluation results for feeder 9 (MW).*

Method		First Node Feeder			Second Node Feeder			Third Node Feeder		
		Min	**Mean**	**Max**	**Min**	**Mean**	**Max**	**Min**	**Mean**	**Max**
PF 1	**Bricks**	10.783	11.253	11.791	11.017	11.314	11.655	9.806	9.851	9.890
	Complete Grid	11.108	11.587	11.957	11.012	11.180	11.310	9.949	9.978	10.015
PF 0.9	**Bricks**	9.716	10.191	10.740	9.772	10.010	10.285	9.858	9.983	10.125
	Complete Grid	10.034	10.522	10.900	9.813	9.981	10.112	9.820	9.848	9.870
Method		**First Node Collateral 1**			**First Node Collateral 2**			**First Node Collateral 3**		
		Min	**Mean**	**Max**	**Min**	**Mean**	**Max**	**Min**	**Mean**	**Max**
PF 1	**Bricks**	10.580	10.700	10.838	10.580	10.700	10.838	10.750	10.873	11.015
	Complete Grid	10.532	10.536	10.541	10.704	10.725	10.742	10.734	10.741	10.750
PF 0.9	**Bricks**	9.494	9.614	9.752	9.494	9.614	9.752	9.597	9.719	9.860
	Complete Grid	9.428	9.432	9.436	9.547	9.569	9.586	9.548	9.554	9.563
Method		**First Node Collateral 4**			**Secon Node Collateral 4**					
		Min	**Mean**	**Max**	**Min**	**Mean**	**Max**			
PF 1	**Bricks**	10.527	10.594	10.651	9.357	9.406	9.448			
	Complete Grid	10.678	10.709	10.748	9.381	9.407	9.440			
PF 0.9	**Bricks**	9.708	9.904	10.128	9.734	9.839	9.957			
	Complete Grid	9.776	9.796	9.811	9.774	9.783	9.793			

Table 4.17: *Comparison between Bricks approach and complete grid model for real feeder 9.*

Bricks Approach		Error			Probability	
		Min Value	**Mean Value**	**Max Value**	**Underestimate**	**Overestimate**
PF 1	**First Node Feeder**	0.0292	0.0288	0.0138	0.2158	0.0001
	Second Node Feder	4.0862e-4	0.0119	0.0305	0.5935	0.0042
	Third Node Feeder	0.0143	0.0127	0.0125	0.6141	0
	First Node Collateral 1	0.0045	0.0155	0.0281	0.0555	0.4123
	Fist Node Collateral 2	0.0115	0.0023	0.0089	0.5147	0.3456
	First Node Collateral 3	0.0014	0.0123	0.0246	0.0940	0.5874
	First Node Collateral 4	0.0141	0.0107	0.0090	0	0.5649
	Second Node Collateral 4	0.0025	7.4410e-5	0.0080	0.1059	0.0458
PF 0.9	**First Node Feeder**	0.0316	0.0314	0.0146	0.2023	0.0001
	Second Node Feder	0.0041	0.0028	0.0171	0.0378	0.2472
	Third Node Feeder	0.0038	0.0136	0.0258	0.0593	0.8519
	First Node Collateral 1	0.0070	0.0193	0.0334	0.0393	0.4694
	Fist Node Collateral 2	0.0055	0.0047	0.0173	0.3959	0.5635
	First Node Collateral 3	0.0051	0.0173	0.0311	0.0519	0.7048
	First Node Collateral 4	0.0069	0.0109	0.0323	0.1420	0.6078
	Second Node Collateral 4	0.0040	0.0057	0.0167	0.2207	0.5748

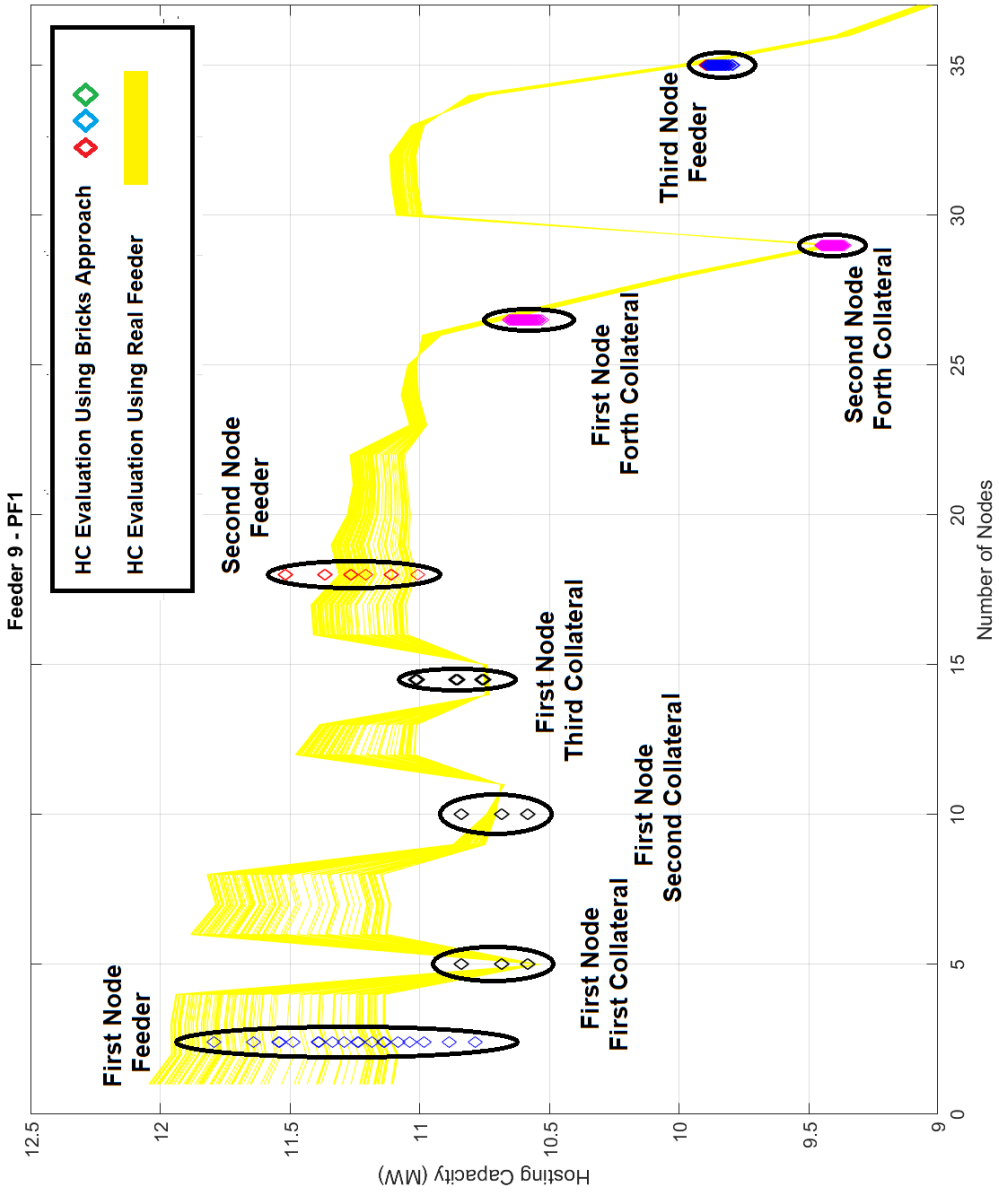

Figure 4.18: *Hosting capacity evaluation of feeder 9, PF1.*

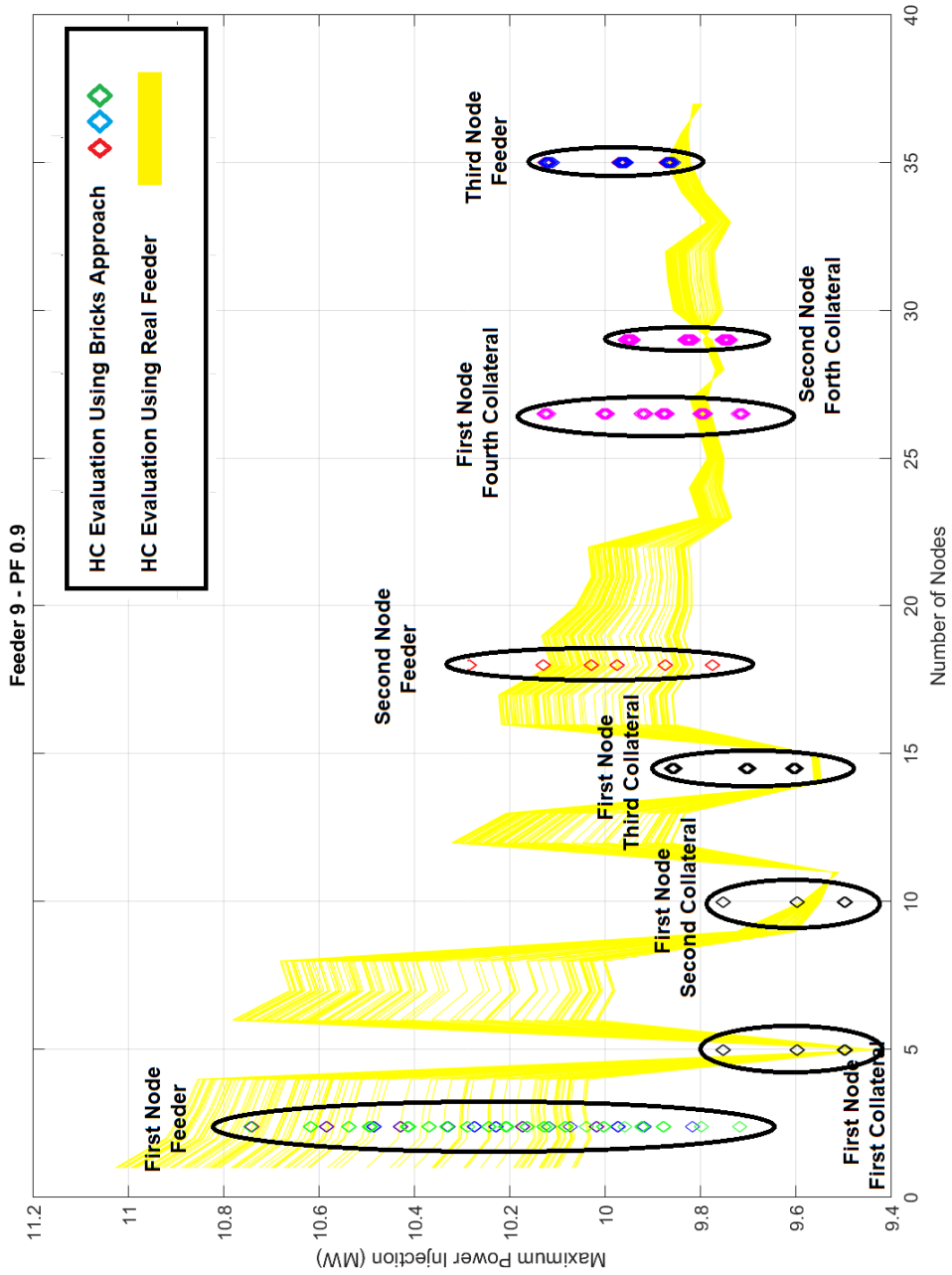

Figure 4.19: *Hosting capacity evaluation of feeder 9, PF 0.9.*

4.3 Multi-Generator Hosting Capacity

Although Nodal HC gives us a right view of injection power to the grid from each node, it cannot give us enough view for the whole grid. In real life, by increasing the number of renewable energy integration at the same time many DG are connecting to the grid which affects other DGs and the grid [227]. Thus, the second step of HC study is evaluating multi generators HC. This is an up-to-date approach and very few works could be found in literature which is motivating a research in such a direction.

The developed procedure within this research takes into account that DGs could be connected to the grid through different plants of different size and connected to various nodes. To evaluate if the distribution grid can host this capacity or if its installation will compromise the performances of the grid, a stochastic approach has been adopted, in particular Monte Carlo simulation is exploited in order to properly consider all the variables.

4.3.1 Proposed Monte Carlo Approach

The procedure in this part is dedicated to analyze the HC of electricity grid to integrate more than one DG plants. The installation of the distributed generation plants in the various nodes of the network is assumed. Since the proposed research wants to be made the approach applicable to a context of Italian regulatory system, where the policy maker does not have the power to decide the size and nodes of the new DG installations, production scenarios are created in which the positioning and sizing of DG is happening in a random way.

The procedure is able to make the generated scenario realistic thanks to the possibility of inserting constraints to the positioning of new plants. These constraints could be related to the node, the type of the DG and its size. Once the scenario has been created with the new DG plants, the operation of the electricity grid is simulated during the year and the solution in which the distribution network meets the installation constraints are identified.

By simulating the mentioned procedure, different scenarios are created. In all scenarios, the installed cumulative capacity for each type of DG is the same, but the number of plants, the size of each plant and the position in the nodes of the network is different.

Obviously, the response of the distribution network would be very different if the power selected for a type of system was installed in a single node positioning with a large plant, or divided into dozens of nodes in which smaller plants were placed. Hence, defining the location and amount of the installed DG is very important in this study. Furthermore, the response of the network would be different if DG were positioned on the network where large loads are supplied, or on sections without loads. Since the position and the size of the installed systems is not generally controllable by the regulator, it is necessary to analyze the network response with different configurations, statistically verifying the probabilities that a certain installed capacity creates problems to the electric network.

To do this, Monte Carlo (MC) simulation has been used here. Monte Carlo simulation evaluates a series of possible composition of a under-study process (in this case a possible series of production scenarios), considering the probability of any occurrence (in this case the probability of a plant with a certain size in a certain node). By evaluating connection of the various DG in different nodes of the MV network, the possible results of the under-study process have been exploit in a dense way. The provide procedure for the creation of scenarios in this study, first selects the type of DG, then its size and at the end its location.

Selecting DG Size: The probability of the installed DG by a certain size rather than another size could be defined by a operator. Actually, to define these probabilities, the operator can rely on the available information thanks to the knowledge of the existing legislation, or even the history of the installations. The set of probabilities that the installation is installed of a certain size can be represented in Monte Carlo simulation by the first roulette wheel represent in Table 4.18. Each sector of the roulette represents an intended size between a minimum and a maximum, and has a surface proportional to the probability that the system is installed of that particular size. Then within the range of the size the system could be selected randomly.

Table 4.18: *Example of a matrix for selecting the size of the DG plant.*

Probability	P_min (kW)	P_max (kW)
0.15	1	5
0.75	5	50
0.1	50	400

Selecting DG Location: For each node of the MV distribution grid, a different possibility to define the type of DG wants to be installed and its size have been considered. if the degree of detail and the constraints increase, a more realistic localization of the systems will be obtained. Two types of constraints are considered: the first valid for all the nodes and independent of the type of the DG, the second one customizable by the operator, based on the node and the considered source. The first constraint is related to the technical or electrical nature and concerns the minimum power required to have a direct connection to the MV network by DG [229], [233]. Mainly, the requested connection less than 100 kW is performed as low voltage connection. This means that if the procedure selects plants with power below 100 kW, these will necessarily be installed in nodes where there is already a secondary substation. While, the second constraint can be of a technical or regulatory issue. From a technical point of view the constraint could be the unavailability of a source, or the impossibility of positioning a large plant in an urban center. Whereas, from the regulatory point of view, there may be several bans on the installation of some types of plant in certain areas of network.

The proposed procedure for each node provides the DG plant maximum size that can be installed on it. In this procedure, it is possible to define four different sizes for each DG, zero size, small size, medium size and large size, which the operators should make a report for the network like Table 4.19 to indicate the maximum possible installation of each type of DG in each node, where N is the number of the nodes and K is the number of DG type.

Table 4.19: *DG size according to the node location.*

Node	DG Type 1	DG Type 2	. . .	DG Type K
1	S	L	. . .	0
2	0	M	. . .	L
.	.	.	.	.
.	.	.	.	.
.	.	.	.	.
N	M	S	. . .	M

Load Flow Inputs: The load flow procedure in Monte Carlo simulation is the same as nodal hosting capacity described in Section 4.2. The only difference is identifying the DG matrix as a new input of LF which in following this matrix has been described in details:

DG Profile Matrix : The DG Profiles defines all the information of the generators and its injected power into the network. The structure of the matrix has a number of rows equal to the number of nodes and a number of columns equal to simulation time step. The multi-generator procedure is able to modify the DG profiles matrix by creating different scenarios. In each scenario the generators are positioned in different nodes, of different sizes and with different types. The matrix is automatically generated by the tool when the Monte Carlo method is given the position, size and type of all installed DG.

Then as it was described before, for creating each scenario of generation, in the Monte Carlo simulation three different roulette wheels selection procedures have been introduced in order to defined the type, size and the connection node of the DGs. Equation 4.12 formulate the power that can be installed by two roulette wheel in the defined node in the third roulette wheel. Fig. 4.20 shows the Monte Carlo simulation flowchart for this procedure.

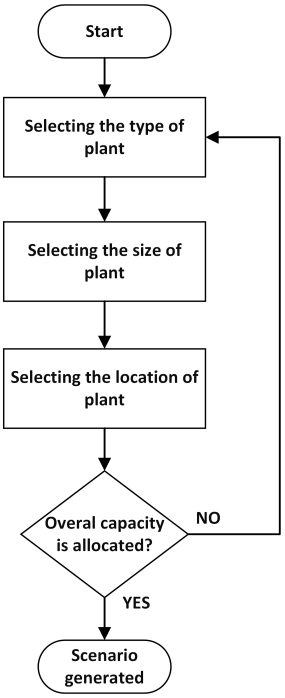

Figure 4.20: *Monte Carlo simulation flowchart for evaluating multi-generator HC.*

$$Power\ to\ Install = \sum_{i=1}^{n} Selected\ Type(DG_i(t)).Selected\ Size(DG_i(t)) \tag{4.12}$$

Once the scenario is created, the hourly (or each required time step simulation) power flow computation as fully-described in the previous section, 4.2 is carried out. By performing power flow computation, system power losses, maximum voltage and maximum current of the grid is calculated.

The Monte Carlo procedure is based on an iterative behavior and equation 4.13 and 4.14 represent

the convergence criterion which is used in this study. μ_{Loss} and σ_{Loss} are the losses mean value, and the losses standard deviation respectively. The variation of these two value should be placed lower than ϵ. In order to have a more robust criterion this procedure is repeating 5 times continuously.

$$\left|\frac{\mu_{Loss}(i) - \mu_{Loss}(i-1)}{\mu_{Loss}(i-1)}\right| < \epsilon_{\mu} \tag{4.13}$$

$$\left|\frac{\sigma_{Loss}(i) - \sigma_{Loss}(i-1)}{\sigma_{Loss}(i-1)}\right| < \epsilon_{\sigma} \tag{4.14}$$

When the number of evaluated scenarios is sufficient according to the convergence criteria, an index that represents the probability of the grid constraints violation, which is called Hosting Capacity Violation Probability (HCVP) through equation 4.15 can be evaluated. In a general way, when a limit in the functioning parameters is set, the number of scenarios in which this limit is violated at least one time can be counted and represented with the variable, so the HCVP can be computed as the fraction of the total number of scenarios evaluated for a specific portfolio in which they violate the constrains.

$$HCVP = \frac{Total\ Number\ of\ Violated\ Scenarios}{Total\ Number\ of\ Scenarios} \tag{4.15}$$

The considered technical constraints, the same as Section 4.2, are steady voltage variation, thermal limit and rapid voltage change. The acceptable probability to violate the limit will define the maximum penetration that can be achieved which here is considered equal to 5%, according to other studies that use similar stochastic approaches [92].

4.3.2 Proposed Monte Carlo and Bricks Approach

Once Monte Carlo simulation has been performed for the under-study complete grid, the Bricks approach has been implemented in MC simulation to create each scenario in order to reduce the evaluation time and required grid information.

To do so, an assumption has been made which the feeders in each grid is marginally affected by the others as transformer automatic voltage regulator could keep the voltage in MV busbars constant. Hence, the full grid could be represented by only one feeder of each category in each time. The full description of the Bricks approach has been explained in Section 4.2.1. After obtaining the type and size of the new DG in Monte Carlo simulation by the defined roulette wheels for each scenario, the locations of aforementioned DGs need to be defined among the considered nodes in Bricks approach. Each scenario is simulated for min, mean and peak load and generator value and the overall HC could be evaluated in shorter time and with less available information. At the end, in order to highlight the accuracy of this method the result of the complete grid and the Monte Carlo with Bricks approach have been compared both in terms of accuracy and processing time.

4.3.3 Validation of the Proposed Approach

To validate the proposed approach in the previous part, a case study which is Aosta city MV distribution grid has been considered. Since this network has been fully-described in Section 4.2.2, here the available DG types in this network has been discussed.

Available DG Types

Distributed generation plants, in general, can exploit different sources and could be made by multiple technologies, it is therefore important to identify which types of plant can potentially be built in the examined network. In the study case of this thesis work, six different types of renewable sources have been exploited: photovoltaic, wind, small and medium-sized hydropower, industrial cogeneration CHP and district heating CHP. Each of these plants produces electricity according to its characteristic time profile, e.g. in the case of solar, wind and hydroelectric plants, electricity production depends on the availability of the sources, while in case of cogeneration plants depends on the request of the associated thermal user. The production profile characteristic, for each of the six types of system, has been normalized in order to represent by the plant energy map. Following the energy maps of the mentioned six types of plant have been described.

Photovoltaic: The normalized profile of photovoltaic production is shown in Fig. 4.21. This profile was created by the irradiation measurements for the city of Aosta reported in satel-light database [234]. From the profile production there are daily and seasonal trends. The daily one is due to the cycle between day and night, so the profile of the photovoltaic system has a "bell" shape; it has the peak of production at the solar noon, while it does not produce at night. The seasonal trend shows how the plant produces less in winter, when the duration of the day and the solar height are minimal. In north part of Italy, the equivalent operating hours of a photovoltaic plant is typically between 1000 and 1300 hour, while the theoretical profile which is built with the radiation data results to have a number of hours equal to 1615. Constructing the profile starting from the theoretical radiation are neglected the non-ideality of the panel, such as the variation in yield with the angle of incidence and shading.

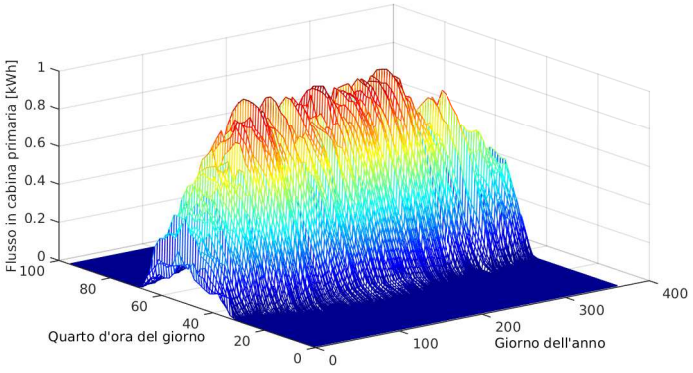

Figure 4.21: *Normalized generation of photovoltaic power plant.*

Wind: The normalized power production of wind turbine is shown in Fig. 4.22. This profile has been created according to the only medium-sized wind farm in Valle d'Aosta today in place. This 2.55 MW plant is consists of three wind turbines of V52-850kW type, with the nominal power of 850 kW. Unlike PV system, this type of plant does not show any specific different trends. Among all of the sources, wind is the least predictable. Despite this, it is possible to notice some characteristics of the production; in the late-winter and spring the production is fairly constant during the day and do not exceed 40% of the

nominal power; during the summer months production changes during the day and the plants operate at nominal power in the late afternoon; the afternoon production goes down slowly in the autumn months, when the plants work at the nominal power for 24 hours in random days. According to the available data, 1573 equivalent hours per year is considered as its working hours.

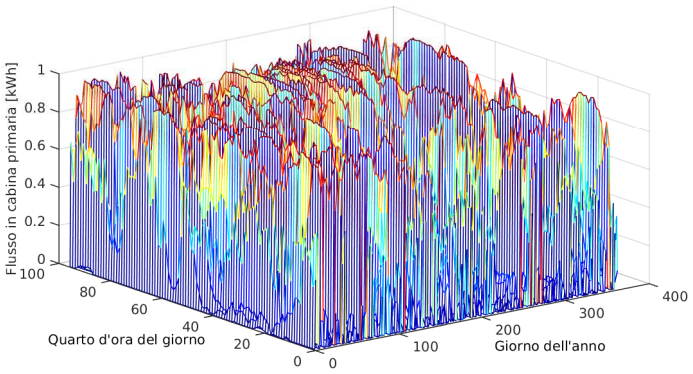

Figure 4.22: *Normalized generation of wind power plant.*

Medium-Size Hydroelectric: In this research, the hydroelectric sources were divided into two classes; small plants and medium-sized plants. The plants with a nominal power more than 1 MW is considered as medium-sized plants, while those with a installed power of hundreds of kW are considered small-sized plants. The same as wind power plant, this profile production has been taken from the real hydroelectric plant in Aosta valley with the nominal power of 3500 kW and the data are sampled in the quarter of an hour. Fig. 4.23 shows this power profile which also represents its strong relationship with seasons. In winter the operating power is around 20% of the nominal power, while in summer because of snow melting and the great availability of water, the systems operate at nominal power. One can see that there is no type of daily periodicity in this profile; since these are often plants that have no possibility of accumulation except in very small quantities, production is carried out when there is availability of water. The number of equivalent operating hours of the plant is calculated in 5092.

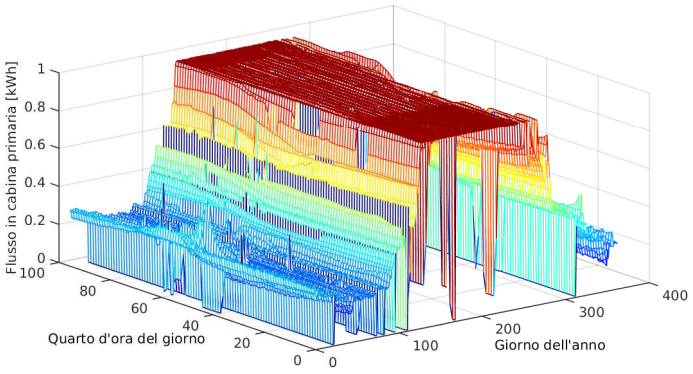

Figure 4.23: *Normalized generation of medium-size hydroelectric power plant.*

Small-Size Hydroelectric: As it was discussed in the previous paragraph, plants with nominal power less than hundreds of kW have been considered small size. The normalized profile of this power plant is shown in Fig. 4.24. It can be seen that the profile is similar to the medium-sized plant, with a nominal power production during summer time and minimum power in winter. The small plants in comparison with medium size plant is more flexible. This characteristic is justified by the fact that the necessary dimensions for the accumulation to make production is more flexible in a small size plant and is less significant compared to medium size plant. The equivalent number of operating hours for small power plant is equal to 4767 which is very close to medium-sized one.

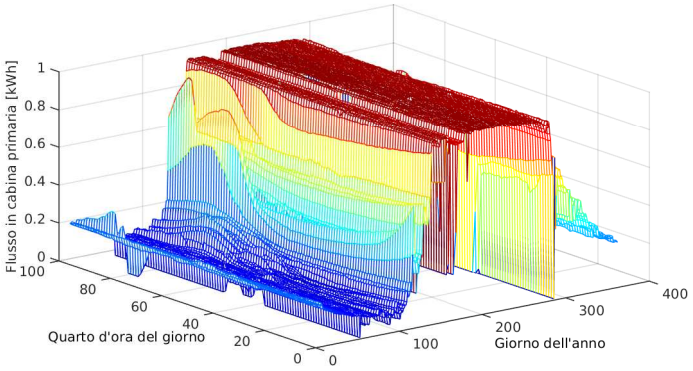

Figure 4.24: *Normalized generation of small-size hydroelectric power plant.*

Industrial CHP: This is the representative of the joint power production of heat and electricity, in which the electric production follows the thermal requirements of an industrial type. The production power profile has been built based on some hypotheses, such as considering the thermal power start request of the industrial user is in around 6 o'clock at morning and ends in the evening around 17 o'clock. While, during these times a production of nominal power is considered. However, the power plant is considered off during night time, weekend and holiday. This plant works for 2722 equivalent hours per year. Fig. 4.25 shows the normalized generation of it.

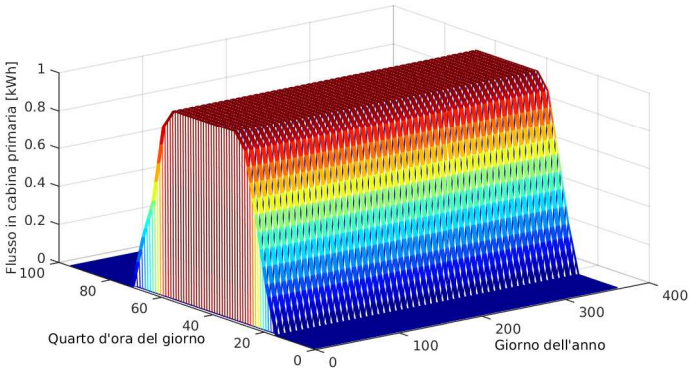

Figure 4.25: *Normalized generation of industrial CHP power plant.*

District Heating CHP: This plant has three biomass boilers with a total production of 20 thermal MW. In winter the turbine works at full load day and night, as the produced heat during the night is stored in two tanks for thermal storage which could be used in the morning in case of maximum load. While, the night demand is lower in the spring and fall seasons, which the operated power is considered about 800 kW. Finally, for a certain summer period, the thermal demand is significantly reduced, which cause electric production interruption;it should be noted that it is difficult to manage under 70% of nominal power for this kind of generation unit. The described power profile has been shown in Fig. 4.26. The theoretical model of the system works for 6671 equivalent hours per year.

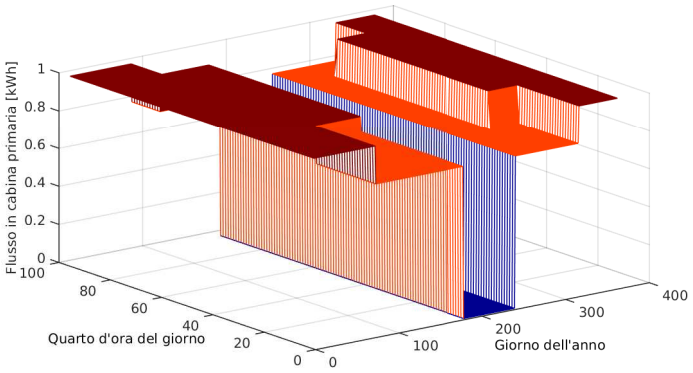

Figure 4.26: *Normalized generation of district heating CHP power plant.*

Installation Regulatory and Geographical Constraints

As it was already mentioned, not all nodes have the ability to accommodate a new connection. Electric regulatory is the first constraint; a generator with power less than 100 kW can not be connected directly to the MV network. For this reason, in the simulation DG with power lower than 100 kW should be connected to node where there is already a secondary substation. In the particular case of the network under analysis, which means that according to Fig. 4.27 this type of generators can be installed in almost half of the nodes. The second type of constraint is the geographical constraints; in each node according to its geographical location some specific sources with specific sizes could be connected. At the following the constraints which have been taken into consideration for each source, and the radial layout of the electrical network with the representation of the size constraints for each node according to [235] is represented. Table 4.20 indicates the considered small, medium or large amount of this study for each generator. If the power is less than the first row it means it has been chosen as the small size, if it is between the value of first and second row it should be medium size and bigger than the last row, goes for large size.

Table 4.20: *DG nominal power in kW for consideration as small, medium or large.*

No.	PV	Wind	Hydroelectric Medium	Hydroelectric Small	Industrial Cogenerator	District CHP
1	5	0	2000	0	250	0
2	50	50	5000	500	500	0

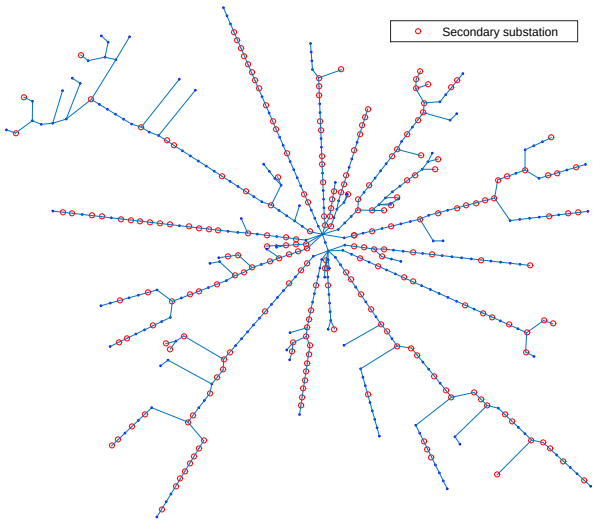

Figure 4.27: *Secondary substation on Aosta MV distribution grid.*

PV Plant Installation Nodes: In the historical center of the city only small size of PV could be installed, as the only available space is the buildings roofs. While, in the suburbs of the city the possibility of installation has been considered medium-sized PV. The installation of large-scale plants has been planned only for the nodes that are located outside the city under study. Fig. 4.28 represents the nodes in Aosta grid which can host PV with different size.

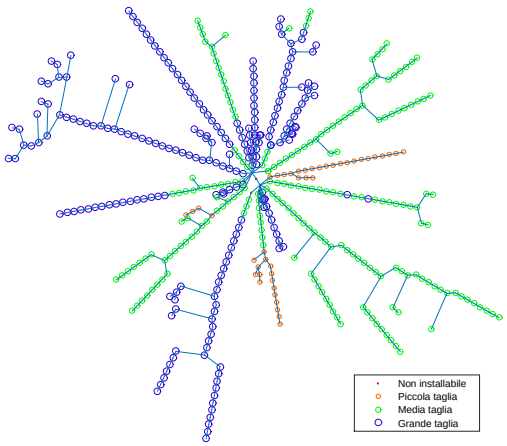

Figure 4.28: *Possible installation point of PV.*

Wind Plant Installation Nodes: Wind turbines have less chance to be considered in the urban context, especially when it comes to large plants. It has been assumed that not any kind can be installed in the central area of the city and near the airport. The medium-sized plants has been considered on the outskirts of the city and in the city agricultural areas. Moreover, large-scale plants have been installed far from the city and the inhabited areas. Fig. 4.29 shows the possible wind turbine installation nodes.

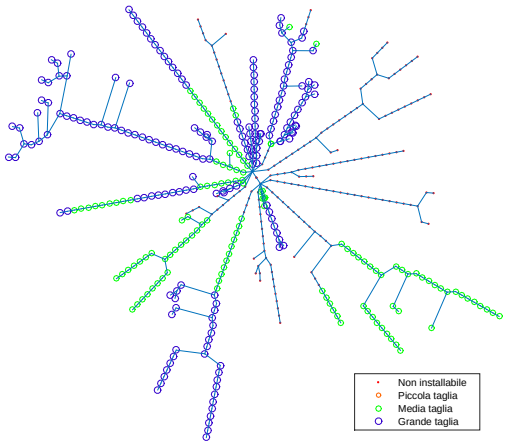

Figure 4.29: *Possible installation point of wind turbine.*

Hydroelectric Plant Installation Nodes: The allowed nodes for installing hydroelectric plants are where there is a probability of exploitable waterways. Hence, the historical center has been excluded and the possibility of installing new large-scale plants in urbanized areas has been excluded. The possible places for installing hydroelectric plants have been shown in Fig. 4.30.

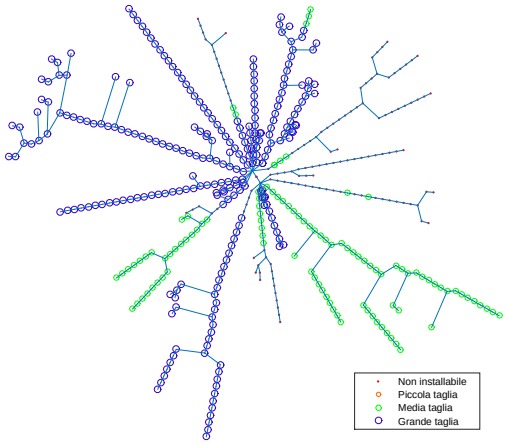

Figure 4.30: *Possible installation point of hydroelectric plant.*

Industrial Cogenerator Plant Installation Nodes: Considering the versatility of the cogeneration plants and the possibility of being connected to various types of industrial or similar utilities, it is assumed that these type of generators could be installed at any node of the network. However, in the historical center the possibility of large-size installation is very low, thus in the nodes of this area the installation is limited to small and medium size plants, fig. 4.31 shows these locations.

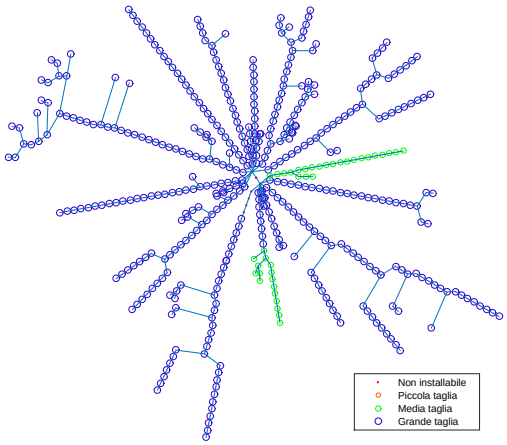

Figure 4.31: *Possible installation point of industrial cogenerator plant.*

District CHP Plant Installation Nodes: For this kind of plants, it is hypothesized that any district heating plants have enough power to be connected to the primary substation with a proper connection. To simulate this condition, the district heating systems are bound to be connected to one of the two MV bars of the primary substations, Fig. 4.32.

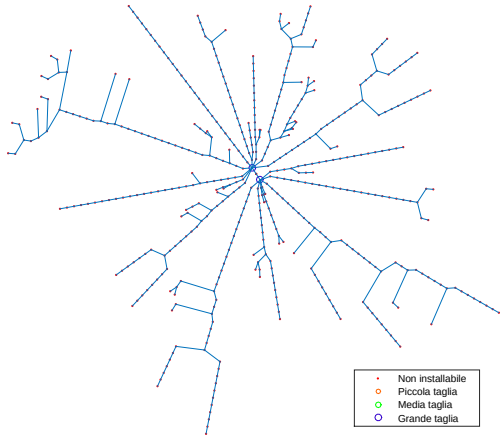

Figure 4.32: *Possible installation point of District CHP plant.*

4.3.4 Results and Discussion

The proposed procedure explained in Section 4.3.1 and 4.3.2 has been applied once again to the case study of the Ponte Pietra primary substation with the aim of evaluating the hosting capacity of the grid in case of multi-genertor connection considering three technical constraints explained in Section 4.2 according to equation 4.15.

Complete Grid Monte Carlo

In this study the total DG installation has been considered from 1 MW to 30 MW. For each installation capacity different combination of DG including different size, type and location is defined through MC simulation and for each single scenario HCVP KPI is evaluated, this index ranges between 0, when no violation are detected in any of the evaluated scenarios, and 1, when all scenarios depicts violations). Table 4.21 in the following identified the total number of violated constraints and also the total number of scenario for each power injection to calculate HCVP. Moreover in this table the average and maximum amount of voltage and current of Aosta grid for each amount of injection has been represent. Figure4.33 below demonstrates this KPI more clear.

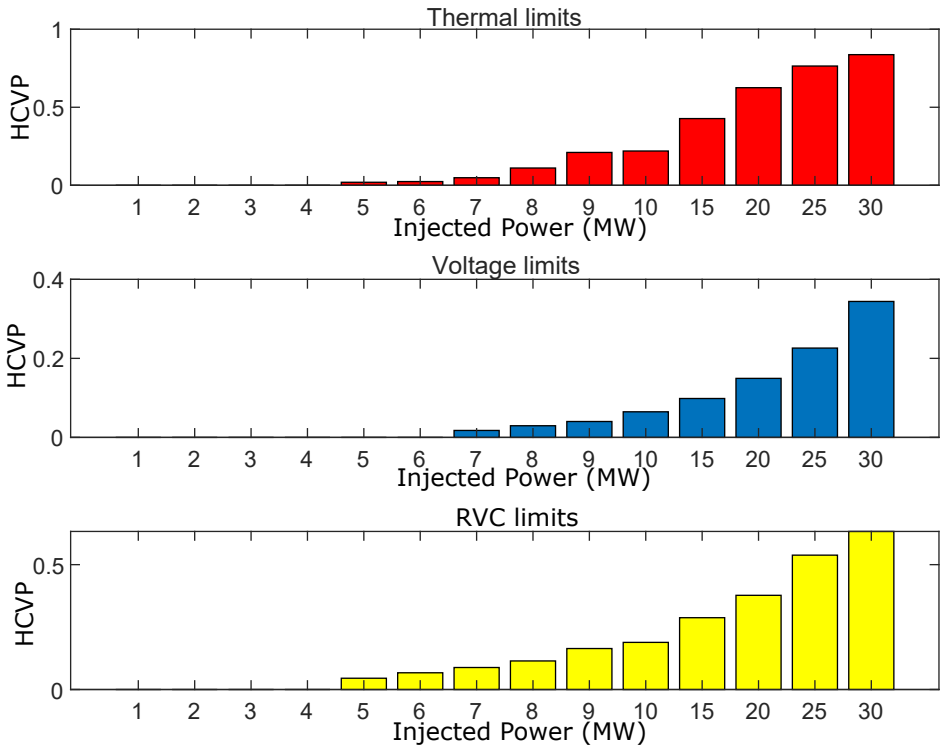

Figure 4.33: *HCVP for complete grid topology with PF1.*

Table 4.21: *Monte Carlo simulation for complete grid topology, PF1.*

Power (MW)	No. of Thermal Limit Violation	No. of Steady State Voltage Violation	No. of RVC Violation	Total No. of Scenario	Current (Mean) pu.	Current (Max) pu.	Voltage (Mean) pu.	Voltage (Max) pu.	RVC (Mean) pu.	RVC (Max) pu.
1	0	0	0	225	0.0512	0.5086	0.9990	1.0307	0.0024	0.0070
2	0	0	0	327	0.0527	0.5086	1.0020	1.0433	0.0041	0.0164
3	0	0	0	215	0.0525	0.5737	1.0032	1.0628	0.0061	0.0307
4	0	0	0	246	0.0597	0.6665	1.0028	1.0556	0.0065	0.0340
5	3	0	7	155	0.0796	1.2122	1.0041	1.0770	0.0071	0.0517
6	5	0	14	209	0.1187	1.2720	1.0047	1.0798	0.0093	0.0737
7	11	4	20	227	0.1542	1.8178	1.0050	1.0903	0.0104	0.0807
8	30	8	31	271	0.1648	1.5286	1.0061	1.1001	0.0125	0.1020
9	68	13	53	323	0.2240	2.0905	1.0069	1.1172	0.0129	0.1220
10	78	23	67	355	0.2091	2.0127	1.0076	1.1368	0.0137	0.1463
15	165	38	111	386	0.3363	2.5918	1.0137	1.1493	0.0205	0.1542
20	247	59	149	395	0.5009	3.1599	1.0158	1.1543	0.0224	0.1500
25	311	92	219	407	0.5102	3.2534	1.0172	1.1635	0.0283	0.1610
30	365	150	276	436	0.5946	3.6777	1.0316	1.1934	0.0360	0.1965

As it can be understood from these data and figure, the limiting factor for complete grid is RVC constraint. At the power injection of more than 6MW RVC limitation and also at 7MW thermal limit could be found, which it could be concluded that for the complete grid of Aosta the total HC is less than 7MW.

In order to evaluate the importance of controlling the voltage by reactive power injection to the grid and making some advantage of HC increasing and also reducing the voltages near boundaries, the above simulation has been performed once again with PF0.9 instead of PF1. Table 4.22 represents these numbers in following. Figure 4.34 has been plotted according to the defined number in the previous table.

According to the mentioned numbers, the total HC of the Aosta grid by considering PF equal to 0.9 has been evaluated by 7MW and the limiting factor is thermal limit here. As the voltage is decreasing by changing the power factor to 0.9 the total HC could be increased also. In order to show the effect of different PF with different power injection in the grid, Fig. 4.35 and Fig. 4.36 demonstrate the voltage profile of Aosta grid in case of 2MW and 7MW power injection for PF1 and PF0.9 respectively in one of the simulated scenario.

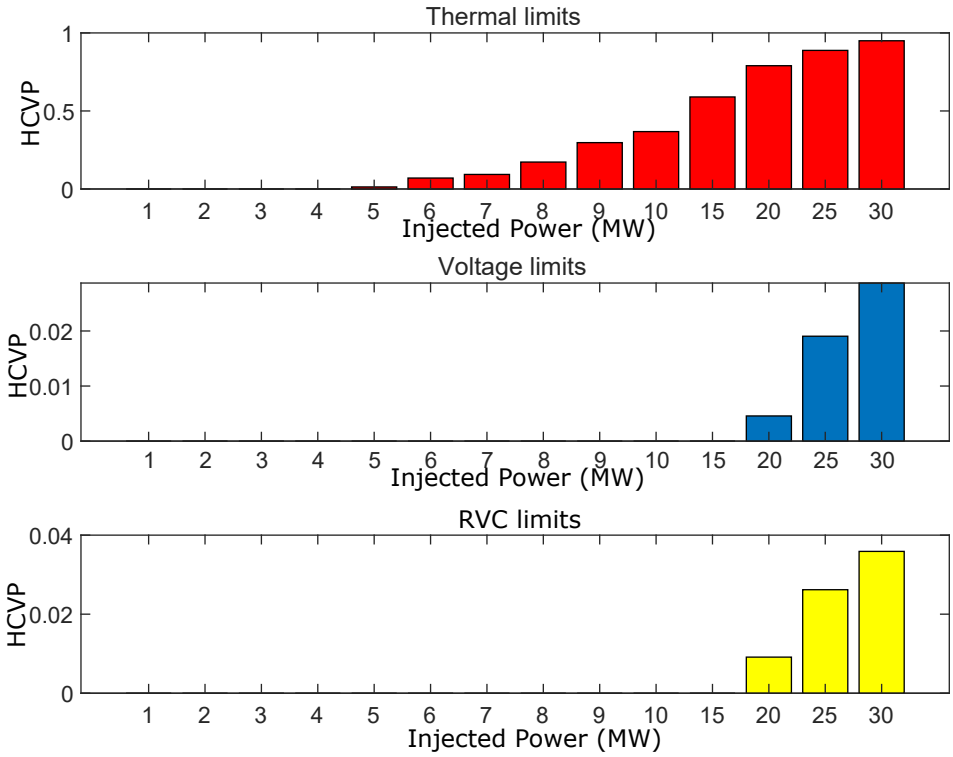

Figure 4.34: *HCVP for complete grid topology with PF0.9.*

Table 4.22: *Monte Carlo simulation for complete grid topology, PF0.9.*

Power (MW)	No. of Thermal Limit Violation	No. of Steady State Voltage Violation	No. of RVC Violation	Total No. of Scenario	Current (Mean) pu.	Current (Max) pu.	Voltage (Mean) pu.	Voltage (Max) pu.	RVC (Mean) pu.	RVC (Max) pu.
1	0	0	0	127	0.1651	0.5086	0.9960	1.0309	0.0043	0.0073
2	0	0	0	187	0.1638	0.5086	1.0006	1.0366	0.0052	0.0082
3	0	0	0	194	0.1593	0.6134	1.0024	1.0448	0.0063	0.0180
4	0	0	0	163	0.1722	0.7431	1.0023	1.0403	0.0075	0.0126
5	2	0	0	151	0.1603	1.1996	1.0035	1.0638	0.0079	0.0370
6	10	0	0	228	0.1610	1.4252	1.0037	1.0542	0.0093	0.0313
7	18	0	1	326	0.1852	2.0540	1.0043	1.0632	0.0103	0.0415
8	53	0	3	307	0.1657	1.9740	1.0057	1.0670	0.0109	0.0436
9	112	0	10	377	0.1709	2.1510	1.0062	1.0724	0.0125	0.0564
10	146	0	13	397	0.2100	2.5216	1.0067	1.0891	0.0143	0.0733
15	253	0	32	429	0.2581	2.9006	1.0124	1.0742	0.0164	0.0579
20	346	2	44	438	0.2903	3.6962	1.0147	1.0880	0.0179	0.0718
25	373	8	67	420	0.3324	3.7003	1.0153	1.1008	0.0197	0.0740
30	397	12	99	418	0.4124	4.2919	1.0178	1.1044	0.0223	0.0886

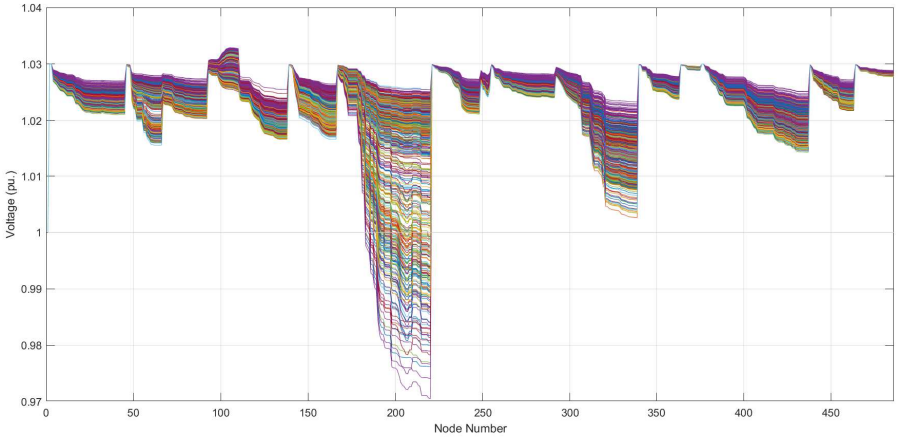

(a) Yearly voltage profile for 2MW injection with PF1.

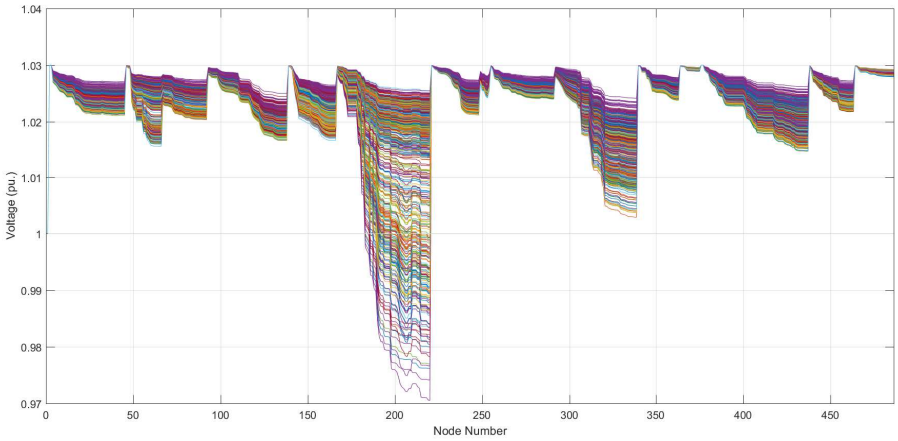

(b) Yearly voltage profile for 2MW injection with PF0.9.

Figure 4.35: *Yearly voltage profile for 2MW injection with different PF.*

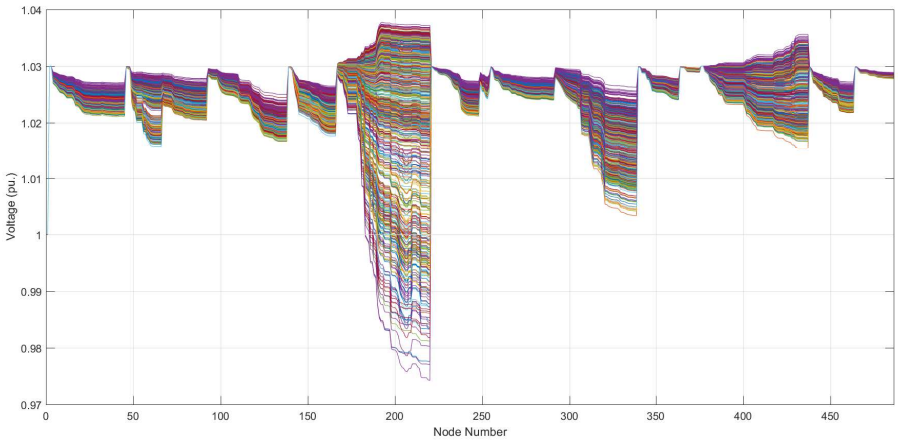

(a) Yearly voltage profile for 7MW injection with PF1.

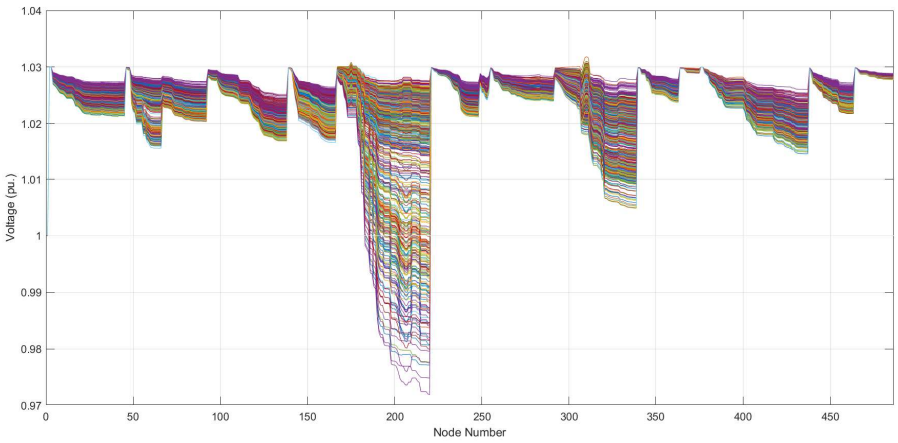

(b) Yearly voltage profile for 7MW injection with PF0.9.

Figure 4.36: *Yearly voltage profile for 7MW injection with different PF.*

Finally, Fig. 4.37 shows the total power injection define by MC simulation by each DG for both 6MW and 7MW injection, where the blue color is representing 7MW and the orange color for 6MW.

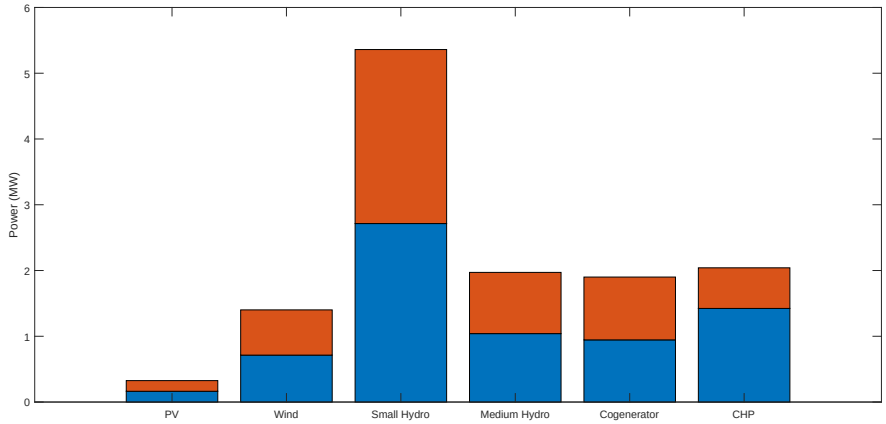

Figure 4.37: *DG grid injection for installed capacity of 6MW and 7MW .*

Monte Carlo and Bricks Approach

Table 4.23 and 4.24 represent the total number of scenarios, the violated one for each defined constraints, the voltage and current characteristics of short feeder categories for PF1 and PF0.9 respectively. Furthermore, their HCVP criteria to estimate the multi-generator HC with 5% acceptance of violation is plotted in the Fig. 4.38 for both PF1 and PF 0.9.

As can be seen from the tables and figures, in short feeder the only limited constraint is thermal limit. Thus changing the power factor from 1 to 0.9 should not have any significant influence on the HC of the network. The total HC for this network with putting more than one generator in each scenario for PF1 is less than 8 MW, whereas for PF 0.9 is less than 7 MW. As it is obvious by increasing the injection to the grid, the total number of violations have been increased which is shown perfectly in the figures.

The same as short feeder category, Table 4.25 and 4.26 express the total number of scenarios for each power injection and the total number of violation of each constraints for medium feeders. Moreover, the average and maximum values of voltage, current and RVC in order to comparison with complete grid model and short category is presented in this tables for PF1 and PF 0.9 respectively. Hereinafter, Fig. 4.39 illustrates the HCVP for medium feeder with different PF.

From the tables and figures it can be seen that, the total number of violation in medium feeder is increasing compare to the short feeder. Although the limiting factor in this category is still thermal limit, steady-state voltage violation and RVC violation also can be seen. These amount of violation by changing the PF1 to PF0.9 have been reduced. The total amount of HC of the grid in case of multi generator injection for medium feeder with PF1 is less than 7 MW and with PF0.9 is less than 6 MW, this could happen due to the problem of reverse power flow. From the estimated HC we could conclude that total HC in medium feeder is less than short feeder.

Table 4.23: *Monte Carlo with Bricks approach for short feeder categories, PF1.*

Power (MW)	No. of Thermal Limit Violation	No. of Steady-State Voltage Violation	No. of RVC Violation	Total No. of Scenario	Current (Mean) pu.	Current (Max) pu.	Voltage (Mean) pu.	Voltage (Max) pu.	RVC (Mean) pu.	RVC (Max) pu.
1	0	0	0	2165	0.0268	0.1651	0.9999	1.0014	0.0005	0.0025
2	0	0	0	2308	0.0349	0.3545	1.0002	1.0038	0.0008	0.0050
3	0	0	0	2867	0.0621	0.5275	1.0006	1.0062	0.0012	0.0075
4	0	0	0	3186	0.0673	0.7224	1.0005	1.0088	0.0011	0.0099
5	0	0	0	3075	0.0992	0.9149	1.0009	1.0113	0.0015	0.0125
6	46	0	0	3403	0.1413	1.0978	1.0014	1.0137	0.0021	0.0148
7	167	0	0	3841	0.1704	1.2796	1.0018	1.0160	0.0025	0.0173
8	312	0	0	3972	0.2117	1.4727	1.0027	1.0184	0.0033	0.0197
9	1453	0	0	4319	0.2606	1.6604	1.0029	1.0209	0.0035	0.0222
10	2866	0	0	4541	0.2286	1.8350	1.0025	1.0234	0.0031	0.0246
15	4443	0	0	5223	0.4268	2.6595	1.0048	1.0346	0.0054	0.0357
20	5030	0	0	5230	0.4810	3.5126	1.0061	1.0460	0.0067	0.0473
25	4761	0	0	4841	0.6986	4.2695	1.0065	1.0548	0.0071	0.0561
30	4873	0	11	4896	0.7683	5.0901	1.0083	1.0660	0.0089	0.0673

Table 4.24: *Monte Carlo with Bricks approach for short feeder categories, PF0.9.*

Power (MW)	No. of Thermal Limit Violation	No. of Steady-State Voltage Violation	No. of RVC Violation	Total No. of Scenario	Current (Mean) pu.	Current (Max) pu.	Voltage (Mean) pu.	Voltage (Max) pu.	RVC (Mean) pu.	RVC (Max) pu.
1	0	0	0	2605	0.0279	0.1944	0.9998	1.0007	0.0004	0.0018
2	0	0	0	2536	0.0362	0.4019	0.9999	1.0025	0.0005	0.0036
3	0	0	0	2945	0.0853	0.5982	1.0003	1.0041	0.0009	0.0054
4	0	0	0	2660	0.0994	0.8177	1.0006	1.0059	0.0012	0.0072
5	17	0	0	3340	0.1010	1.0321	1.0004	1.0078	0.0010	0.0089
6	143	0	0	3622	0.1933	1.2268	1.0011	1.0095	0.0017	0.0106
7	326	0	0	4117	0.2211	1.4429	1.0013	1.0112	0.0019	0.0124
8	1602	0	0	4207	0.1887	1.6347	1.0009	1.0130	0.0015	0.0141
9	3016	0	0	4580	0.2223	1.8480	1.0014	1.0147	0.0020	0.0158
10	3574	0	0	4772	0.2828	2.0633	1.0021	1.0164	0.0027	0.0175
15	4277	0	0	4834	0.3563	2.9926	1.0029	1.0240	0.0035	0.0252
20	5164	0	0	5319	0.5795	3.8465	1.0043	1.0305	0.0049	0.0316
25	4985	0	0	5035	0.8721	4.7777	1.0056	1.0384	0.0062	0.0398
30	4528	0	0	4541	0.9254	5.2063	1.0063	1.0419	0.0069	0.0430

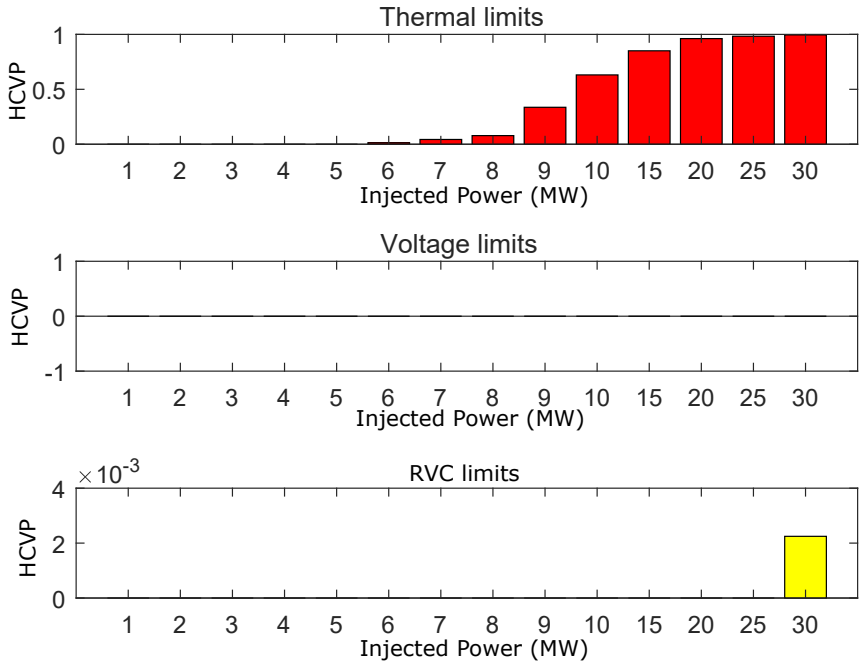

(a) HCVP for short feeder category with PF1.

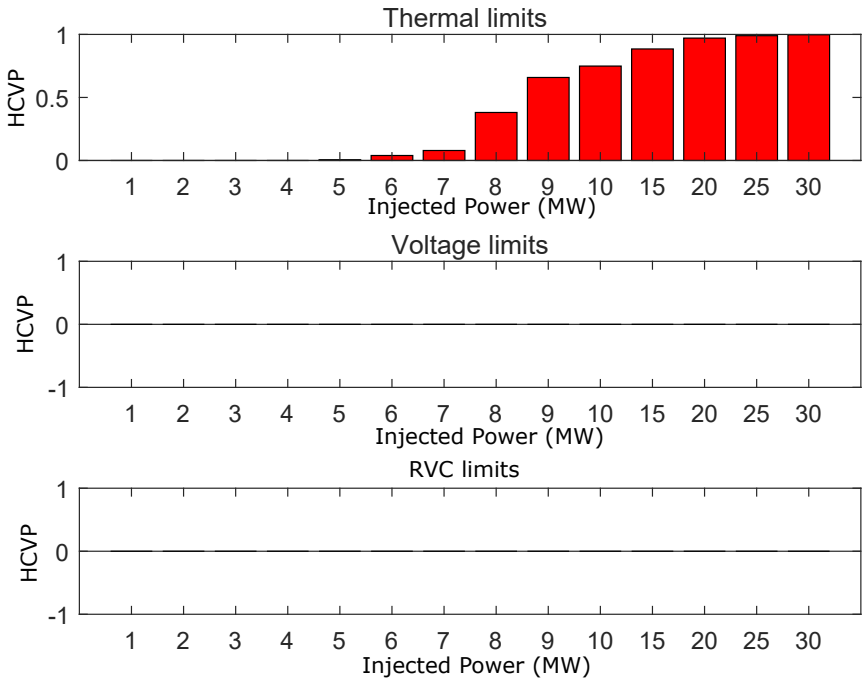

(b) HCVP for short feeder category with PF0.9.

Figure 4.38: *HCVP for short feeder category with different PF.*

Table 4.25: *Monte Carlo with Bricks approach for medium feeder categories, PF1.*

Power (MW)	No. of Thermal Limit Violation	No. of Steady-State Voltage Violation	No. of RVC Violation	Total No. of Scenario	Current (Mean) pu.	Current (Max) pu.	Voltage (Mean) pu.	Voltage (Max) pu.	RVC (Mean) pu.	RVC (Max) pu.
1	0	0	0	8495	0.0333	0.1870	0.9987	1.0021	0.0024	0.0090
2	0	0	0	9346	0.0356	0.3403	0.9993	1.0103	0.0030	0.0173
3	0	0	0	9493	0.0384	0.5276	0.9998	1.0182	0.0036	0.0254
4	0	0	0	10661	0.0526	0.7161	1.0008	1.0268	0.0045	0.0337
5	0	0	0	13252	0.0764	0.8971	1.0013	1.0353	0.0050	0.0420
6	149	0	0	14623	0.1078	1.0941	1.0029	1.0428	0.0066	0.0500
7	963	0	0	15586	0.1154	1.2758	1.0047	1.0507	0.0083	0.0577
8	2133	0	75	17173	0.1632	1.4578	1.0066	1.0582	0.0103	0.0651
9	2901	0	267	16137	0.1997	1.6440	1.0057	1.0657	0.0094	0.0728
10	9701	0	633	17544	0.1836	1.8159	1.0086	1.0731	0.0123	0.0801
15	15555	16	3834	17892	0.3088	2.7248	1.0139	1.1082	0.0176	0.1148
20	16739	440	7497	17414	0.4177	3.5482	1.0194	1.1359	0.0231	0.1427
25	15609	1520	9609	15769	0.5443	4.4778	1.0209	1.1600	0.0246	0.1680
30	15420	3293	11673	15464	0.6106	5.0409	1.0268	1.1887	0.0305	0.1964

Table 4.26: *Monte Carlo with Bricks approach for medium feeder categories, PF0.9.*

Power (MW)	No. of Thermal Limit Violation	No. of Steady-State Voltage Violation	No. of RVC Violation	Total No. of Scenario	Current (Mean) pu.	Current (Max) pu.	Voltage (Mean) pu.	Voltage (Max) pu.	RVC (Mean) pu.	RVC (Max) pu.
1	0	0	0	8605	0.0748	0.3548	0.9922	1.0000	0.0082	0.0285
2	0	0	0	8647	0.0798	0.3796	0.9929	1.0000	0.0087	0.0285
3	0	0	0	9438	0.0818	0.5939	0.9944	1.0043	0.0100	0.0317
4	0	0	0	11693	0.1145	0.7956	0.9957	1.0105	0.0111	0.0362
5	40	0	0	13457	0.1055	1.0049	0.9955	1.0164	0.0110	0.0469
6	905	0	0	14693	0.1527	1.2040	0.9980	1.0220	0.0134	0.0530
7	2047	0	0	15999	0.1653	1.4147	0.9996	1.0272	0.0149	0.0571
8	3601	0	0	16966	0.2171	1.6128	1.0011	1.0321	0.0164	0.0620
9	12212	0	0	18346	0.2161	1.8158	1.0023	1.0370	0.0175	0.0658
10	13690	0	0	17700	0.2160	2.0341	1.0042	1.0407	0.0194	0.0708
15	16307	0	196	17962	0.3810	2.9881	1.0083	1.0592	0.0235	0.0871
20	15813	0	1412	16148	0.5037	3.9395	1.0106	1.0729	0.0258	0.1017
25	15538	0	3811	15613	0.7482	4.7803	1.0168	1.0827	0.0319	0.1119
30	15064	9	5827	15097	0.7300	5.6168	1.0188	1.0915	0.0339	0.1210

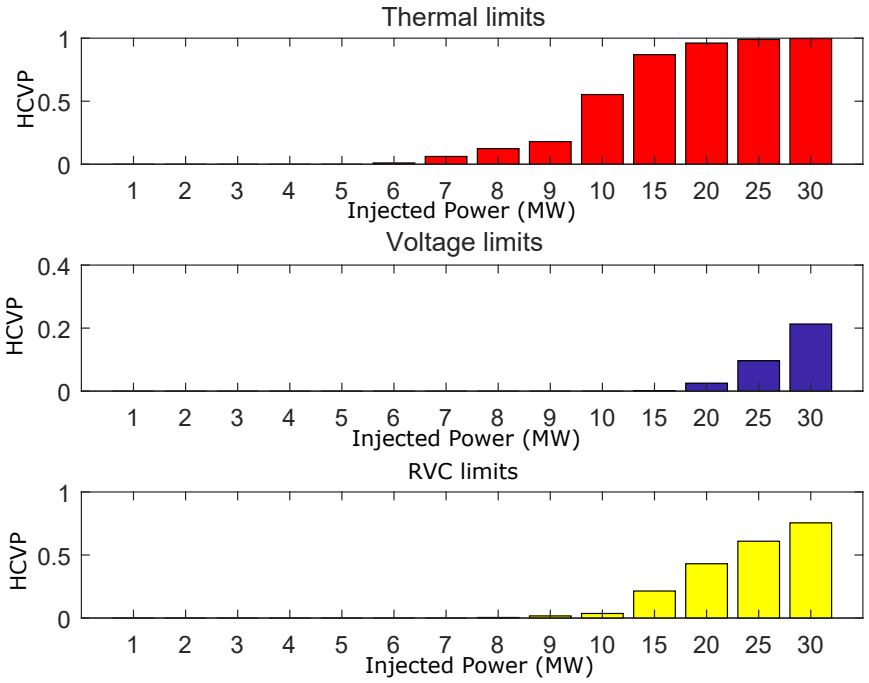

(a) HCVP for medium feeder category with PF1.

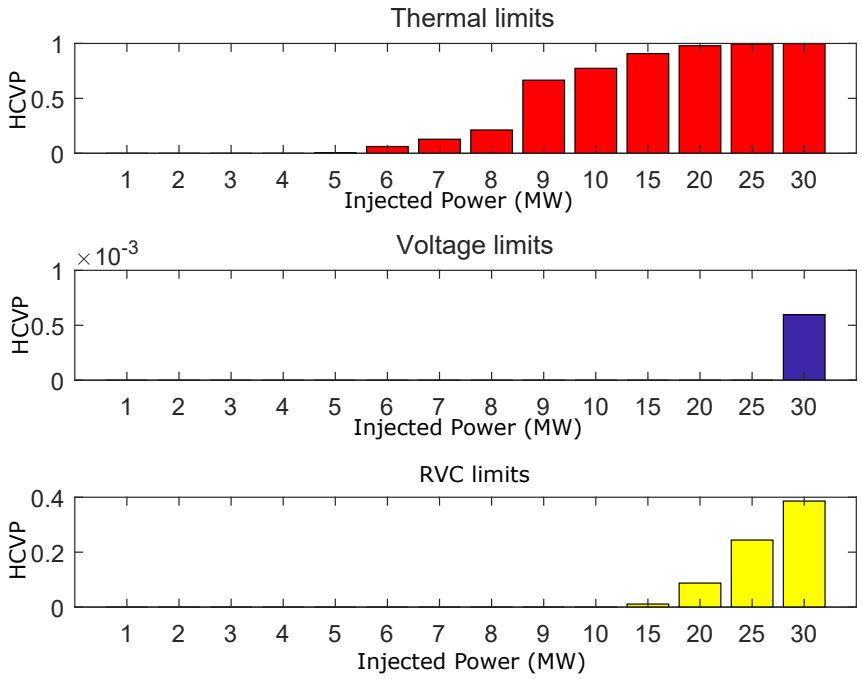

(b) HCVP for medium feeder category with PF0.9.

Figure 4.39: *HCVP for medium feeder category with different PF.*

Finally, Table 4.27 and 4.28 stress out the total number of violation of each constraints and the total number of scenarios for each active power injection by DGs to grid to calculate the HCVP for long feeder categories. In this tables also the amount of average and maximum values of current and voltage could be found. Then HCVP for this kind of feeder for both PF have been shown in Fig. 4.40.

By combining the three mentioned category to only one and finalize the results, there would be a possibility to compare the Monte Carlo for the complete grid and the Monte Carlo with combination of the Bricks approach. Hence, Table 4.29 and 4.30 represent the quantity of violated constraints, current and voltage of Aosta grid for the proposed method. Fig. 4.41 illustrates HCPV here.

The comparison between two different PF indicates that in case of reactive power injection the voltage could be controlled and the violated scenarios related to steady-state voltage and RVC could be decreased significantly. However, in this case due to some reverse power flow in the lines the number of violated thermal limit could be increased which in this case by changing the PF to 0.9 the total HC of Aosta city has increased slightly from 6MW to 7MW.

Table 4.27: *Monte Carlo with Bricks approach for long feeder categories, PF1.*

Power (MW)	No. of Thermal Limit Violation	No. of Steady-State Voltage Violation	No. of RVC Violation	Total No. of Scenario	Current (Mean) pu.	Current (Max) pu.	Voltage (Mean) pu.	Voltage (Max) pu.	RVC (Mean) pu.	RVC (Max) pu.
1	0	0	0	311	0.0688	0.3548	0.9927	1.0000	0.0086	0.0285
2	0	0	0	404	0.0575	0.3541	0.9948	1.0077	0.0103	0.0346
3	0	0	0	415	0.0555	0.5056	0.9966	1.0190	0.0120	0.0461
4	0	0	1	449	0.0629	0.6926	0.9989	1.0319	0.0142	0.0601
5	0	0	349	515	0.0817	0.8748	0.9977	1.0453	0.0132	0.0734
6	46	0	1699	631	0.1192	1.0508	1.0049	1.0565	0.0201	0.0863
7	646	0	3440	598	0.1468	1.2336	1.0020	1.0704	0.0172	0.0975
8	1653	0	5292	516	0.1449	1.3975	1.0088	1.0818	0.0240	0.1109
9	2779	0	7168	630	0.1769	1.6175	1.0096	1.0936	0.0247	0.1225
10	3928	42	9025	702	0.2092	1.8073	1.0106	1.1042	0.0257	0.1333
15	14769	2268	12732	632	0.3020	2.5701	1.0210	1.1573	0.0361	0.1838
20	18541	7545	16644	755	0.4372	3.5101	1.0271	1.1963	0.0422	0.2279
25	15694	8806	14875	585	0.5266	4.3063	1.0356	1.2390	0.0507	0.2656
30	16812	10513	16469	595	0.7327	4.9065	1.0476	1.2762	0.0627	0.3117

Table 4.28: *Monte Carlo with Bricks approach for long feeder categories, PF0.9.*

Power (MW)	No. of Thermal Limit Violation	No. of Steady-State Voltage Violation	No. of RVC Violation	Total No. of Scenario	Current (Mean) pu.	Current (Max) pu.	Voltage (Mean) pu.	Voltage (Max) pu.	RVC (Mean) pu.	RVC (Max) pu.
1	0	0	0	7267	0.0748	0.3548	0.9922	10.000	0.0082	0.0285
2	0	0	0	8406	0.0798	0.3796	0.9929	10.000	0.0087	0.0285
3	0	0	0	9096	0.0818	0.5939	0.9944	10.043	0.0100	0.0317
4	0	0	0	11301	0.1145	0.7956	0.9957	10.105	0.0111	0.0362
5	5	0	0	13433	0.1055	1.0049	0.9955	10.164	0.0110	0.0469
6	641	0	0	15123	0.1527	1.2040	0.9980	1.0220	0.0134	0.0530
7	1775	0	0	16324	0.1653	1.4147	0.9996	1.0272	0.0149	0.0571
8	3073	0	7	18315	0.2171	1.6128	1.0011	1.0321	0.0164	0.0620
9	10396	0	147	19368	0.2161	1.8158	1.0023	1.0370	0.0175	0.0658
10	14091	0	679	19036	0.2160	2.0341	1.0042	1.0407	0.0194	0.0708
15	16006	0	4731	17868	0.3810	2.9881	1.0083	1.0592	0.0235	0.0871
20	16806	0	8474	17196	0.5037	3.9395	1.0106	1.0729	0.0258	0.1017
25	16685	0	11422	16785	0.7482	4.7803	1.0168	1.0827	0.0319	0.1119
30	15552	0	12540	15591	0.7300	5.6168	1.0188	1.0915	0.0339	0.1210

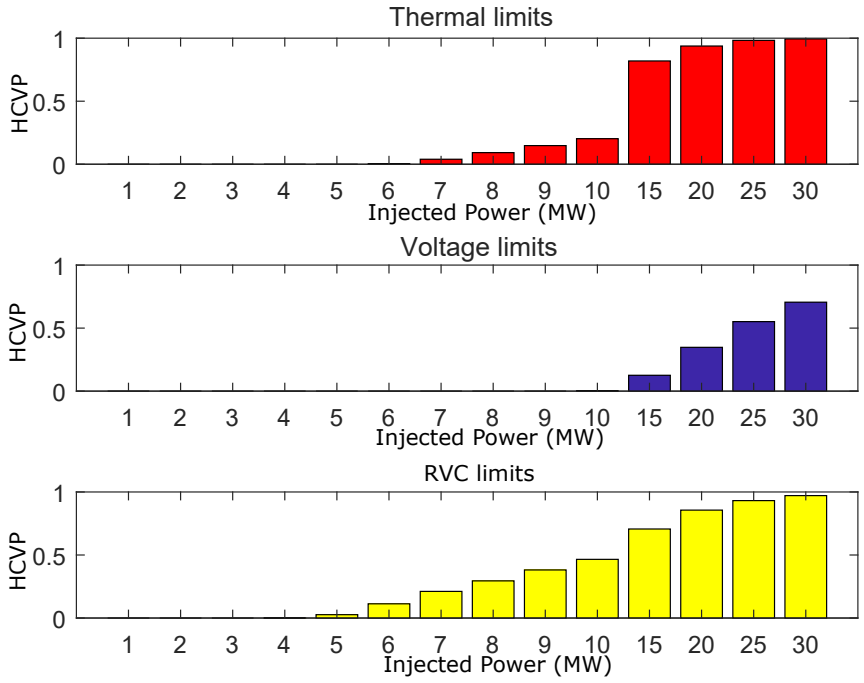

(a) HCVP for long feeder category with PF1.

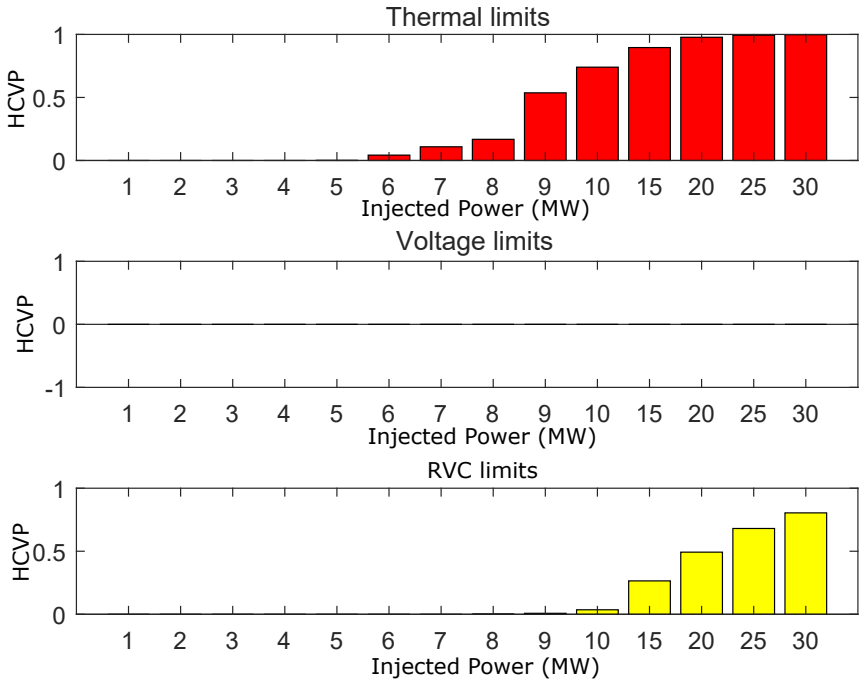

(b) HCVP for long feeder category with PF0.9.

Figure 4.40: *HCVP for long feeder category with different PF.*

Table 4.29: *Monte Carlo with Bricks approach for PF1.*

Power (MW)	No. of Thermal Limit Violation	No. of Steady-State Voltage Violation	No. of RVC Violation	Total No. of Scenario	Current (Mean) pu.	Current (Max) pu.	Voltage (Mean) pu.	Voltage (Max) pu.	RVC (Mean) pu.	RVC (Max) pu.
1	0	0	0	6563	0.0430	0.2356	0.9971	1.0012	0.0038	0.0133
2	0	0	0	6631	0.0427	0.3496	0.9981	1.0073	0.0047	0.0190
3	0	0	0	7075	0.0520	0.5202	0.999	1.0145	0.0056	0.0263
4	0	0	0	8036	0.0609	0.7104	1.0001	1.0225	0.0066	0.0346
5	0	0	116	9824	0.0858	0.8956	1	1.0306	0.0066	0.0426
6	80	0	566	11030	0.1228	1.0809	1.0031	1.0377	0.0096	0.0504
7	592	0	1147	11902	0.1442	1.2630	1.0028	1.0457	0.0093	0.0575
8	1366	0	1789	13033	0.1733	1.4427	1.0060	1.0528	0.0125	0.0652
9	2378	0	2478	13083	0.2124	1.6406	1.0061	1.0601	0.0125	0.0725
10	5498	14	3219	13824	0.2071	1.8194	1.0072	1.0669	0.0137	0.0793
15	11589	761	5522	13714	0.3459	2.6515	1.0132	1.1000	0.0197	0.1114
20	12603	2128	7380	13250	0.4453	3.5236	1.0175	1.1261	0.0240	0.1393
25	12021	3442	8161	12193	0.5898	4.3512	1.0210	1.1513	0.0275	0.1632
30	11702	4602	8718	11753	0.7039	5.0125	1.0276	1.1770	0.0340	0.1918

Table 4.30: *Monte Carlo with Bricks approach for PF0.9.*

Power (MW)	No. of Thermal Limit Violation	No. of Steady-State Voltage Violation	No. of RVC Violation	Total No. of Scenario	Current (Mean) pu.	Current (Max) pu.	Voltage (Mean) pu.	Voltage (Max) pu.	RVC (Mean) pu.	RVC (Max) pu.
1	0	0	0	6159	0.0592	0.3013	0.9947	1.0002	0.0056	0.0196
2	0	0	0	6530	0.0653	0.3870	0.9952	1.0008	0.0060	0.0202
3	0	0	0	7160	0.0830	0.5953	0.9964	1.0042	0.0070	0.0229
4	0	0	0	8551	0.1095	0.8030	0.9973	1.0090	0.0078	0.0265
5	21	0	0	10077	0.1040	1.0140	0.9971	1.0135	0.0077	0.0342
6	563	0	0	11146	0.1662	1.2116	0.9990	1.0178	0.0095	0.0389
7	1383	0	0	12147	0.1839	1.4241	1.0002	1.0219	0.0106	0.0422
8	2759	0	2	13163	0.2076	1.6201	1.0010	1.0257	0.0114	0.0460
9	8541	0	49	14098	0.2182	1.8265	1.0020	1.0296	0.0123	0.0491
10	10452	0	226	13836	0.2383	2.0438	1.0035	1.0326	0.0138	0.0530
15	12197	0	1642	13555	0.3728	2.9896	1.0065	1.0475	0.0168	0.0665
20	12594	0	3295	12888	0.5290	3.9085	1.0085	1.0588	0.0188	0.0783
25	12403	0	5078	12478	0.7895	4.7794	1.0131	1.0679	0.0233	0.0879
30	11715	3	6122	11743	0.7951	5.4800	1.0146	1.0750	0.0249	0.0950

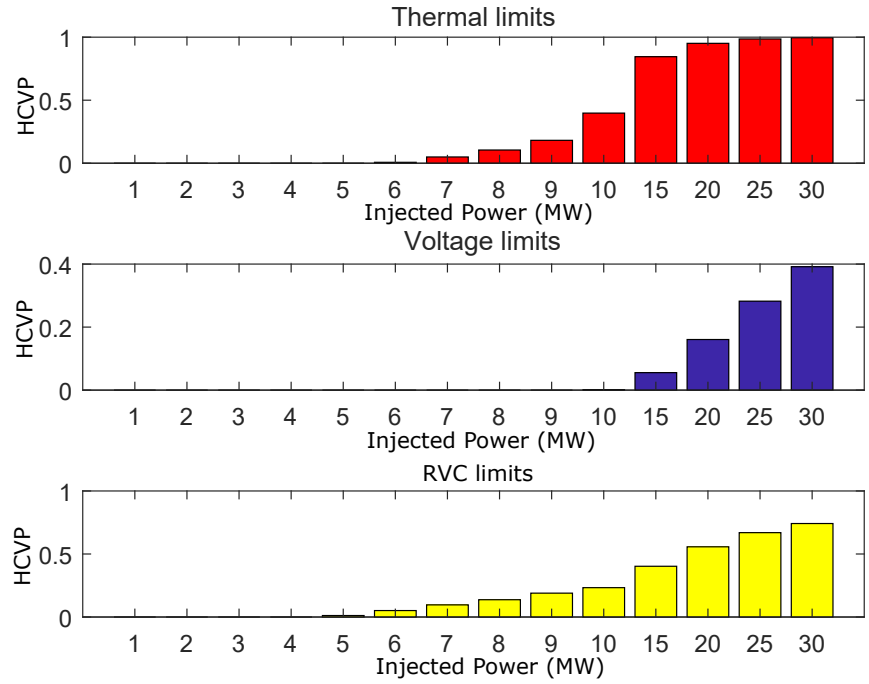

(a) HCVP for Bricks approach with PF1.

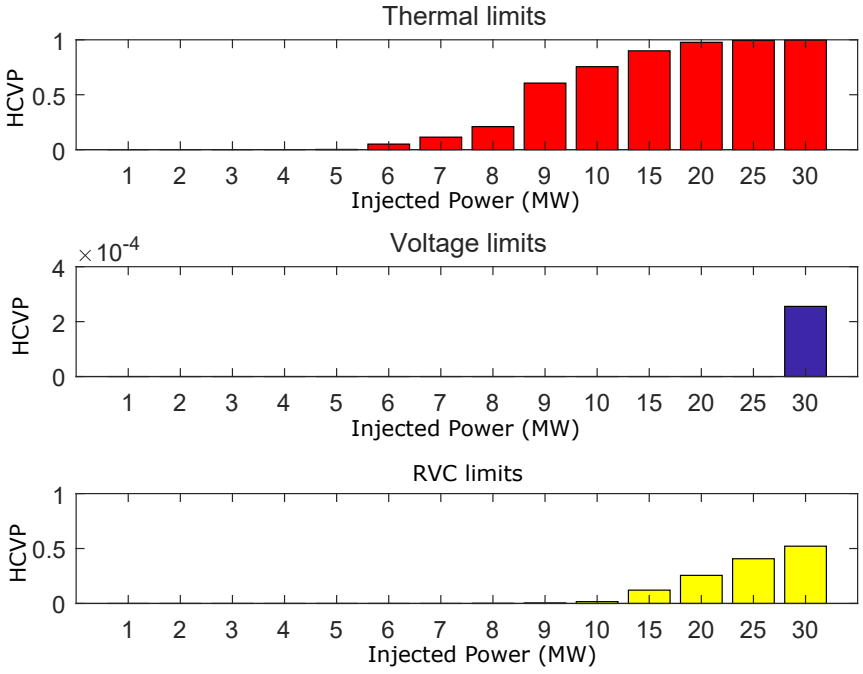

(b) HCVP for Bricks approach with PF0.9.

Figure 4.41: *HCVP for Bricks approach with different PF.*

Complete grid and Bricks Comparison

The main advantage of using combined MC simulation and Bricks approach in comparison with MC simulation for the complete grid is less computation time and required data. The computational time of MC simulation for the full grid is more than 680 hours, whereas for the combined method this amount is about 7 hours (intel i7 7700 - 16 GB Calculator).

As it has been discussed in the past paragraphs, the total HC of the Aosta grid for both methods is almost equal to 6MW for PF1 and in case of reactive power injection (PF0.9) this amount has been defined as 7MW. Hence, in order to show the accuracy of the proposed method, HCVP comparison for PF1 and PF0.9 have been demonstrated in Fig.4.42 and the relative error has been shown in Fig. 4.43. As it is clear from this picture, the median of all the boxes are less than 0.05% which shows a promising results.

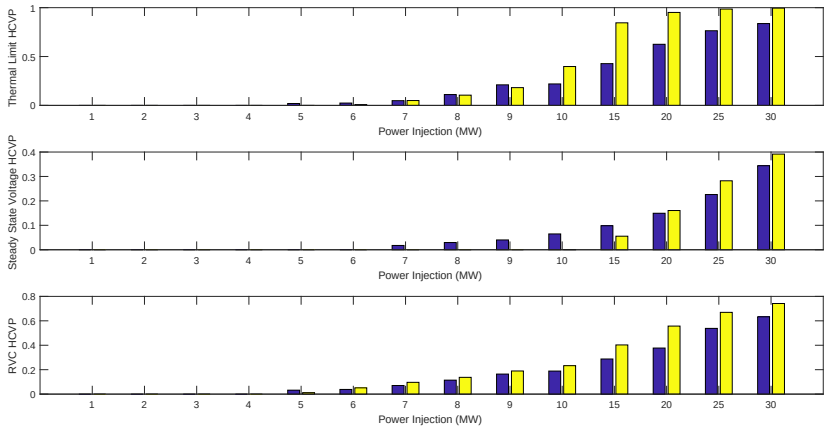

(a) HCVP comparison between complete grid and Bricks approach, PF1.

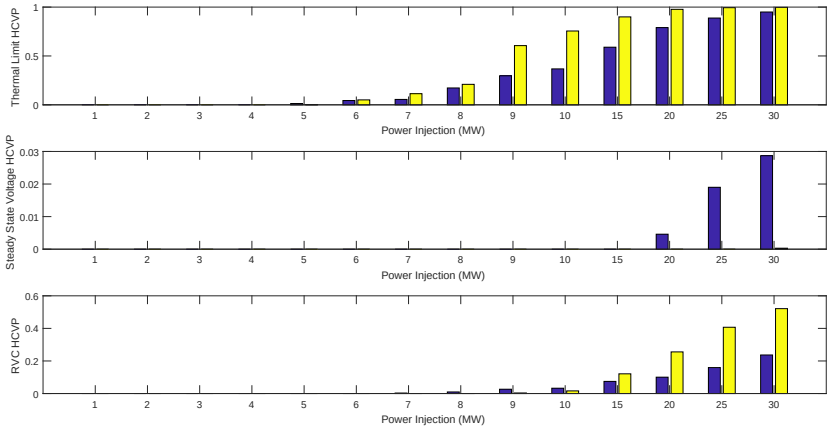

(b) HCVP comparison between complete grid and Bricks approach, PF0.9.

Figure 4.42: *HCVP comparison between complete grid and Bricks approach with different PF.*

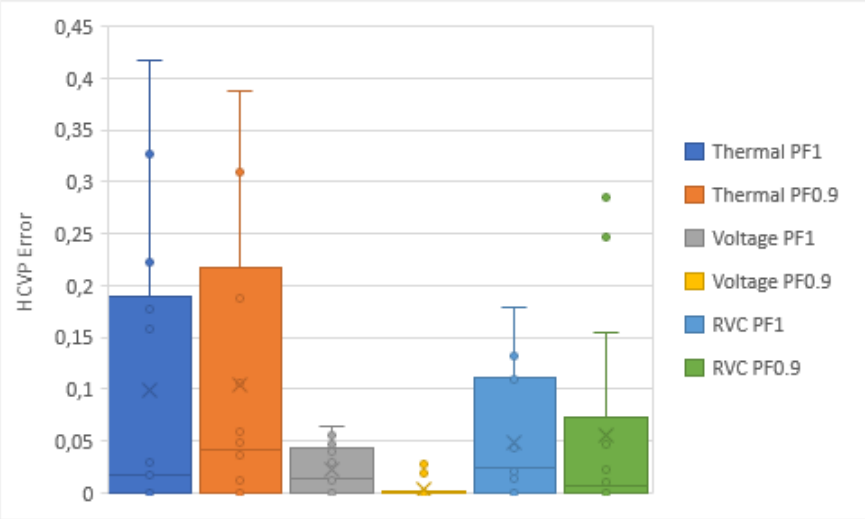

Figure 4.43: *HCVP error (%) both MC simulation and MC with Bricks approach.*

4.4 Electric Vehicle Hosting Capacity

The goal of this section is to evaluate the impact of the e-mobility hosting capacity charging processes on the electric grid, in a real-life study case. An effective approach is proposed to quantify the increase in the energy consumption on the grid with respect to both grid operation and efficiency.

Renewable energy sources are the main driver of the ongoing energy revolution all over the world. In order to manage RES, electric networks infrastructure, and the relevant regulatory and market frameworks, need to be properly updated. Similarly, there is a significant effort in the energy world toward a low carbon framework: one of the sectors which is experiencing important improvements is transportation. In 2011, the road transportation greenhouse gas emission was estimated 17% of the total 24% in the European Economic Area. Hence, European Commission has adopted a roadmap to cut 20% of transportation emission by 2030 and 60% by 2050 [236], [237], [238]. Therefore, transportation sector is shifting to electric mobility (e-mobility) and EVs that could reduce the CO2 emissions [239]. Actually, it is particularly important to evaluate which role the electric mobility could play in the new framework of the RES based electric grids.

Electric mobility could act as an elastic load; it could theoretically change its energetic behavior in order to fit at best with the energy balance of the grid. It is well known that a first step of integration in the electric grid is relevant to a control of the charging processes, in order to schedule them at best [240] or to limit them in case of a grid congestion [241]. A second, more advanced, step is the so called vehicle-to-grid approach, that is an active role of the e-mobility batteries injecting when is necessary (e.g. in case of a system under-frequency transient). The research of this part of the thesis is focused on the first step, i.e. the goal of the work is to evaluate the impact of the e-mobility charging processes on the distribution grid, in a real life study case, to manage such an increase in the energy consumption with respect to both the grid operational and efficiency parameters.

Some research has been done focusing on EVs management in the literature to schedule the charge of EVs optimally. In [241], [242], [243], [244], [245] the day-ahead forecasting techniques of EV load have been used to minimize the energy cost or to maximize the operators profit by creating the charging

process schedule. Heuristic approach based on particle swarm optimization is used in [246] to determine the allocation of EVs. In this study, the power flow procedure is run before the optimization process. The possibility of discharging batteries to provide energy to the grid is evaluated in [246]. The offline optimization which has been used in this research presents some limitations in terms of flexibility in the management of unexpected working conditions. The works in [243] and [242] are based on online procedures. The method proposed in [242] is based on using the preliminary optimization that could define the set-point for each charging station. Moreover, a controller implemented in the charging station schedules the charge requests. The network operation effects on the charge requests constraints, and the advantages of the scheduling procedure on the power system, have not been studied in depth, as the infrastructure of electricity distribution is not modeled in this study. In [243], the power grid is divided in zones; the spatially distributed optimization procedure performed for each zone independently leads to local optimal. For this reason, this method does not address network-wide issues and constraints.

Another important topic to be addressed evaluating the E-mobility evolution is relevant to the regulatory framework. In fact, charging stations could be classified in public and private points. In the first case, private users will have to activate two different supply contracts and two different meters; this could open to advanced energy price tariff focused on e-mobility. Similarly, private charging stations could be activated and managed for a public use; in this case the owner will act as an energy supplier, eventually providing additional services. In case of public charging points, it is mandatory to guarantee a nondiscriminatory access to the area; they could be managed by DSO or in order to foster competition, by new e-mobility operators. Investment cost could be covered by revenues on the access fees, eventually incentive schemes could be proposed by the National Regulatory Authorities in order to foster the e-mobility growth. Since this topic is particularly debated and worth an investigation, in the following a focus is dedicated to the regulatory framework evaluation.

4.4.1 Sustainable Mobility Legislation

The Italian legislation concerning the alternative fuels adopted in the transport sector evolved in the last decade moving from the acknowledgment and the adoption of European Directives, contextualized in the energy strategy "EU2020" put in place by the European Commission (EC). In particular, the strategy for Europe-2020 [247] promotes the diffusion of sustainable mobility looking after three main issues:

- The definition of common technical standards.
- The development of the required infrastructure.
- The incentivization of research in transport field.

Specifically, foreseen policies in Transport2050 [237] roadmap by EC has ambitious targets:

- CO2 emissions reduction from the transport sector by 60%.
- Strong effort towards the usage of zero and low emissions EV and Hybrid Electric vehicles (HEV).
- Prevalent presence of ecological vehicles in urban areas.

Moreover Directive 2009/33/EC [248], concerning the promotion of green and low consumption vehicles, defined the target of 10% renewable energy quota in transport sector by 2020; these actions

are included in a general framework where the diffusion of EV and HEV is promoted together with a required continuous reduction of green house gases emission by traditional, internal combustion engine based vehicles [249].

Following the 2020 package and the actions urged for the transport sector by EC, many associations have been called to express their position at European and national level; the relevant documents have been exploited to define policies to be implemented in Italy [250], [251], [252].

As a first result of the EU directives, since 2010 ARERA, the National Regulation Authority of Italy, sustained electrical mobility through a series of actions, with reference to both private charging systems and public ones. With Decision 56/2010 [253] ARERA introduced a general system charge and a grid services tariff for private charging systems, deleting the legislative constraints that could impede the installation of new charging points; right after, with Decision 242/2010 [254], a new tariff for public charging systems has been introduced: this tariff entered in force in 2011 and is updated every three months. Within the same decision, ARERA launched a series of pilot projects concerning the development of infrastructures for the charging of EV; these pilot projects have been selected with the Decision 96/2011 [255] and ended in 2015, bringing to relevant results.

More recently, the European and Italian legislation concerning the promotion of EV moved from two main measures:

- EU Directive 2014/94/EU.
- Law of 7 August 2012 n. 134 by the Italian Parliament.

Starting from the guidelines identified by the two documents at European and Italian level, it has been possible to define the deployment plans for EV charging infrastructures, the technical rules concerning modes and type of connections required for EV charging systems, and all regulatory aspects concerning the management of EV charging points. On October 2014, European Parliament published the Directive 2014/94/EU [256] defining the main options for the diffusion of alternative fuels in the transport sector. The document individuated main obstacles for the diffusion of new mobility solutions in:

- Absence of a physical infrastructure for distribution of alternative fuels.
- Absence of a common reference framework concerning technical rules and standards.

These two issues are correlated to the lack of awareness regarding alternative fuels by EU citizens, the inability to develop economy of scale in this sector, in terms of both demand and offer of zero emissions vehicles. The directive sets four main classes of actions to be taken by the member states:

- Deployment of an adequate number of public charging points by 2020 in urban areas and by 2025 in sub-urban and high-density areas, with the request to guarantee different technical solutions (AC/DC technologies with different power and voltage levels) and a non-discriminatory access to charging infrastructure both from the operators side, promoting a competitive market for charging points management, and from the user side, allowing the purchasing of different types of services involving the charging process.
- Definition of a national strategic framework for an effective development of the alternative fuels market, taking into consideration the key issues for the transport sector at a national level and the requests coming from regional and local entities.

- Provision of all the information needed by citizens and stakeholders in a clear and coherent way, in order to favor the use of advanced technological solutions within the charging infrastructures and the diffusion of new mobility habits.
- Requirement to present a document to EC within November 2019 (and since then every three years) to report about all national measures undertaken in order to sustain the diffusion of alternative fuels from the juridical, strategic and development point of view.

Italy has acknowledged and applied the EU directive with Law n.134 of August 2012, defining the development of a national charging infrastructure for EV as a priority among the actions to be implemented in the 2020 panorama. Under the light of this law, since 2013 Italy defined a national infrastructural plan for the charging of electric vehicles (PNire [257]), further developed with Law of 16 December 2016 n.257 [258]. The plan defines the guidelines to establish a diffuse development of charging stations for EV all over the Italian territory, starting from a series of measures involving:

- Institution of an EV charging service, for both private and public transport, which is coherent with the EU framework.
- Introduction of management procedures for the services to be delivered in charging stations, particularly concerning the costs to be sustained by the users, the presence of a differentiated system tariffs and the regulation of modes, time and connections required for the charging process, taking care of the needs of users and electric grid.
- Introduction of incentives and facilitation for the operators of the charging stations to favor the updating of services offered.
- Realization of specific programs to promote the technological update of the existing private and public buildings, in order to integrate EV charging solutions.
- Promotion of research activities in all the fields concerning the development of new solutions for EV charging processes, and all the aspects related to sustainable mobility.

The PNire implementation has been divided into two different steps:

- Phase 1 (2013-2016), where institutions are called to define a reference framework for the infrastructural development and implement a first technological deployment which can guarantee the EV motion within urban areas.
- Phase 2 (2017-2020), where EU member states, stakeholders (such as car builders and normative entities) and national authorities are called to define harmonized standards to favor the diffusion of sustainable solutions, and charging infrastructure must be completed to be able to host a high and increasing level of EV penetration.

According to EU directives, Italian legislation defined four main charging modes, differentiated on the basis of the power provided during charging process, and consequently the time needed to charge an EV's battery. This classification distinguishes slow, fast and very fast charging process, going from 7.4 kW of power provided (slow) up to more than 50 kW (very fast). The different technological solutions which can be adopted have been declined by Italian legislation according to different charging scenarios.

In the first scenario the charging process is supposed to last for a long time: this is the case of charging points at workplaces or in residential areas, where charging process is carried out during the whole day or at night-time. In this case low power (7 kW) charging points are required, and two connection plugs are needed.

In the second scenario the charging process lasts for less than two hours, such as in the case of commercial areas where tertiary services are provided; therefore, medium power charging points are requested, with the possibility to charge more than one vehicle at the same time from a single charging station. In this case the typical power provided is around 20 kW.

In the third scenario the time foreseen for the charging process is reduced, typically below 30 minutes. In this case, high power solutions, both in AC and in DC, are required, to guarantee flexibility and high performances; hence, advanced combined charging systems must be implemented. It is important to notice that in every case the charging process must be guaranteed independently from the necessity for the user to conclude a deal exclusively with the operators of charging stations; moreover, the provision of the charging process should be developed as the selling of a service and not of a good. Consequently, advanced solutions concerning the metering of energy provided, the monitoring of relevant parameters and the optimization of charging process can be a part of the service purchased by the user.

Finally, the realization of charging infrastructure must be carried out through proper agreements with the local administrations and DSOs, in order to exploit the knowledge of the territorial needs and to verify the limits due to the electricity distribution grid.

4.4.2 Proposed E-mobility Hosting Capacity Charging Process

One of the biggest challenge for DSOs is the use of an intelligent control for managing power fluctuation due to passive and active users, to have more reliable and efficient networks [259]. In the DSO perspective, it is very important to guarantee a reliable management of the distribution grid, consequently proper planning and operational tools are required. Actually, the increasing of EV utilization may cause overload and undervoltage disturbances on the distribution grid [260], [261].

With respect to DGs, in the literature a lot of works propose a KPI approach, Section 2.2, to evaluate the maximum amount of incremental generation that system can manage according to grid technical constraints (such as steady-state voltage variation, thermal limits and Rapid Voltage Changes RVC). On the other hand, increasing the end-user electricity requirements is the main issue from the demand side, which is leading to evaluate the operational margins [241]. Hence, here a similar approach is proposed in order to evaluate the maximum amount of e-mobility charging processes which the grid could manage.

The KPI approach proposed for the evaluation of the e-mobility charging processes on the distribution grid is based on a Monte Carlo algorithm discussed in Section 4.3.1. Scenarios are evaluated thanks to performance indices typically adopted for hosting capacity evaluation in Section 2.2: steady-state voltage variation, line thermal limit and rapid voltage change and grid efficiency which is explained in the following.

Grid Efficiency: Losses on MV feeders can be evaluated as a further performance index; in particular such an index will be adopted to compare the efficiency of the electric grid in supporting different e-mobility penetration scenarios, and allow to compare each other the grid performances with respect to different assumptions in the e-mobility parameters.

In order to model e-mobility energy needs, the developed MC procedure is based on different assumptions. In the performed simulation, a charging station has been supposed in place in every secondary substation of the passive grid and for the second step in the active grid, in order to evaluate the impact of DG presence on the electric vehicle on distribution grid. In this regard, three different charging modes have been proposed, coherently with the scenarios detailed in Section 4.4.1. Namely, 3 kW (the most common solution in place in Italy for domestic and slow charging process), 20 kW (selected to represent fast public charging station) and 50 kW (a charging power equal to 50 kW has been supposed as a realistic, short/medium term assumption for very fast charging station) have been selected as slow, fast and very fast recharge processing respectively. Each charging station has the same probability to be selected, while a roulette wheel selection has been used in order to select the node where a new e-car is asking for a recharge.

A second roulette wheel has been adopted in order to choose the nominal power of each charging process, i.e. to simulate different charging technologies for different vehicles. Three different distributions of each mode have been considered; the first distribution has been tested for mainly slow domestic recharge process, the second one is mainly fast process and the last one is considered prevalence very fast process. In the following the probability of each technology has been mentioned.

- Simulation SET1: 80% slow + 10% fast + 10% vary fast.

- Simulation SET2: 20% slow + 60% fast + 20% very fast.

- Simulation SET3: 10% slow + 10% fast + 80% very fast.

Similarly, adopting a third roulette wheel, a different distribution of arrival-departure time has been modeled for each vehicle (i.e. different charging time). For each hour of the year, the algorithm simulates the charging processes (increasing them iteratively) and checks the KPI devoted to evaluating the quality of supply, up to a predefined operational limit. Simulations are defined with respect to different assumptions. The slow recharge process time is concentrated on late evening and each charging process will last for 7 hours (21 kWh). In this charging process, only one recharge per car in each single day is allowed. High probability for using fast recharge process in late morning and afternoon has been assumed, each charging process will last for 2 hours (40 kWh) and (as domestic charging process) only one recharge per each car in each single day is permissible. The very fast process time has more probability from 8 a.m. to 22 p.m. as the charging process will last only one single hour (50 kWh) and two recharge processes in each day could be done by each electric car. Table 4.31 represents the summary of time probability adopted for the study and Fig. 4.44 and 4.45 show the flowchart of the proposed approach for passive and active network respectively.

Table 4.31: *Time distribution in different charging technology.*

Charging Mode	Power (kW)	Time Probability		Charging Time (h)	Daily Charge (each car)
Slow	3	12am-6pm 6pm-12am	0.1 1	7	1
Fast	20	12am-10am 10am-3pm 3pm-6pm 6pm-12am	0.1 1 0.1 1	2	1
Very Fast	50	8am-10pm 10pm-8am	1 0.1	1	2

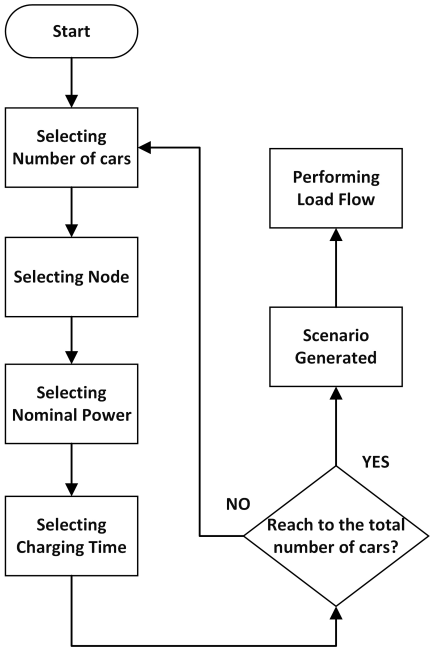

Figure 4.44: *Monte Carlo flowchart for E-mobility charging process for passive network.*

The same as evaluating HC for multi-generator scenario the Monte Carlo procedure is based on an iterative behavior and equation 4.13 and 4.14 represent the convergence criterion based on μ_{Loss} and σ_{Loss}, the losses mean value and the losses standard deviation respectively. The variation of these two values should be placed lower than ϵ. In order to have a more robust criterion this procedure is repeating 5 times continuously.

Once the simulation for passive network has performed and the results are obtained, the procedure has been implemented again to evaluate the e-mobility charging process on the active network, as it is expected the presence of DG could increase the capacity of electrical vehicle on the grid. To do so, two Monte Carlo simulation need to be performed. The first one is devoted to locating and sizing different DGs for the under-studied grid according to the total HC of the it, and the second MC simulation is related to e-mobility charging process. In Section 4.4.4, both passive and active network results are presented.

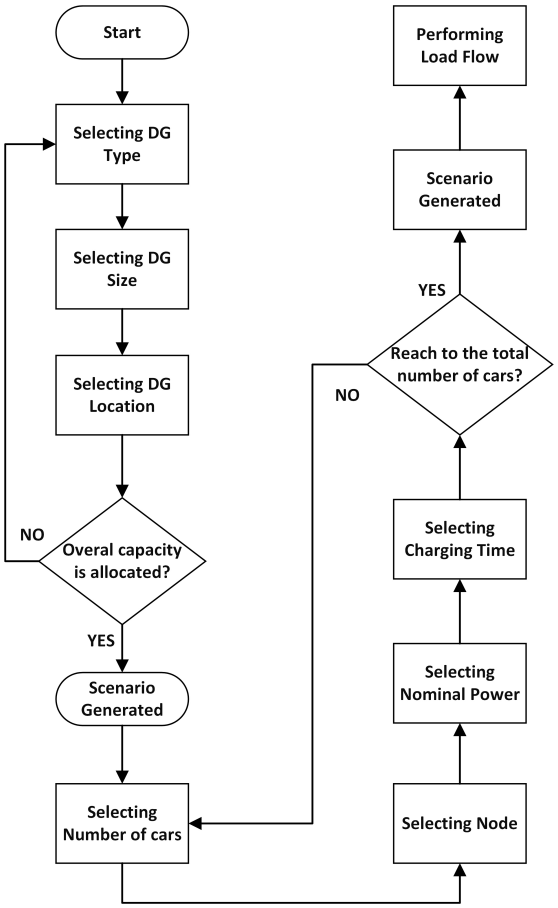

Figure 4.45: *Monte Carlo flowchart for E-mobility charging process for active network.*

4.4.3 Validation of the Proposed Approach

San Severino Marche, with 193 km^2 area, is a small town in the center of Italy; its 20 kV distribution grid has a total length of 180 km. Fig 4.46 shows the energy demand during a year, simulated in this research exploiting the realistic assumptions on the load. Two transformers are placed in the primary substation; six feeders depart from one transformer and seven from the other one. Fig. 4.47 shows this structure, in which the red busbar has 104 km and the green busbar has 76 km. In the past, the area reported a significant amount of hydro resources while, recently, photovoltaic penetration rises each year. Moreover, due to the agricultural activities, good opportunities are also related to biomasses. The energy needs of the loads are quite limited, consequently a reverse power flow regularly occurs, especially during summer time. Figure 4.48 demonstrates the power exchange measured at the HV/MV interface, the green color is standard (passive) operation and the red one is in reverse power flow condition.

A peak demand of the grid is 53.55 MW where 370 generators by total amount of 27.6 MW are connected to it. The main typologies of generators are solar, wind, and hydro from rivers, where the generation profile of them have been presented in Fig. 4.49 (a)-(c).

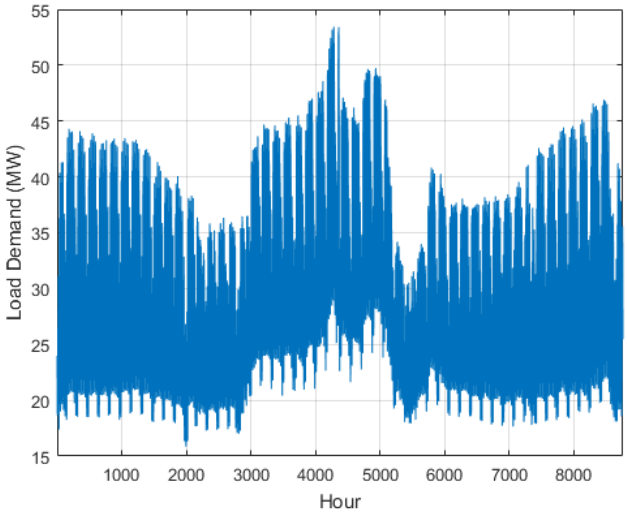

Figure 4.46: *Yearly energy demand in San Severino Marche..*

Thanks to past experimental projects, the area is already provided with an advanced communication architecture, allowing the exchange of real-time signals/data between the DSO's control center and the users; in particular the communication system is based on fiber optic, Wi-Fi bridges, and mobile network (LTE). Moreover, the Smart Grid core unit is linked to the DSO SCADA/DMS and to a set of monitoring apparatuses deployed in primary and secondary substations to properly collect real time measurements about the grid operation [262]. Finally, weather nowcast and forecast equipment are going to be deployed in order to estimate in real time and in advance RES production [246].

Actually, the Smart Grid architecture is designed to provide in perspective advanced services to the DSO:

- DERs production forecast on a multi-scale time window to provide advices to DSO.
- Real-time and predictive state estimation of MV network.
- Evaluation of the network performance indexes (energy losses, hosting capacity, etc.).
- Identification of the optimal grid topology to be adopted (i.e. which switching devices should be opened or closed, and for how long, to optimize the grid operation according to given KPIs).
- Warnings about possible problems expected on the network in the next future.
- Provision of ancillary services from the active users equipped with Energy Storage Systems.

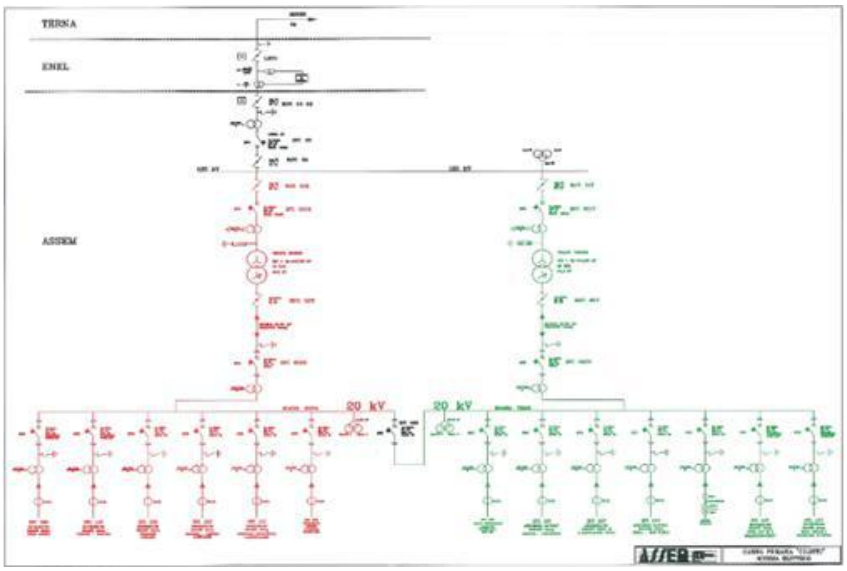

Figure 4.47: *San Severino Marche PS detailed in two transformers and 13 feeders.*

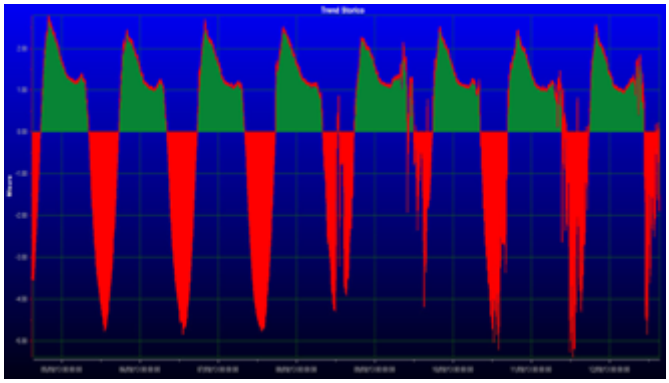

Figure 4.48: *Reverse power flow in San Severino Marche network.*

4.4.4 Results and Discussion

In order to validate the proposed procedure in section 4.4.2, it has been tested on an equivalent model of the San Severino distribution grid, and several simulations have been performed for both passive and active network. In particular, for each single simulation set, the number of 1000, 2000, 3000 and 4000 electric cars have been connected to the grid nodes.

Passive Distribution Network

In the following, Table 4.32, Fig. 4.50 and 4.51, a detailed analysis of the aforementioned simulations for the passive network is reported; results are relevant to a whole year scenario and samples are detailed for each single hour. The focus is in the evaluation of the distribution grid e-mobility hosting capacity and in the quantification of the relevant impact on losses. Simulated Scenarios are detailed with respect to different assumptions on the e-mobility penetration in the area (power absorbed during the charge processes, number of charges in a day, travel length average, etc.).

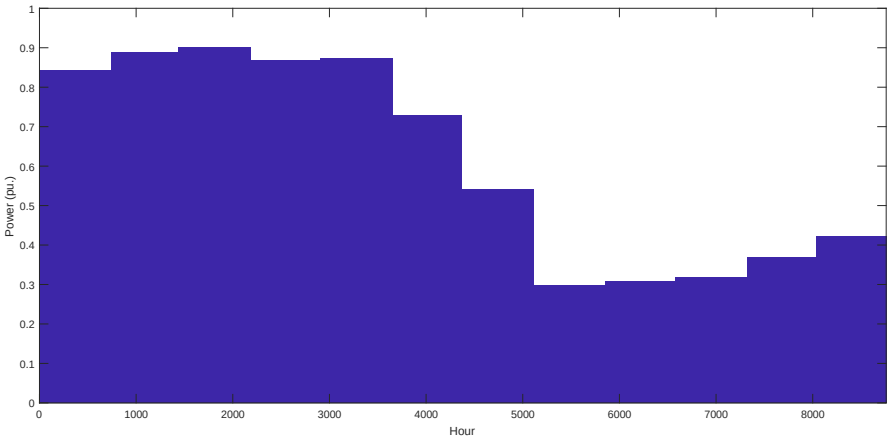

(a) Yearly Hydroelectric profile.

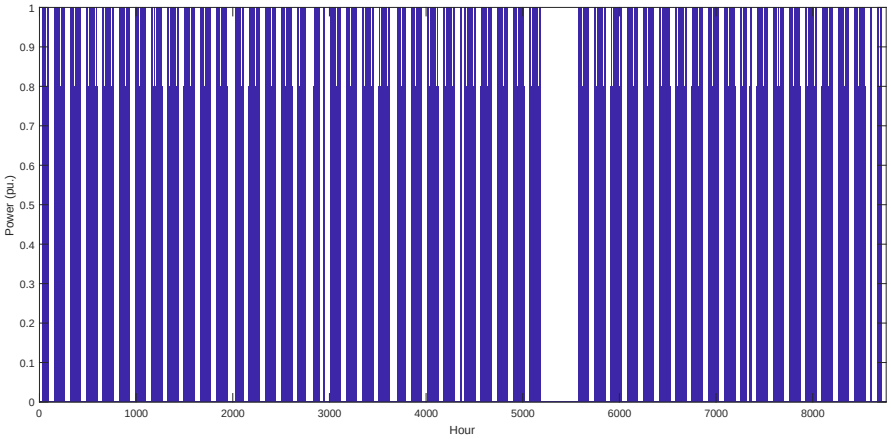

(b) Yearly Thermoelectric profile.

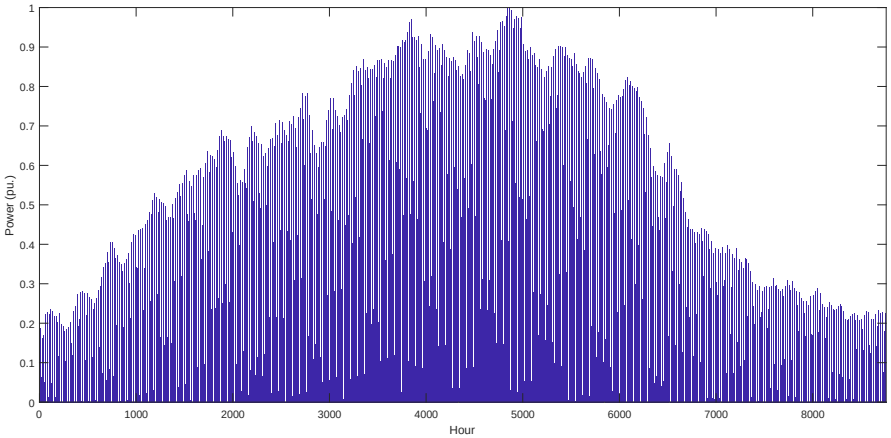

(c) Yearly PV profile.

Figure 4.49: *San Severino Marche DG yearly profile.*

After performing MC simulation for the mentioned number of cars and for each simulation set, the results were evaluated according to the technical constraints; Table 4.32 represents these results. For each simulation set hosting capacity limits are reported: min voltage steady state, max current over the feeders, rapid voltage changes and yearly losses over lines. According to this table, we can conclude that the hosting capacity of connecting electric cars to San Severino Marche grid is less than 4000, 2000 and 2000 cars for simulation SET1, SET2 and SET3 respectively. Actually, the table reports the KPI analysis up to the identification of an index violation. In all the performed simulations the limiting factor results to be the maximum current over the grid branches. Based on the classified assumptions in the Simulation SET1 (charging processes mainly based on domestic and slow processes) the grid under study shows an overcurrent equal to 114.94% of the nominal one in managing lower than 4000 e-cars. Adopting assumption corresponding to the Simulation SET2 (charging processes mainly based on fast public charging station) the hosting capacity results limited to less than 2000 cars (overcurrent up to 120.81% are detected). Finally, Simulation SET3 assumption drives to an even higher overcurrent, depicting a grid hosting capacity slightly higher than 1000 e-cars. Moreover, faster charging process could bring increase of system losses.

Figure 4.50 shows the transformer power flow after adding 1000 cars in the grid for each simulation set. As obvious, the power flow increased where the charging process is faster. In addition, Figure 4.51 magnifies these amounts for one single week. It can be seen that, in simulation SET1 and SET2 the peak values could be changed in hours of the day by high probability of charging cars, however in simulation SET3 the peak values are focused in daylight hours, that is critical load fluctuation over a single day could arise (such a result is coherent with respect to the assumptions adopted in the models developed for this study).

Table 4.32: *Monte Carlo results for 3 different recharge processing distribution in passive network.*

Test Case Without Gen		Voltage (pu.)			Thermal Limit (I/Imax)		RVC (pu.)		Loss/Energy
		Min	Mean	Max	Mean	Max	Mean	Max	Mean
SET1	1000 Cars	0.9843	0.9965	1.0004	0.0442	0.7872	1.1e-4	1.8e-3	0.8427
	2000 Cars	0.9764	0.9954	1.0003	0.0628	0.8765	2.3e-4	2.17e-3	0.9854
	3000 Cars	0.9698	0.9943	1.0002	0.0768	0.9860	3.4e-4	2.49e-3	1.1519
	4000 Cars	0.9619	0.9932	1.0001	0.0910	1.1494	4.5e-4	3.12e-3	1.3525
SET2	1000 Cars	0.9665	0.9945	1.0002	0.0742	0.0876	1.8e-4	1.53e-3	0.9597
	2000 Cars	0.9676	0.9941	1.0001	0.0788	1.0546	5.3e-4	3.94e-3	1.2736
	3000 Cars	0.9556	0.9923	1.0001	0.1010	1.3077	7.1e-4	4.12e-3	1.6102
SET3	1000 Cars	0.9665	0.9945	1.0002	0.0742	1.0472	3.2e-4	3.16e-3	1.2403
	2000 Cars	0.9466	0.9913	1.0001	0.1139	1.4737	6.4e-4	4.87e-3	1.9212

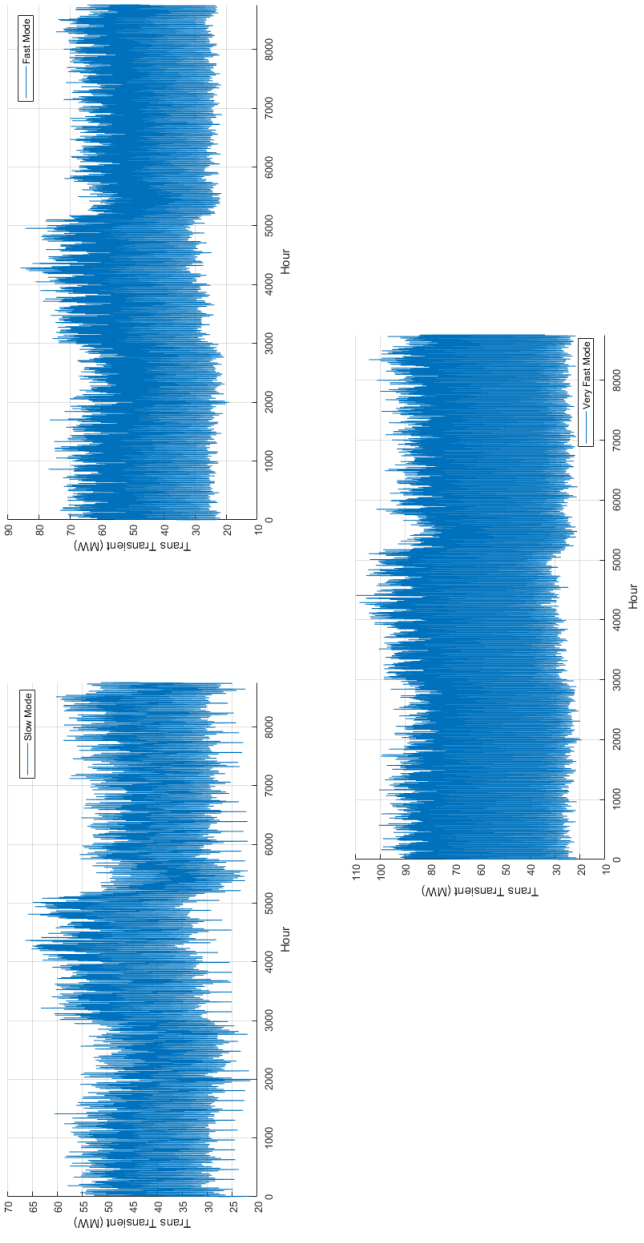

Figure 4.50: *Different testing mode transformer transient for 1000 cars.*

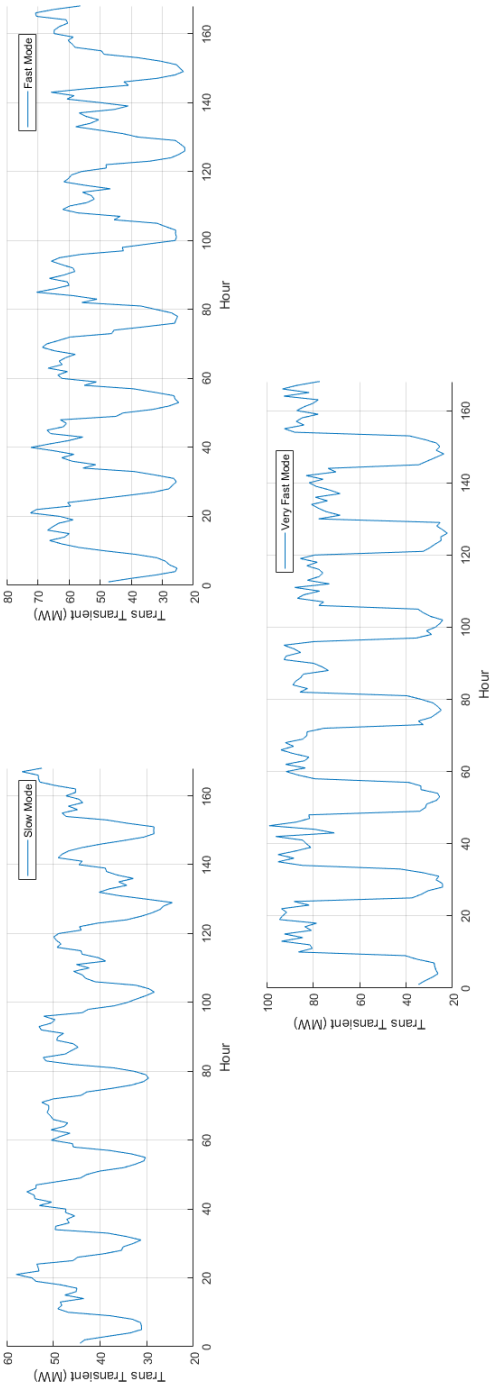

Figure 4.51: *Different testing mode transformer transient for 1000 cars in one week.*

Active Distribution Network

As already mentioned in the introduction, the aim of this thesis is expecting different impact on the grid. Hence, DG could be useful to manage more e-cars on the grid. In order to have an active distribution grid considering three defined type of DG, in san Severino Marche including PV, hydroelectric and thermoelectric a Monte Carlo simulation has been performed to find a distribution of the DG in the grid. Fig. 4.52 shows the percentage of each DG type in this network for the total HC of 7MW.

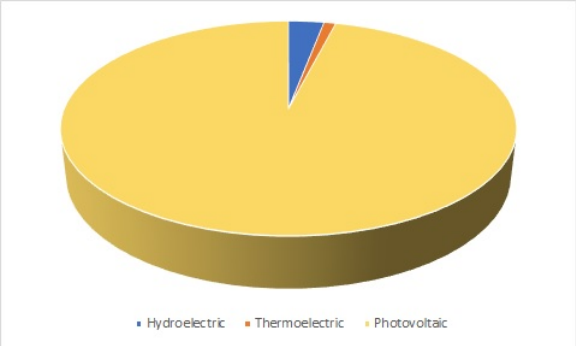

Figure 4.52: *Installed different DG percentage in San Severino Marche.*

After locating 7MW DGs in the grid, by performing MC simulation the possible number of charging cars without causing any grid reliability issues could be defined. The aforementioned procedure has been repeated for different power factor. In the following, Table 4.33 and 4.34 report the system losses and the value for each constraints.

Table 4.33: *Monte Carlo results for 3 different recharge processing distribution in active network, PF1.*

Test Case Without Gen		Voltage (pu.)			Thermal Limit (I/Imax)		RVC (pu.)		Loss/Energy
		Min	Mean	Max	Mean	Max	Mean	Max	Mean
SET1	1000 Cars	0.9847	0.9971	1.0032	0.0467	0.6723	1.9e-4	2.30e-3	0.7523
	2000 Cars	0.9815	0.9960	1.0029	0.0595	0.8102	3.1e-4	2.73e-3	0.8791
	3000 Cars	0.9745	0.9949	1.0025	0.0730	0.9661	4.3e-4	2.99e-3	1.0445
	4000 Cars	0.9669	0.9937	1.0021	0.0867	1.1338	5.3e-4	3.34e-3	1.2311
SET2	1000 Cars	0.9821	0.9965	1.0033	0.0542	0.7322	2.4e-4	1.61e-3	0.8567
	2000 Cars	0.9682	0.9947	1.0034	0.0752	1.1401	5.8e-4	4.32e-3	1.1450
	3000 Cars	0.9608	0.9929	1.0030	0.0969	1.2864	7.9e-4	4.83e-3	1.4747
SET3	1000 Cars	0.9734	0.9963	1.0036	0.0711	1.0248	3.8e-4	3.54e-3	1.1340
	2000 Cars	0.9536	0.9923	1.0035	0.1100	1.4588	6.9e-4	5.35e-3	1.7936

By comparing the results of these tables with the similar table in passive network it could be found that the losses are decreasing in active network. Moreover, it can be decresed more, if there will be an ability of voltage control by reactive power injection. Active grid leads slightly voltage increasing, however by reactive power injection from DG, the voltage rising could be controlled, Fig 4.53 shows this trend. Since the limiting factor in this network is thermal limit, by reactive power voltage control the amount of hosting capacity is still remain almost the same.

Table 4.34: *Monte Carlo results for different recharge processing distribution in active network, PF0.9.*

Test Case Without Gen		Voltage (pu.)			Thermal Limit (I/Imax)		RVC (pu.)		Loss/Energy
		Min	Mean	Max	Mean	Max	Mean	Max	Mean
SET1	1000 Cars	0.9847	0.9965	1.0021	0.0489	0.6736	1.6e-4	2.12e-3	0.7519
	2000 Cars	0.9765	0.9954	1.0018	0.0628	0.8436	2.8e-4	2.52e-3	0.8784
	3000 Cars	0.9704	0.9943	1.0015	0.0768	0.9709	3.9e-4	2.73e-3	1.0439
	4000 Cars	0.9634	0.9932	1.0009	0.0910	1.1498	4.9e-4	3.14e-3	1.2309
SET2	1000 Cars	0.9739	0.9853	1.0021	0.0542	0.7852	2.1e-4	1.47e-3	0.8557
	2000 Cars	0.9512	0.9932	1.0026	0.0752	1.1544	5.3e-4	3.97e-3	1.1416
	3000 Cars	0.9403	0.9901	1.0029	0.0969	1.3113	7.5e-4	4.36e-3	1.4703
SET3	1000 Cars	0.9727	0.9951	1.0034	0.0721	1.0389	3.2e-4	3.32e-3	1.1260
	2000 Cars	0.9470	0.9919	1.0032	0.1110	1.5181	6.3e-4	4.59e-3	1.7915

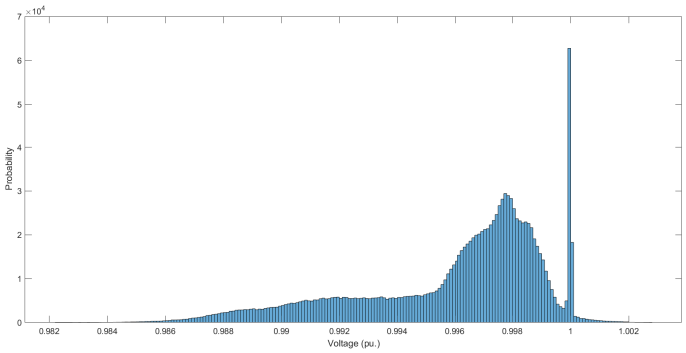

(a) Voltage histogram for 2000 cars with slow charging technology, PF1.

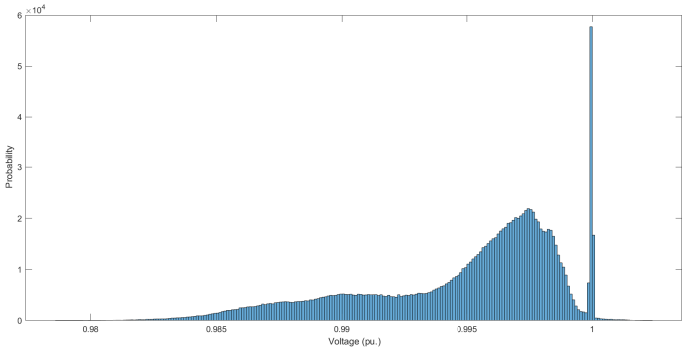

(b) Voltage histogram for 2000 cars with slow charging technology, PF0.9.

Figure 4.53: *Yearly voltage profile histogram.*

4.5 Summary

Increasing penetration of distributed energy resources in distribution network needs active network management as it could cause system voltage violations and overloading. Hence, nowadays evaluating the maximum hosted generation by distribution grid (Hosting Capacity) is vital for distribution system operators. In the first and second part of this chapter a new effective computative method (Bricks approach) and its combination with Monte Carlo simulation to evaluate the hosting capacity in case of grid parameter uncertainties and multi-generator connection in a real-life case study was proposed. Bricks approach is useful when network data are complex to collect or when the computational effort could result critical. According to Bricks approach, feeders and collaterals are classified in given categories according to their electrical characteristics. The tests performed, taking into account 3 main technical constraints (steady-state voltage variations, rapid voltage changes and thermal limits), proved the method to be effective in estimating the HC in real-life distribution networks, if compared to the method based on the complete grid model.

Then in the last part of this chapter, the impact of e-mobility charging processes on the electric grid in a real-life study case was evaluated. The aim is to propose HC as an effective index not only for evaluate DG but also in order to evaluate the impact of e-cars on distribution grid. Hence, a similar procedure to the one developed for DG have been adopted for e-car. The study was developed according to three different recharging modes, the first based on slow charging process, the second relevant to fast charging station, the latter based on enhanced, very fast, public charging stations. Afterwards, three different test case (SET1, SET2 and SET3) had been tested. The charging processes impact on the grid, in both case of active and passive grid, were evaluated adopting a KPI procedure, devoted to quantify the hosting capacity of the grid. In all the performed simulation, no criticalities have been detected with respect to the feeders voltage profile. As a matter of fact, the limiting factor in the grid charging process hosting capacity resulted to be the lines thermal limit, i.e. the maximum current the feeders could manage. In addition, the results showed that although SET3 distribution (mainly very fast charging) provides high speed charging process, it could cause some critical load fluctuation over a single day limiting the capacity of the grid to host recharge process, or, similarly, decreasing the efficiency of the distribution grid. Moreover, the total losses in active distribution network shows a lower amount in comparison with passive one.

CHAPTER 5

Voltage Control

5.1 Introduction

The increasing penetration of dispersed generation mainly based on renewable energy sources, as a supplement to centralized generation, has caused new challenges in modeling, operation and controlling of the MV distribution grid. Although DGs could take some advantages from RES production such as sustainability, less maintenance and low carbon emission, since DGs power injections to the grid are not coordinated with the actual distribution grid, it can cause power quality and reliability degradation such as harmonics, voltage profile and interface protection problems and moreover it may increase system losses and operational costs [67].

The fast increasing of DG connections may affect the supply quality. In fact, voltage profile along the feeder have been influenced and overvoltage at the DG's Point of Common Coupling (PCC) may occur [5], [152]. The voltage increase along the feeder leads to power flow decreasing in the HV/MV transformer which cause load compensation decreasing. Thus, new voltage regulation approaches are required which have to act not only through substation measurements [263], [226].

In order to overcome these issues, distributed system operators have to evaluate the maximum generation that can be hosted by distribution grids without violating the technical constraints and find the ways to increase as it was discussed in Section 2.3.3. In this chapter voltage control as one of these approach has been discussed. After a brief introduction of voltage rise issue, the proposed set-up for voltage control has been introduced, and finally the tested results has been reported.

5.2 Voltage Rise Issue

Due to the increasing number of DG in distribution grid, the voltage problems are also increasing (voltage increasing issue has been discussed in Section 2.2.2). This cause sever problem in case of no demand as all the exceed generation by DG should be exported to the primary substation. Authors in [264] categorized the voltage issues in distribution grid into short term and long term group. Short term category takes place between a half-cycle and sixty seconds which usually caused by a fault in power system and leads to voltage dip. Whereas, the second group such as overvoltage and undervoltage takes longer time and could cause more sever issues in power system. In case of voltage rise issues, a management system could assist to eliminate the voltage rise problems.

5.2.1 Voltage Control Architecture

In order to keep the voltage of distribution grid inside its boundaries, it is important to use a control scheme to reduce the voltage profile in case of voltage rise and increase it in case of voltage drop. To do so, there are several methods to improve the distribution system voltage regulation in unidirectional power flow such as [265]:

- MV PS voltage set-point increasing
- Feeder conductor size increasing
- Generator voltage regulator
- Primary feeder shunt capacitor
- Primary feeder series capacitor
- Substation capacitor
- Substation voltage-regulator apparatus
- Feeder section changing to multiphase
- Load transferring to the new feeder

Always at each secondary substation an automatic voltage regulation and feeder regulator are provided. Moreover, primary substation is equipped by OLTC which has the ability to automatically regulate the reference voltage. However, depending on the system requirements one of the mentioned techniques could be used.

Voltage regulator equipments are configured in order to regulate the voltage level in case of load variation. When the load is increasing, voltage regulators are working in direction of increasing the voltage in order to compensate the feeder voltage drop. On the other hand, when the load consumption is decreasing, the voltage needs to be decreased as well.

In all feeders and in each secondary substation capacitors have been installed in sufficient quantities in order to set up power factor. For having an automatic switching, in many of these installations a control system has been equipped. Fixed capacitor is not a voltage regulation device by itself, however the automatically switching procedure could help to make them a replacement for traditional voltage regulators [38].

By increasing the number of DG in the distribution grid, the traditional voltage control such as OLTC and capacitor bank are not enough. Hence for the new situation, new control regulation is necessary. Each DG unit has an indirect influence on the other DG unit in the grid; a reactive power increasing in on of them cause injection decreasing in the others. Hence, more coordination and higher infrastructure between apparatuses is necessary. Moreover, as DG units are mainly based on RES with periodic behavior, voltage regulator respond time is also increasing [266]. DG causes the increasing number of tap positions in OLTC leading to shortening its life. Hence, tap position minimization in active distribution network is required [267].

In the literature, several methods are proposed for voltage regulation. The first step of distribution grid control strategies is based on local management which is already expressed by national standard, e.g. the Italian Technical Committee, and international standard IEC [233]. Since the possibility of reverse power flow by increasing the penetration of DGs into the grid is arising, distribution system is transforming to the active distribution network. By this transformation, DSOs can solve voltage problems by controlling grid generation and consumption [268]. To do so, an active network management will be needed which, by real-time communication and control, may provide better DG integrations [269].

There are several ways in the category of advanced control voltage such as centralized voltage control, coordinated voltage control, local voltage control, hierarchical voltage control and distributed voltage control. Each of the aforementioned control has different strength, complexity, communication required and cost [264]. It is worth mentioning that the purpose of voltage regulation is not only the elimination of voltage rises and the increasing of hosting capacity. Voltage regulation is a resource to improve and optimize the entire electrical grid according to different objective functions, such as system losses reduction or power factor optimization.

The aforementioned methods have many advantages such as flexibility, efficiency and reliability. As an example STATCOM are able to provide solution in a very rapid response time, thus it could provide a dynamic voltage control. However, one of the disadvantage of some advanced voltage control especially centralized voltage control is their communication requirement leading to a really high cost. In contrast, local voltage control has provided a promising solution [264]. In following different voltage control have been discussed and compared.

Local Voltage Control

Local voltage control, known as decentralized method, uses local information to allow more DG to connect to the grid leads to increase HC. This method is used where the communication and optimization tools are limited. Thus, each DG works separately and uncoordinated with other devices, leading to less expenses [270]. The local voltage control is obtained with two contributions: the regulatory of on load tap changer in primary substation and the power factor control of DG units.

On Load Tap Changer: The automatic tap changer controls the voltage of MV bus-bar at primary substation. To do so, the voltage set-point is determined (in the best case) by offline optimal power flow in order to provide a suitable voltage profile for the whole feeder [143]. In order to manage the increasing number of DGs, studies related to the operating power factor, size and location of the DGs are required [271], [272].

Usually, OLTC regulation performs considering a line drop compensation, based on the resistance

(R) and reactance (X) of the feeder to regulate the voltage at transformer terminal [272]. Actually, line drop compensator measuring the secondary current simulates the voltage drop along the feeder between transformer terminal and load [273], [274]. The fundamental operation of OLTCs with or without using line drop compensator has been studied in [275].

Since the voltage rise may affect the automatic voltage control relay and subsequently causes regulation problems, in [145] different modern control schemes are discussed. The methods for voltage control improvement are including enhanced transformer automatic paralleling package, to reduce the circulating current between transformers, and super TAPP n+ relay, the enhanced TAPP scheme which has the ability to estimate the RES output current. In [276], a set-point control algorithm of automatic voltage control is proposed. State estimation-based OLTC is suggested in [146].

Reactive Power and Power Factor Control: It is already discussed that DG injections drive a voltage rise in the MV feeders, however they could be coupled with additional compensator to regulate the voltage in its limits [277]. Static compensator (STATCOM), D-STATCOM, static VAR compensator, fixed capacitor banks and shunt capacitor banks have been investigated in [147], [149], although some of these devices are costly.

Generally speaking, PFC could control the system voltage by increasing the hosting capacity of the distribution grid [269], [278]. There are many studies about the combination of various methods with PFC, which allow for some advantages such as reliability, efficiency and flexibility [279].

The authors in papers [280], [281] have indicated that PFC could be implemented by fixed Q, fixed PF, PF as a function of active power ($cos\phi(P)$) and as a function of PCC measured voltage ($cos\phi(U)$). Traditionally, DSOs obligatory have made all DG to operate under PFC control. Although it is less troublemaking compared to OLTC, it has some disadvantages, such as PFC at fixed Q mode needs load and DG power profiles. Moreover, at fixed PF, undesired level of system losses could occur when the generated power is low, as reactive power is proportional to active power, in this case reactive power control is meaningless. The mentioned problem for fixed PF can be solved by $cos\phi(P)$. Fig. 5.1 shows this improvement by changing the amount of $cos\phi(P)$ from $C1$ to $C2$ in case of low active power injection [281]. The other solution is $cos\phi(U)$, however again the reactive power is directly linked to active power injection. Hence, these two voltage controls should be performed when DG units active power injection is close to nominal values [151].

In $Q(U)$ method, Fig. 5.1 at bottom, local voltage information in the neighborhood has been used. Therefore, the control activity could be reduced in case of low voltage penalty factor. To do so, the contribution of reactive power of DG units placed close to the transformer is required for weak voltage supporting. In dead band, the possibility of seeing any reactive power absorption by DG units which are sited near to the transformer is very low, even though the voltage at the end of the feeder is beyond than boundaries [281].

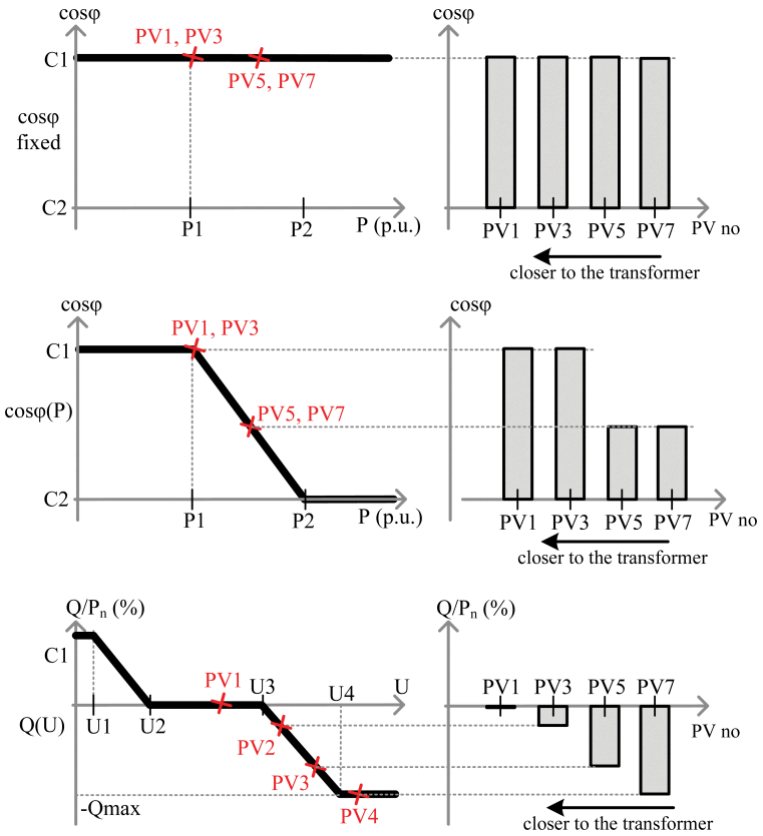

Figure 5.1: *Standard PFC by Fixed cos$\phi(U)$, Fixed cos$\phi(P)$ and $Q(U)$.*

Figure 5.2 shows the hysteresis incorporation in $Q(U)$ control strategy as different points could be chosen for controlling voltage rise which would be different from the controlling points of voltage drop [279].

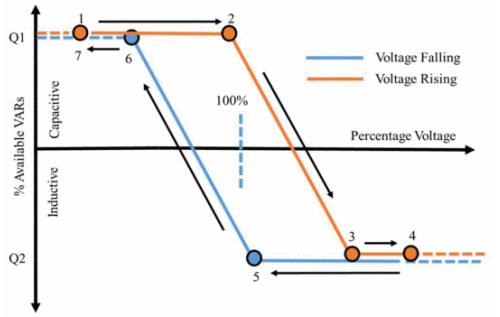

Figure 5.2: *$Q(U)$ control with hysteresis incorporation.*

Moreover in [152] four different local control strategies have been exploited according to European technical standards, as listed in the following: $LawA$) control of tangent of ϕ according to the PCC voltage ($\tan\phi = f(u)$); $LawB$) control of reactive power according to the PCC voltage ($q = f(u)$); $LawC$) control of tangent of ϕ according to the real power injected ($\tan\phi = f(p)$); $LawD$) control of reactive power according to the real power injected ($q = f(p)$). In Fig. 5.3 the aforementioned control laws are presented.

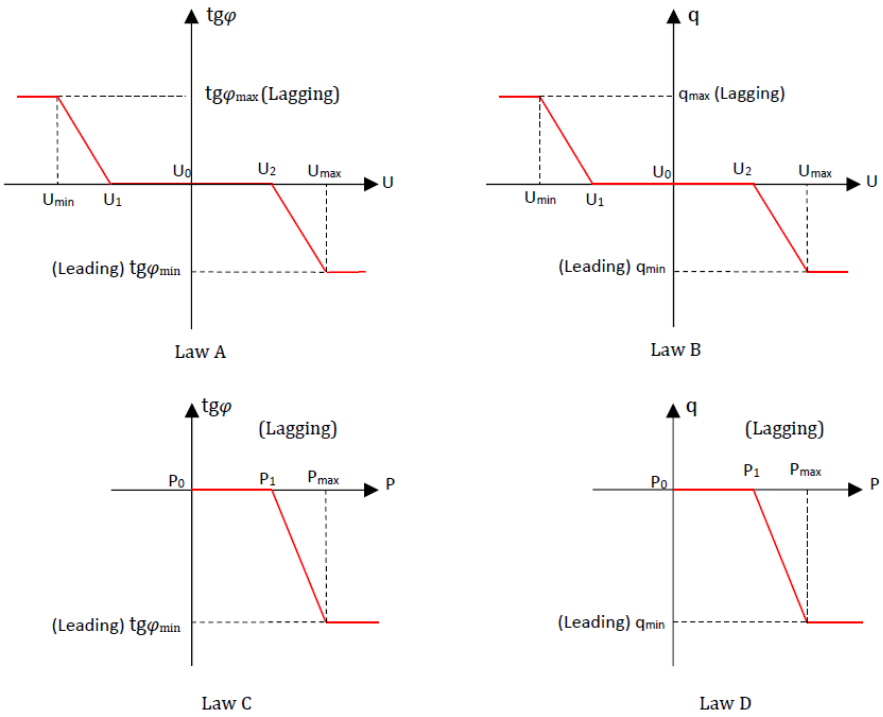

Figure 5.3: *Local voltage control strategy.*

Among all of presented strategies for local voltage control, volt-var control ($Q(U)$) shows better performance regarding increasing hosting capacity and decreasing energy losses [152]. This control is a dynamic close-loop system where the reactive power has been defined by the measured voltage. Hence, the explained drop-based control (also known as non-incremental) in the previous paragraphs has some unwanted oscillatory behaviors. In order to solve this problem, Gradient Projection method has been used for designing an incremental voltage control which can be represented as follow:

$$q(t+1) = [1-\alpha(t))].q(t) + \alpha(t)[q(t) - D.\nabla f(q(t))]_{q_{min}}^{q_{max}} \tag{5.1}$$

where, α is the weighting parameter with a value from 0 to 1, q_{max} and q_{min} are the maximum and minimum amount of reactive power which is acceptable for the next loop cycle and D is the diagonal matrix of each bus containing the step size d_j. In the literature, there are several strategies for incremental control which some of them have been discussed in following.

1. **Droop-var control**: The most important goal of this control is scaling the output reactive power using the bus voltage mismatches. This linear control does not have any dead band however, it has a negative slop equal to ($d = -c_j^{-1}$), where c_j is the penalty coefficient. Hence, equation 5.1 could be rewritten in equation 5.2.

$$q_j(t+1) = [-c_j.(V_j(t) - \mu_j)]_{q_{min}}^{q_{max}}, \forall j \tag{5.2}$$

This control is more unstable for large scale distribution system and in case of small penalty coefficient.

2. **Scaled-var control**: This control has better flexibility in terms of reactive power penalty choosing and boosting the convergence rate as it considers other approach to define D for local voltage control. In this control, D would be defined by the inverse diagonal matrix of $(X + C)$, where X is the inverse of bus sensitivity matrix and C is a diagonal matrix of penalty coefficient, equation 5.3 represents D calculation.

$$D = \epsilon.[diag(X + C)]^{-1} \tag{5.3}$$

3. **Delayed-var control**: This method, could improve also an unstable droop control. The stability and error norm is improving in this control as the step size has been chosen for lower value than 1. The step size could be defined by droop or the scaled-droop control, equation 5.4 shows its design.

$$q_j(t+1) = [1 - \alpha(t))].q(t) + \alpha(t)[-d_j.(V_j(t) - \mu_j)]_{q_{min}}^{q_{max}} \tag{5.4}$$

Coordinated Voltage Control

This real time control acts according to control rules taking into account the needs of the whole distribution network. This method is suitable for simple networks with less control possibilities and optimization tools. The Coordinated Voltage Control (CVC) holds the information of network topology and electrical characteristic of each feeder connected to the PS. The voltage control logic is based on two categories: 1) In case of normal operation condition no signal is sent to the CVC and the system is working according to the local voltage control strategy; 2) in case of critical condition, after receiving a warning signal CVC will elaborate the collected information to apply proper regulation actions. The goal of CVC is to improve the system operation toward an optimum.

The easiest method of CVC, which is controlling substation voltage based on voltage lower and upper bound, has been studied in [282]. In some proposed approaches, only reactive power compensator have been used in order to keep the voltage at the permissible level [283]. A new CVC method with reactive power managment scheme has been studied in [284]. Besides, in [285], [286], the authors proposed a combined method of SVC by injecting reactive power and step voltage regulator by changing tap position according to the received information from sensors in the distribution line which could be able to keep the voltage lower than the maximum allowed. Moreover, in [287], [288], active power control has been implemented in order to control the voltage, while distributed methods using multiagent systems for CVC have been studied in [289].

The aforementioned approaches are useful in simple and small networks, however by increasing the number of objectives, the control rules could become complicated. Hence, optimization algorithms have been used in many research papers. Genetic Algorithm has been used in [290], [291]. In addition, Particle Swarm Optimization algorithm has been investigated in [292]. Two new CVC algorithms, focused on time domain simulation and statistical distribution network planning, have been discussed in [293]. The combination of local-learning algorithm and nonlinear programming for computational time reduction was implemented in [294], [290]. In [295], a new two-stage voltage control scheme for controlling OLTC, capacitor banks and DGs using micro genetic algorithm and recursive genetic algorithm has been used. This method is based on finding the optimal reactive injection looking for the minimization of the

power losses. Structural changes to minimize the operational conflicts by giving the priority in action to the resources close, based on the electrical distance, has been proposed in [296]. Finally, the importance of reliable communication infrastructure and the quality of service in CVC was discussed in [297].

The importance of Remote Terminal Unit (RTU) in DG units for estimation the voltage profile in CVC has been discussed in [298]. The selection of DG in a multi-Gen system for voltage regulation has been done according to the sensitivity methods. The OLTC could be updated if the DG support is not able to put the voltage in the boundaries. One of the advantage of putting RTU in each DG and each line capacitor for this control strategy is communication cost reduction.

Centralized Voltage Control

This last-step-regulation procedure needs a complete and continuous communication between PS and the sensors widespread on the distribution network. It is based on continuous OPF calculations of the network model which is obtained by the state estimator. In each cycle, the obtained voltage set-points are delivered to the local DG. Actually, the centralized voltage control is an advanced control based on OPF, it has to generate a new voltage set-point by comparing the optimum value created by OPF and the measured value in order to adopt the optimum according to the current network status.

There are many intelligent techniques which are used for centralized control to formulate different type of objective functions [299], [300]. The advantage of using these methods is to provide optimized solution compared to the conventional methods and, as they have flexibility in defining constraints, to effectively handle the nonlinear programming. GA, PSO, Evolutionary PSO, Discrete PSO, sensitivity theory, tabu search, Artificial Neural Network, fuzzy logic and multi agent are extensively report in literature review [301], [302]. In these studies, by solving a constraint optimization problem for minimizing the system losses, control actions are scheduled to reactive power suppliers.

An improved centralized voltage control of OLTC and Static Voltage Regulator based on standard communication lines and automation server has been studied in [303]. The voltage fluctuations are forecasted using JIT modeling. Similarly, in [304], day-ahead load forecasts using GA are exploited in order to define the optimal dispatch schedule of OLTC and shunt capacitor. The PSCAD/EMTDC network model with different load profiles and dynamic loads is validated by the OPF developed in [305].

Hierarchical voltage control

This control splits the distribution grid in different zones an area to add time-delays between them in order to minimize the computational processing time. In [306], for optimal voltage regulation, a hierarchical zone based on volt-var control has been proposed.

For a big-size PV plant, a multistage "time-grated" in a cascade OLTC and capacitor bank has been introduced in [307]. In an unbalanced MV distribution grid, a multi-stage volt-var optimization algorithm is projected to regulate the voltage. The aim of this optimization is relaxing the cascade switch regulators operations, and minimizing the PV inverter output curtailment.

Distributed voltage control

In case of real-time voltage regulation request, which is very complex and demanding, each single DG unit needs to have its own local voltage control and an optimization algorithm where each algorithm gathers their neighbors data. Hence, the probability of communication technical problem is getting lower because of local voltage control incorporation. Furthermore due to OPF performing, the energy losses has been decreased [308], [309].

As discussed in the this sections, voltage control methodologies and approaches are investigated and discussed in the literature as a means of enhancing the distribution grid HC. Table 5.1, shows the different approaches comparison [264]; for some approaches to regulate the voltage along the system and hold it in the allowable limits, an accurate knowledge about voltage in each node is required. However, due to lack of (or limited number of) SCADA in distribution networks, real time measurements are rarely available through feeders and only are available at PS. To compensate this shortage, state estimation of measurements has to be done by sensors and communication assets to evaluate voltage profiles and to dispatch the DG units and the other resources available in the network accordingly. However, state estimation procedures based on a very limited number of measures typically are affected by uncertainty and errors which may cause wrong decisions. On the other hand, aligning sensors for each node of the distribution system is very costly and unaffordable. Hence, a cost effective approach to set up the voltage law has to be proposed to cope with all of these problems.

Table 5.1: *Decentralized, coordination and centralized voltage control comparison.*

Decentralized Methods	**Coordinated and Centralized Methods**
Local Control	Vast Control
Needs no communication	Needs vast communication
With no coodination	With vast coordination
Affordable	Costly

5.3 Proposed Set-up Procedure for Local Voltage Control Law

The proposed strategy in this thesis has been developed according to the DSO needs and European technical standards. DSO are in charge to set the local voltage control on DG power plants according to Fig. 5.3. Thus, generation units could be considered in order to develop new algorithms for the reactive resources management in the MV distribution networks. It is worth to mention reactive-based voltage control of DG is operated only in MV, since the Thevenin impedance seen from a LV node is basically resistive, so reactive power control would be ineffective in LV grids. This can be done by corrective adjustments of the reactive production of a single generator. In particular, each generating unit has to give reactive support in those situations in which its production would lead to voltage violation, according to the standard EN 50160. However, no literature could be found for this purpose. The procedure has been proposed in this thesis is based on the Optimal Reactive Power Flow (ORPF) (similar to OPF), a non linear problem with continue and discrete variables. In the proposed strategy, the ORPF operates off-line on the basis of a historical network behavior. The goal of the procedure is to statistically set up the parameters of the local voltage control law. According to the proposed approach, each reactive resource operates locally and the parameters of the local characteristic are adjusted based on the output

of an optimum computation. Hence, the proposed approach is aimed to improve the operation of today distribution grid without requiring investments in TLC or ICT equipment. Therefore, no communication infrastructure is necessary since still is a local voltage control. ORPF objective function could be losses minimization, generator reactive power minimization and voltage deviation of each node from the related value minimization. ORPF constraints can be defined as: voltage limits of buses, reactive power capability limits of generators and power factor limits at the substation. The final goal is to properly define the local voltage regulation setting.

To do so, MATPOWER package has been used in this thesis. MATPOWER is a MATLAB package for performing OPF and PF simulation [54]. The focus of this chapter of thesis is mainly on developing the data preparation, tool set-up, post processing and automation procedure. The present section has been explained the set-up procedure for Local Voltage Control (LVC). The final goal of this procedure is to find a new setting which is performing better than standard local voltage control that currently is performing. To do so a generalization of LVC setting is required to support different DG and loading conditions, hence a wide range of loading hours, nodes, nominal active power injections should be deeply assessed. However, this needs a huge computational time as well which make it a critical issue. Therefore, a selection procedure to define the suitable nodes, loading hours and active power injections is required (such as Bricks Approach). In addition, the new LVC settings should not only related to the specific grid nodes, but it needs to be associated with grid characteristics. To do so, a cluster procedure is necessary to categorized nodes with similar characteristics to have a technically viable approach for DSO. At the end, in order to highlight the strength of the new LVC setting, its results have been compared with standard LVC, OPF simulation and simple load flow. Fig. 5.4 in following shows the flowchart of this new-set-up in LVC.

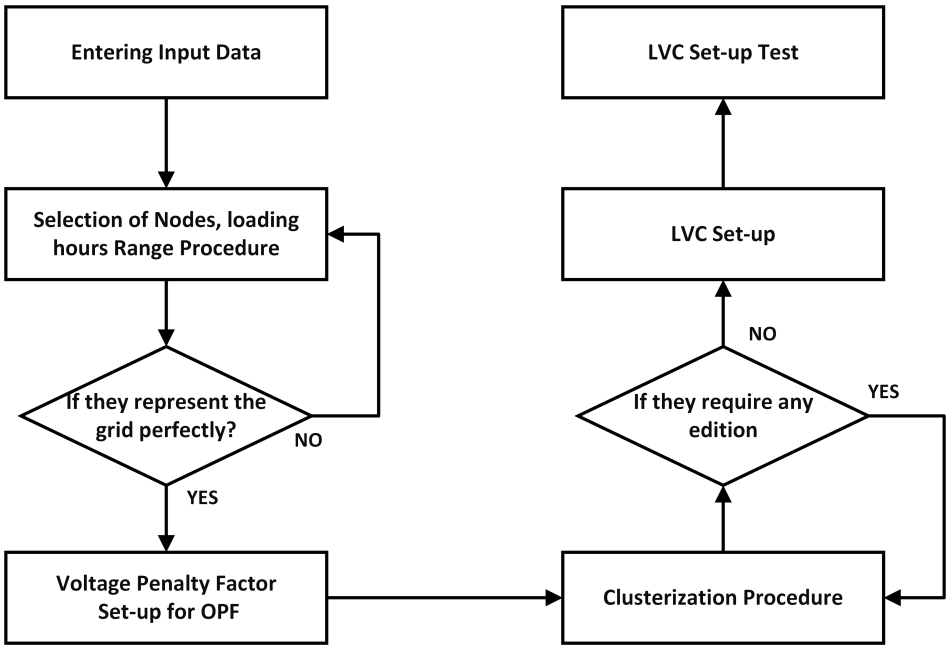

Figure 5.4: *Proposed procedure for LVC set-up flowchart.*

The flowchart has been started with entering the required input data such as the structure and characteristic of the grid in different defined matrix that is explained in Section 5.3.1 followed by load and

accumulated feeder impedance analysis in order to define the selected nodes and loading hours (such as Bricks approach selection procedure). After that best-fit voltage penalty factor, by performing several OPF with different penalty factor and dead band to find the best set-up, needs to be defined. Then the clusterization process has been performed for each MV busbar based on defined hours. In order to check the accuracy of the clusterization process, OPF should be launched for each cluster. If the results are not satisfying, the clusters need to be changed. As the next step, an OPF based on keeping MV voltage constant has been performed and then the results have been linearized for achieving the new LVC set-up. Finally, the results of the new LVC set-up, the standard LVC, OPF and simple load flow with PF1 have been compared. In following after a full description of MATPOWER package and optimal power flow procedure, a brief introduction of each step has been provided.

5.3.1 Optimal Power Flow

Input Data Modeling

The required input data for MATPOWER in this thesis is based on case struct, which has all the necessary data to perform OPF. The struct input variable is including baseMVA, version, bus matrix, branch matrix, gen matrix and gencost matrix which gencost matrix is not mandatory to be defined. A short description for each mentioned variables has been reported in the following.

BaseMVA: This value is devoted to the grid parameters p.u. conversion and is a single value.

Version: It defines if the input variables are set as struct or independently. As it was mentioned before, in this thesis the struct form has been chosen.

Branch Matrix: All the information related to distribution lines, transformers and phase shifter are collected in the Branch matrix. In order to define these variables, π transmission model in Fig. 3.2 has been used in this study.

Bus Matrix: In this matrix, bus type, bus voltage and its angel, consumed active power and reactive power at each bus as loads and moreover the voltage boundaries have been defined.

Generator Matrix: Each generator model has been set in the Gen matrix variable by its active power, reactive power and its voltage limitation.

Gencost Matrix: In order to perform OPF, active power and reactive power penalty factor could be saved in this matrix.

MATPOWER Different Options: There are several set-up options in MATPOWER for performing OPF, PF and other integrated solvers, such as algorithm, DC or AC modeling, convergence tolerance, maximum number of iteration, generator reactive power limits. Depends on each case study these variables should be defined.

AC Optimal Power Flow Solver

There are several solver in MATPOWER for performing AC/DC OPF and PF. The focus of this thesis is on AC OPF. In this study, in order to perform an optimal power flow, MATPOWER Interior Point Solver (MIPS) has been defined among all of the other solver. MIPS could also use separately and outside of MATPOWER for nonlinear optimization problem which equation 5.5-5.9 represent its model.

$$min_x f(x) \tag{5.5}$$

subject to

$$g(x) = 0 \tag{5.6}$$

$$h(x) \leq 0 \tag{5.7}$$

$$l \leq A.x \leq u \tag{5.8}$$

$$x_{min} \leq x \leq x_{max} \tag{5.9}$$

where, equation 5.5 is a minimization objective function with equality and inequality constraints in 5.6 and 5.7 respectively. A general linear restrictions for all optimization variables are saved in matrix A with a lower and upper limitation of l and u in equation 5.8 and at the end, equation 5.9 shows the optimization variables limitation.

The main difference between MIPS and MATLAB Optimization Toolbox is summarized in equation 5.8 where the linear constraints in MATLAB Optimization Toolbox is splited to an equality and upper bounded function ($A_{eq}.x = b_{eq}, A.x \leq b$).

The algorithm which is used by MIPS to find a solution for optimization problem is called Primal-Dual Interior Point Algorithm and could be implemented by combining both linear constraints and variables into g(x) and h(x). In this algorithm, n_i inequality constraints are converted into equality constraints using a barrier function in following.

$$min[f(x) - \gamma \sum_{m=1}^{n_i} ln(Z_m)] \tag{5.10}$$

subject to

$$g(x) = 0 \tag{5.11}$$

$$h(x) + Z = 0 \tag{5.12}$$

$$Z > 0 \tag{5.13}$$

The Lagrangian, γ for this equality constrained problem can be defined as follow:

$$\iota^{\gamma}(X, Z, \lambda, \mu) = f(c) + \lambda^{T}.g(x) + \mu^{T}.(h(x) + Z) - \gamma.\sum_{m=1}^{n_i} ln(Z_m) \tag{5.14}$$

The optimal first order condition for this problem would be satisfied when the partial derivatives of the Lagrangian are set to zero. Hence, the optimal first order conditions could be solved using Newton's method written bellow.

$$\begin{bmatrix} \iota^{\gamma}_{XX} & 0 & g^{T}_{X} & h^{T}_{X} \\ 0 & [\mu] & 0 & [Z] \\ g_x & 0 & 0 & 0 \\ h_x & 0 & 0 & 0 \end{bmatrix} . \begin{bmatrix} \Delta X \\ \Delta Z \\ \Delta \lambda \\ \Delta \mu \end{bmatrix} = - \begin{bmatrix} \iota^{\gamma^{T}}_{X} \\ [\mu].Z - \gamma.e \\ g(X) \\ h(X) + Z \end{bmatrix} \tag{5.15}$$

This complex equation is simplified by solving explicitly for $\Delta\mu$ in terms of ΔZ and ΔZ in terms of ΔX.

In order to have a strict feasibility for the trial solution, the algorithm needs to approximate the Newton step by scaling the primal (α_p) and dual variables (α_d). Then the variables have been updated according to this new scale such as bellow.

$$X \leftarrow X + \alpha_p \,.\, \Delta X \tag{5.16}$$

$$Z \leftarrow Z + \alpha_p \,.\, \Delta Z \tag{5.17}$$

$$\lambda \leftarrow \lambda + \alpha_p \,.\, \Delta \lambda \tag{5.18}$$

$$\mu \leftarrow \mu + \alpha_p \,.\, \Delta \mu \tag{5.19}$$

Finally, γ should be updated according to the next equation, where σ is set to 0.01 in MIPS.

$$\gamma \leftarrow \sigma.\frac{Z^{T}.\mu}{n_i} \tag{5.20}$$

MATPOWER is also able to solve the quadratic optimization problem where this kind of problem would be defined in following.

$$min\frac{1}{2}w^{T}Hw + C^{T}w \tag{5.21}$$

$$l \leq A.x \leq u \tag{5.22}$$

$$x_{min} \leq x \leq x_{max} \tag{5.23}$$

The objective function is expressed by parameters H for quadratic term and C for linear term which are the quadratic penalty factor coefficient. If H assumed to be zero, problem converts to linear problem.

Standard AC Optimal Power Flow

A DG-connected bus should be chosen as a slack bus in MATPOWER to mate the role of active power and slack voltage angle. At the slack bus the voltage angle is known, while the active power is unknown, and the other nodes should be defined by their characteristic as PQ or PV buses.

In the following, vector X as an optimization vector for the OPF in this research is including $n_b \times 1$ vector of voltage magnitude (V_m) and its angle (Θ), and also a $n_g \times 1$ vector for generators active and reactive power (P_g, Q_g).

$$x = \begin{bmatrix} \Theta \\ V_m \\ P_g \\ Q_g \end{bmatrix} \tag{5.24}$$

Hence, the objective function expressed in equation 5.5 is the summation of the individual polynomial cost function (f_P^i, f_Q^i) of active and reactive power injection of each DG shows in equation 5.25.

$$min_{\Theta, V_m, P_g, Q_g} \sum_{i=1}^{n_g} f_P^i(p_g^i) + f_Q^i(q_g^i) \tag{5.25}$$

Then, the nonlinear active and reactive power balance equations have been defined as the equality constraints in equation 5.6. According to the conventional combination of power flow formulation, the power balance equation has divided into active component and reactive component (such as equation 5.26 and 5.27) which has been calculated as the function of voltage magnitude and its angel plus generator active and reactive injections, while load assumed to be constant and known.

$$g_p(\Theta, V_m, P_g) = P_{bus}(\Theta, V_m) + P_d - C_g P_g = 0 \tag{5.26}$$

$$g_p(\Theta, V_m, P_g) = Q_{bus}(\Theta, V_m) + Q_d - C_g Q_g = 0 \tag{5.27}$$

where, the status of generator in the distribution grid can be defined by the generator connection matrix (C_g). The inequality constraints discussed in equation 5.7 is including the two vectors of branch flow limits as a function of bus voltage magnitudes and their angles which one of them represents the flow from end and one for the to end as follows.

$$h_f(\Theta, V_m) = |F_f(\Theta, V_m)| - F_{max} \leq 0 \tag{5.28}$$

$$h_f(\Theta, V_m) = |F_t(\Theta, V_m)| - F_{max} \leq 0 \tag{5.29}$$

The flows could be one of the following forms of the constraints:

$$F_f(\Theta, V_m) = \begin{cases} S_f(\Theta, V_m) \\ P_f(\Theta, V_m) \\ I_f(\Theta, V_m) \end{cases} \tag{5.30}$$

where, as it was explained before $I_f = Y_f.V$ and $S_f(V) = [C_f V]I_f^* = [C_f V].Y_f^* V^*$. The flow limits value for performing OPF in this research have been identified in branch matrix, column 6 as F_{max}. Setting zero value to this column give us an unconstrained line.

The variables constraints in equation 5.9 consists on slack buses voltage angle, voltage magnitude, generators active and reactive power injection.

$$\Theta_i^{ref} \leq \Theta_i \leq \Theta_i^{ref}, i \exists I_{ref} \tag{5.31}$$

$$v_m^{i,min} \leq v_m^i \leq v_m^{i,max}, i = 1, ...n_b \tag{5.32}$$

$$p_g^{i,min} \leq p_g^i \leq p_m^{i,max}, i = 1, ...n_g \tag{5.33}$$

$$q_g^{i,min} \leq q_g^i \leq q_m^{i,max}, i = 1, ...n_g \tag{5.34}$$

The voltage magnitude limitation and voltage angle of the reference buses have been defined in the column 12, 13 and 9 of bus matrix respectively. Similarly, the generator active and reactive limitation have been determined in columns 4, 5,9 and 10 of gen matrix.

Extended AC Optimal Power Flow

Users have the ability to modify MATPOWER problem formulation in the way which is necessary without rewriting the standard OPF formulation [310]. This ability could be done through optional input parameters, preserving the power of using pre-compiled solvers. Hence, the standard formulation needs to be modified according to the user-defined costs constraints and variable z as follow:

$$min_{x,z} f(x) + f_u(x, z) \tag{5.35}$$

subject to

$$g(x) = 0 \tag{5.36}$$

$$h(x) \leq 0 \tag{5.37}$$

$$x_{min} \leq x \leq x_{max} \tag{5.38}$$

$$l \leq A \begin{bmatrix} x \\ z \end{bmatrix} \leq u \tag{5.39}$$

$$z_{min} \leq z \leq z_{max} \tag{5.40}$$

where the equality and equality constraints and the variable limitation is the same as previous section. Moreover, cost function (f_u) in equation 5.21 which is specified in terms of H and C, N, $\hat{r}$, k, d and

m should be defined by user. All of the mentioned parameters are vectors by the dimension of $n_w \times 1$ except matrix H by $n_w \times n_w$, and matrix N by $n_w \times (n_x + n_z)$ size. The user cost function is written as follow.

$$f_u(x, z) = \frac{1}{2} w^T H w + C^T w \tag{5.41}$$

where, w should be defined by some steps; first of all by applying linear transformation (N) and shifting to the optimization variables ($\hat{r}$), the new vector u is obtained.

$$r = N \begin{bmatrix} x \\ z \end{bmatrix} \tag{5.42}$$

$$u = r - \hat{r} \tag{5.43}$$

Second, a scaled function with a dead band has been applied to vector u to achieve the elements of w.

$$w_i = \begin{cases} m_i f_i(u_i + k_i) & u_i \leq -k_i \\ 0 & -k_i \leq u_i \leq k_i \\ m_i f_i(u_i - k_i) & u_i \geq k_i \end{cases} \tag{5.44}$$

where, k_i determined the size of the dead band, m_i is scale factor, and f_i is a predefined scalar function chosen by d_i. At this moment, only linear and quartic options are implemented by MATPOWER.

$$f_i(\alpha) = \begin{cases} \alpha & \text{if } d_i = 1 \\ \alpha^2 & \text{if } d_i = 2 \end{cases} \tag{5.45}$$

Fig. 5.5 show linear (a) and quadratic (b) user-defined cost function. In this thesis for implementing a voltage penalty factor the quadratic option has been used. The voltage penalty factor is required to reduce the reactive power injection in case of high voltage level.

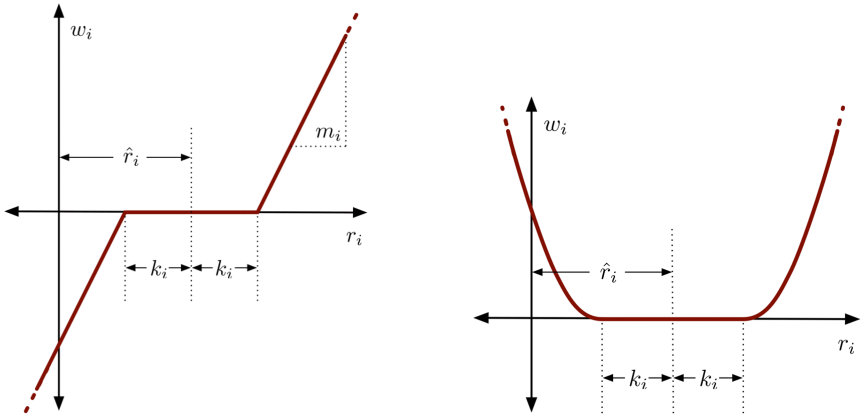

(a) User linear cost function.

(b) User quadratic cost function.

Figure 5.5: *User defined cost function.*

5.3.2 Loading Hours and Node Selection Procedure

In order to have a generalized LVC setting, it is required to support different DG and loading conditions. Hence a wide range of loading hours, nodes, nominal active power injections should be deeply assessed. However, this needs a huge computational time as well which make it a critical issue. Therefore, a selection procedure to define the suitable nodes and loading hours is required. In the following the procedure of defining the representative of the under-study distribution network has been explained.

Node Selection

As it was discussed in Section 4.2.1 in order to choose some nodes for performing OPF, a rule for feeders and collaterals has been defined. The selected nodes for short feeder category are located at 10%, 50%, 90% and 100% of the feeder, while for the medium and long categories the selected node have been considered at 10%, 25%, 50%, 75%, 90% and 100%.

The applied rule for collaterals depends on its total impedance has been expressed in following:

- If the collateral has one node and the total impedance of collateral is less than the 10% of maximum feeder impedance, no node has been considered for this category.
- If the collateral has more than one node and the total impedance of the collateral is less than the 10% of the total feeder impedance, the last nod in collateral has been considered.
- If the collateral has less than four nodes and the total impedance of it is lower than 50% and higher than 10% of the total feeder impedance, the last collateral mode has been considered.
- If the collateral has more than three nodes and the total impedance of it is lower than 50% and higher than 10% of the total feeder impedance, the last node of the collateral and a node located in 50% of the total impedance of the collateral have been considered.
- If the collateral impedance id higher or equal to 50% of the total feeder impedance, the last collateral node, a node with 50% and a node with 10% of the total collateral impedance have been considered.

Load Hour Selection

As the load is oscillating daily, a clear idea of the typical daily load value is very important in this research, to do so grid load behavior should be analyzed. The goal is to define a group of hour which are the representative of the loading behavior in the full grid along a defined time range.

In order to have general picture of the study range, the first step is finding the maximums and minimums loading of MV bus bars and feeders. Then, to have an idea about the possible grouping of loading hours to reduce the computational time, a relative hours classification (hours referred to time line of a day) based on loading behavior have been done. At the end, all the under-studied loading feeder days should be overlapped to find a the load behavior along the year. Mainly the maximum and minimum load value for the full grid at the MV bus bars and feeders are occurred at around the same time for different days.

Thus, for each distribution grid a maximum and minimum loading time, in addition with specific hour of the day including low peak, first high peak, second high peak, middle, drop up and drop down could be defined as the most important time of loading for performing the simulation. Fig. 5.6 shows single day time division for load.

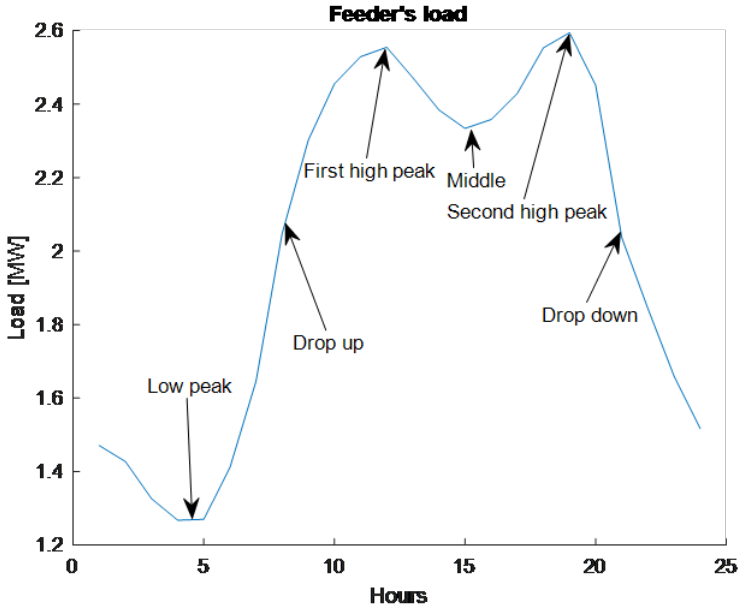

Figure 5.6: *Daily load behavior and chosen relevant points .*

5.3.3 Voltage Penalty Factor Set-Up

When the active power penalty factor for all the nodes assumed to be equal, the default OPF relies on grid energy losses minimization. Hence, the voltage could be increased until its boundaries. In order to finding a trade-off between energy losses and voltage increasing, there are two possible solution: reactive power penalty factor and voltage penalty factor.

Reactive power penalty factor is based on the fact that reactive power injection leads to increase voltages and its absorption leads to decrease voltages. The main problem in this approach is to find a link between voltage level and reactive power absorption, in case of low voltage value for avoiding unnecessary reactive power absorption. Moreover, the voltage rise looks complex to be defined to reduce energy losses. Hence, the other solution is voltage penalty factor for each node. Since, the active power in these nodes is constant (except the slack bus), OPF could be performed based on reactive power. Hence, reactive power injection or absorption is linked to voltage level, OPF has been motivated to increase reactive power in low voltage value as voltage penalty factor is low or zero. However, if the voltage is high, OPF is forced for reactive power absorption.

Therefore, reactive power penalty factor is decided to be set at zero to avoid unwanted optimization behavior and voltage penalty factor needs to be set up which can be done with the extended OPF formulation in Section 5.3.1.

5.3.4 Clusterization Procedure

After defining the nodes, loading hours and setting up the OPF, several OPF with constant active power have been performed to define the generator reactive power and nodes voltage (PCC voltage) which results a big cloud. However, an independent cloud for each node is not useful and the nodes with similar characteristic needs to be categorized. The clusterization process in this research has been done with cluster functions incorporated in MATLAB Statistics and Machine Learning Toolbox [311]. The aforementioned tool is a partitioning method and is based on K-mean clustering. This tool handles measurement in the data as objects having locations and distances from each other, where this distance could be evaluated by the square Euclidean distance. K-means partitions the objects into K mutually exclusive clusters, such that objects within each cluster are as close to each other as possible, and as far from objects in other clusters as possible. Therefore, it is required to define K for each clusterization.

The chosen points in each cluster has been defined by injected reactive power, accumulated impedance and R/X ratio for the selected nodes and loading hours. First, a smaller range of loading hour has been used for clusterization, then OPF has been performed for wider range of loading hours and the clusterization has been checked in case of modifications requirement, such as joining two clusters due to their similarities or removing some nodes from one cluster and moving to other one.

Fig. 5.7 shows this cluster procedure where each color represents a cluster.

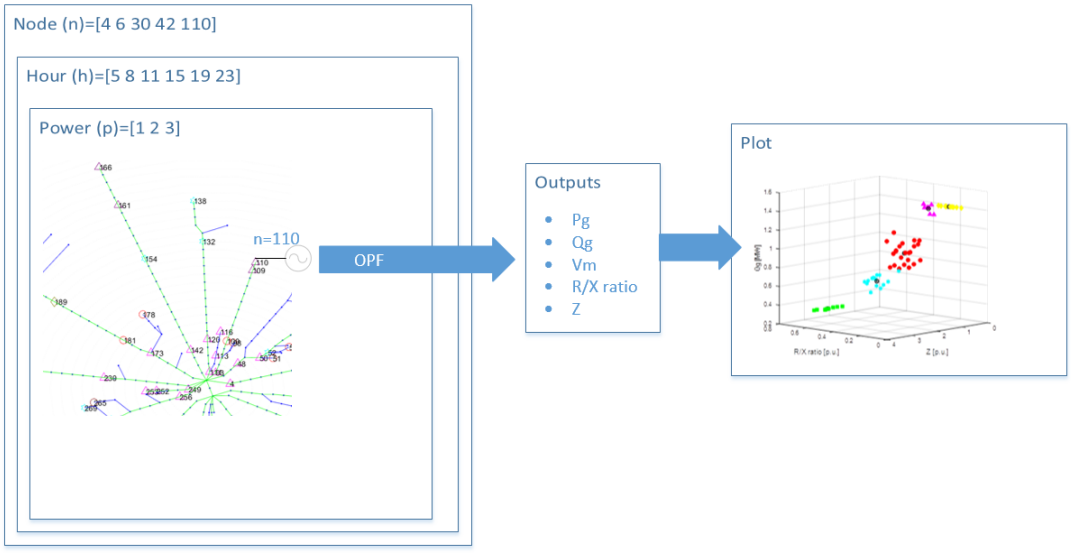

Figure 5.7: *Cluster procedure.*

5.3.5 Local Voltage Control Set-Up

After performing OPF for wider range of loading hour (including relative hour of one day and the maximum and minimum loading hour) for each defined cluster in the previous section, a bigger cloud has been obtained. In the next step, the center of each cloud has been defined and linearized to achieve the LVC setting. The enhanced LVC set-up is more complex in comparison with the standard LVC reported in CEI 0-16 [229], Fig. 5.8 demonstrates both LVC. The enhanced LVC consists on five sections instead of three sections.

- First Section: For voltage increasing near boundaries (e.g. voltage equal and lower than 0.92).
- Second Section: Dead band with the aim of reducing energy losses by increasing the voltage. It is a constant line with a value equal to the maximum defined reactive power in section three.
- Third Section: It should be defined by the LVC set up procedure explained here.
- Forth Section: This section has been defined to connect section three and five together.
- Fifth Section: For voltage decreasing near boundaries (voltage higher than 1.08).

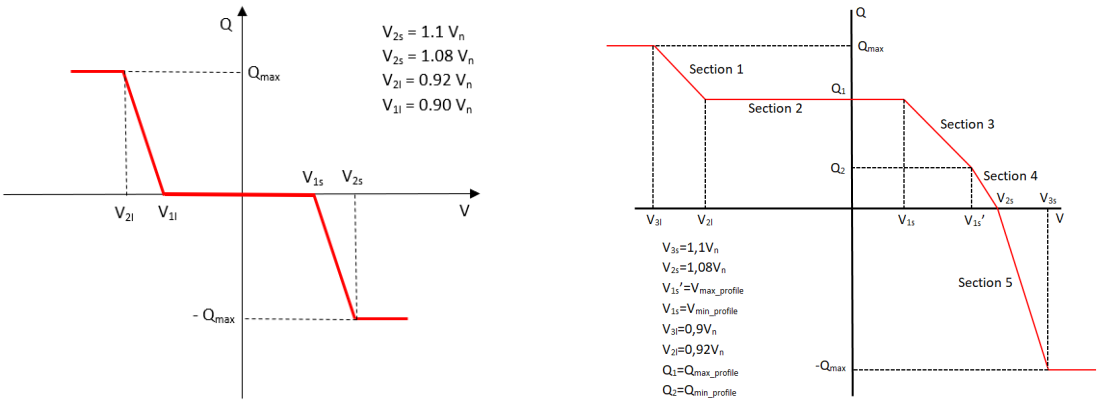

(a) Standard local voltage control.

(b) Enhanced local voltage control.

Figure 5.8: *Local Voltage Control.*

At the end, enhanced LVC needs to be tested in order to validate the procedure. Fig. 5.9 shows the flowchart of this procedure. In the first step, importing grid case characteristics and initialization have been done, then a load flow procedure is run to acquire the nodes state. In case of simulation failure due to convergence problem or grid limitations, the procedure has been performed load flow simulation once again with higher voltage boundaries. This procedure is useful when the voltages have the values close to the voltage limitations, due to the fact that the initial iterations may ask for a solution outside this limitation. After that if the simulation succeed, the new voltage has been compared with the old one. The new voltage has been considered as a right value if the difference between the old an new voltage is lower than 0,001. This step is repeated for four consecutive simulation for each node. The whole load flow simulation is repeated 40 times in order to ensure the voltage stability.

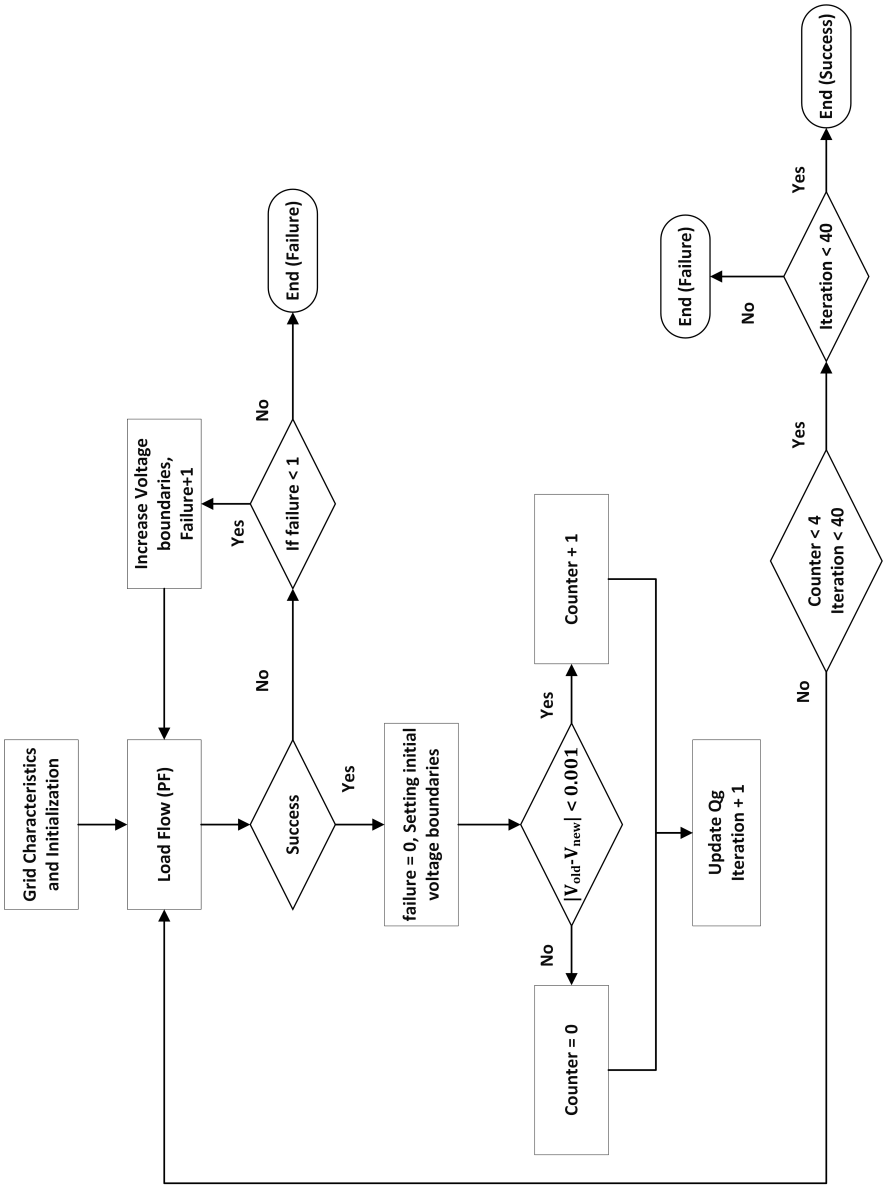

Figure 5.9: *Enhanced LVC set-up flowchart.*

5.4 Validation of the Proposed LVC Set-Up

The proposed procedure explained in the previous section could be implemented and tested for different distribution grids. The studied real grid for this topic is Aosta grid explained in Chapter 4. In this chapter some other useful information and analysis of this grid which is required for implementation of LVC set-up procedure have been reported.

Aosta MV distribution grid supplies 29,118 LV (60.5 MVA) and 63 MV users (20.3 MVA). Among these MV users, two of them (Node 238 and 253) have interconnection with another MV distribution grid rolled by another company (CEG). By doing some investigations, it can be understood that there is a clear separation between MV and LV supplied feeder. Mainly, the feeders which are supplying MV users are located at city skirt, whereas for LV users are located in the city center. Fig. 5.10 shows load positions in the grid by red circles, main feeders by green color and collaterals by blue. Generators are located in node 101, 198, 331 and 377, also the big loads are placed in 60, 148, 253 and 446 which supply ski track, Heineken manufactory, CEG company and general hospital.

5.4.1 Loading Hour Selection

As the load distribution has a vital influence on the voltage level of the distribution grid, in this section this effect has been studied over Aosta grid. Hence, it is necessary to choose a range of hours to reduce the processing time.

Figure 5.11 (a) and 5.11 (b) represent the load oscillation along a year for whole distribution grid and for each MV busbar respectively. The maximum amount of load for the full grid is around 44.2MW and has happened at the beginning and ending of the year when there are more tourists at the city and the minimum value is 11.48MW at the middle of the year. The MV busbars have different loading, MV busbar 1 has higher load with maximum of 22.12MW and minimum of 5.74MW, while busbar 2 has maximum 11.04MW and minimum 3.13MW. In order to get better view of the grid, Fig. 5.12 (a) and 5.12 (b) show the load profile for each separate feeder and for each node respectively. In Fig. 5.12 (b) the nodes with high load values have been highlighted.

Moreover, Fig. 5.13 (a) shows the load profile for full grid and each MV busbar for the first week of the year. From this plot it could be found that in the full grid during 5 and 7 o'clock there is a minimum, while there are two maximums around 11 and 19 o'clock for each day. This peaks at the weekends and the first day of the year is lower than the weekdays value. Moreover, the weekly load profile of each feeder has been presented in Fig. 5.13 which almost shows the same trend as the full grid.

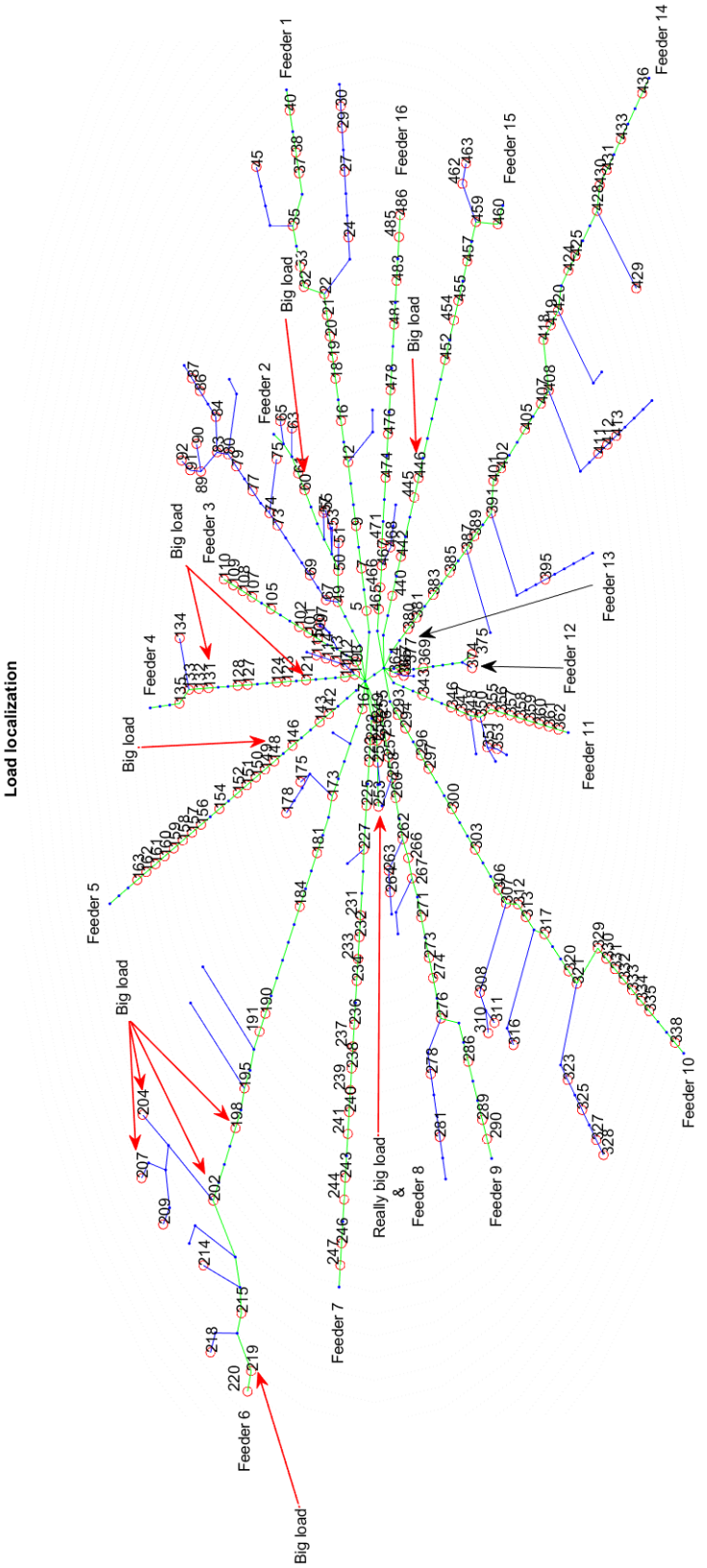

Figure 5.10: *Aosta MV grid load localization.*

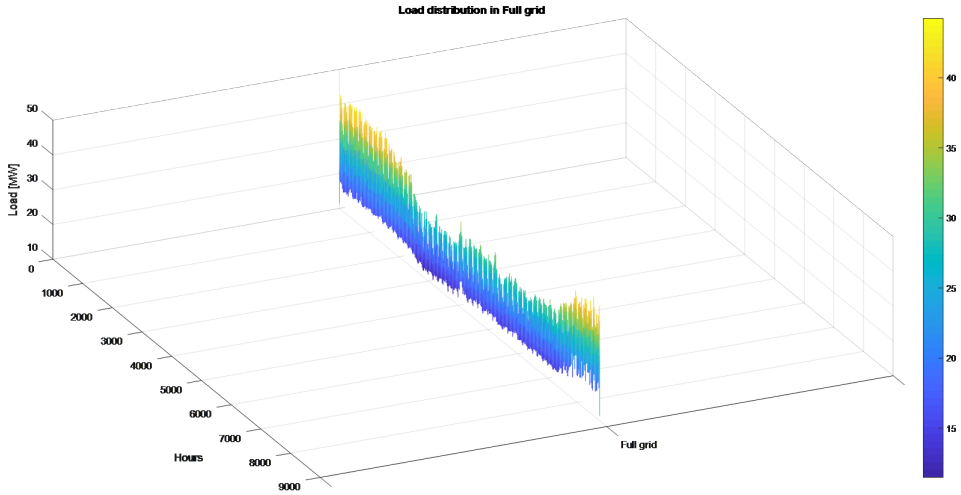

(a) Full grid load distribution.

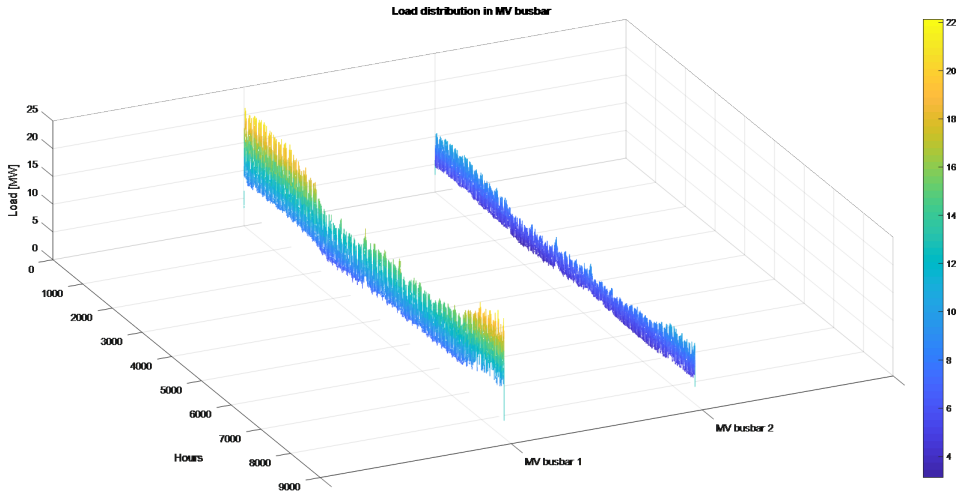

(b) MV busbars load distribution.

Figure 5.11: *Yearly load distribution in Aosta grid (PS, Busbars).*

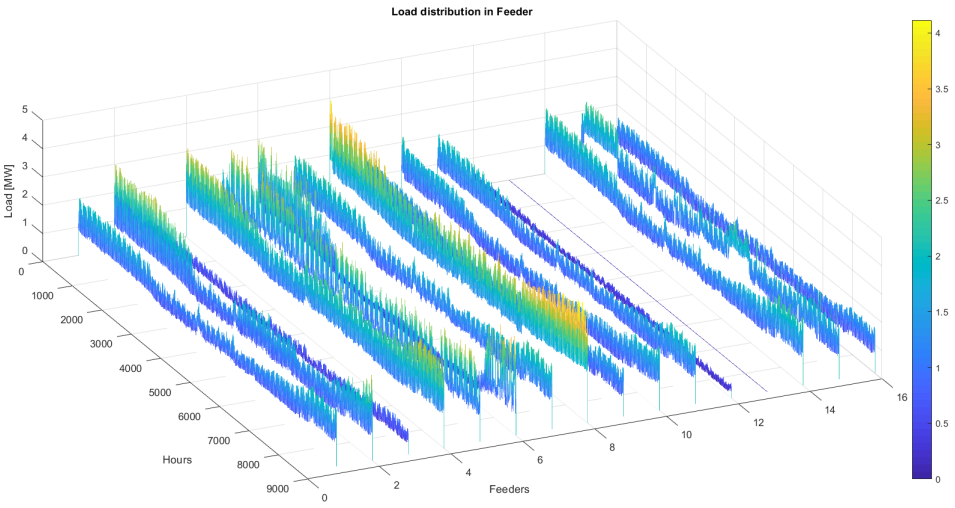

(a) Feeders load distribution.

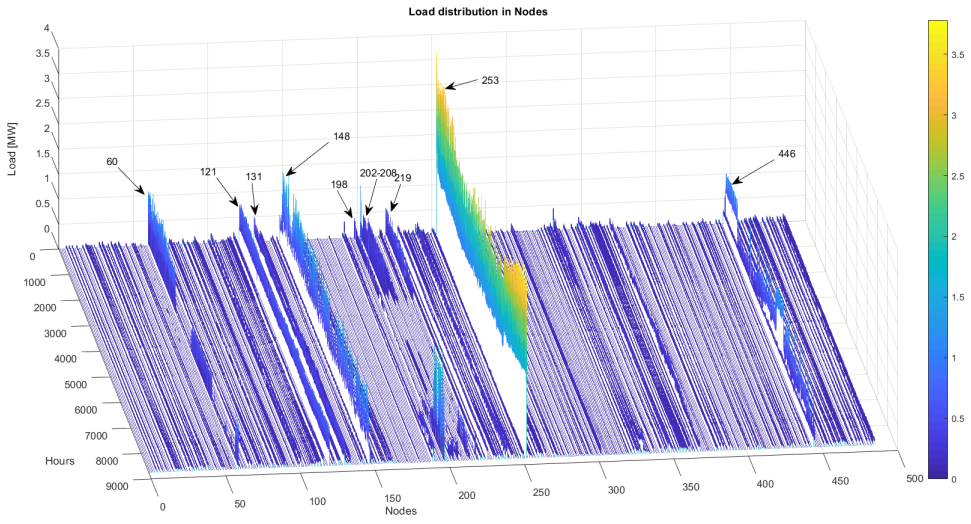

(b) Nodes load distribution.

Figure 5.12: *Yearly load distribution in Aosta grid (Feeders, Nodes).*

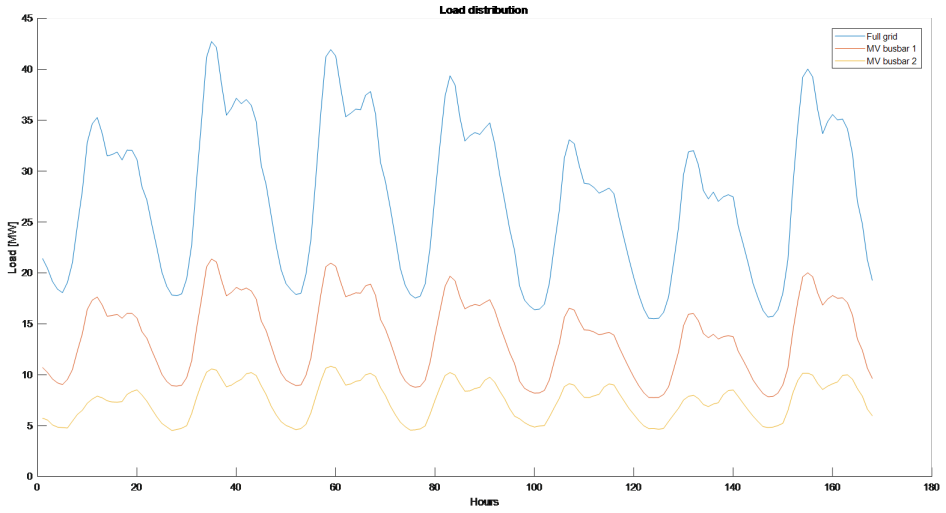

(a) Full grid and each MV busbar weekly load profile.

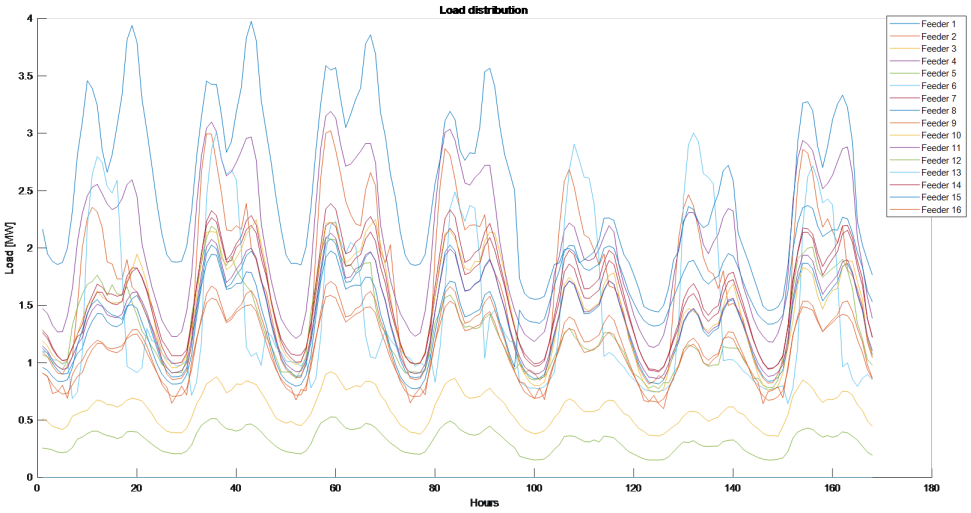

(b) Feeders weekly load profile.

Figure 5.13: *Weekly load profile*

Table 5.2: *Maximum and minimum loading hours for Aosta MV distribution grid.*

		Full Grid	MV busbar	
			1	2
Maximum	**Active Power (MW)**	44.2391	22,1195	11,0446
	Absolute Hour	8555	8555	347
	Daily Relative Hour	11	11	11
Minimum	**Active Power (MW)**	11.4848	5.7424	3.1307
	Absolute Hour	3151	3151	3151
	Daily Relative Hour	7	7	7

From Fig. 5.13 and Table 5.2 it can be seen that the maximum and minimum load of full grid, the MV busbars and feeders have been occurred almost in the same hour of each different day. The maximum loading hour of MV full grid is 8555 which is the same as MV busbar 1 and for MV busbar 2 is 347 where the daily relative hour of all of them is 11 o'clock. The minimum loading hour for all of them was happened at 3151 and daily relative hour of 7 o'clock.

Using all of this deep investigations about loading hours in the grid and mentioned approach in Section 5.3.2, each day can be divided into five zones, have been shown by green continuous line in Fig. 5.14.

- Load demand zone: 1am-6am.
- Drop up zone: 7am-8am.
- Middle high demand zone: 9am and 1pm-8pm.
- Peak demand zone: 10am-12am.
- Drop down zone: 9pm-12am.

Fig. 5.14 represents the loading of feeder 1 in four different groups consists of winter period, summer period, workdays and weekends and holidays. (The other feeders loading have been presented in Appendix A). As it can be gotten from these figures, workdays and weekends do not present a strong difference, Weekends and holidays have a slightly lower active power level. The different hours presents dispersion between $\pm$0.5MW and $\pm$1MW in most of the cases.

Hence, if representative hours have been chosen by 5h from low peak, 8h from drop up, 23h from drop down, 15h from middle load, 11h from first high peak and 19h from second high peak (red discontinuous lines in Fig. 5.14) could cover all the different feeders loading along the year.

5.4.2 Node Selection

According to the selecting node procedure in Section 5.3.2 the number of selected nodes depends on the accumulative impedance of the feeders and collaterals could be changed. By applying the same rules discussed in Section 5.3.2, 106 nodes have been selected. Fig. 5.15, 5.16 and 5.17 compare the full grid R/X ratio, Q-V sensitivity and bus impedance matrix with the selected nodes respectively. The peak value in these figures is indicating the feeders end and the lowest value is indicating the beginning of the feeders. The comparisons highlight the accuracy of those chosen nodes as representatives of the full grid as it could be seen that all the peaks and lower values of the full grid feeders are also presented in the chosen nodes.

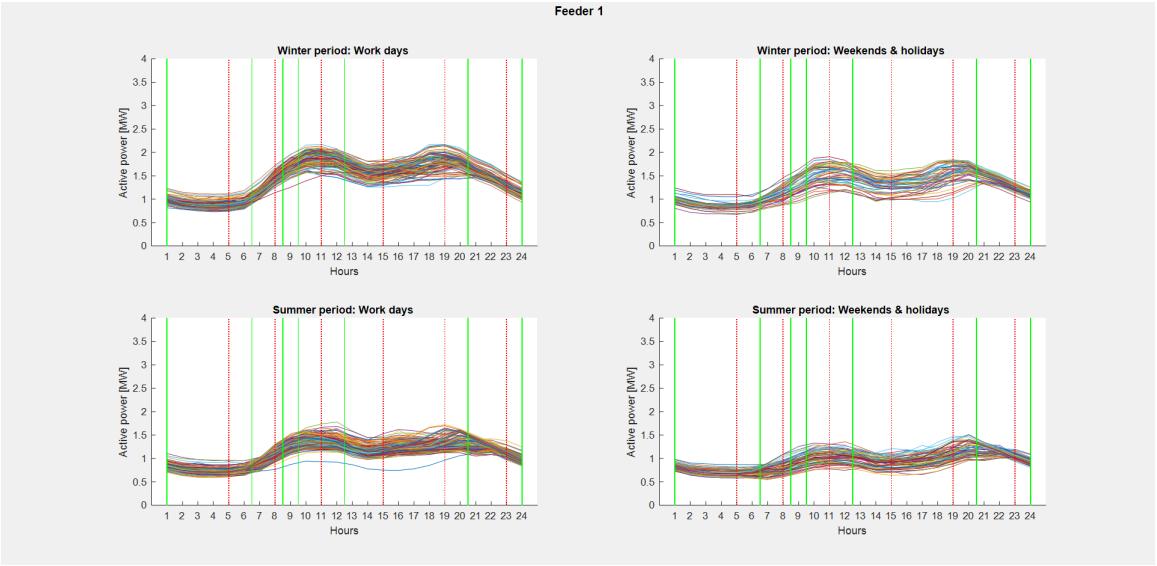

Figure 5.14: *Feeder1 loading profile for winter, summer, workdays and weekends categories.*

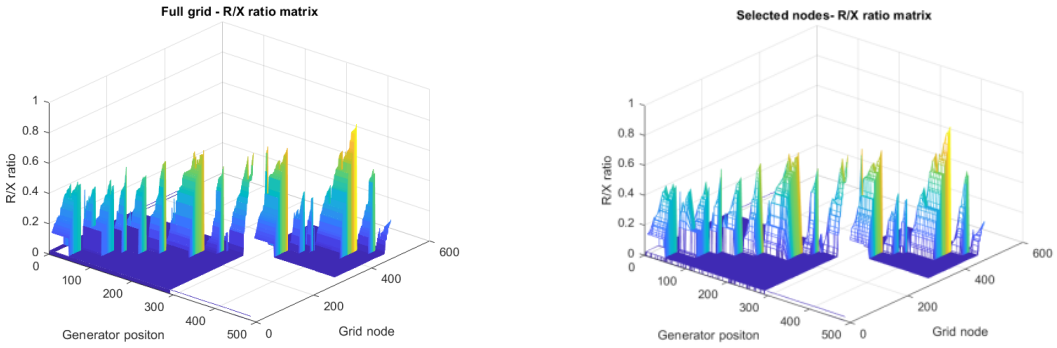

(a) Full grid R/X ratio.

(b) Selected nodes R/X ratio.

Figure 5.15: *R/X ration comparison between full grid and selected nodes.*

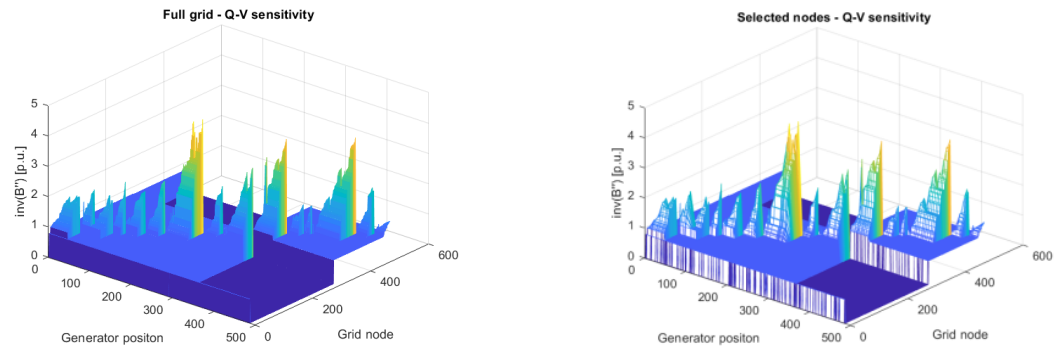

(a) Full grid Q-V sensitivity.

(b) Selected nodes Q-V sensitivity.

Figure 5.16: *Q-V sensitivity comparison between full grid and selected nodes.*

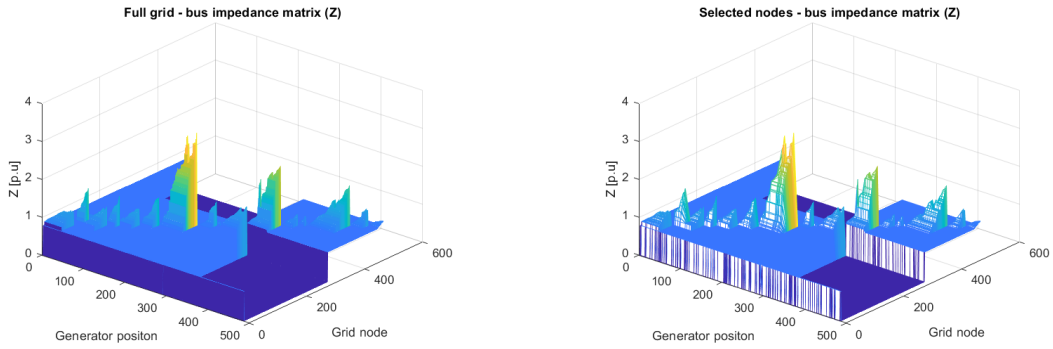

(a) Full grid bus impedance matrix.

(b) Selected nodesbus impedance matrix.

Figure 5.17: *Bus impedance matrix comparison between full grid and selected nodes.*

In the following Fig. 5.18 shows the selected nodes in the Aosta MV distribution grid, 63 of these nodes are located in the MV busbar1 and 43 of them are placed in MV busbar2, as MV busbar2 has less feeders in comparison with busbar1. The voltage profile of these selected nodes has been reported in Fig. 5.19, nodes 220 and 311 have higher voltage value which they have been marked in this figure. Once again, the peaks in this figure represents the feeders end and the lower values represent the beginning og the feeders.

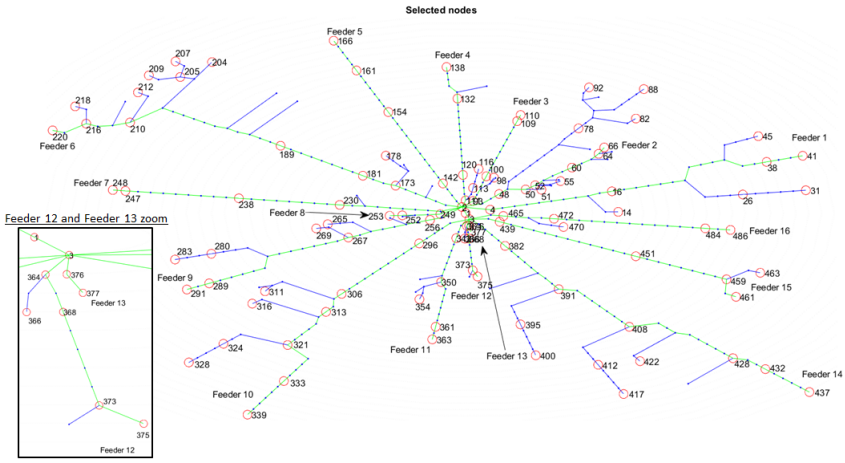

Figure 5.18: *Representatives of Aosta full grid nodes.*

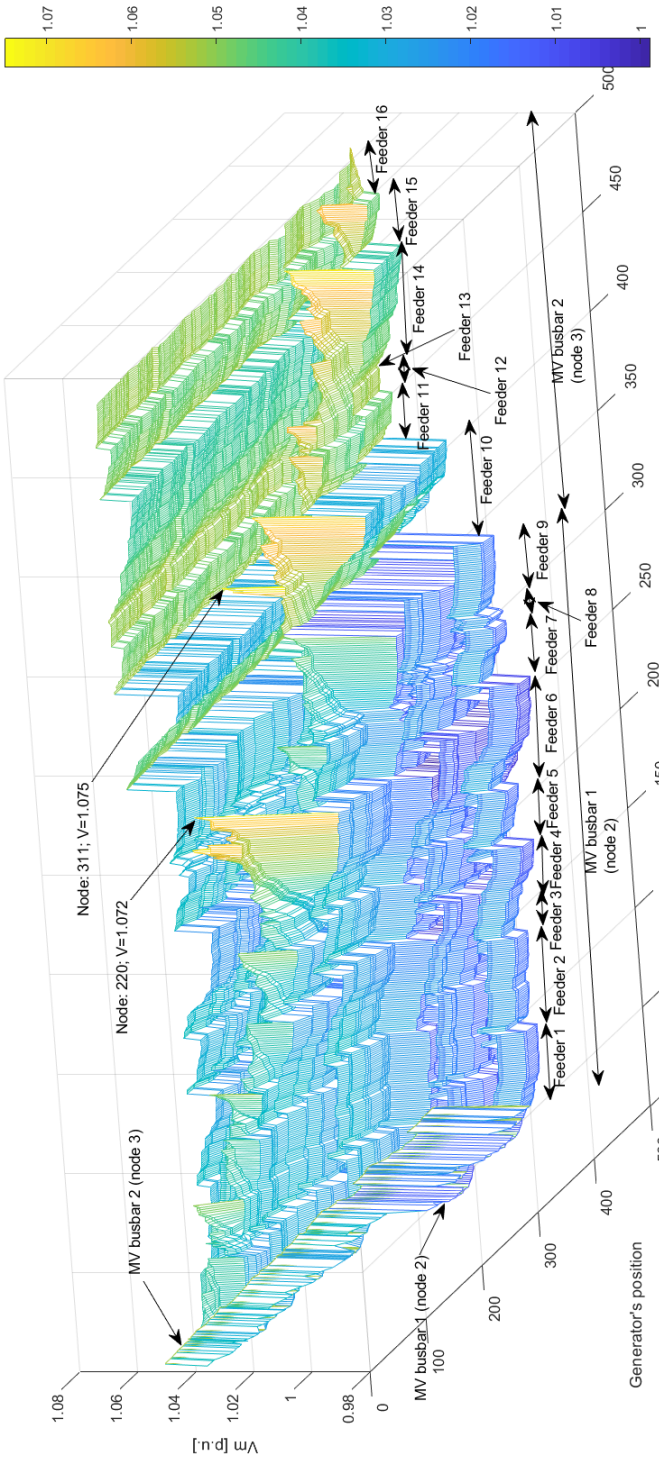

Figure 5.19: *Voltage profile of the selected nodes.*

5.4.3 Penalty Factor Setting

In order to perform OPF, three main penalty factors need to be defined, active, reactive and voltage penalty factor. As it was discussed, the active penalty factor for all the nodes has been considered constant and equal to 100 €/MW and reactive power penalty factor has been considered zero as described in Section 5.3.3. Hence in this Section, voltage penalty factor parameters needs to be defined.

In order to get a better view of the under-study voltage range and its behavior, a brief analysis for the influence of active and reactive power injection on voltage has been done (All of these simulations have been done without considering voltage penalty factor). Figure 5.20 shows voltage profile of selected nodes of Aosta grid at hour of 19 (selected loading hour as second high peak) for 0MW, 1MW and 3MW. As it can be seen from these figures, in case of zero active power injection, voltage drop is clearly visible where it inverts to voltage rise even in other connected feeders to the same MV busbar with increasing active power injection.

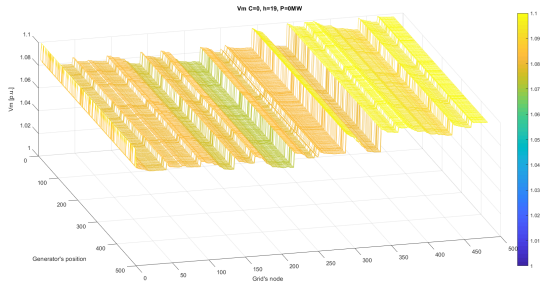

(a) Voltage profile in case of 0MW active power injection.

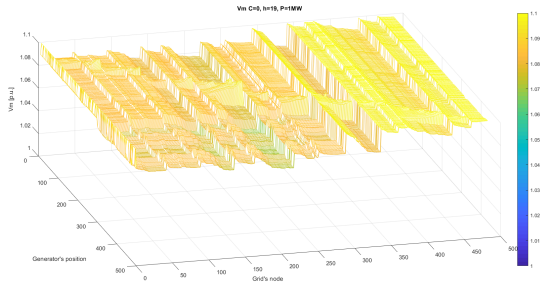

(b) Voltage profile in case of 1MW active power injection.

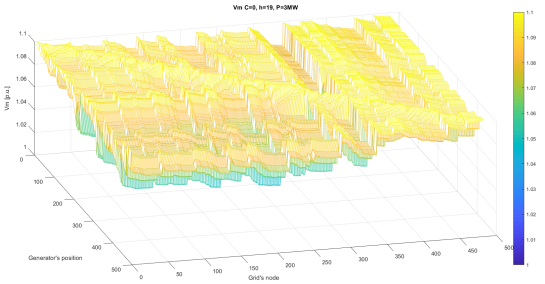

(c) Voltage profile in case of 3MW active power injection.

Figure 5.20: *Aosta grid voltage profile in case of different active power injection.*

In the following the reactive power influence on grid for minimum and maximum loading (3151, 8555) have been reported in Fig. 5.21, as the extrem loadings in the system results the highest difference. When the loading are in its lowest position, the reactive power injection is in its lowest amount, while with higher loading condition, reactive power injection needs to be increased as OPF is able to move the MV busbars voltage close to boundaries. There is a negative reactive power injection possibility in some nodes to avoid upper voltage limit and keep the rest of the feeders at high voltages to minimize losses. Hence, OPF without voltage penalty factor leads all of the nodes voltage to the boundaries in order to reduced energy losses.

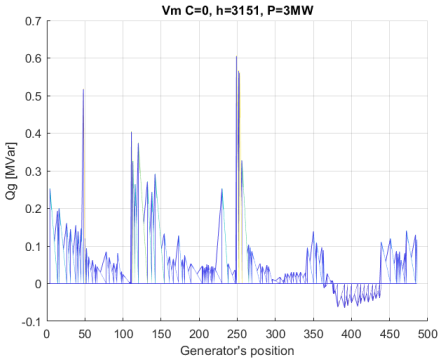

(a) Reactive power injection in case of minimum loading.

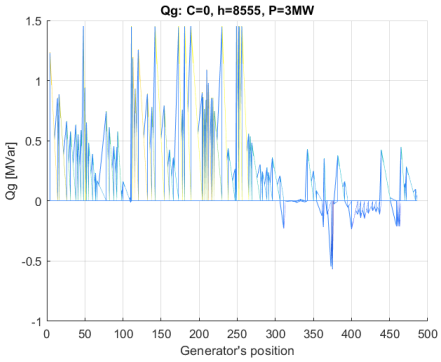

(b) Reactive power injection in case of maximum loading.

Figure 5.21: *Reactive power injection in case of different loading.*

Voltage penalty factor in OPF applies defined penalty to each unit with the voltage above dead band. Voltage penalty factor parameters as it was discussed in Section 5.3.1 is including six parameters: parameter H is considered zero in order to have a linear programming problem, parameter m_i is considered one, parameter r_i for making center 1 for the cost function, equal to one, parameter N is an identity matrix to select voltage nodes. Parameter dead band (k_i) and the penalty factor (C) needs to be defined according to several grid investigations in following.

The penalty factor (C) could be chosen among the wide range of zero to positive infinitive. In this thesis further studies have been done with considering the value from 0 to 100 with different steps in between. For dead band value (k_i) more than zero value has been considered to avoid adding penalty factor to acceptable voltage values and therefore avoid unnecessary energy losses increasing. Hence, in this thesis 0.04, 0.05 and 0.06 have been considered.

The OPF is performed considering a generator in each studied node with different active power from 1MW, 2 MW and 3MW. Table 5.3 represents the results of OPF for different penalty factor, dead band and active power for the worst Asota grid node and for the loading hour of 19 as an agreement between the maximum and minimum grid loading. As it can be seen from the table by increasing the voltage penalty factor, the voltage in this node is decreasing, while increasing the injected active power has a negative effect on energy losses. That is why, OPF works on the direction of increasing the voltage according to the defined dead band to reduce the losses.

Table 5.3: *Different voltage penalty factor, dead band and active power injection influence on voltage.*

	Dead Band (p.u.)																					
	0.04						0.05						0.06									
	Injected Active Power (MW)																					
	1		2		3		1		2		3		1		2		3					
Penalty Factor	**V (p.u.)**	**ΔV (p.u.)**	**V (p.u.)**	**ΔV (p.u.)**	**V (p.u.)**	**ΔV (p.u.)**	**V (p.u.)**	**ΔV (p.u.)**	**V (p.u.)**	**ΔV (p.u.)**	**V (p.u.)**	**ΔV (p.u.)**	**V (p.u.)**	**ΔV (p.u.)**	**V (p.u.)**	**ΔV (p.u.)**	**V (p.u.)**	**ΔV (p.u.)**				
0	1,1	-	1,1	-	1,1	-	1,1	-	1,1	-	1,1	-	1,1	-	1,1	-	1,1	-				
1	1,0951	0,0049	1,1000	-7,19e-09	1,1000	2,57e-08	1,1000	9,35e-06	1,1000	1,50e-09	1,1000	-1,39E-10	1,1000	5,66e-08	1,1000	1,14e-09	1,1000	-8,77e-11				
2	1,0776	0,0224	1,0951	0,0049	1,1000	1,15e-07	1,0871	1,29e-02	1,1000	6,99e-08	1,1000	1,19e-08	1,0966	3,42e-03	1,1000	-1,45e-08	1,1000	1,65e-08				
3	1,0709	0,0291	1,0884	0,0116	1,1000	6,82e-09	1,0806	0,0194	1,0979	2,09e-03	1,1000	7,02e-08	1,0903	0,0097	1,1000	1,99e-08	1,1000	-3,41e-08				
4	1,0673	0,0327	1,0847	0,0153	1,1000	0,0000	1,0771	0,0229	1,0943	5,72e-03	1,1000	1,23e-07	1,0869	0,0131	1,1000	7,59e-08	1,1000	9,20e-09				
5	1,0650	0,0350	1,0823	0,0177	1,0994	0,0006	1,0748	0,0252	1,0919	0,0081	1,1000	-1,76e-08	1,0846	0,0154	1,1000	0,0000	1,1000	2,84e-08				
10	1,0594	0,0406	1,0760	0,0240	1,0925	0,0075	1,0693	0,0307	1,0857	0,0143	1,1000	0,0000	1,0791	0,0209	1,0954	0,0046	1,1000	0,0000				
15	1,0568	0,0432	1,0729	0,0271	1,0888	0,0112	1,0667	0,0333	1,0825	0,0175	1,0983	0,0017	1,0765	0,0235	1,0922	0,0078	1,1000	0,0000				
20	1,0552	0,0448	1,0707	0,0293	1,0862	0,0138	1,0650	0,0350	1,0803	0,0197	1,0957	0,0043	1,0747	0,0253	1,0900	0,0100	1,1000	0,0000				
30	1,0531	0,0469	1,0678	0,0322	1,0825	0,0175	1,0630	0,0370	1,0775	0,0225	1,0920	0,0080	1,0728	0,0272	1,0872	0,0128	1,1000	0,0000				
40	1,0519	0,0481	1,0659	0,0341	1,0799	0,0201	1,0617	0,0383	1,0756	0,0244	1,0895	0,0105	1,0716	0,0284	1,0854	0,0146	1,0991	0,0009				
50	1,0510	0,0490	1,0644	0,0356	1,0779	0,0221	1,0608	0,0392	1,0742	0,0258	1,0875	0,0125	1,0707	0,0293	1,0840	0,0160	1,0971	0,0029				
75	1,0494	0,0506	1,0618	0,0382	1,0740	0,0260	1,0594	0,0406	1,0716	0,0284	1,0836	0,0164	1,0693	0,0307	1,0814	0,0186	1,0933	0,0067				
100	1,0485	0,0515	1,0599	0,0401	1,0710	0,0290	1,0584	0,0416	1,0697	0,0303	1,0807	0,0193	1,0683	0,0317	1,0795	0,0205	1,0903	0,0097				

In the following, Table 5.4 categorizes the voltage level of Aosta grid with different dead band and penalty factor in case of 3MW active power injection as the highest possibility of voltage rise happens with higher active power injections. From the reported results, the increasing of voltage penalty factors causes higher voltage nodes number decreasing. However, increasing the amount of dead band leads to voltage increasing. Therefore, by considering energy losses trend a trade off between theses two values need to be defined.

Therefore, Fig. 5.22 - 5.24 show the energy losses for different dead bands and active power injections. The significant changes in these figures happened when there is a bigger R/X ratio and Q-V sensitivity (mostly end the feeders or collaterals connected to the end). Overall, as discussed before energy losses are lower when dead band is higher and voltage penalty factor is smaller.

Table 5.4: *Aosta grid voltage classified for different dead band and voltage penalty factor.*

	Dead Band (p.u.)													
	0.04													
	Voltage Penalty Factor													
Voltage Range (p.u.)	**0**	**1**	**2**	**3**	**4**	**5**	**10**	**15**	**20**	**30**	**40**	**50**	**75**	**100**
1.06 - 1.07	0	0	53	129	265	274	193	133	104	67	55	46	30	22
1.07 - 1.08	0	0	206	291	153	97	33	13	11	15	12	11	4	2
1.08 - 1.09	0	122	193	47	18	11	13	12	9	3	0	0	0	0
1.09 - 1.1	485	363	33	18	14	12	3	0	0	0	0	0	0	0
	0.05													
	Voltage Penalty Factor													
Voltage Range (p.u.)	**0**	**1**	**2**	**3**	**4**	**5**	**10**	**15**	**20**	**30**	**40**	**50**	**75**	**100**
1.06 - 1.07	0	0	0	0	59	101	252	312	318	297	244	230	205	180
1.07 - 1.08	0	0	89	141	250	268	190	123	101	63	52	39	29	21
1.08 - 1.09	0	0	206	290	145	93	29	14	12	14	12	11	3	1
1.09 - 1.1	485	485	190	54	31	23	14	11	7	3	0	0	0	0
	0.06													
	Voltage Penalty Factor													
Voltage Range (p.u.)	**0**	**1**	**2**	**3**	**4**	**5**	**10**	**15**	**20**	**30**	**40**	**50**	**75**	**100**
1.06 - 1.07	0	0	0	0	0	0	0	36	54	122	179	208	253	286
1.07 - 1.08	0	0	0	0	87	112	265	305	317	284	244	228	203	179
1.08 - 1.09	0	0	107	157	236	271	184	120	95	65	50	38	26	19
1.09 -1.1	485	485	378	328	162	102	36	24	19	14	12	11	3	1

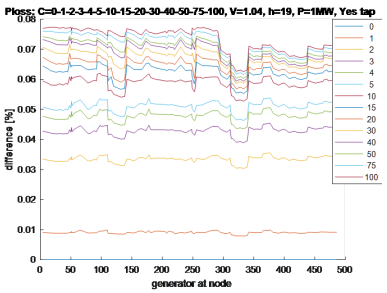

(a) Aosta energy losses with dead band ±0.04 and 1MW injection.

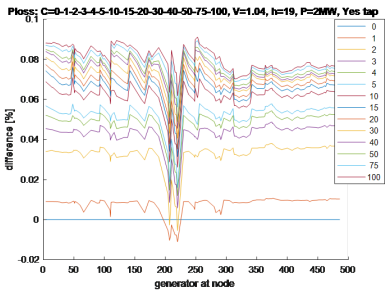

(b) Aosta energy losses with dead band ±0.04 and 2MW injection.

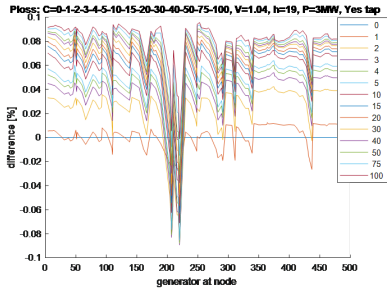

(c) Aosta energy losses with dead band ±0.04 and 3MW injection.

Figure 5.22: *Aosta energy losses for dead band ±0.04.*

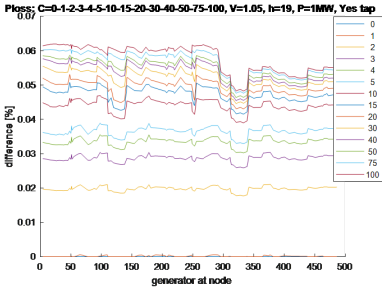

(a) Aosta energy losses with dead band ±0.05 and 1MW injection.

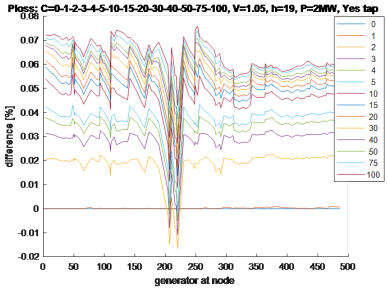

(b) Aosta energy losses with dead band ±0.05 and 2MW injection.

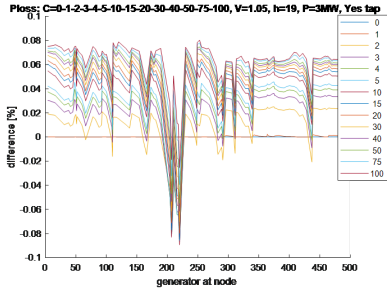

(c) Aosta energy losses with dead band ±0.05 and 3MW injection.

Figure 5.23: *Aosta energy losses for dead band ±0.05.*

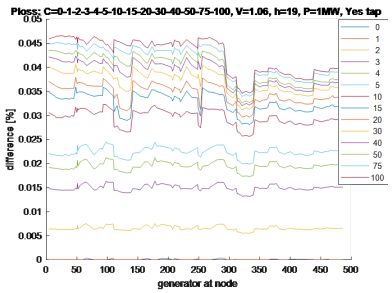

(a) Aosta energy losses with dead band ±0.06 and 1MW injection.

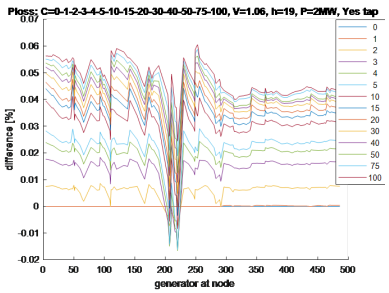

(b) Aosta energy losses with dead band ±0.06 and 2MW injection.

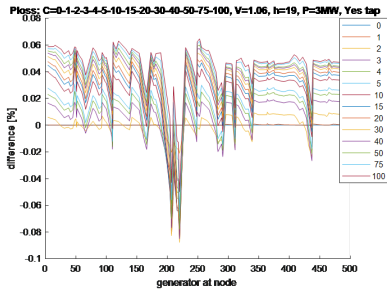

(c) Aosta energy losses with dead band ±0.06 and 3MW injection.

Figure 5.24: *Aosta energy losses for dead band ±0.06.*

Figure 5.25 represents the voltage level and energy losses of Node 220 (as a node with high voltage level) for different dead band, penalty factor and active.

According to all of this deep investigations, choosing a dead band equal to 0,05 and a voltage penalty factor equal to 10 could be a wise option as the number of nodes at the last voltage range is few (14 nodes) and the energy loses increasing is around 0,04%-0,06% for an injected power equal to 3MW. The voltage profile of selected nodes of Aosta grid by implementing these values to OPF and performing it for active power of 1MW and 3MW has been compared in Fig. 5.26. As it can be understood from this figures, the existence of penalty factor has a significant effect on voltage profile especially in higher power injection.

5.4.4 Clusterization Procedure

The clusterization process has been performed by MATLAB tools cluster analysis from Statistics and Machine Learning Toolbox. In this study OPF results are the used data in the clusterization. Selected variables in this study are R/X ratio, bus impedance matrix (Z) and generator reactive power injection. R/X ratio and Z have been selected in order to process different grid characteristics separately from the load, while reactive power is considered to gather or pull apart nodes with similar ro different behavior due to loads or voltage levels.

The clusters are required to classify the nodes depending on their behavior. The clusters in this studies need to cover different loading situation along the year. Hence, first nodes have been clusterized according to two different loading hours with different reactive power behaivour. Then, in order to make a comparison the clusters are crossed. If the nodes are not in the same cluster in both hours, they split

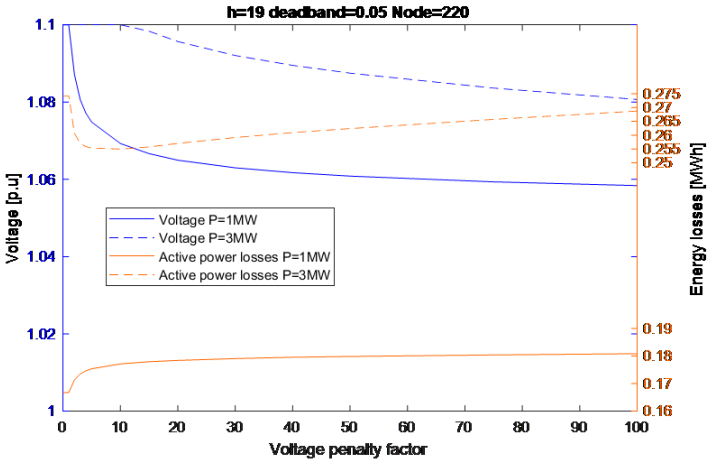

(a) Voltage and energy losses with different voltage penalty factor and dead band equal to ± 0.05.

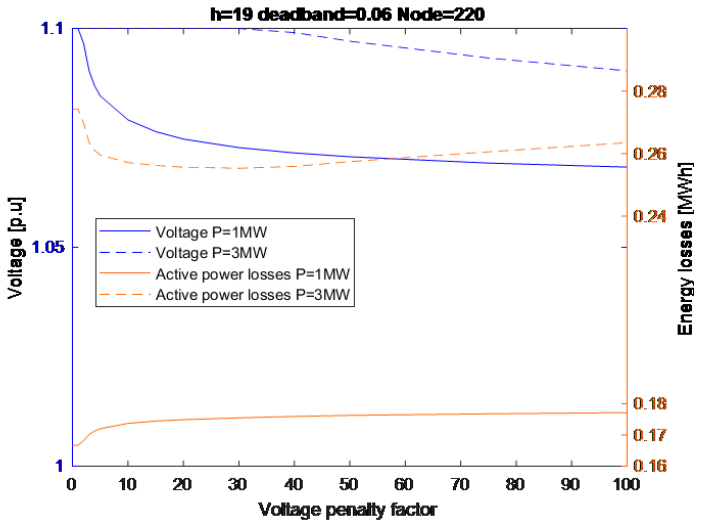

(b) Voltage and energy losses with different voltage penalty factor and dead band equal to ± 0.06.

Figure 5.25: *Voltage and energy losses with different voltage penalty factor and dead band.*

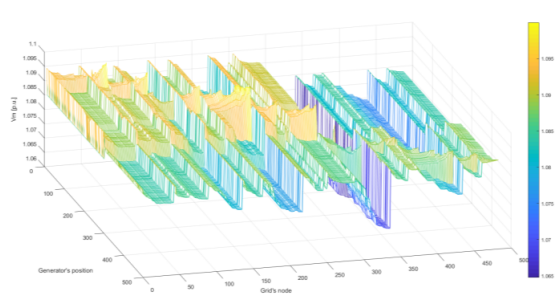

(a) Aosta voltage profile with C=0, P=1MW.

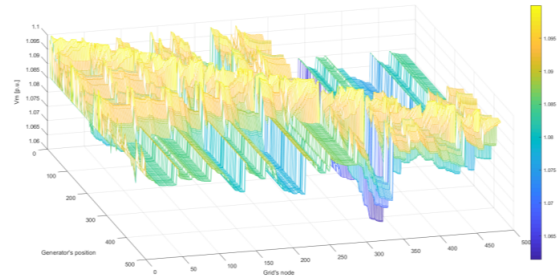

(b) Aosta voltage profile with C=0, P=3MW.

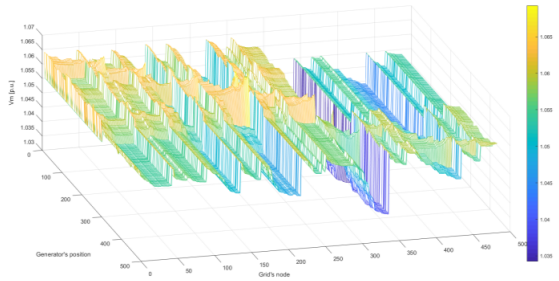

(c) Aosta voltage profile with C=10, P=1MW.

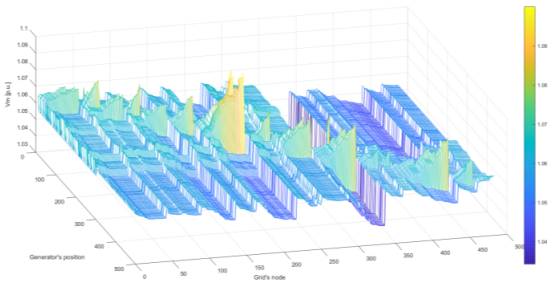

(d) Aosta voltage profile with C=10, P=3MW.

Figure 5.26: *Comparing voltage profile of selected nodes with and without penalty factor.*

in two or more clusters. After that by checking the volt-var representation of the clusters, in case of necessity some cluster are joined together or some nodes have been moved. In the last step, a manual check have been done for the selected wider range of loading hour (5, 8, 11, 15, 19, 23, 347, 3151 and 8555) and required modifications have been performed.

In the following, Fig. 5.27 represents the clusterization for two different loading hours, different colors define different clusters. R/X ratio in both loading hours is the same, while the reactive power changes where these variation produces different clusters. After that by crossing these two clusterizations, separation procedure for the nodes which are in the same cluster but behaving differently have been done.

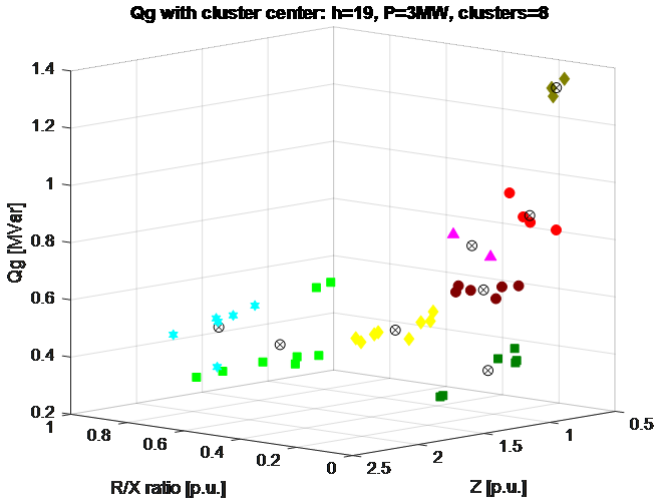

(a) OPF output clusterization for selected loading hour 19h.

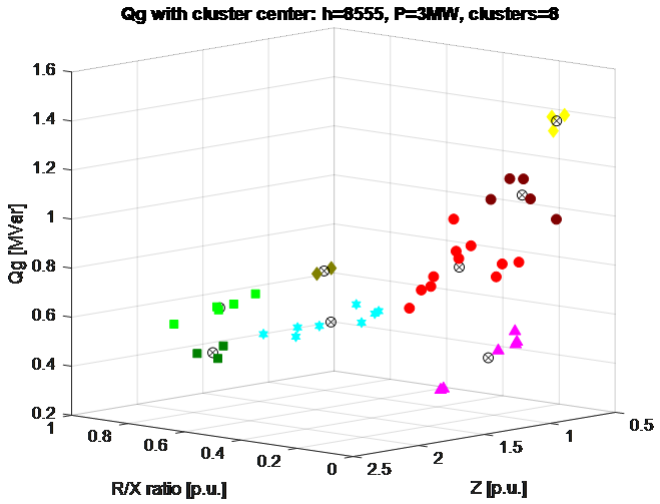

(b) OPF output clusterization for selected loading hour 8555h.

Figure 5.27: *OPF output clusterization for different loading hour.*

Therefore, Fig. 5.28 show the final clusterization of MV busbar1 and 2. MV busbar1 has 9 clusters and MV busbar2 has 10. In general, clusters do not have any overlapping and in some minor cases the overlapped points have completely different behavior.

In the following figures, the map of the grid considering the clusterization for two busbars have been presented. As it can be seen from these figures, feeders with higher loading have been presented by more clusters such as feeder 6 where cluster 2, 6 and 9 are presenting this feeder.

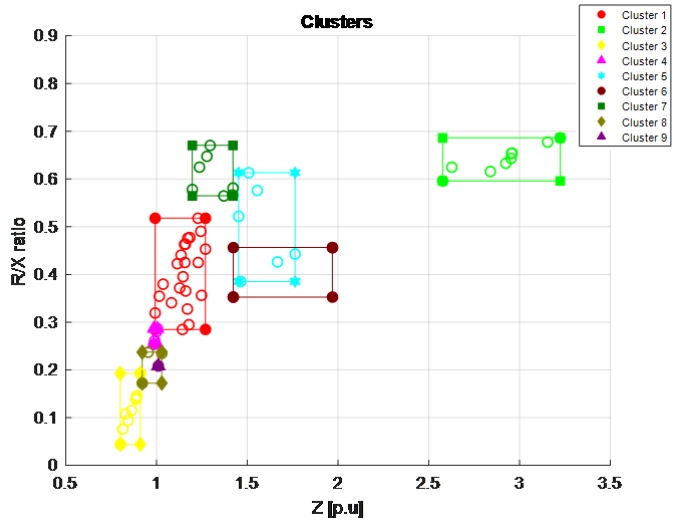

(a) Final clusterization of MV busbar1.

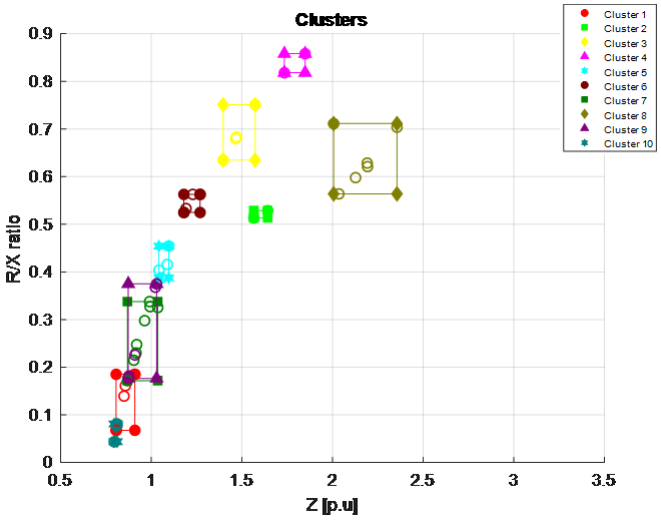

(b) Final clusterization of MV busbar2.

Figure 5.28: *Final clusterization of MV busbar1 and MV busbar2.*

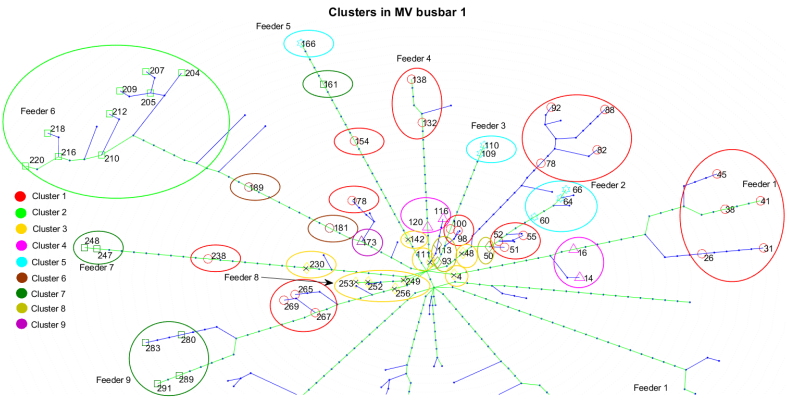

(a) Representing MV busbar1 clusterization on the grid map.

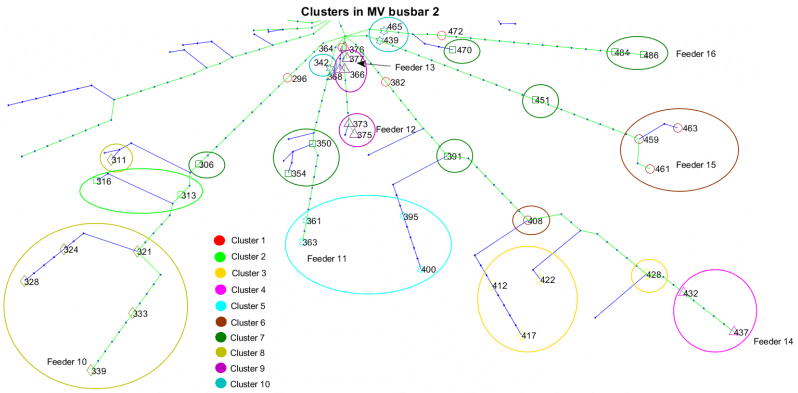

(b) Representing MV busbar2 clusterization on the grid map.

Figure 5.29: *Representing MV busbars clusterization on the grid map.*

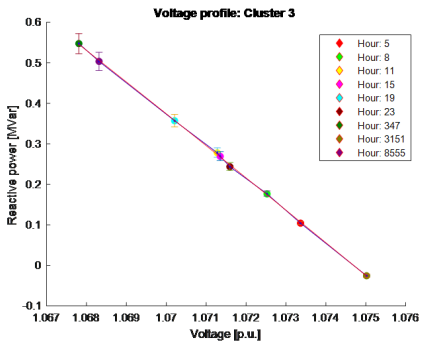

Figure 5.30: *Linearization of cluster 3.*

5.5 Results and Discussion

The performed simulation in this section considers 3MW active power injection; this amount has been chosen based on the maximum power injection that the studied node can accept due to thermal limit

violation, whereas reactive power boundaries in this simulation has been characterized by power factor equal to 0.9. Moreover, the two different voltage of 1.02p.u. and 1.055p.u. for MV busbars have been simulated. The first value, 1.02p.u., has been chosen as the typical used voltage value by DSO is between 1.02p.u. and 1.03p.u., and the second value was chosen in order to test a higher value which does not move voltages too close to upper boundaries (as dead band is equal to $\pm$ 0.05p.u.).

Before making comparison between the proposed approach and the other available approaches, more discussion about the proposed LVC test have been expressed as follows. In the linearization procedure, each point has its own reactive power error. In the following, the linearization of cluster 1 and cluster 2 of MV busbar1 have been shown for both busbar voltages (1.02p.u. and 1.055p.u.) in Fig. 5.31 with the same scale. From the figures it could be seen that the reactive power error in cluster 1 is higher than the error in cluster 2. Hence, cluster 2 shows much closer behaivour to OPF results than cluster 1. However, in all of the reported figures reactive power injections from higher values move to close zero. It is because in high loading hour, there is a high energy flow which leads to high energy losses and voltage drop as well. Then, OPF by injecting reactive power wants to compensate the voltage drop and energy losses reduction. Moreover, the presented voltage profiles with lower MV busbar value have lower values compare to the higher one. The clusters of MV busbar2 cover a shorter reactive power range as it supplies a lower loading in comparison with busbar1. All the clusters for both MV busbars at different voltages have been presented in Appendix A.

Once the LVC setting has been completed by defining section 3 described in the previous Section, the LVC test can be executed. The performing load flow is based on the bisection method which the obtained reactive power in the privious iteration has been used as an input to define the new reactive power defined by LVC, equation 5.46.

$$q(t+1) = [1-\alpha(t)].q(t) + \alpha(t)[q(v(t))]_{q_{min}}^{q_{max}} \tag{5.46}$$

The tested LVC for MV busbar1 with voltage at 1.055p.u. have been reported in the following for four different clusters, Fig. 5.32.

Hence, by recognizing the different behaivour of various clusters it can be conclude that reactive power effect on voltage is playing an important role for energy losses reduction. Table 5.5 represents the results of load flow calculation for MV busbar fixed at 1.055p.u. for different combination of real and reactive power for Cluster1 and Cluster2 in the maximum and minimum loading hours. Cluster1 and Cluster2 have been chosen as an example of a cluster with strong reactive power drop and low reactive power drop respectively.

From this table it can be seen that the effect of active and reactive power on voltage in Cluster1 is lower than Cluster2. Energy losses increase significantly by arising active power injection. Moreover, reactive power injection is not able to reduce the losses as it has a low effect on voltages and even it increases the energy losses. Therefore, the reactive power injection has been reduced to avoid unnecessary energy losses increase. On the other hand in cluster2, energy losses could be decreased slowly by reactive power injection as it is able to compensate the energy losses reduction thanks to the voltages rise.

The aim of this part is evaluate and comparison the results of the proposed LVC, standard LVC, OPF and simple power flow with PF equal to 1. Hence the following Table 5.6 reports the average energy losses for both MV busbars for mentioned approaches.

Performing OPF simulation guarantees the best settings for voltage and reactive power injection,

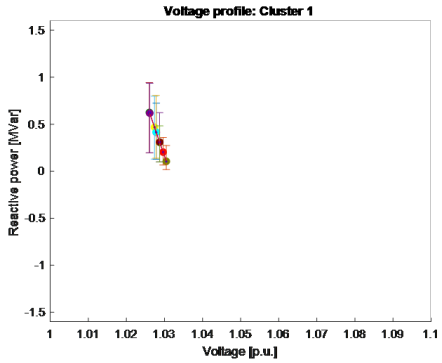

(a) LVC section 3 for MV busbar1 1.02p.u., Cluster 1.

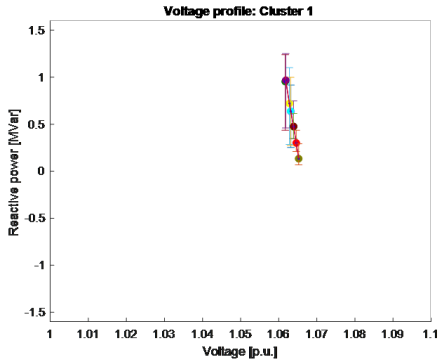

(b) LVC section 3 for MV busbar1 1.055p.u., Cluster 1.

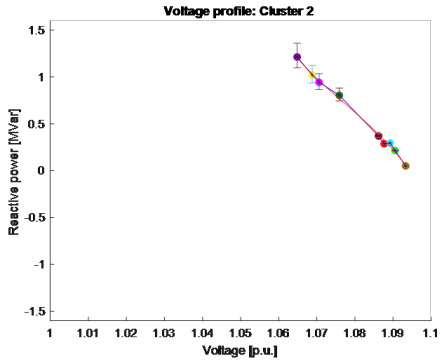

(c) LVC section 3 for MV busbar1 1.02p.u., Cluster 2.

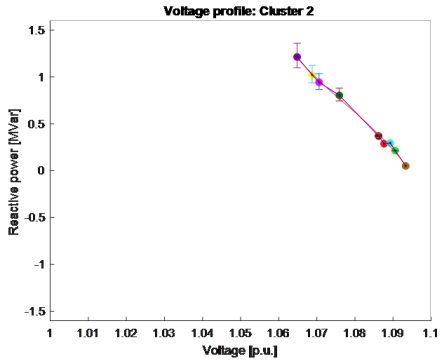

(d) LVC section 3 for MV busbar1 1.055p.u., Cluster 2.

Figure 5.31: *Different clusters LVC setup section 3 for MV busbar1 with different voltage.*

Table 5.5: *Voltage and energy losses comparison for different clusters in MV busbar1.*

Voltage (p.u.)						
	Cluster 1 (Feeder 3)			**Cluster 2 (Feeder 6)**		
Hour	**3151**	**19**	**8555**	**3151**	**19**	**8555**
P = 0 (MW)	1,0536	1,0524	1,0516	1,0407	1,0424	1,0004
P = 3 (MW), Q = 0 (Mvar)	1,0633	1,0621	1,0614	1,0768	1,0784	1,0398
P = 3 (MW), Q = 1.5 (Mvar)	1,0678	1,0667	1,0659	1,0963	1,0978	1,0604
Energy Losses (MWh)						
	Cluster 1 (Feeder 3)			**Cluster 2 (Feeder 6)**		
Hour	**3151**	**19**	**8555**	**3151**	**19**	**8555**
P = 0 (MW)	0,0006	0,0017	0,0026	0,0096	0,0077	0,1284
P = 3 (MW), Q = 0 (Mvar)	0,0209	0,0175	0,0156	0,0562	0,0599	0,0283
P = 3 (MW), Q = 1.5 (Mvar)	0,0270	0,0225	0,0199	0,0686	0,0735	0,0092

therefore the amount of energy losses is in lower value. The energy losses for standard LVC and normal load flow with PF1 is almost similar for the MV busbar equal to 1.02p.u. as the operational voltage range in all the nodes is less than the voltage dead band value (1.05p.u.). However, this amount is going higher when the voltage at MV busbar sets at 1.055p.u. as in the standard LVC the reactive power injection has been started after the dead band value to decrease the voltages. Therefore, the enhanced LVC (proposed LVC in this thesis) performs better with the defined setting compared to standard LVC, as it can be seen from Table 5.6 the energy losses in this LVC is not so far from OPF results. In order to analyze the

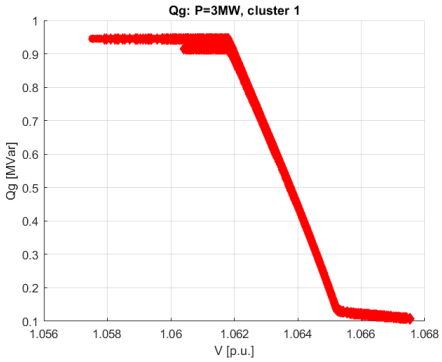

(a) LVC setting test for MV busbar1 1.055p.u., Cluster 1.

(b) LVC setting test for MV busbar1 1.055p.u., Cluster 2.

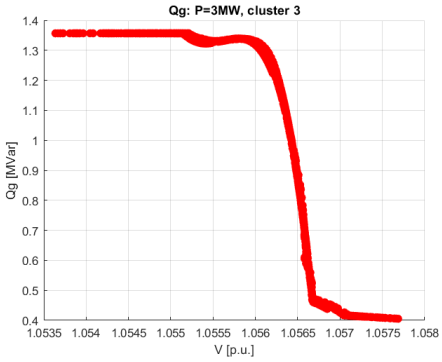

(c) LVC setting for MV busbar1 1.055p.u., Cluster 3.

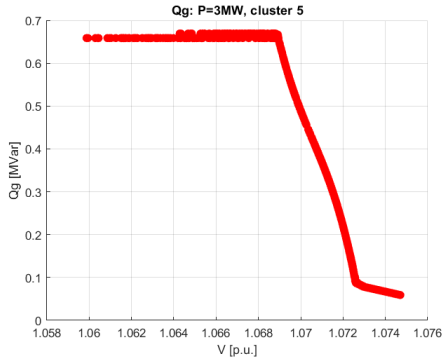

(d) LVC setting test for MV busbar1 1.055p.u., Cluster 5.

Figure 5.32: *Different clusters LVC setting test for MV busbar1 with 1.055p.u. voltage.*

Table 5.6: *Energy losses comparison for different approaches.*

	Energy Losses			
	MV busbar fix at 1.02p.u.		**MV busbar fix at 1.055p.u.**	
	MV busbar1	**MV busbar2**	**MV busbar1**	**MV busbar2**
OPF (MWh)	17,0148	9,2790	23,2243	8,4413
Enhanced LVC	+0,06%	+0,51%	+0,27%	+3,06%
Standard LVC	+1,42%	+1,78%	+3,95%	+8,55%
Load Flow, PF=1	+1,39%	+1,78%	+1,34%	+4,22%

influence of the different aforementioned approaches on Aosta grid, Table 5.7 presents the average of energy losses for each cluster with both voltage values at MV busbars.

The results in Table 5.7 follows the results of Table 5.6. As it was discussed before, Cluster2 in MV busbar1 has the lowest reactive power drop and the highest energy loss compare to the others. Moreover, as the voltage profile of Cluster9 in MV busbar2 is very close to zero enhanced LVC does not show a better performance compare to the other methods. In general, the energy losses is lower with the higher MV busbar voltage (here 1.055p.u.) due to voltage increasing.

Table 5.7: *Energy losses comparison for different approaches in different clusters.*

MV busbar1, V=1.02p.u.										
Cluster	**1**	**2**	**3**	**4**	**5**	**6**	**7**	**8**	**9**	
OPF	3,4255	10,5816	0,8194	1,6409	6,6007	5,4699	6,2691	1,6054	5,5353	
Enhanced LVC	+0,39%	+0,11%	+1,22%	+0,16%	+0,15%	+0,40%	+0,05%	+0,59%	+0,01%	
Standard LVC	+3,53%	+8,67%	+13,62%	+10,38%	+1,51%	+9,86%	+0,94%	+6,80%	+3,36%	
Load Flow, PF=1	+3,53%	+8,31%	+13,62%	+10,38%	+1,51%	+9,86%	+0,94%	+6,80%	+3,36%	
MV busbar2, V=1.02p.u.										
Cluster	**1**	**2**	**3**	**4**	**5**	**6**	**7**	**8**	**9**	**10**
OPF	1,4691	4,3854	6,0367	9,0835	3,1944	4,3486	1,8134	7,8397	2,8017	0,6331
Enhanced LVC	+0,59%	+0,02%	+0,10%	+0,04%	+0,09%	+0,04%	+0,51%	+0,10%	+10,80%	+0,39%
Standard LVC	+2,74%	+7,37%	+1,97%	+1,45%	+2,57%	+2,63%	+4,29%	+4,80%	+10,81%	+3,51%
Load Flow, PF=1	+2,74%	+7,37%	+1,97%	+1,45%	+2,57%	+2,63%	+4,29%	+4,80%	+10,81%	+3,51%
MV busbar1, V=1.055p.u.										
Cluster	**1**	**2**	**3**	**4**	**5**	**6**	**7**	**8**	**9**	
OPF	3,2031	9,9455	0,7643	1,5333	6,1812	5,1141	5,8715	1,4995	5,1464	
Enhanced LVC	+1,23%	+1,17%	+2,22%	+1,99%	+0,29%	+0,99%	+0,43%	+2,42%	+0,03%	
Standard LVC	+9,56%	+24,29%	+17,25%	+16,42%	+8,40%	+14,77%	+8,42%	+10,50%	+4,43%	
Load Flow, PF=1	+3,42%	+7,88%	+13,45%	+10,18%	+1,44%	+9,50%	+0,88%	+6,64%	+3,27%	
MV busbar2, V=1.055p.u.										
Cluster	**1**	**2**	**3**	**4**	**5**	**6**	**7**	**8**	**9**	**10**
OPF	1,3680	4,1054	5,6543	8,5170	2,9862	2,9863	1,6942	7,3509	2,6212	+0,5904
Enhanced LVC	+1,14%	+0,00%	+0,13%	+0,06%	+0,28%	+0,27%	+1,11%	+0,14%	+11,27%	+1,56%
Standard LVC	+4,53%	+18,21%	+12,88%	+16,22%	+8,28%	+8,28%	+9,03%	+19,51%	+12,49%	+5,08%
Load Flow, PF=1	+2,62%	+7,03%	+1,78%	+1,30%	+2,45%	+2,45%	+4,14%	+4,54%	+10,81%	+3,44%

As the loading behavior is changing along each time span, the voltage of the nodes is also changing. Fig. 5.33 in the following shows the percentage of the nodes in each voltage range for each busbar and with different voltage values in one week.

From Fig. 5.33, it is clear that the OPF has higher voltage level than the other approaches when the voltage of MV busbar is fixed at 1.02p.u., while when the voltage is fixed at 1.055p.u. the voltages is shifted to the right as the voltage penalty factor has been started at 1.05p.u. and OPF tries to keep the voltages close to the dead band to reduce the system cost. Therefore, the enhanced LVC with the MV busbar voltage fixed at 1.055p.u. also has higher voltage value in comparison with the fixed voltage at 1.02p.u. due to the high reactive power injections which leads to higher voltage values. Whereas, the voltage profile trend of standard LVC and normal load flow with PF1 by changing the MV busbar voltage to the higher value have been changed, the standard LVC setting starts to absorb reactive power and reduce the voltages as the voltage dead band is 1.05p.u., however in the other case more nodes with the voltage higher than 1,07p.u compared to standard LVC could be found due to zero reactive power injections. The difference between the voltage distribution of busbars is due to the different busbars loading, which the lower load OPF requires less voltage rise for energy losses compensation.

At the end, Table 5.8 and 5.9 represent the energy losses for each studied node of each cluster. Some clusters in MV busbar1 and MV busbar2 due to the high voltage error have different results compare to the OPF result. However, the rest of the results has the value between OPF simulation results and standard LVC which is a proven of the great performance of enhance LVC as it was expected.

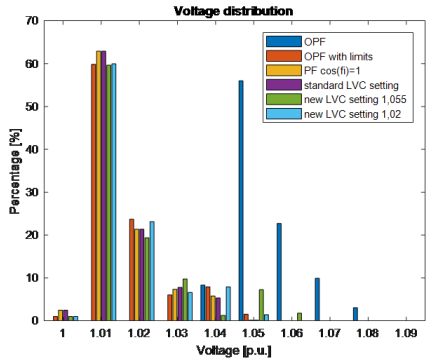

(a) Voltage distribution for MV busbar1, V=1.02p.u..

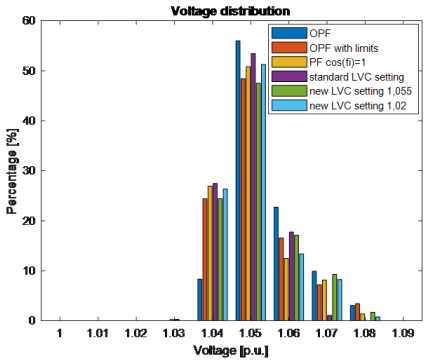

(b) Voltage distribution for MV busbar1, V=1.055p.u..

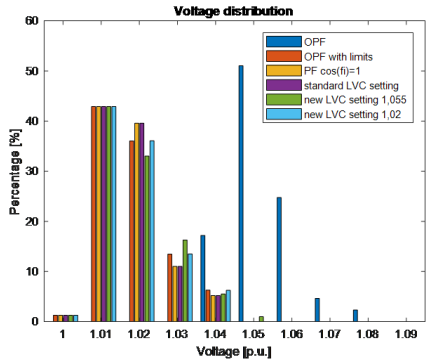

(c) Voltage distribution for MV busbar2, V=1.02p.u..

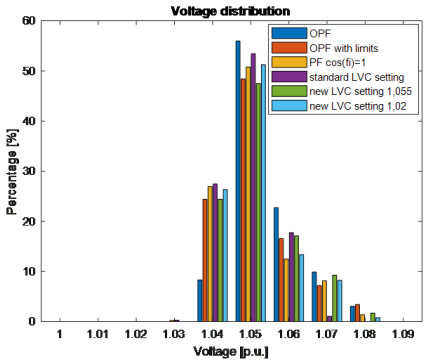

(d) Voltage distribution for MV busbar2, V=1.055p.u..

Figure 5.33: *Voltage distribution for both MV busbars with different fixed voltages and approaches.*

Table 5.8: *Energy losses comparison for selected nodes, MV busbar1.*

MV busbar 1																
	Cluster 1															
Nodes	**26**	**31**	**38**	**41**	**45**	**51**	**52**	**55**	**78**	**82**	**88**	**92**	**98**	**100**	**132**	**138**
OPF (MWh)	154,05	191,82	166,43	203,91	187,4	266,22	148,18	211,79	123,99	166,12	251,22	233,28	180,08	179,29	141,35	183,93
Enhanced LVC	+0,03%	+0,34%	+0,13%	+0,51%	+0,32%	+0,12%	+0,40%	+0,01%	+0,58%	+0,03%	+0,36%	+0,30%	+0,76%	+0,34%	+0,79%	+1,24%
Standard LVC	+3,85%	+2,86%	+3,57%	+2,69%	+3,00%	+0,88%	+2,58%	+1,51%	+3,48%	+2,46%	+1,42%	+1,60%	+0,18%	+0,41%	+9,68%	+6,89%
	Cluster 1						Cluster 2									Cluster 3
Nodes	**154**	**178**	**238**	**265**	**267**	**269**	**204**	**205**	**207**	**209**	**210**	**212**	**216**	**218**	**220**	**4**
OPF (MWh)	122,71	316,38	178,71	129,18	141,34	162,63	693,02	739,42	872,34	761,28	580,17	630,72	762,53	764,66	896,99	57,27
Enhanced LVC	+0,33%	+0,02%	+0,01%	+1,23%	+0,66%	+0,28%	+0,02%	+0,00%	+0,12%	+0,01%	+0,33%	+0,18%	+0,01%	+0,01%	+0,17%	+0,32%
Standard LVC	+6,00%	+0,66%	+1,77%	+1,43%	+1,49%	+1,21%	+3,24%	+3,36%	+3,95%	+3,42%	+3,35%	+3,14%	+3,56%	+3,57%	+4,25%	+3,86%
	Cluster 3								Cluster 4				Cluster 5			
Nodes	**48**	**111**	**142**	**230**	**249**	**252**	**253**	**256**	**14**	**16**	**116**	**120**	**60**	**64**	**66**	**109**
OPF (MWh)	48,53	60,82	62,63	40,5	28,45	13,42	11,43	31,58	86,51	81,02	128,03	60,84	263,18	352,19	395,82	370,37
Enhanced LVC	+0,53%	+1,66%	+0,09%	+0,14%	+1,18%	+5,30%	+7,19%	+1,09%	+0,04%	+0,01%	+0,04%	+0,47%	+0,53%	+0,02%	+0,07%	+0,04%
Standard LVC	+0,77%	+14,39%	+4,88%	+3,23%	+19,60%	+68,61%	+85,30%	+1,45%	+4,66%	+5,73%	+4,82%	+20,53%	+1,66%	1,20%	+1,05%	+0,24%
	Cluster 5		Cluster 6		Cluster 7							Cluster 8			Cluster 9	
Nodes	110	166	181	189	161	247	248	280	283	289	291	50	93	113	173	
OPF (MWh)	441,75	365,7	251,67	361,03	304,55	311,59	340,51	305,43	372,87	343,07	389,41	89,72	75,35	91,17	172,8	
Enhanced LVC	+0,04%	+0,10%	+0,68%	+0,23%	+0,08%	+0,00%	+0,03%	+0,18%	+0,02%	+0,01%	+0,07%	+0,33%	+0,74%	+0,39%	0,01%	
Standard LVC	+0,21%	+1,59%	+3,43%	+3,86%	+2,01%	+1,01%	+0,90%	+0,60%	+0,45%	+0,52%	+0,44%	+4,24%	+0,36%	+8,12%	2,18%	

Table 5.9: *Energy losses comparison for selected nodes, MV busbar2.*

MV busbar 2											
	Cluster 1				Cluster 2		Cluster 3				Cluster 4
Nodes	**296**	**364**	**382**	**472**	**313**	**316**	**412**	**417**	**422**	**428**	**432**
OPF (MWh)	113,58	22,27	74,04	40,75	269,43	291,40	305,74	363,75	328,18	383,75	476,26
Enhanced LVC	+0,58%	+2,45%	+0,11%	+0,37%	+0,01%	+0,02%	+0,16%	+0,00%	+0,00%	+0,21%	+0,03%
Standard LVC	+1,84%	+0,15%	+2,18%	+2,99%	+2,97%	+2,87%	+1,23%	+0,97%	+1,28%	+1,18%	+0,96%
	Cluster 4	**Cluster 5**				**Cluster 6**				**Cluster 7**	
Nodes	**437**	**361**	**363**	**395**	**400**	**408**	**459**	**461**	**463**	**306**	**350**
OPF (MWh)	548,24	153,71	179,46	162,87	209,78	218,40	236,19	274,93	244,62	151,86	63,74
Enhanced LVC	+0,05%	+0,00%	+0,13%	+0,22%	+0,03%	+0,04%	+0,00%	+0,10%	+0,00%	+0,34%	+0,12%
Standard LVC	+0,82%	+2,46%	+1,99%	+1,55%	+1,06%	+1,89%	+2,10%	+1,70%	+2,01%	+2,57%	+6,37%
	Cluster 7					**Cluster 8**					
Nodes	**354**	**391**	**451**	**470**	**484**	**486**	**311**	**321**	**324**	**328**	**333**
OPF (MWh)	103,00	110,13	104,26	71,81	78,46	89,58	673,95	363,80	418,05	459,21	453,29
New LVC setting	+0,34%	+0,10%	+0,89%	+1,73%	+0,37%	+0,13%	+0,01%	+0,24%	+0,04%	+0,00%	+0,00%
Standard LVC	+3,27%	+2,72%	+4,94%	+0,85%	+1,81%	+1,51%	+0,65%	+3,06%	+2,68%	+2,45%	+2,55%
	Cluster 8	**Cluster 9**						**Cluster 10**			
Nodes	**339**	**366**	**368**	**373**	**375**	**376**	**377**	**342**	**439**	**465**	
OPF (MWh)	576,56	96,57	115,75	225,39	231,45	99,97	102,43	34,97	42,69	12,93	
Enhanced LVC	+0,24%	+0,01%	+0,03%	+0,04%	+0,03%	+0,07%	+122,16%	+0,47%	+0,25%	+0,90%	
Standard LVC	+2,00%	+0,02%	+0,13%	+0,06%	+0,06%	+0,00%	+122,13%	+3,26%	+3,40%	+2,13%	

5.6 Summary

This chapter introduced a new set-up for local voltage control, called Enhanced Local Voltage Control. The procedure has been tested on the real life case study, Aosta city in Italy. In order to reduce the computational time, a selection procedure has been done to find some nodes and loading hours as the representatives of the full grid. Then the nodes are classified into different clusters with specific voltage profile. At the end the new set-up for local voltage control has been tested and compared with OPF, standard local voltage control and normal load flow with PF1. The proposed local voltage control performed better than standard local voltage control and slightly lower than OPF which is a proven of the accuracy of the proposed model.

CHAPTER 6

Conclusions

Distributed energy resources connections demand, mostly based on renewables, at the medium voltage and low voltage distribution networks is continuously increasing; due to this fact, the importance of distributed energy resources and distributed generation compared to classical centralized generation has increased. However, one of the important practical problems to carry out a study on a grid in some countries, especially emerging countries, is lack of available data. This motivates the need of a reverse engineering procedure (Parameter Estimation) to estimate branch parameters starting from typical available data, i.e., approximated values of bus voltages, active and reactive power flows of each branch. The parameter estimation model that can be applied to large systems makes it possible to derive estimations for the series resistance, the series reactance and the line charging of each branch.

Parameter Estimation is based on the developed theory for state estimation which is an application of statistics that estimates the values of parameters based on measured data and their stochastic behavior. The parameters describe a fundamental physical setting in a way that their value affects the distribution of the measured data. In addition, the best usage of resources decision depends judgmentally on current parameters or states. However, system parameters estimation by imprecise measurements in the energy systems operation is a critical problem. Hence, their values are defined indirectly by settlement between the mathematical model of the system and existing measurements by an inverse estimation procedure, such as state estimation.

The real-life case study for the proposed parameter estimation procedure in this thesis was Tanzania network with 38 buses and 81 branches. The provided data by Tanzania electric supply company were including active, reactive power in each branch and voltage in each bus. Obtaining the rest necessary data including impedance, impedance characteristic angle, bus angles and line charging was modeled in

MATLAB through Quasi-Newton method which was based on minimizing total error in this electrical grid with more than 100 unknown and the results compared with the result obtained from a rough geographical feature of the grid including line lengths. This comparison shows the proposed method in this thesis is, as expected, more reliable and accurate, especially for reactive power estimations.

After defining some unknown grid information, the influence of distributed generation on distribution grid should be carried out as high levels penetration of distributed energy resources have many undesired consequences on the grid, such as overvoltage, overcurrent and harmonic distortions. For this reason, the hosting capacity for distributed energy resources identifies the acceptable degree of distributed energy resources penetration under specific conditions. In other words, hosting capacity is the maximum distributed energy resources penetration which the power system can support satisfactorily. It depends on different parameters such as the configuration and operation of the network, the characteristics of the generation units, the loads requirements, and national and regional requirements. In this thesis, different methodologies for hosting capacity evaluation were reviewed, and a novel model to determine the hosting capacity considering grid parameters uncertainties (called Bricks approach) and multi-generator connection was proposed.

In order to perform hosting capacity analysis, a complete model of the distribution grid is required. Actually, hosting capacity is impacted by the topology of the grid, grid parameters and also power profiles of the loads and generators, resulting in a quite heavy data set to be properly managed. Practically speaking, distribution system operators could not have all the required data (or, eventually, gathering them could results quite complex) and in some cases, e.g. in emerging countries scenarios, even distribution system operators could be unable to gather all the required information, where highlight the importance usage of Bricks approach.

Actually, the standard structure of distribution grid is including the main feeder and connected branches to the main line which is typically named collaterals. The new method is based on the assumption that hosting capacity in one feeder is marginally affected by the other feeders. Moreover, in order to limit the computational effort of the study, the grid is modeled as an aggregation of "bricks", each one representing a portion of the grid which can be added, removing and replacing stochastically to evaluate all the possibility of the grid structure in shorter time. In addition, only critical nodes of the grid being assessed by Bricks approach.

According to Bricks approach, feeders and collaterals are classified in given categories according to their electrical characteristics. The tests performed, taking into account three main technical constraints (steady-state voltage variations, rapid voltage changes and thermal limits), proved the method to be effective in estimating the hosting capacity in real-life distribution networks, if compared to the method based on the complete grid model. Aosta city distribution grid in north west of Italy with 486 nodes, 16 feeders and two medium voltage busbars was considered in this test. The results were confirmed with two different reactive power control contributions by distributed generation. The benefits of Bricks approach are less-required information (i.e. is not required the detailed topology of the grid and the detailed power profile for all the nodes) and limited computational time, e.g. in the presented case-study, hosting capacity computation required a processing time with Bricks approach of 5 minutes and 37 seconds, whereas with the complete model approach it was over 92 hours.

Although Nodal HC gives us a right view of injection power to the grid from each node, it cannot give us enough view for the whole grid. In real life, by increasing the number of renewable energy integration at the same time many DG are connecting to the grid which affects other distributed gener-

ations and the grid. Thus, the next step of hosting capacity study is evaluating multi generators hosting capacity. The procedure developed takes into account that distributed generation could be connected to the grid through different plants of different size and connected to various nodes. To evaluate if the distribution grid can host this capacity or if its installation will compromise the performances of the grid, a stochastic approach has been adopted, in particular Monte Carlo simulation is exploited in order to properly consider all the variables. For creating each scenario of generation, in the Monte Carlo approach three different roulette wheel selection procedures have been introduced in order to defined the type, size and the connection node of the distributed generation. At the end a combination of Bricks approach and Monte Carlo simulation for medium voltage distribution grid of Aosta city was compared with the Monte Carlo simulation for the complete grid. The main advantage of using combined approach is less computation time and required data as the computational time of MC simulation for the full grid was more than 680 hours, whereas for the combined method this amount was about 7 hours.

The evaluation of the impact of e-mobility charging processes on the distribution grid, in a real-life case study with respect to both the grid operational and efficiency parameters as one of the hosting capacity application was done in this thesis. Hence, scenarios based on Monte Carlo algorithm are studied thanks to the KPI approach (steady-state voltage variation, transformer and lines thermal limits, rapid voltage change and grid efficiency) typically adopted for DG Hosting capacity evaluation, and here proposed also for the evaluation of the e-mobility hosting capacity charging processes. The case-study for this research was San Severino Marche, with 193 km^2 area, a small town in the center of Italy. Two transformers are placed in the primary substation, six feeders depart from one transformer and seven from the other one.

For each single simulation set, the different number of electric cars were connected to the grid nodes. The focus was the evaluation of the distribution grid hosting capacity in front of e-mobility and in the quantification of the relevant impact on losses. After performing Monte Carlo simulation for the mentioned number of cars and for each different simulation set and different technology, the results were evaluated according to the technical constraints. The results showed that in all the performed simulations, the limiting factor of the grid charging process hosting capacity resulted to be the line thermal limit. Although mainly very fast charging provides high speed charging process, it could cause some critical load fluctuation over a single day limiting the capacity of the grid to host recharge process or decreasing the efficiency of the distribution grid. Then, In order to evaluate the impact of DG on this study, all of these procedures were repeated for the active network, where as it was expected the results showed the higher e-car hosting capacity charging process.

For the last step of this thesis, voltage control as one of the possible approach for increasing the hosting capacity was studied. In fact, several EU countries consider local voltage control with standard setting. However, the standard setting has some limitation such as hosting capacity maximization and energy losses minimization. That is why, the focus of this thesis was a new set-up local voltage control procedure for connected generator to MV distribution grid.

This procedure was based on the deployment of the generator with constant active power injection in different nodes of the grid. Then optimal power flow were performed by considering injected active power and voltage penalty factor. In order to reduce the computational time, a novel procedure were applied to select some nodes and loading hours as representative of the grid. After that the results of optimal power flow were clustered according to R/X ratio, impedance matrix diagonal and reactive power. Once the nodes are classified in clusters, linearization procedure was performed on generated

clouds and the new local voltage control setting were stressed. Finally, the new set-up law was tested on Aosta grid and compared with OPF and standard local voltage control, where the results showed a better performance for new voltage profile in terms of energy losses compared to standard local voltage control and very close to OPF performance.

For the future work, the proposed local voltage control in this thesis could be implemented for the multi-generator scenario. Moreover, study on a distributed control, where different local voltage controls have been shared among them and primary substation, could provide interesting capabilities to optimize the medium voltage grid. In addition, transient behaivour of the grid and its impact on the voltage drop reduction could be studied further by an electromagnetic modeling of the grid.

Appendices

APPENDIX A

Additional Information

A.1 Aosta Feeders Loading

Aosta grid is not a homogeneous grid which covers a specific type of loading for the feeders. Overall, the feeders in this MV grid could be divided into feeders bellow 1MW, feeders more than 1MW and bellow 2.5MW, Feeders above 2.5MW and feeders without clear behavior.

Feeders 3, 12, 13 are below than 1MW, with almost flat shape. Feeder 1, 7, 9, 10, 11, 15 and 16 are categorized for the second group and Feeder 2, 4, 8, and 14 are in the third group. Feeder 5 and Feeder 6 in this grid due to suppling ski resort and industry have stronger difference compared to the other feeders and could be grouped in the category of feeders without clear trend. Here, all the loading of sixteen feeders of Aosta grid for different categories of winter period, summer period, weekdays and weekend and holidays have been reported

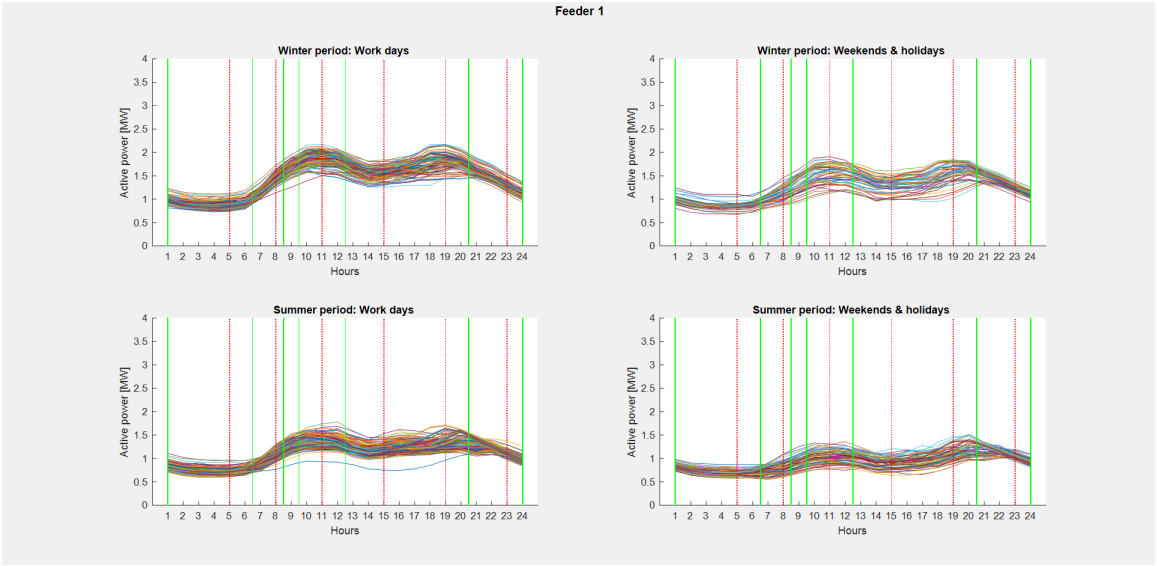

Figure A.1: *Daily load profile of feeder1 for different categories.*

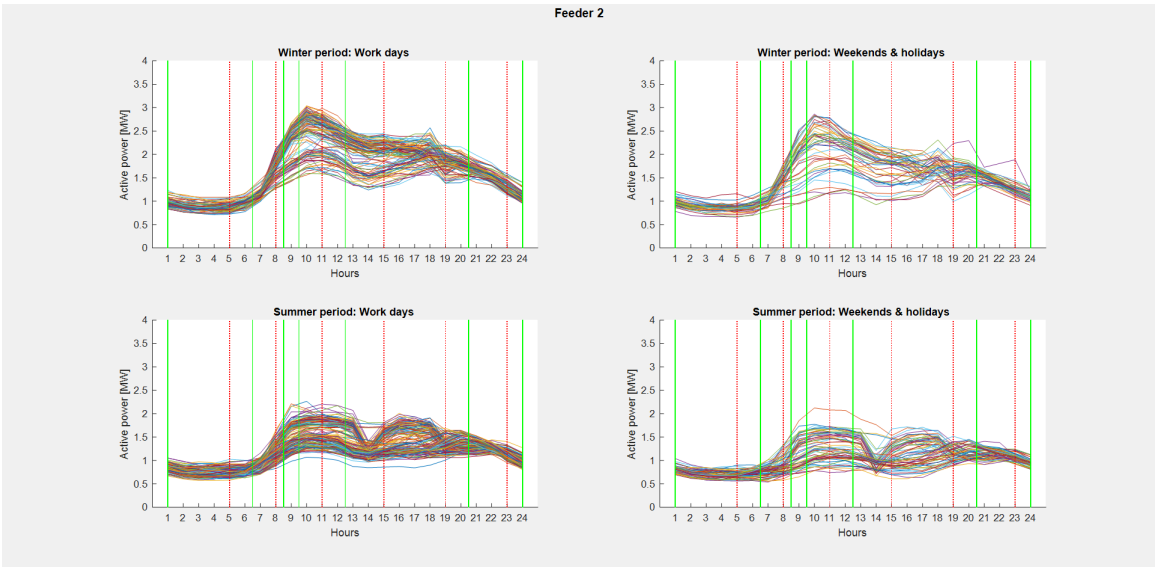

Figure A.2: *Daily load profile of feeder2 for different categories.*

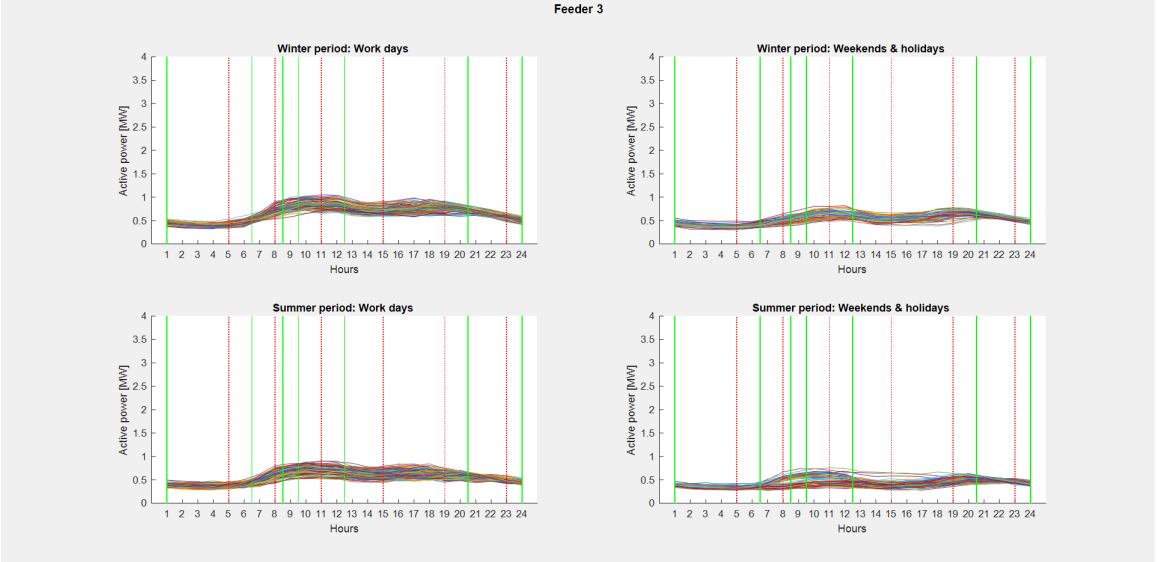

Figure A.3: *Daily load profile of feeder3 for different categories.*

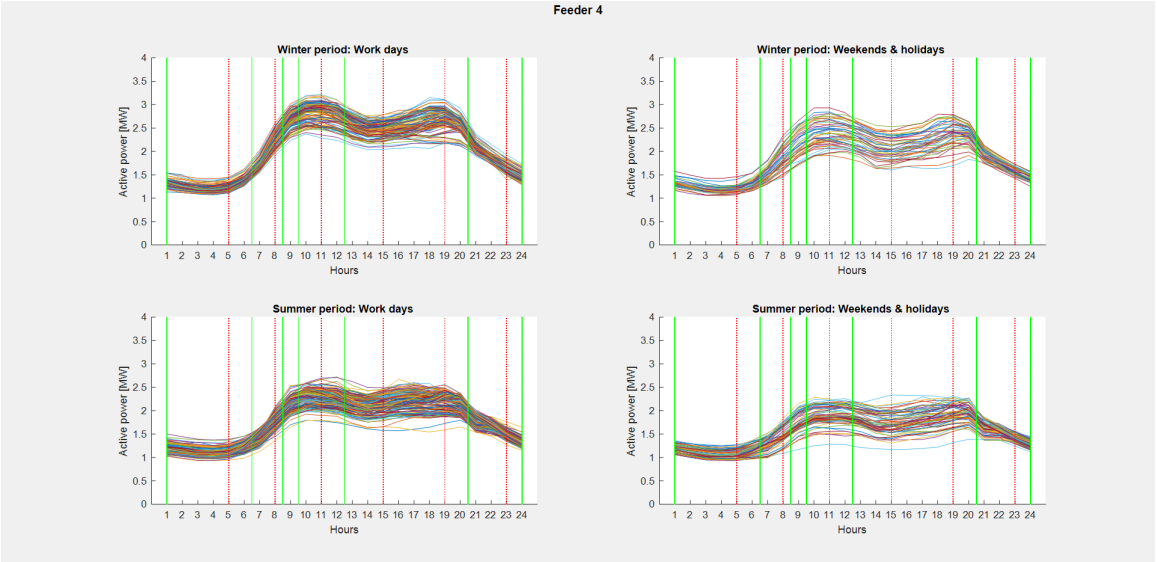

Figure A.4: *Daily load profile of feeder4 for different categories.*

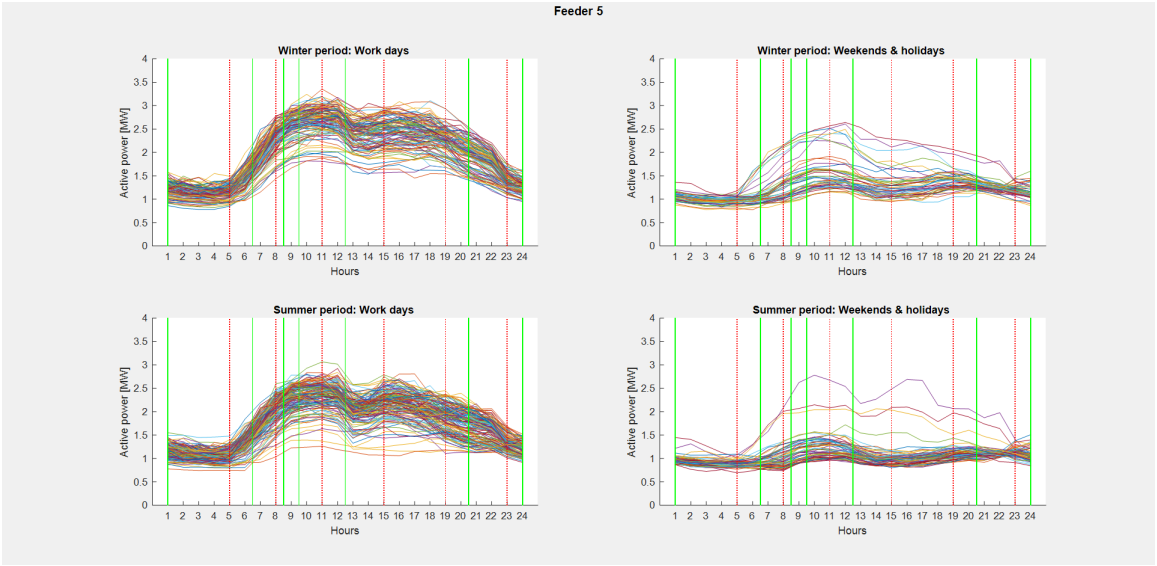

Figure A.5: *Daily load profile of feeder5 for different categories.*

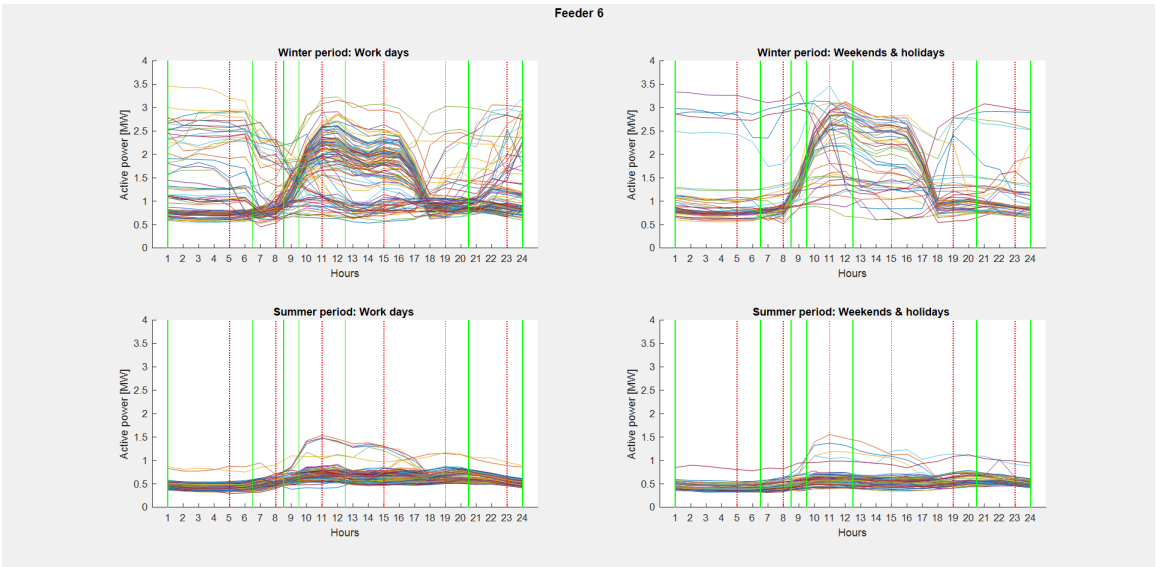

Figure A.6: *Daily load profile of feeder6 for different categories.*

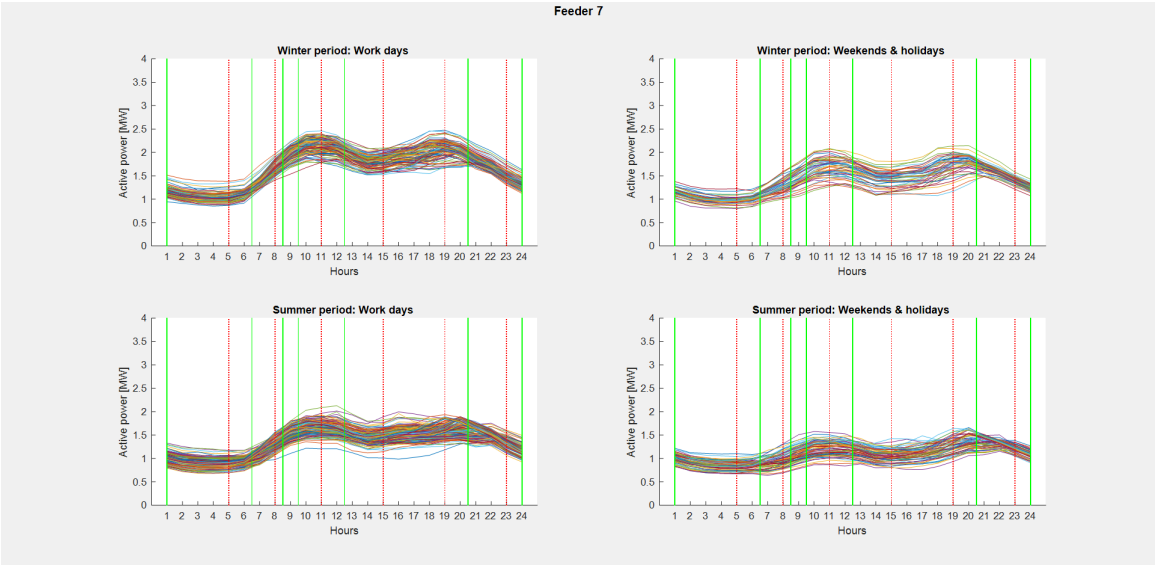

Figure A.7: *Daily load profile of feeder7 for different categories.*

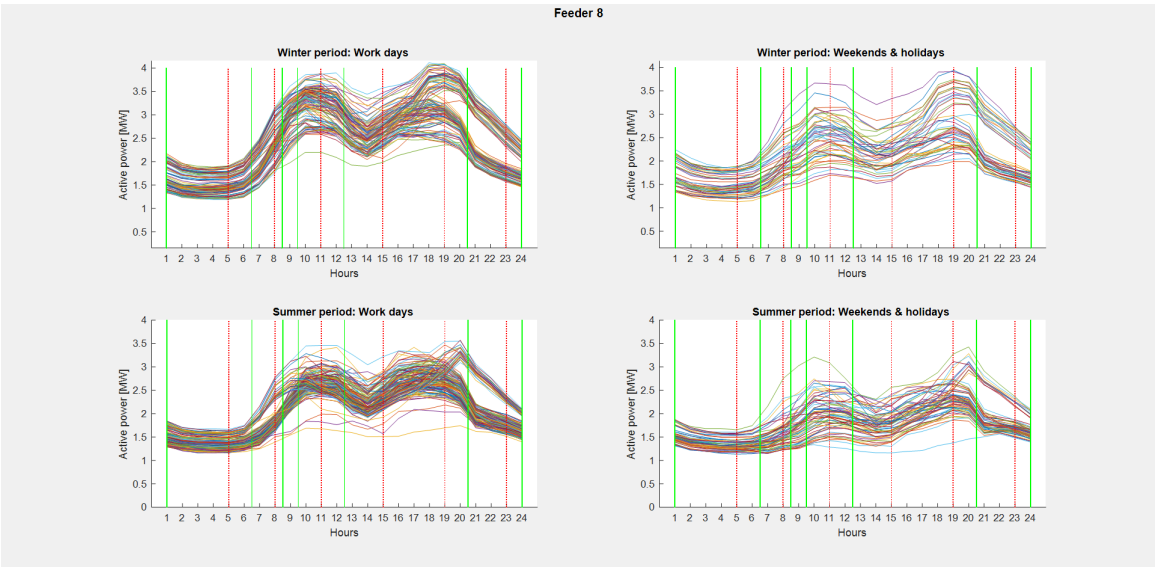

Figure A.8: *Daily load profile of feeder8 for different categories.*

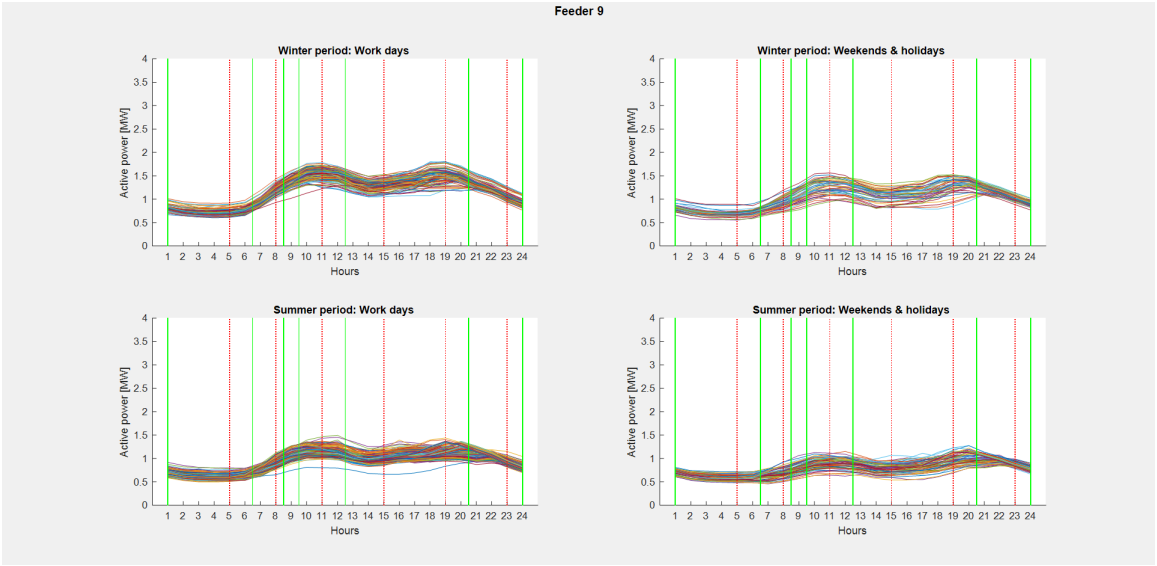

Figure A.9: *Daily load profile of feeder9 for different categories.*

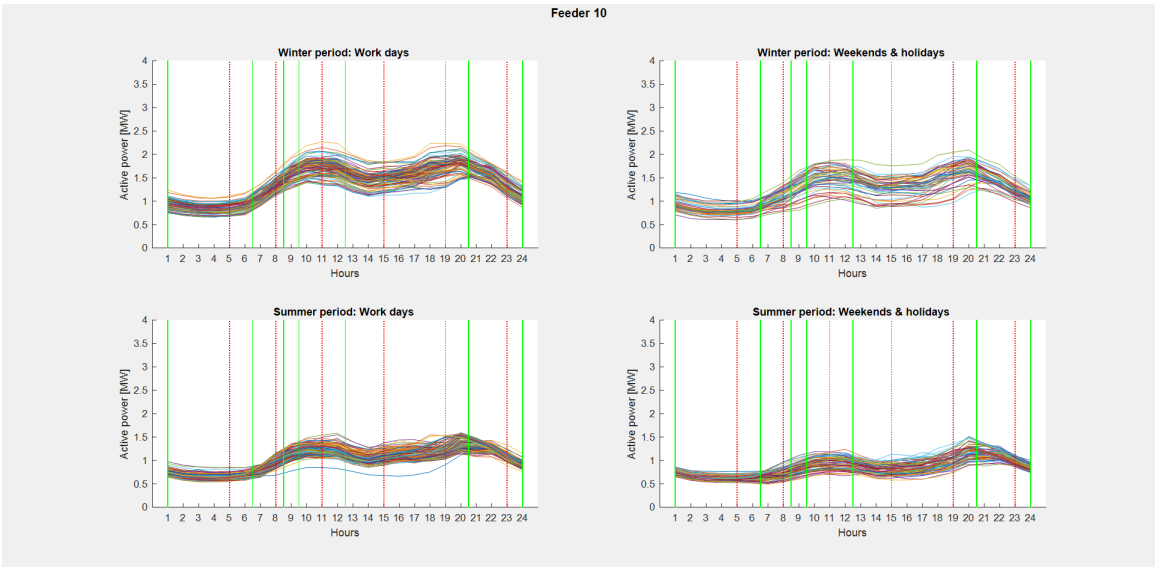

Figure A.10: *Daily load profile of feeder10 for different categories.*

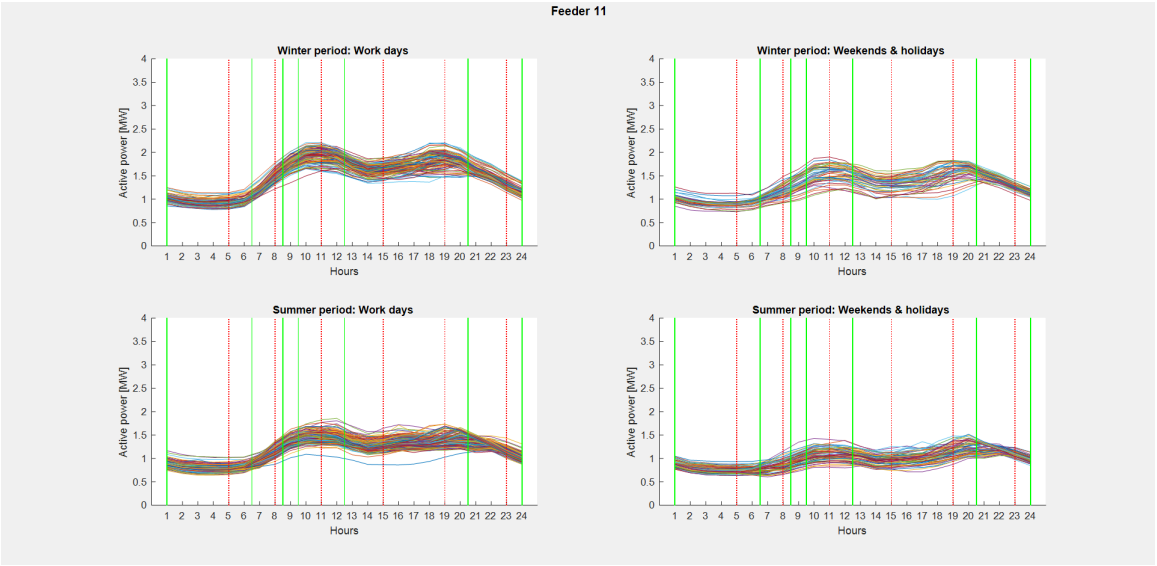

Figure A.11: *Daily load profile of feeder11 for different categories.*

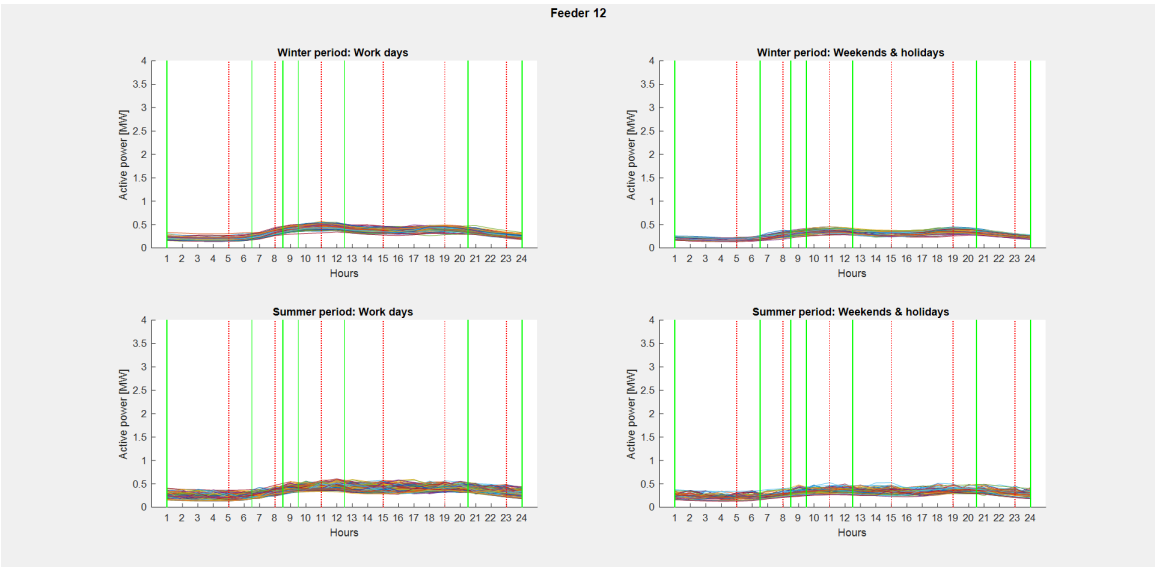

Figure A.12: *Daily load profile of feeder12 for different categories.*

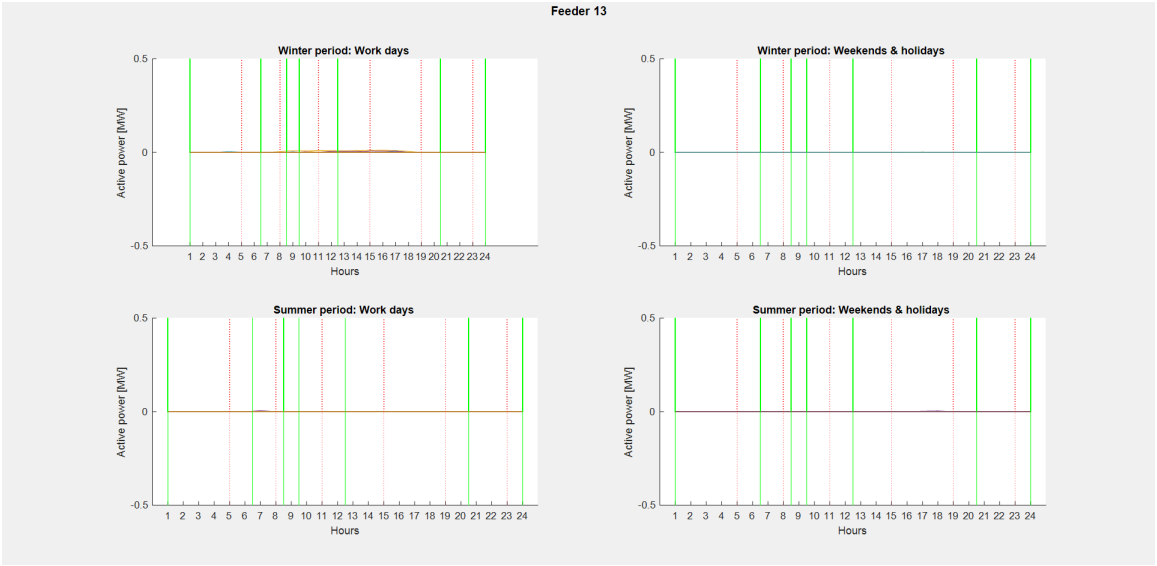

Figure A.13: *Daily load profile of feeder13 for different categories.*

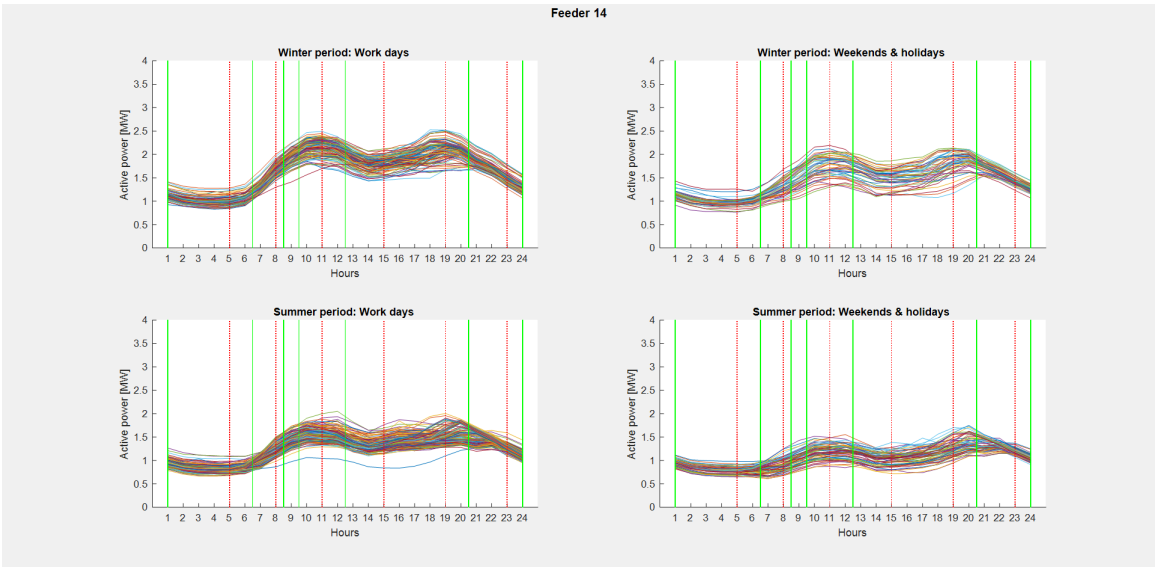

Figure A.14: *Daily load profile of feeder14 for different categories.*

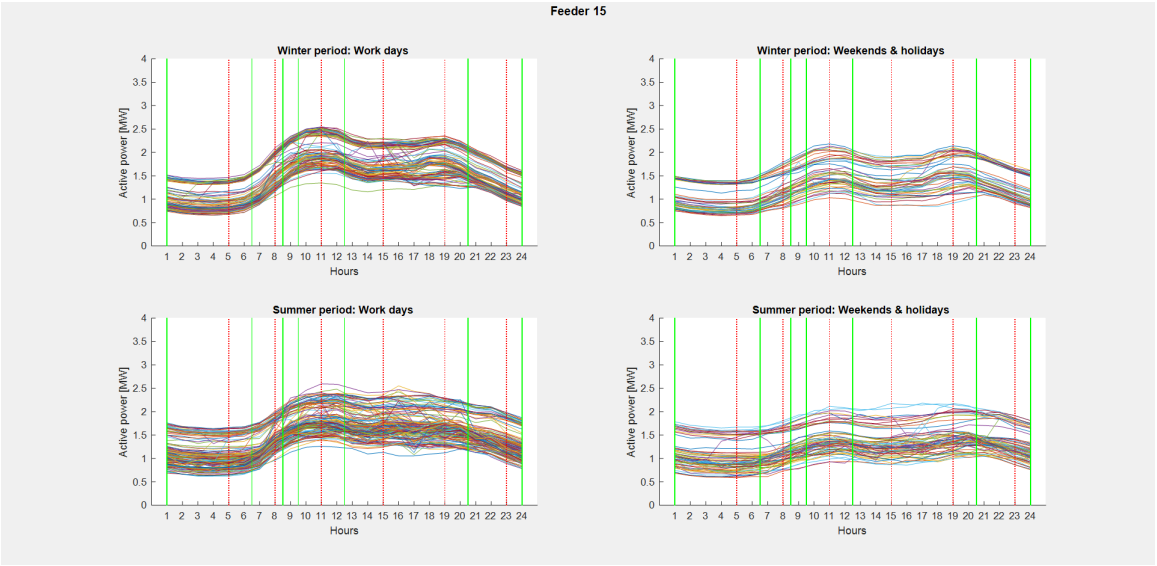

Figure A.15: *Daily load profile of feeder15 for different categories.*

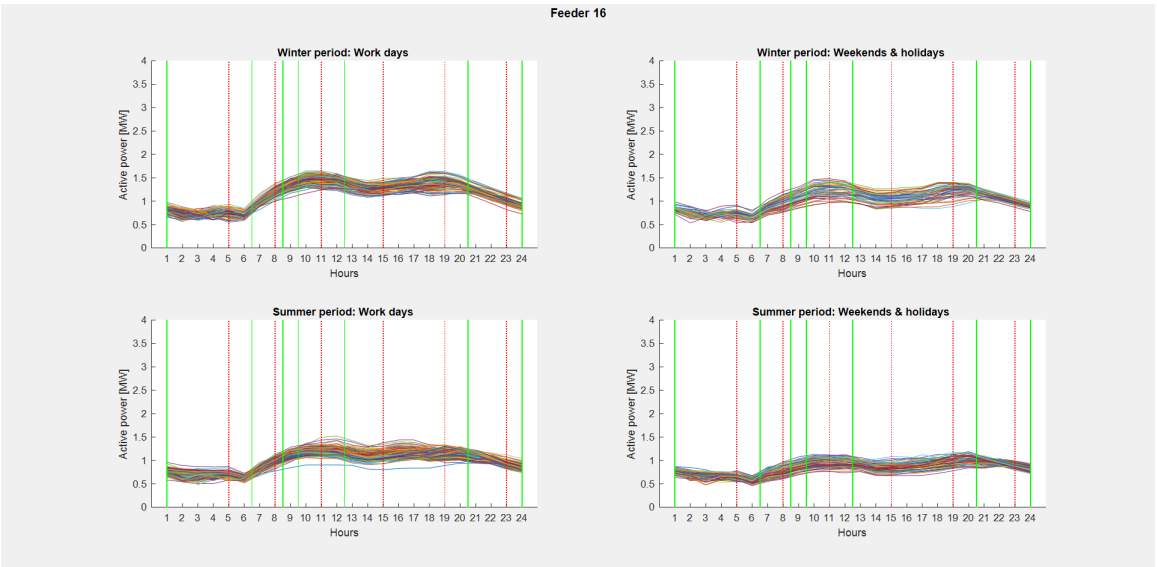

Figure A.16: *Daily load profile of feeder16 for different categories.*

A.2 LVC Section Three Setting

In the following figures the section three of the proposed LVC has been reported. The figures are presented for both MV busbars and for both discussed voltage (1.02p.u. and 1.055p.u.).

From these figures, Cluster2 and cluster6 (both of them are located in the same feeder) have shown a lower reactive power drop compared to the others. In the mentioned clusters, voltage severely influenced by reactive power. Hence, it could lead to energy losses reduction. In addition, Cluster9 (located at the beginning of Feeder6) shows a strange voltage profile, which is related to the strong loading variation along the year and the selected loading hours could significantly change its behaivour.

MV busbar2 covers a shorter reactive power range as it has a lower loading. Hence, it accepts lower amount of reactive power injection without increasing the energy losses. Cluster9 and Cluster10 present a vertical line which is unacceptable for a real control system. However, their results for enhanced LVC in comparison with OPF and standard LVC show an acceptable performance, Table 5.7.

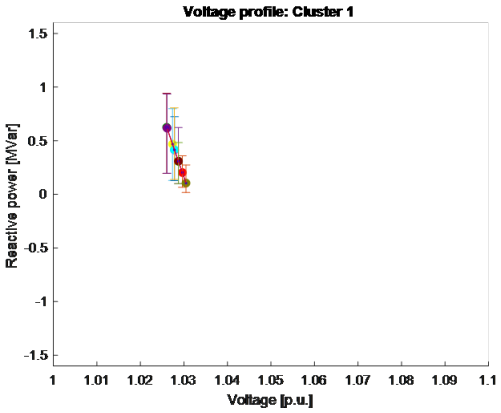

Figure A.17: *LVC section 3 fro MV busbar1 1.02p.u., Cluster1.*

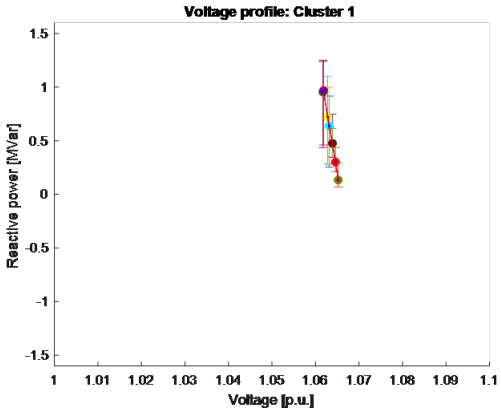

Figure A.18: *LVC section 3 fro MV busbar1 1.055p.u., Cluster1.*

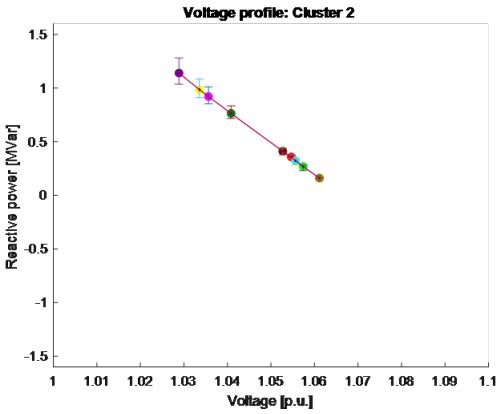

Figure A.19: *LVC section 3 fro MV busbar1 1.02p.u., Cluster2.*

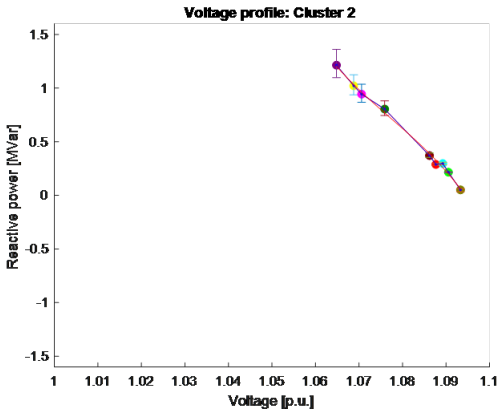

Figure A.20: *LVC section 3 fro MV busbar1 1.055p.u., Cluster2.*

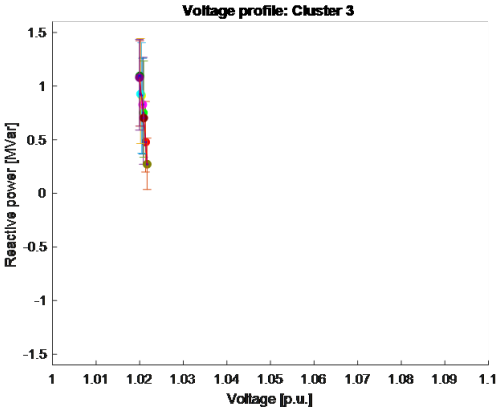

Figure A.21: *LVC section 3 fro MV busbar1 1.02p.u., Cluster3.*

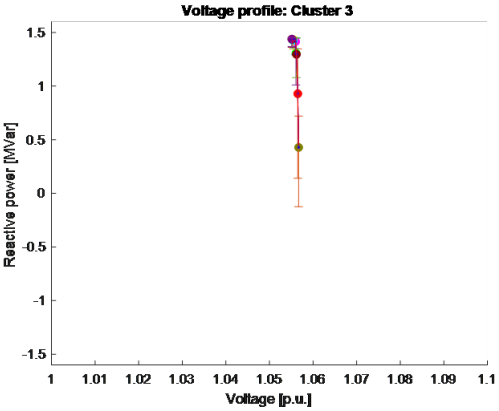

Figure A.22: *LVC section 3 fro MV busbar1 1.055p.u., Cluster3.*

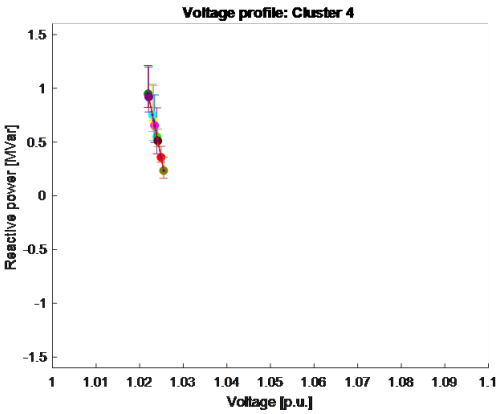

Figure A.23: *LVC section 3 fro MV busbar1 1.02p.u., Cluster4.*

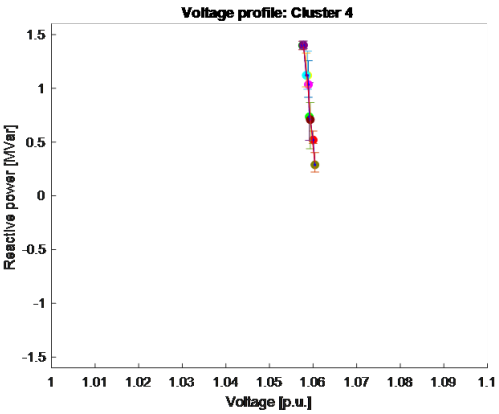

Figure A.24: *LVC section 3 fro MV busbar1 1.055p.u., Cluster4.*

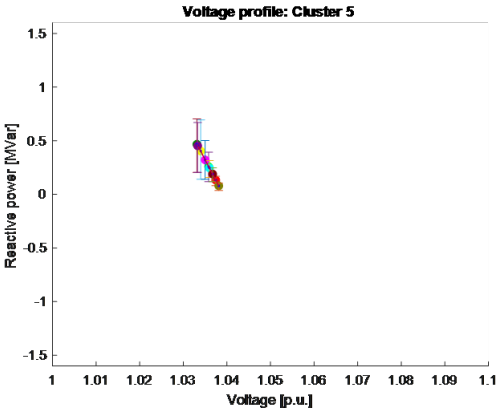

Figure A.25: *LVC section 3 fro MV busbar1 1.02p.u., Cluster5.*

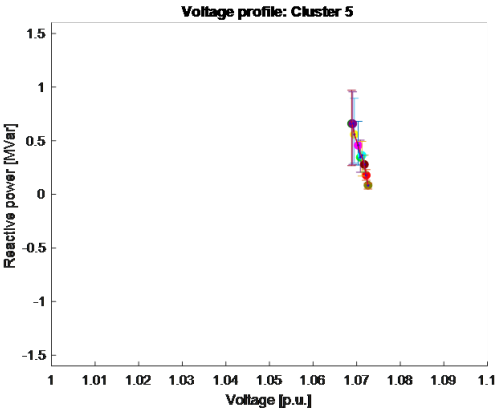

Figure A.26: *LVC section 3 fro MV busbar1 1.055p.u., Cluster5.*

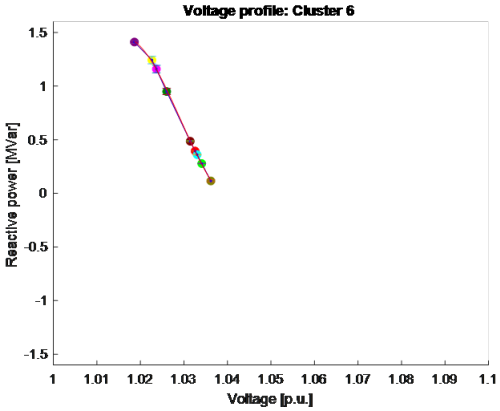

Figure A.27: *LVC section 3 fro MV busbar1 1.02p.u., Cluster6.*

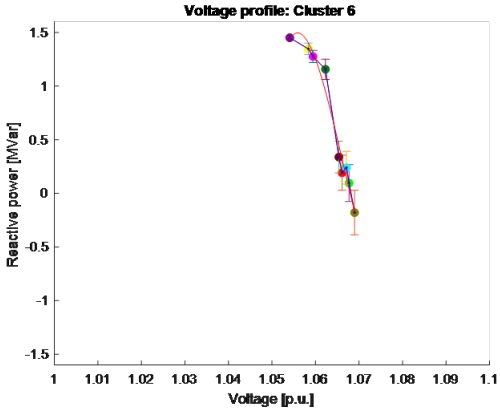

Figure A.28: *LVC section 3 fro MV busbar1 1.055p.u., Cluster6.*

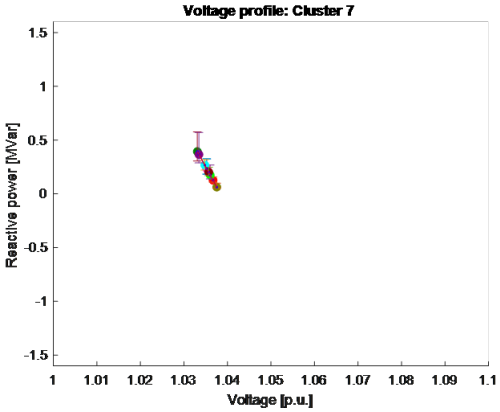

Figure A.29: *LVC section 3 fro MV busbar1 1.02p.u., Cluster7.*

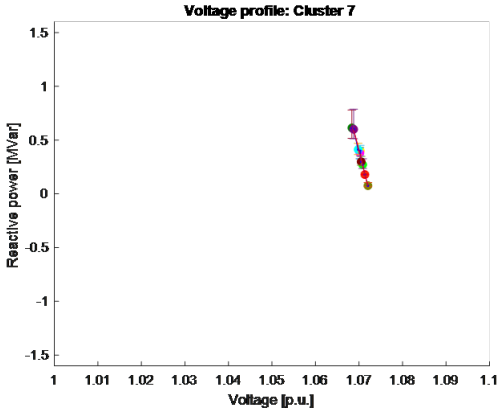

Figure A.30: *LVC section 3 fro MV busbar1 1.055p.u., Cluster7.*

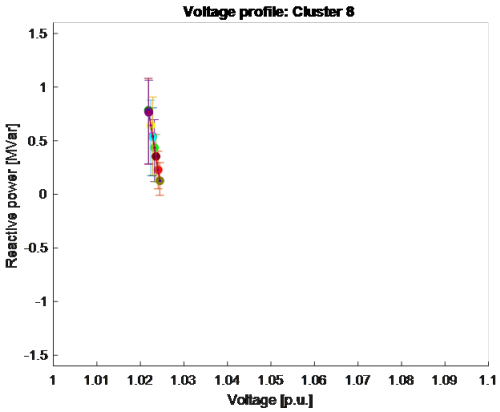

Figure A.31: *LVC section 3 fro MV busbar1 1.02p.u., Cluster8.*

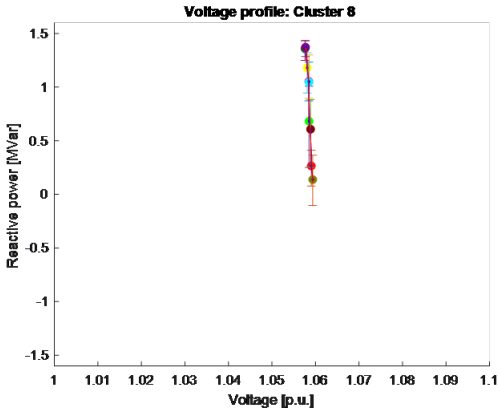

Figure A.32: *LVC section 3 fro MV busbar1 1.055p.u., Cluster8.*

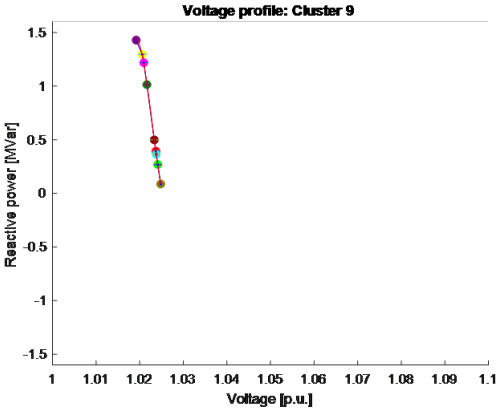

Figure A.33: *LVC section 3 fro MV busbar1 1.02p.u., Cluster9.*

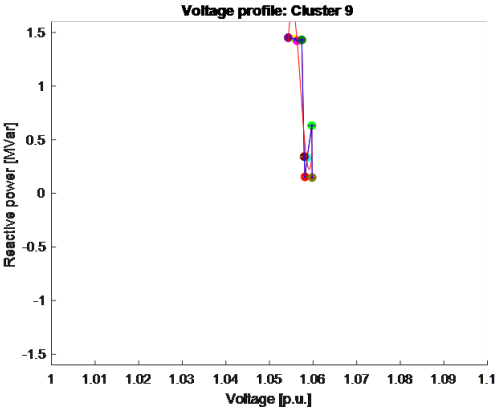

Figure A.34: *LVC section 3 fro MV busbar1 1.055p.u., Cluster9.*

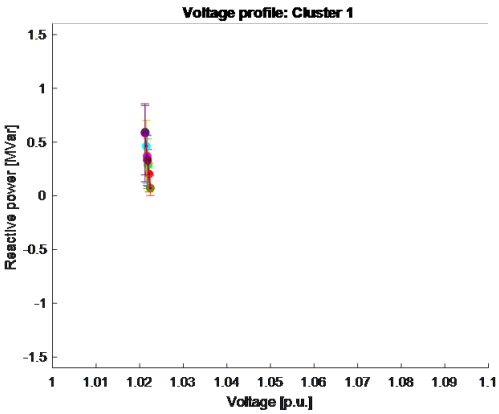

Figure A.35: *LVC section 3 fro MV busbar2 1.02p.u., Cluster1.*

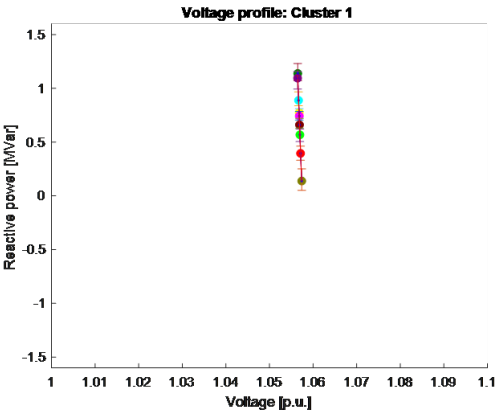

Figure A.36: *LVC section 3 fro MV busbar2 1.055p.u., Cluster1.*

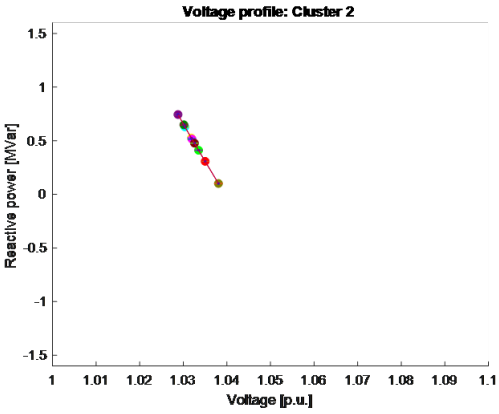

Figure A.37: *LVC section 3 fro MV busbar2 1.02p.u., Cluster2.*

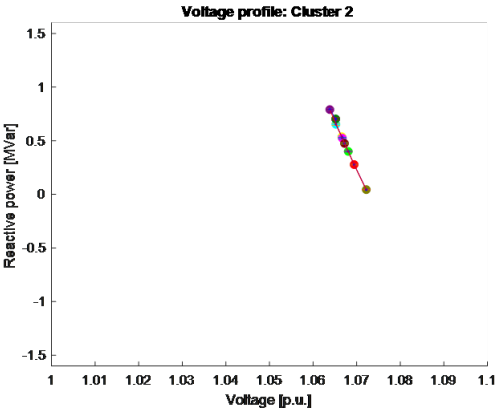

Figure A.38: *LVC section 3 fro MV busbar2 1.055p.u., Cluster2.*

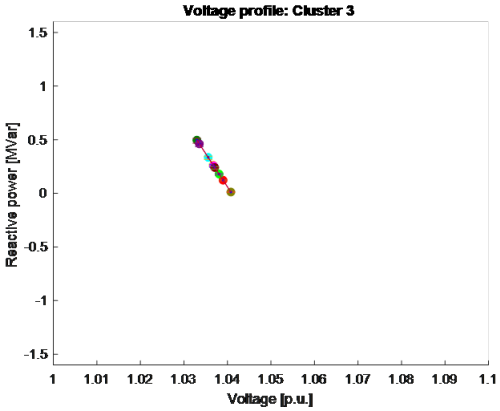

Figure A.39: *LVC section 3 fro MV busbar2 1.02p.u., Cluster3.*

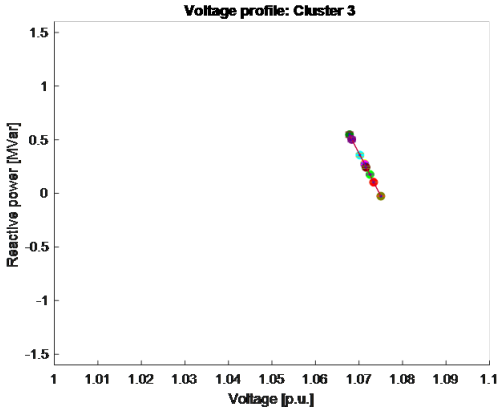

Figure A.40: *LVC section 3 fro MV busbar2 1.055p.u., Cluster3.*

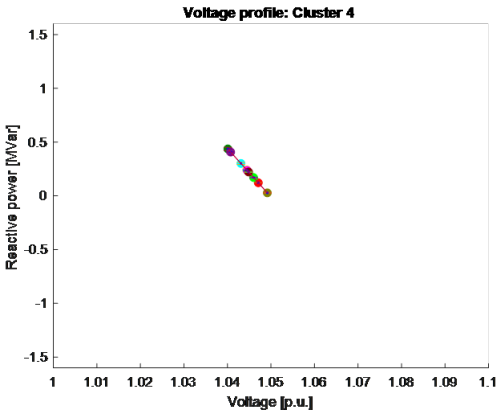

Figure A.41: *LVC section 3 fro MV busbar2 1.02p.u., Cluster4.*

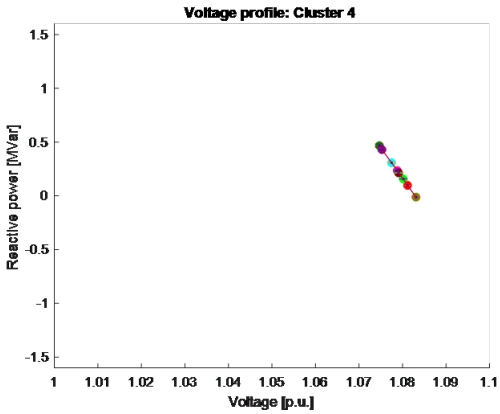

Figure A.42: *LVC section 3 fro MV busbar2 1.055p.u., Cluster4.*

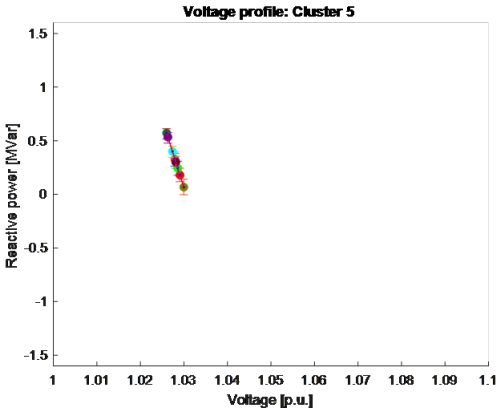

Figure A.43: *LVC section 3 fro MV busbar2 1.02p.u., Cluster5.*

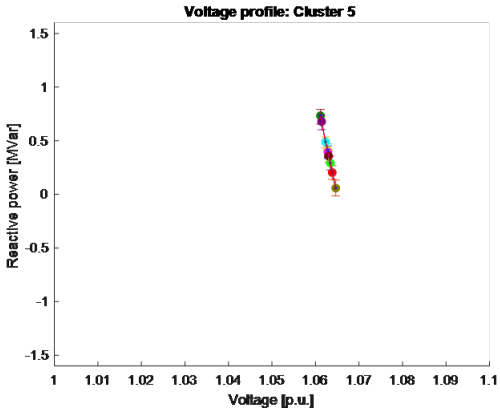

Figure A.44: *LVC section 3 fro MV busbar2 1.055p.u., Cluster5.*

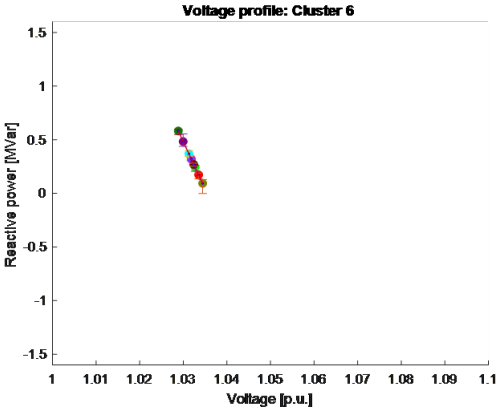

Figure A.45: *LVC section 3 fro MV busbar2 1.02p.u., Cluster6.*

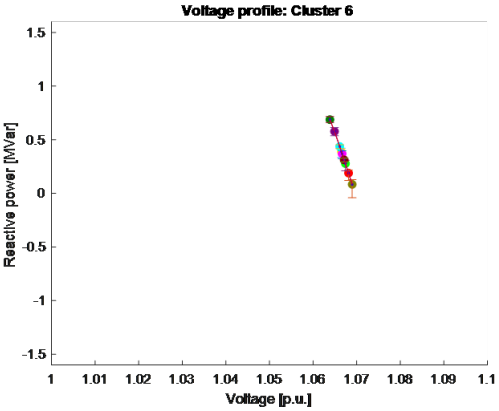

Figure A.46: *LVC section 3 fro MV busbar2 1.055p.u., Cluster6.*

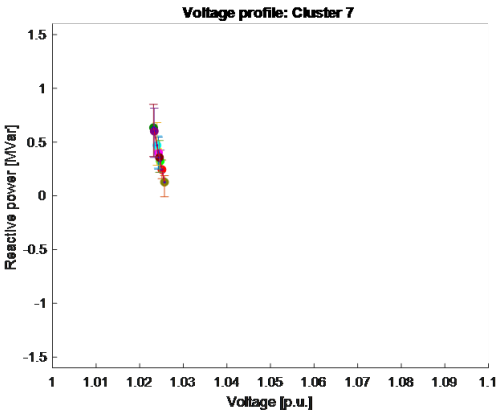

Figure A.47: *LVC section 3 fro MV busbar2 1.02p.u., Cluster7.*

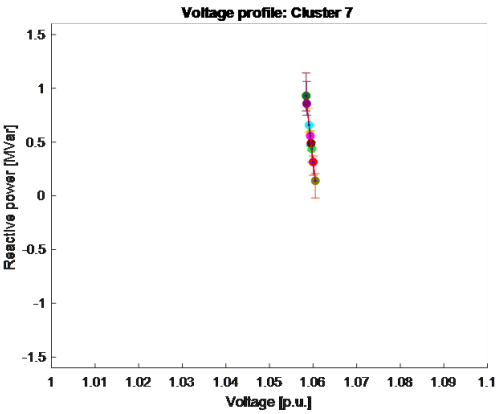

Figure A.48: *LVC section 3 fro MV busbar2 1.055p.u., Cluster7.*

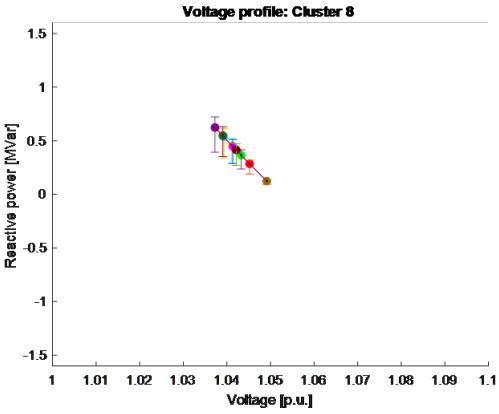

Figure A.49: *LVC section 3 fro MV busbar2 1.02p.u., Cluster8.*

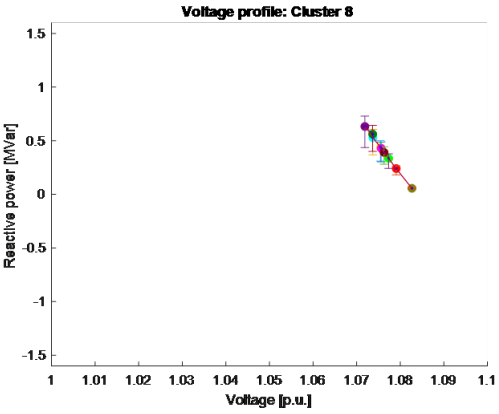

Figure A.50: *LVC section 3 fro MV busbar2 1.055p.u., Cluster8.*

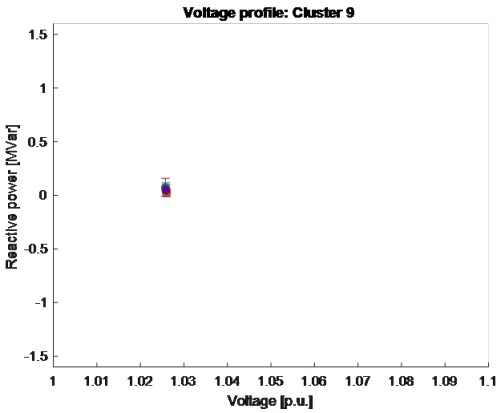

Figure A.51: *LVC section 3 fro MV busbar2 1.02p.u., Cluster9.*

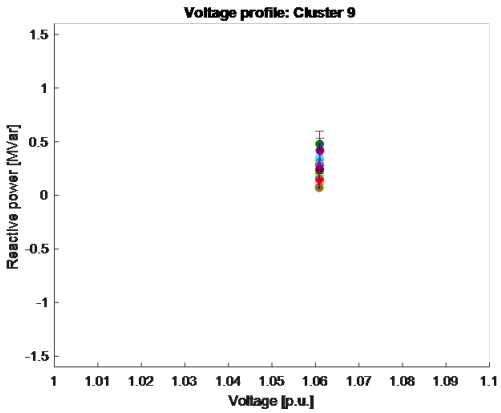

Figure A.52: *LVC section 3 fro MV busbar2 1.055p.u., Cluster9.*

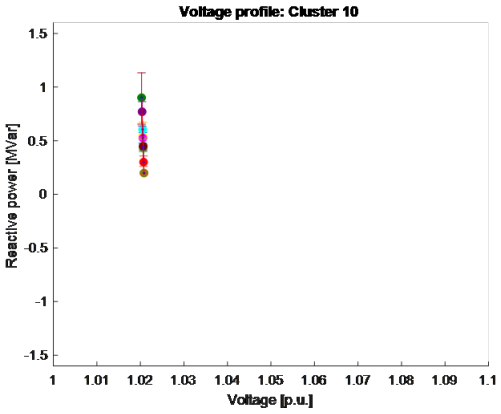

Figure A.53: *LVC section 3 fro MV busbar2 1.02p.u., Cluster10.*

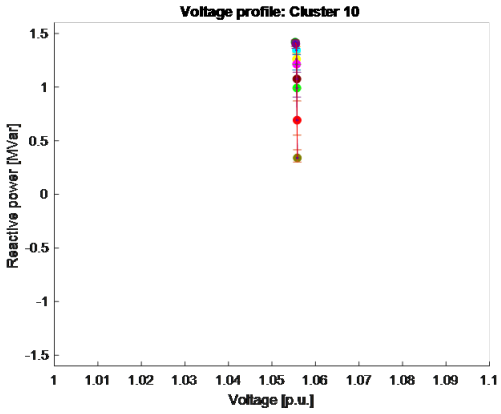

Figure A.54: *LVC section 3 fro MV busbar2 1.055p.u., Cluster10.*

Bibliography

[1] S. M. Mirbagheri, J. F. Mushi, V. Ilea, M. Merlo, and A. Berizzi, "Grid parameter estimation procedure for emerging countries scenario," in *Clean Electrical Power (ICCEP), 2017 6th International Conference on*, IEEE, 2017, pp. 327–333.

[2] S. M. Mirbagheri, M. Moncecchi, D. Falabretti, and M. Merlo, "Hosting capacity evaluation in networks with parameter uncertainties," in *Proceedings of International Conference on Harmonics and Quality of Power, ICHQP*, 2018, ISBN: 9781538605172. DOI: 10.1109/ICHQP.2018.8378891.

[3] S. M. Mirbagheri, F Bovera, D Falabretti, M Moncecchi, M Delfanti, M Fiori, and M Merlo, "Monte Carlo Procedure to Evaluate the E-mobility Impact on the Electric Distribution Grid," in *2018 International Conference of Electrical and Electronic Technologies for Automotive*, IEEE, 2018, pp. 1–6.

[4] S. M. Mirbagheri, V. Ilea, D. Falabretti, and M. Merlo, "Hosting Capacity Analysis: A Review and A New Evaluation Method in Case of Parameters Uncertainty and Multi-Generator," in *18th International Conference on Electricity Distributionth annual conference of the International Conference on Environmental and Electrical Engineering*, 2018, pp. 1–6.

[5] S. M. Mirbagheri, D. Falabretti, and M. Merlo, "Voltage Control in Active Distribution Grids: A Review and a New Set-Up Procedure for Local Control Laws," in *2018 International Symposium on Power Electronics, Electrical Drives, Automation and Motion (SPEEDAM)*, IEEE, 2018, pp. 1203–1208 (cit. on p. 143).

[6] D. Falabretti, M. Moncecchi, M. Mirbagheri, F. Bovera, M. Fiori, M. Merlo, and M. Delfanti, "San Severino Marche Smart Grid Pilot within the InteGRIDy project," *Energy Procedia*, vol. 155, pp. 431–442, 2018.

[7] S. Corgliano, M. Moncecchi, S. M. Mirbagheri, M. Merlo, and M. Molinas, "Microgrid Design: Sensitivity on Models and Parameters," in *13th IEEE PES PowerTech Conference (Submitted)*, 2019.

[8] C. UNFCCC, *United Nations framework convention on climate change*, 1992 (cit. on p. 8).

[9] K. Protocol, "United Nations framework convention on climate change," *Kyoto Protocol, Kyoto*, vol. 19, 1997 (cit. on p. 8).

[10] P. Agreement, "United nations framework convention on climate change," *Paris, France*, 2015 (cit. on p. 8).

[11] European Commission, "EU climate and energy package - Citizens' summary," Tech. Rep., 2008 (cit. on p. 8).

[12] P. Europeo, "Consiglio dell'Unione Europea," *Decisione N. 1600/2002/CE che istituisce il 6 Programma Quadro Comunitario di Azione in materia di Ambiente*, 2014 (cit. on p. 9).

[13] P. Europeo, "Direttiva 2009/28/CE del Parlamento Europeo e del Consiglio del 23 aprile 2009 sulla promozione dell'uso dell'energia da fonti rinnovabili, recante modifica e successiva abrogazione delle direttive 2001/77/CE e 2003/30/CE," *Gazzetta ufficiale dell'Unione europea*, vol. 5, p. 2009, 2009 (cit. on p. 9).

[14] Commissione Europea, "Renewable Energy Progress Report," Tech. Rep., 2017. [Online]. Available: `https://ec.europa.eu/transparency/regdoc/rep/1/2017/EN/COM-2017-57-F1-EN-MAIN-PART-1.PDF` (cit. on pp. 9, 11).

[15] C. Europeo, "Conclusioni sul quadro 2030 per le politiche dell'energia e del clima," Tech. Rep., 2014 (cit. on p. 9).

[16] Commissione Europea, "Comunicazione della Commissione al Parlamento europeo, al Consiglio, al Comitato economico e sociale europeo e al Comitato delle regioni - Tabella di marcia per l'energia 2050," Tech. Rep., 2011 (cit. on p. 9).

[17] European Commission, "National Action Plans," Tech. Rep. (cit. on p. 10).

[18] Ministero dello Sviluppo Economico, "Piano di azione nazionale per le energie rinnovabili dell'Italia," Tech. Rep., 2010 (cit. on pp. 10, 12).

[19] Ministero dello Sviluppo Economico, "SEN - Strategia energetica nazionale," Tech. Rep., 2013 (cit. on p. 11).

[20] Ministero dello Sviluppo Economico, "Decreto 15 marzo 2012 del Ministero dello Sviluppo Economico - Decreto burden sharing," Tech. Rep., 2015 (cit. on p. 13).

[21] L. Schrattenholzer, "Some issues in energy policy and planning," *Encyclopedia of Life Support Systems (EOLSS)*, 2005 (cit. on p. 14).

[22] R. Thery and P. Zarate, "Energy planning: a multi-level and multicriteria decision making structure proposal," *Central European Journal of Operations Research*, vol. 17, no. 3, pp. 265–274, 2009 (cit. on p. 14).

[23] R. B. Hiremath, S Shikha, and N. H. Ravindranath, "Decentralized energy planning; modeling and application—a review," *Renewable and Sustainable Energy Reviews*, vol. 11, no. 5, pp. 729–752, 2007 (cit. on p. 14).

[24] G. N. Koutroumpezis, A. S. Safigianni, G. S. Demetzos, and J. G. Kendristakis, "Investigation of the distributed generation penetration in a medium voltage power distribution network," *International Journal of Energy Research*, 2010, ISSN: 0363907X. DOI: `10.1002/er.1573` (cit. on p. 15).

[25] J. H. R. Enslin, "Integration of photovoltaic solar power - The quest towards dispatchability," *IEEE Instrumentation and Measurement Magazine*, 2014, ISSN: 10946969. DOI: 10.1109/MIM.2014.6810041 (cit. on p. 16).

[26] The European Wind Energy Associationstatistics, *Wind Power*, 2016. [Online]. Available: http://www.ewea.org/Statistics/ (cit. on p. 16).

[27] SolarPower Europestatistics, *Solar Power*, 2016. [Online]. Available: www.solarpowereurope.org/.Accessed:2016-09-21 (cit. on p. 16).

[28] J. K. Kaldellis and D. Zafirakis, "The wind energy (r) evolution: A short review of a long history," *Renewable energy*, vol. 36, no. 7, pp. 1887–1901, 2011 (cit. on p. 16).

[29] K Balamurugan, D. Srinivasan, and T. Reindl, "Impact of distributed generation on power distribution systems," in *Energy Procedia*, 2012, ISBN: 9781467323086. DOI: 10.1016/j.egypro.2012.07.013 (cit. on p. 18).

[30] S. A. Rahman and B. Das, "Impact of Distributed Generation on Power System Protection," (cit. on p. 18).

[31] T. Basso, "System Impacts from Interconnection of Distributed Resources: Current Status and Identification of Needs for Further Development," *NREL Technical Report*, 2009 (cit. on p. 18).

[32] M. Chiandone, R. Campaner, A. M. Pavan, G. Sulligoi, P. Mania, and G. Piccoli, "Impact of Distributed Generation on power losses on an actual distribution network," in *3rd International Conference on Renewable Energy Research and Applications, ICRERA 2014*, 2014, ISBN: 9781479937950. DOI: 10.1109/ICRERA.2014.7016537 (cit. on p. 18).

[33] I. P.o.C. C. IPCC, "Climate Change 2014 Synthesis Report. Summary for Policymakers.," Tech. Rep., 2014. DOI: 10.1017/CBO9781107415324. arXiv: arXiv:1011.1669v3 (cit. on p. 18).

[34] N. Etherden and M. H. J. Bollen, "Overload and overvoltage in low-voltage and medium-voltage networks due to renewable energy - Some illustrative case studies," *Electric Power Systems Research*, 2014, ISSN: 03787796. DOI: 10.1016/j.epsr.2014.03.028 (cit. on p. 18).

[35] M. Bollen, Y. Chen, and N. Etherden, "Risk analysis of alternatives to N-1 reserves in a network with large amounts of wind power," 2013 (cit. on p. 19).

[36] International Electrotechnical Commission, *Electropedia*, 2012. [Online]. Available: www.electropedia.org (cit. on p. 19).

[37] S. Heinen, D. Elzinga, S.-K. Kim, and Y. Ikeda, "Impact of smart grid technologies on peak load to 2050," 2011 (cit. on p. 19).

[38] W. H. Kersting, *Distribution system modeling and analysis*. CRC press, 2006 (cit. on pp. 20, 144).

[39] M. A. Mahmud, M. J. Hossain, H. R. Pota, and A. B. M. Nasiruzzaman, "Voltage control of distribution networks with distributed generation using reactive power compensation," in *IECON 2011-37th Annual Conference on IEEE Industrial Electronics Society*, IEEE, 2011, pp. 985–990 (cit. on p. 21).

[40] *Smart Grid Resource Center*. [Online]. Available: http://smartgrid.epri.com/ (cit. on p. 21).

[41] M. Bollen and M. Häger, "Power quality: interactions between distributed energy resources, the grid, and other customers," *Leonardo Energy*, 2005 (cit. on pp. 22, 28, 32, 67, 68).

[42] R. A. Walling, R. Saint, R. C. Dugan, J. Burke, and L. A. Kojovic, "Summary of distributed resources impact on power delivery systems," *IEEE Transactions on power delivery*, vol. 23, no. 3, pp. 1636–1644, 2008 (cit. on pp. 22, 67).

[43] M. Delfanti, D. Falabretti, M. Merlo, G. Monfredini, and V. Olivieri, "Dispersed generation in mv networks: performance of anti-islanding protections," in *Harmonics and Quality of Power (ICHQP), 2010 14th International Conference on*, IEEE, 2010, pp. 1–6 (cit. on pp. 22, 67).

[44] C. J. Mozina, "Impact of green power distributed generation," *IEEE Industry Applications Magazine*, vol. 16, no. 4, pp. 55–62, 2010 (cit. on p. 22).

[45] M. Delfanti, E. Fasciolo, V. Olivieri, and M. Pozzi, "A2A project: A practical implementation of smart grids in the urban area of Milan," *Electric Power Systems Research*, vol. 120, pp. 2–19, 2015 (cit. on p. 22).

[46] A. Berizzi, C. Bovo, D. Falabretti, V. Ilea, M. Merlo, G. Monfredini, M. Subasic, M. Bigoloni, I. Rochira, and R Bonera, "Architecture and functionalities of a smart Distribution Management System," in *Harmonics and Quality of Power (ICHQP), 2014 IEEE 16th International Conference on*, IEEE, 2014, pp. 439–443 (cit. on pp. 22, 32).

[47] A. Berizzi, C. Bovo, J. Allahdadian, V. Ilea, M. Merlo, A Miotti, and F Zanellini, "Innovative automation functions at a substation level to increase res penetration," in *CIGRE Symposium The electric power system of the future*, 2011, pp. 1–7 (cit. on p. 22).

[48] M. H. J. Bollen, Y. Yang, and F. Hassan, "Integration of distributed generation in the power system-a power quality approach," in *Harmonics and Quality of Power, 2008. ICHQP 2008. 13th International Conference on*, IEEE, 2008, pp. 1–8 (cit. on pp. 22, 27, 67).

[49] N. Jenkins, "Embedded generation," *Power engineering journal*, vol. 9, no. 3, pp. 145–150, 1995 (cit. on pp. 22, 67).

[50] AEEG, "Integrated Text of the technical and economic conditions for connection to electricity grids with the obligation to connect third of the production facilities of electricity," Tech. Rep., 2008. [Online]. Available: `http://www.autorita.energia.it/it/docs/08/099-08arg.htm` (cit. on pp. 22, 67).

[51] G. Celli, E. Ghiani, S. Mocci, and F. Pilo, "A multiobjective evolutionary algorithm for the sizing and siting of distributed generation," *IEEE Transactions on power systems*, vol. 20, no. 2, pp. 750–757, 2005 (cit. on p. 22).

[52] P. Prakash and D. K. Khatod, "Optimal sizing and siting techniques for distributed generation in distribution systems: A review," *Renewable and Sustainable Energy Reviews*, vol. 57, pp. 111–130, 2016 (cit. on p. 22).

[53] The European Network of Transmission System Operators, "European Electricity Grid Initiative Roadmap and Implementation plan," Tech. Rep., 2010 (cit. on pp. 23, 33).

[54] European Regulators Group for Electricity and Gas, "Position paper on smart grids," Tech. Rep., 2010 (cit. on pp. 23, 33).

[55] J. Deuse, S. Grenard, K. Karoui, O. Samuelsson, L. Gertmar, P. Karlsson, V. Chuvychin, A. Sauhats, L. Ribickis, M. H. J. Bollen, M. Häger, F. Söllerkvist, and M. Speychal, "Interactions of dispersed energy resources with power system in normal and emergency conditions," *41st International Conference on Large High Voltage Electric Systems 2006, CIGRE 2006*, 2006 (cit. on pp. 23, 24, 68).

[56] P. J.A.P. B. J. Deuse, D. Benintendi, "Power System and Market Integration of DER, the EU-Deep approach," *18th International Conference on Electricity Distribution*, 2005, ISSN: 05379989 (cit. on pp. 23, 32).

[57] J. Deuse, S Grenard, M. Bollen, M Häger, and F Sollerkvist, "Effective impact of DER on distribution system protection," in *International Conference on Electricity Distribution: 21/05/2007-24/05/2007*, AIM, 2007 (cit. on pp. 23, 28).

[58] F Bollen, M. ; Hassan, "Protection," in *Integration of Distributed Generation in the Power System*, 2011, ISBN: 9781118029039. DOI: 10.1038/nphys2063. arXiv: arXiv:1011.1669v3 (cit. on p. 23).

[59] M. Bollen, M. Häger, and F. Sollerkvist, "Power Quality and EMC State of the Art and new Developments," (cit. on pp. 24, 28).

[60] M. H. J. Bollen and M. Häger, "Impact of increasing penetration of distributed generation on the number of voltage dips experienced by end-customers," in *Electricity Distribution, 2005. CIRED 2005. 18th International Conference and Exhibition on*, IET, 2005, pp. 1–5 (cit. on pp. 24, 28).

[61] Michael Viotto, "Present status of dg in germany: national codes, standards, requirements and rules for grid-interconnection and operation.," Tech. Rep., 2005 (cit. on p. 24).

[62] M. Hable, C. Schwaegerl, L. Tao, A. Ettinger, R. Koberle, and E.-P. Meyer, "Requirements on electrical power infrastructure by electric vehicles," in *Emobility-Electrical Power Train, 2010*, IEEE, 2010, pp. 1–6 (cit. on pp. 24, 30).

[63] G. P. Harrison and A. R. Wallace, "Optimal power flow evaluation of distribution network capacity for the connection of distributed generation," *IEE Proceedings - Generation, Transmission and Distribution*, 2005, ISSN: 13502360. DOI: 10.1049/ip-gtd:20041193 (cit. on p. 25).

[64] K. N. Maya and E. A. Jasmin, "A three phase power flow algorithm for distribution network incorporating the impact of distributed generation models," *Procedia Technology*, vol. 21, pp. 326–331, 2015 (cit. on p. 25).

[65] M. H. J. Bollen and F. Hassan, *Integration of distributed generation in the power system*. John wiley & sons, 2011, vol. 80 (cit. on p. 26).

[66] N. Etherden, M. H. J. Bollen, S. Ackeby, and O. Lennerhag, "The Transparent Hosting Capacity Approach – Overview, Applications And Developments," in *23 rd International Conference on Electricity Distribution*, 2015 (cit. on pp. 26, 27).

[67] M. H. J. Bollen and M. Häger, "Power Quality : Interactions Between Distributed Energy Resources , the Grid , and Other Customers and With Distributed Energy," *Electrical Power Quality and Utilisation, Magazine*, 2005 (cit. on pp. 26, 28, 143).

[68] C. Schwaegerl and M. Bollen, "Voltage control in distribution systems as a limitation of the hosting capacity for distributed energy resources," *Electricity Distribution, ...*, 2005, ISSN: 05379989. DOI: 10.1049/cp:20051229 (cit. on pp. 26, 28).

[69] J. Deuse, S Grenard, and M. Bollen, “EU-DEEP integrated proect: technical implications of the" hosting-capacity" of the sytem for DER,” *International Journal of Distributed Energy Resources*, vol. 4, no. 1, pp. 17–34, 2008 (cit. on p. 26).

[70] G. Bourgain, J. Deuse, S. Galant, A. Vafeas, G. Bercq, C. Alvarez, and Others, “Integrating distributed energy resources into today’s electrical system,” *ExpandDER, June*, 2009 (cit. on p. 26).

[71] K. Büdenbender, M. Braun, T. Stetz, and P. Strauss, “Multifunctional PV Systems Offering Additional Functionalities and Improving Grid Integration,” *International Journal of Distributed Energy Resources*, 2011, ISSN: 1614-7138 (cit. on p. 26).

[72] T. Stetz, W. Yan, and M. Braun, “Voltage Control in Distribution Systems with High Level PV-Penetration,” in *25th European PV Solar Energy Conference*, 2010 (cit. on p. 26).

[73] G. P. Harrison, A. Piccolo, P. Siano, and A. R. Wallace, “Hybrid GA and OPF evaluation of network capacity for distributed generation connections,” *Electric Power Systems Research*, 2008, ISSN: 03787796. DOI: 10.1016/j.epsr.2007.03.008 (cit. on p. 27).

[74] D. Menniti, M. Merlo, N. Scordino, and F. Zanellini, “Distribution network analysis: A comparison between hosting and loading capacities,” in *SPEEDAM 2012 - 21st International Symposium on Power Electronics, Electrical Drives, Automation and Motion*, 2012, ISBN: 9781467312998. DOI: 10.1109/SPEEDAM.2012.6264635 (cit. on pp. 27, 29).

[75] D. Bertini, D. Falabretti, D. Moneta, M. Merlo, and A. Silvestri, “Hosting Capacity of Italian Distribution Networks,” *CIRED 21st International Conference on Electricity Distribution*, 2011 (cit. on pp. 27, 29, 68, 69).

[76] F. AlAlamat, “Increasing the hosting capacity of radial distribution grids in Jordan,” PhD thesis, Uppasala, 2015 (cit. on p. 27).

[77] N. Etherden, “Increasing the hosting capacity of distributed energy resources using storage and communication,” PhD thesis, Luleåtekniska universitet, 2014 (cit. on p. 27).

[78] M. Alturki, “Hosting Capacity Calculations in Power Systems,” 2014 (cit. on p. 27).

[79] N. Etherden and M. H. J. Bollen, “Increasing the hosting capacity of distribution networks by curtailment of renewable energy resources,” in *PowerTech, 2011 IEEE Trondheim*, IEEE, 2011, pp. 1–7 (cit. on pp. 27, 30, 31, 68).

[80] M. Delfanti, M. Merlo, G. Monfredini, V. Olivieri, M. Pozzi, and A. Silvestri, “Hosting dispersed generation on Italian MV networks: Towards smart grids,” in *ICHQP 2010 - 14th International Conference on Harmonics and Quality of Power*, 2010, ISBN: 9781424472444. DOI: 10.1109/ICHQP.2010.5625442 (cit. on pp. 27, 29, 68).

[81] A. Kulmala, S. Repo, and J. Pylvänäinen, “Generation curtailment as a means to increase the wind power hosting capacity of a real regional distribution network,” *CIRED-Open Access Proceedings Journal*, vol. 2017, no. 1, pp. 1782–1786, 2017 (cit. on p. 27).

[82] M. Delfanti, M. Merlo, M. Pozzi, V. Olivieri, and M. Gallanti, “Power flows in the Italian distribution electric system with dispersed generation,” in *Electricity Distribution-Part 1, 2009. CIRED 2009. 20th International Conference and Exhibition on*, IET, 2009, pp. 1–5 (cit. on pp. 27, 68).

[83] D. Menniti, M. Merlo, N. Scordino, N. Sorrentino, and F. Zanellini, "A DSO-oriented mathematical model for dispersed generation management on MV networks," in *Power and Energy Society General Meeting, 2012 IEEE*, IEEE, 2012, pp. 1–8 (cit. on pp. 27, 28).

[84] L. J. Thomas, A Burchill, D. J. Rogers, M Guest, and N Jenkins, "Assessing distribution network hosting capacity with the addition of soft open points," in *5th IET International Conference on Renewable Power Generation (RPG) 2016*, 2016, ISBN: 978-1-78561-300-5. DOI: 10.1049/cp.2016.0553 (cit. on p. 27).

[85] L. D. Campello, P. M. Duarte, P. F. Ribeiro, and T. E. De Oliveira, "Hosting capacity of a university electrical grid considering the inclusion of wind-turbines for different background distortions," in *Proceedings of International Conference on Harmonics and Quality of Power, ICHQP*, 2016, ISBN: 9781509037926. DOI: 10.1109/ICHQP.2016.7783335 (cit. on p. 28).

[86] M. Merlo, N. Scordino, and F. Zanellini, "Optimal power flow approach to manage dispersed generation rise and passive load energy needs over a distribution grid," *International Review of Electrical Engineering*, 2013, ISSN: 18276660 (cit. on p. 28).

[87] H. Iyer, S. Ray, and R. Ramakumar, "Assessment of distributed generation based on voltage profile improvement and line loss reduction," in *Proceedings of the IEEE Power Engineering Society Transmission and Distribution Conference*, 2006, ISBN: 0780391942. DOI: 10.1109/TDC.2006.1668671 (cit. on pp. 28, 67).

[88] A. Rabiee and S. M. Mohseni-Bonab, "Maximizing hosting capacity of renewable energy sources in distribution networks: A multi-objective and scenario-based approach," *Energy*, 2017, ISSN: 03605442. DOI: 10.1016/j.energy.2016.11.095 (cit. on p. 28).

[89] J. Le Baut, P. Zehetbauer, S. Kadam, B. Bletterie, N. Hatziargyriou, J. Smith, and M. Rylander, "Probabilistic evaluation of the hosting capacity in distribution networks," in *IEEE PES Innovative Smart Grid Technologies Conference Europe*, 2017, ISBN: 9781509033584. DOI: 10.1109/ISGTEurope.2016.7856213 (cit. on p. 28).

[90] E. Zio, M. Delfanti, L. Giorgi, V. Olivieri, and G. Sansavini, "Monte Carlo simulation-based probabilistic assessment of DG penetration in medium voltage distribution networks," *International Journal of Electrical Power and Energy Systems*, 2015, ISSN: 01420615. DOI: 10.1016/j.ijepes.2014.08.004 (cit. on p. 28).

[91] T. Walla, *Hosting capacity for photovoltaics in Swedish distribution grids*, 2012 (cit. on p. 28).

[92] M. Kolenc, I. Papič, and B. Blažič, "Assessment of maximum distributed generation penetration levels in low voltage networks using a probabilistic approach," *International Journal of Electrical Power and Energy Systems*, 2015, ISSN: 01420615. DOI: 10.1016/j.ijepes.2014.07.063 (cit. on pp. 28, 97).

[93] A. Navarro-Espinosa and L. F. Ochoa, "Probabilistic Impact Assessment of Low Carbon Technologies in LV Distribution Systems," *IEEE Transactions on Power Systems*, 2016, ISSN: 08858950. DOI: 10.1109/TPWRS.2015.2448663 (cit. on p. 28).

[94] M. Delfanti, M. S. Pasquadibisceglie, M. Pozzi, M. Gallanti, and R. Vailati, "Limits to dispersed generation on Italian MV networks," in *Electricity Distribution-Part 1, 2009. CIRED 2009. 20th International Conference and Exhibition on*, IET, 2009, pp. 1–4 (cit. on pp. 28, 29, 68).

[95] E. Haesen, F. Minne, J. Driesen, and M. Bollen, *Hosting capacity for motor starting in weak grids*, 2005. DOI: 10.1109/FPS.2005.204291 (cit. on pp. 28, 29).

[96] L. Gertmar, P. Karlsson, and O. Samuelsson, "On DC injection to AC grids from distributed generation," in *2005 European Conference on Power Electronics and Applications*, 2005, ISBN: 90-75815-09-3. DOI: 10.1109/EPE.2005.219420 (cit. on p. 28).

[97] F. Demailly, A. Even, O. Ninet, and J. Bouckaert, "Optimal design of the distribution infrastructure and the impact of distributed generation," in *Electricity Distribution, 2005. CIRED 2005. 18th International Conference and Exhibition on*, IET, 2005, pp. 1–5 (cit. on p. 28).

[98] S.-K. K. S. Heinen, D. Elzinga and Y. Ikeda, "Impact of Smart Grid," *International Energy Agency*, 2011 (cit. on p. 28).

[99] M. Bollen, F. Sollerkvist, A. Larsson, and M. Lundmark, "Limits to the hosting capacity of the grid for equipment emitting high-frequency distortion," in *Nordic Distribution and Asset Management Conference: 21/08/2006-22/08/2006*, 2006 (cit. on p. 29).

[100] M. H. J. Bollen, P. F. Ribeiro, E. O. A. Larsson, and C. M. Lundmark, "Limits for voltage distortion in the frequency range 2 to 9 kHz," *IEEE Transactions on Power Delivery*, vol. 23, no. 3, pp. 1481–1487, 2008 (cit. on p. 29).

[101] V. Chuvychin, A. Sauhats, and V. Strelkovs, "Problems of frequency control in the power system with massive penetration of distributed generation," in *8th International Conference CONTROL OF POWER SYSTEMS*, vol. 8, 2008, pp. 11–13 (cit. on p. 29).

[102] M. Bollen, "Overvoltages due to wind power: hosting capacity, deterministic and statistical approaches," *Electrical Power Quality and Utilization*, vol. 3, no. 2, pp. 2–15, 2008 (cit. on p. 29).

[103] J. Deuse and K. Purchala, "DER profitability, distribution network development and regulation," in *Electricity Distribution-Part 1, 2009. CIRED 2009. 20th International Conference and Exhibition on*, IET, 2009, pp. 1–4 (cit. on p. 29).

[104] ARERA, "Monitoraggio Dello Sviluppo Degli Impianti Di Generazione Distributa Per L'anno 2006," (cit. on p. 29).

[105] Italian Regulatory Authority for Electricity and Gas (Aeeg), "Resolution ARG/elt 25/09 "Monitoring of the development of distributed generation plants in Italy for the year 2006 and analysis of the possible effects of distributed generation on the national electricity system," Tech. Rep., 2009 (cit. on pp. 29, 68).

[106] L. L. Schiavo, M. Delfanti, E. Fumagalli, and V. Olivieri, "Changing the regulation for regulating the change: Innovation-driven regulatory developments for smart grids, smart metering and e-mobility in Italy," *Energy policy*, vol. 57, pp. 506–517, 2013 (cit. on pp. 29, 33).

[107] J. Meyer, M. Klatt, and P. Schegner, "Power quality challenges in future distribution networks," in *Innovative Smart Grid Technologies (ISGT Europe), 2011 2nd IEEE PES International Conference and Exhibition on*, IEEE, 2011, pp. 1–6 (cit. on p. 29).

[108] B. Bletterie, A. Goršek, B Uljanic, B Blazic, A. Woyte, T. Vu Van, F. Truyens, and J. Jahn, "Enhancement of the network hosting capacity – clearing space for/with PV," in *25th European Photovoltaic Solar Energy Conference and Exhibition*, 2010, ISBN: 3-936338-26-4. DOI: 10.4229/25thEUPVSEC2010-5AO.7.3 (cit. on p. 29).

[109] T. Fawzy, D. Premm, B. Bletterie, and A. Goršek, "Active contribution of PV inverters to voltage control - From a smart grid vision to full-scale implementation," *Elektrotechnik und Informationstechnik*, 2011, ISSN: 0932383X. DOI: 10.1007/s00502-011-0820-z (cit. on pp. 30, 33).

[110] D. Geibel, T. Degner, T. Reimann, B. Engel, T. Bülo, J. P. Da Costa, W. Kruschel, B. Sahan, and P. Zacharias, "Active intelligent distribution networks-Coordinated voltage regulation methods for networks with high share of decentralised generation," 2012 (cit. on p. 30).

[111] B. Bletterie, A. Goršek, T. Fawzy, D. Premm, W. Deprez, F. Truyens, A. Woyte, B. Blazič, and B. Uljanič, "Development of innovative voltage control for distribution networks with high photovoltaic penetration," *Progress in Photovoltaics: Research and Applications*, vol. 20, no. 6, pp. 747–759, 2012 (cit. on p. 30).

[112] T. Stetz, F. Marten, and M. Braun, "Improved low voltage grid-integration of photovoltaic systems in Germany," *IEEE Transactions on Sustainable Energy*, 2013, ISSN: 19493029. DOI: 10.1109/TSTE.2012.2198925 (cit. on p. 30).

[113] T. Van Loon, T. Van Vu, A. Woyte, F. Truyens, B. Bletterie, J. Reekers, B. Blazic, and R. Engelen, "Increasing photovoltaics grid penetration in urban areas through active distribution systems: First large scale demonstration," in *3rd International Conference on Next Generation Infrastructure Systems for Eco-Cities, INFRA 2010 - Conference Proceedings*, 2010, ISBN: 9781424484775. DOI: 10.1109/INFRA.2010.5679214 (cit. on p. 30).

[114] M. Braun, T. Stetz, R. Bründlinger, C. Mayr, K. Ogimoto, H. Hatta, H. Kobayashi, B. Kroposki, B. Mather, M. Coddington, K. Lynn, G. Graditi, A. Woyte, and I. MacGill, "Is the distribution grid ready to accept large-scale photovoltaic deployment? State of the art, progress, and future prospects," in *Progress in Photovoltaics: Research and Applications*, 2012, ISBN: 1099-159X. DOI: 10.1002/pip.1204. arXiv: 1303.4604 (cit. on p. 30).

[115] W. S. J. Smith, B. Seal and R. Dugan, "Simulation of Solar Generation with Advanced Volt-var Control," in *Proceedings of 21st International Conference on Electricity Distribution (CIRED)*, Frankfurt, 2011 (cit. on p. 30).

[116] M. Coddington, A. Ellis, K. Lynn, A. Razon, T. Key, B. Kroposki, B. Mather, R. Hill, K. Nicole, and J. Smith, "Updating technical screens for PV interconnection," in *Photovoltaic Specialists Conference (PVSC), 2012 38th IEEE*, IEEE, 2012, pp. 1768–1773 (cit. on p. 30).

[117] J. W. Smith, R Dugan, M Rylander, and T Key, "Advanced distribution planning tools for high penetration PV deployment," in *Power and Energy Society General Meeting, 2012 IEEE*, IEEE, 2012, pp. 1–7 (cit. on p. 30).

[118] E. F. G. Mauri and S. Fratti, "Electric Vehicles' Impact on the Planning of Milan Distribution Network," in *Proceedings of 21st International Conference on Electricity Distribution (CIRED)*, Frankfurt, 2011 (cit. on p. 30).

[119] G. Mauri, P. Gramatica, E. Fasciolo, and S. Fratti, "Recharging of EV in a typical Italian urban area: Evaluation of the hosting capacity," in *PowerTech, 2011 IEEE Trondheim*, IEEE, 2011, pp. 1–5 (cit. on p. 30).

[120] M. Cresta, F. M. Gatta, A. Geri, L. Landolfi, S. Lauria, M. Maccioni, M. Paulucci, and M. Pompili, "Prospective installation of EV charging points in a real LV network: two case studies," in *Energy Conference and Exhibition (ENERGYCON), 2012 IEEE International*, IEEE, 2012, pp. 725–730 (cit. on p. 30).

[121] K. Clement-Nyns, E. Haesen, and J. Driesen, "The impact of vehicle-to-grid on the distribution grid," *Electric Power Systems Research*, vol. 81, no. 1, pp. 185–192, 2011 (cit. on p. 30).

[122] J. Kirby and F. Hassan, "AC Recharging Infrastructure for EVs and future smart grids—A review," in *Universities Power Engineering Conference (UPEC), 2012 47th International*, IEEE, 2012, pp. 1–6 (cit. on p. 30).

[123] S. Grenard, O. Devaux, and J. Maire, "New automation functions under development to enable French distribution networks to integrate efficiently large share of Dispersed Energy Resources and Renewable Energy Sources," *Power*, 2010. DOI: 10.1109/PESGM.2012.6345361 (cit. on p. 30).

[124] A. Q. S. Grenard and O. Carre, "NoTechnical and economic assessment of centralised voltage control functions in presence of DG in the French MV network," in *Proceedings of21st International Conference on Electricity Distribution (CIRED)*, 2011, Frankfurt (cit. on p. 30).

[125] M. M. D. Moneta, P. Mora, M. Gallanti, G. Monfredini and V. Olivieri, "MV network with Dispersed Generation: voltage regulation based on local controllers," in *Proceedings of the 21st International Conference on Electricity Distribution (CIRED),*, Frankfurt, 2011 (cit. on p. 30).

[126] C. Bovo, M. Merlo, R. Bonera, F. Corti, I. Rochira, F. Zanellini, and M. Rodolfi, "Computation server architecture and advanced functions for distribution control centers," in *2012 IEEE International Energy Conference and Exhibition, ENERGYCON 2012*, 2012, ISBN: 9781467314541. DOI: 10.1109/EnergyCon.2012.6348217 (cit. on p. 30).

[127] A. Einfalt, F. Zeilinger, H. Brunner, and F. Kupzog, "Control concept for active low voltage distribution networks," *Tagungsband ComForEn*, 2012 (cit. on pp. 30, 31).

[128] F. Kupzog, P. Dimitriou, M. Faschang, R. Mosshammer, M. Stifter, and F. Andrén, *Co-simulation of power-and communication-networks for low voltage smart grid control*. na, 2012 (cit. on p. 30).

[129] F. G. L. Pilo, E. Ghiani, G. Celli, and G. Soma, "Planning of Reliable Active Distribution Systems," in *44th International Conference on Large High Voltage Electric Systems 2012*, CIGRE', 2012 (cit. on p. 30).

[130] G. Bianco, G. Di Lembo, and G. Sapienza, "Interface for energy regulation: An application for distributed generation control," 2012 (cit. on p. 31).

[131] E. Diskin and T. Fallon, "Implementation of demand side management as a solution for distribution network operation and management," in *Integration of Renewables into the Distribution Grid, CIRED 2012 Workshop*, IET, 2012, pp. 1–4 (cit. on p. 31).

[132] A. Kulmala, A. Mutanen, A. Koto, S. Repo, and P. Järventausta, "Demonstrating coordinated voltage control in a real distribution network," in *Innovative Smart Grid Technologies (ISGT Europe), 2012 3rd IEEE PES International Conference and Exhibition on*, IEEE, 2012, pp. 1–8 (cit. on p. 31).

[133] A. Kulmala, S. Repo, and P. Järventausta, "Active voltage control-From theory to practice," 2012 (cit. on p. 31).

[134] I. Leisse, O. Samuelsson, and J. Svensson, "Coordinated voltage control in distribution systems with DG-Control algorithm and case study," 2012 (cit. on p. 31).

[135] M. Meuser, H. Vennegeerts, and P. Schäfer, "Impact of voltage control by distributed generation on hosting capacity and reactive power balance in distribution grids," 2012 (cit. on p. 31).

[136] F. Capitanescu, L. F. Ochoa, H. Margossian, and N. D. Hatziargyriou, "Assessing the potential of network reconfiguration to improve distributed generation hosting capacity in active distribution systems," *IEEE Transactions on Power Systems*, vol. 30, no. 1, pp. 346–356, 2015 (cit. on p. 31).

[137] V. Calderaro, A. Piccolo, and P. Siano, "Maximizing DG penetration in distribution networks by means of GA based reconfiguration," in *Future Power Systems, 2005 International Conference on*, IEEE, 2005, 6–pp (cit. on p. 31).

[138] P. C. Ramaswamy, P. Vingerhoets, and G. Deconinck, "Reconfiguring distribution grids for more integration of distributed generation," 2013 (cit. on p. 31).

[139] A. Bayat, A. Bagheri, and R. Noroozian, "Optimal siting and sizing of distributed generation accompanied by reconfiguration of distribution networks for maximum loss reduction by using a new UVDA-based heuristic method," *International Journal of Electrical Power & Energy Systems*, vol. 77, pp. 360–371, 2016 (cit. on p. 31).

[140] A. Bayat, "Uniform voltage distribution based constructive algorithm for optimal reconfiguration of electric distribution networks," *Electric Power Systems Research*, vol. 104, pp. 146–155, 2013 (cit. on p. 31).

[141] B. Bletterie, S. Kadam, and J. Le Baut, "Increased hosting capacity by means of active power curtailment," 2016 (cit. on p. 31).

[142] W. Sun and G. P. Harrison, "Influence of generator curtailment priority on network hosting capacity," 2013 (cit. on p. 31).

[143] C. Gao and M. A. Redfern, "A review of voltage control techniques of networks with distributed generations using On-Load Tap Changer transformers," in *Universities Power Engineering Conference (UPEC), 2010 45th International*, IEEE, 2010, pp. 1–6 (cit. on pp. 32, 145).

[144] K. Rauma, F. Cadoux, N. Hadj-Said, A. Dufournet, C. Baudot, and G. Roupioz, "Assessment of the MV/LV on-load tap changer technology as a way to increase LV hosting capacity for photovoltaic power generators," 2016 (cit. on p. 32).

[145] C. R. Sarimuthu, V. K. Ramachandaramurthy, K. R. Agileswari, and H. Mokhlis, "A review on voltage control methods using on-load tap changer transformers for networks with renewable energy sources," *Renewable and Sustainable Energy Reviews*, vol. 62, pp. 1154–1161, 2016 (cit. on pp. 32, 146).

[146] S. N. Salih and P. Chen, "On coordinated control of OLTC and reactive power compensation for voltage regulation in distribution systems with wind power," *IEEE Transactions on Power Systems*, vol. 31, no. 5, pp. 4026–4035, 2016 (cit. on pp. 32, 146).

[147] M. Elnashar, M. Kazerani, R. El Shatshat, and M. M. A. Salama, "Comparative evaluation of reactive power compensation methods for a stand-alone wind energy conversion system," in *Power Electronics Specialists Conference, 2008. PESC 2008. IEEE*, IEEE, 2008, pp. 4539–4544 (cit. on pp. 32, 146).

[148] M. Aggarwal, S. K. Gupta, G. Kasal, and Others, "D-statcom control in low voltage distribution system with distributed generation," in *Emerging Trends in Engineering and Technology (ICETET), 2010 3rd International Conference on*, IEEE, 2010, pp. 426–429 (cit. on p. 32).

[149] D. Caples, S. Boljevic, and M. F. Conlon, "Impact of distributed generation on voltage profile in 38kV distribution system," in *Energy Market (EEM), 2011 8th International Conference on the European*, IEEE, 2011, pp. 532–536 (cit. on pp. 32, 146).

[150] D. Kumar and S. R. Samantaray, "Implementation of multi-objective seeker-optimization-algorithm for optimal planning of primary distribution systems including DSTATCOM," *International Journal of Electrical Power & Energy Systems*, vol. 77, pp. 439–449, 2016 (cit. on p. 32).

[151] M. Delfanti, L. Frosio, G. Monfredini, M. Merlo, C. Rosati, D. Rosati, and G. Marchegiani, "Part I of II: Technical Strategies for Voltage Power Regulation in LV Distribution Networks," *Distributed Generation & Alternative Energy Journal*, vol. 30, no. 3, pp. 57–80, 2015 (cit. on pp. 32, 146).

[152] M. Delfanti, M. Merlo, and G. Monfredini, "Voltage control on LV distribution network: Local regulation strategies for DG exploitation," *Research Journal of Applied Sciences, Engineering and Technology*, vol. 7, pp. 4891–4905, 2014 (cit. on pp. 32, 143, 147, 148).

[153] Council of European Energy Regulators, "CEER status review of regulatory approaches to smart electricity grids," Tech. Rep., 2011 (cit. on p. 33).

[154] V. Olivieri, M. Delfanti, and L. L. Schiavo, "The Italian regulatory framework for developing smart distribution grids," *International Journal of Emerging Electric Power Systems*, vol. 13, no. 5, 2012 (cit. on p. 33).

[155] W. Tayati and H. Bui, "PV Generation Hosting Capacity of Remote Area Power Supply Systems," in *Proceedings of the 50th Annual Conference*, Melbourne, 2012 (cit. on p. 33).

[156] Horizon Power, *Renewable energy buyback hosting capacity*. 2013. [Online]. Available: `www.horizonpower.com.au`, (cit. on p. 34).

[157] F. C. Schweppe and D. B. Rom, "Power system static-state estimation, Part II: Approximate model," *IEEE Transactions on Power Apparatus and Systems*, no. 1, pp. 125–130, 1970 (cit. on pp. 35–37).

[158] J. B. A. LONDON JR and N. G. BRETAS, "Power system parameter estimation," in *Congreso Brasileiro de Automatica, Gramado, Rio Grande do Sul (Paper-cba-542)*, 2004 (cit. on p. 35).

[159] I. A. Hiskens and A. Koeman, "Power system parameter estimation," *Journal of Electrical and Electronics Engineering Australia*, vol. 19, pp. 1–8, 1999 (cit. on p. 35).

[160] E. Walter and L. Pronzato, *Identification of parametric models from experimental data*. Springer Verlag, 1997 (cit. on p. 35).

[161] A. P. S. Meliopoulos, B. Fardanesh, and S. Zelingher, "Power system state estimation: Modeling error effects and impact on system operation," *Proceedings of the Hawaii International Conference on System Sciences*, 2001, ISSN: 10603425. DOI: 10.1109/HICSS.2001.926269 (cit. on pp. 36, 37).

[162] F. C. Schweppe and J Wildes, "Power system static-state estimation, Part I: Exact model," *IEEE Transactions on Power Apparatus and systems*, no. 1, pp. 120–125, 1970 (cit. on pp. 36, 37).

[163] Schweppe, Fred C. and D. B. Rom, "Power System Static-State Estimation, Part III: Implementation," *IEEE Trans. On Power Apparatus and Systems*, vol. 89, no. 1, pp. 130–135, 1970 (cit. on pp. 36, 37).

[164] P. Zarco and A. G. Expósito, "Power system parameter estimation: a survey," *IEEE Transactions on Power Systems*, 2000, ISSN: 08858950. DOI: 10.1109/59.852124 (cit. on p. 36).

[165] J. Chen and Y. Liao, "State Estimation and Power Flow Analysis of Power Systems.," *JCP*, vol. 7, no. 3, pp. 685–691, 2012 (cit. on p. 36).

[166] Y. Liao, "State estimation algorithm considering effects of model inaccuracies," in *SoutheastCon, 2007. Proceedings. IEEE*, IEEE, 2007, pp. 450–453 (cit. on p. 36).

[167] A. Gomez-Exposito and A. Abur, *Power system state estimation: theory and implementation*. CRC press, 2004 (cit. on p. 36).

[168] N. R. Shivakumar and A. Jain, "A review of power system dynamic state estimation techniques," in *2008 Joint International Conference on Power System Technology POWERCON and IEEE Power India Conference, POWERCON 2008*, 2008, ISBN: 9781424417629. DOI: 10.1109/ICPST.2008.4745312 (cit. on pp. 37, 41).

[169] A. Monticelli, "Electric power system state estimation," *Proceedings of the IEEE*, 2000, ISSN: 00189219. DOI: 10.1109/5.824004. arXiv: arXiv:1011.1669v3 (cit. on p. 37).

[170] W. G. Li, J. Li, A. Gao, and J. H. Yang, "Review and research trends on state estimation of electrical power systems," in *Asia-Pacific Power and Energy Engineering Conference, APPEEC*, 2011, ISBN: 9781424462551. DOI: 10.1109/APPEEC.2011.5749095 (cit. on p. 37).

[171] D. M. Falcão and A. M. L. da Silva, "Bibliography on power system state estimation (1968 - 1989)," *IEEE Transactions on Power Systems*, 1990, ISSN: 15580679. DOI: 10.1109/59.65925 (cit. on p. 37).

[172] A. Gómez-Expósito, A. De La Villa Jaén, C. Gómez-Quiles, P. Rousseaux, and T. Van Cutsem, "A taxonomy of multi-area state estimation methods," *Electric Power Systems Research*, 2011, ISSN: 03787796. DOI: 10.1016/j.epsr.2010.11.012 (cit. on pp. 37, 43).

[173] T. E. D. Liacco, "The role and implementation of state estimation in an energy management system," *International Journal of Electrical Power & Energy Systems*, vol. 12, no. 2, pp. 75–79, 1990 (cit. on p. 37).

[174] E. A. Blood, M. D. Ilic, and B. H. Krogh, "A Kalman filter approach to quasi-static state estimation in electric power systems," in *Power Symposium, 2006. NAPS 2006. 38th North American*, IEEE, 2006, pp. 417–422 (cit. on p. 37).

[175] A. Bose and K. A. Clements, "Real-time modeling of power networks," *Proceedings of the IEEE*, vol. 75, no. 12, pp. 1607–1622, 1987 (cit. on p. 37).

[176] J. J. Allemong, L Radu, and A. M. Sasson, "A fast and reliable state estimation algorithm for AEP's new control center," *IEEE Transactions on Power Apparatus and Systems*, 1982, ISSN: 00189510. DOI: 10.1109/TPAS.1982.317159 (cit. on p. 39).

[177] A. Abur and A. G. Expósito, *Power System State Estimation: Theory and Implementation*. 2004, ISBN: 0824755707. DOI: 10.1201/9780203913673 (cit. on p. 40).

[178] H. P. Horisberger, J. C. Richard, and C Rossier, "A fast decoupled static state-estimator for electric power systems," *IEEE Transactions on Power Apparatus and Systems*, 1976, ISSN: 00189510. DOI: 10.1109/T-PAS.1976.32093 (cit. on p. 40).

[179] A. Garcia, A. Monticelli, and P. Abreu, "Fast decoupled state estimation and bad data processing," *IEEE Transactions on Power Apparatus and Systems*, no. 5, pp. 1645–1652, 1979 (cit. on p. 40).

[180] M. C. De Almeida, A. V. Garcia, and E. N. Asada, "Regularized least squares power system state estimation," *IEEE Transactions on Power Systems*, 2012, ISSN: 08858950. DOI: 10.1109/TPWRS.2011.2169434 (cit. on p. 40).

[181] F. Kazempour and S. Poshtkouhi, "Power system state estimation: methods, Implementation and evaluation," in *Electrical & Computer Engineering (CCECE), 2012 25th IEEE Canadian Conference on*, IEEE, 2012, pp. 1–4 (cit. on p. 40).

[182] J. L. Durán-Paz, F Perez-Hidalgo, and M. J. Duran-Martinez, "Bad Data Detection of Unequal Magnitudes in State Estimation of Power Systems [Power Engineering Letters]," *IEEE Power Engineering Review*, vol. 22, no. 4, pp. 57–60, 2002 (cit. on p. 40).

[183] L. Mili and T. Van Cutsem, "Implementation of the hypothesis testing identification in power system state estimation," *IEEE Transactions on Power Systems*, vol. 3, no. 3, pp. 887–893, 1988 (cit. on p. 40).

[184] S. Zhong and A. Abur, "Combined state estimation and measurement calibration," *IEEE Transactions on Power Systems*, 2005, ISSN: 08858950. DOI: 10.1109/TPWRS.2004.841237 (cit. on p. 40).

[185] F. F. Wu and A Monticelli, "Network observability: theory," *IEEE Transactions on Power Apparatus and Systems*, no. 5, pp. 1042–1048, 1985 (cit. on p. 40).

[186] A. Monticelli and F. F. Wu, "Network observability: Identification of observable islands and measurement placement," *IEEE Transactions on Power Apparatus and Systems*, no. 5, pp. 1035–1041, 1985 (cit. on p. 40).

[187] F. F. Wu, "Power system state estimation: a survey," *International Journal of Electrical Power & Energy Systems*, vol. 12, no. 2, pp. 80–87, 1990 (cit. on p. 41).

[188] Z. Morvaj, "A mathematical model of an electric power system for DSE," *Electric Power Systems Research*, vol. 8, no. 3, 1985 (cit. on p. 41).

[189] J. M. Lin, S. J. Huang, and K. R. Shih, "Application of sliding surface-enhanced fuzzy control for dynamic state estimation of a power system," *IEEE Transactions on Power Systems*, 2003, ISSN: 08858950. DOI: 10.1109/TPWRS.2003.810894 (cit. on pp. 41, 43).

[190] K. R. Shih and S. J. Huang, "Application of a robust algorithm for dynamic state estimation of a power system," *IEEE Transactions on Power Systems*, 2002, ISSN: 08858950. DOI: 10.1109/59.982205 (cit. on pp. 41, 42).

[191] A. M. L. Da Silva, M. B. Do Coutto Filho, and J. F. De Queiroz, "State forecasting in electric power systems," in *IEE Proceedings C-Generation, Transmission and Distribution*, IET, vol. 130, 1983, pp. 237–244 (cit. on p. 41).

[192] J. K. Mandal, A. K. Sinha, and L Roy, "Incorporating nonlinearities of measurement function in power system dynamic state estimation," *IEE Proceedings-Generation, Transmission and Distribution*, vol. 142, no. 3, pp. 289–296, 1995 (cit. on p. 41).

[193] M. Zima-Bockarjova, M. Zima, and G. Andersson, "Analysis of the state estimation performance in transient conditions," *IEEE Transactions on Power Systems*, vol. 26, no. 4, pp. 1866–1874, 2011 (cit. on p. 41).

[194] A. K. Sinha and J. K. Mondal, "Dynamic state estimator using ANN based bus load prediction," *IEEE Transactions on Power Systems*, vol. 14, no. 4, pp. 1219–1225, 1999 (cit. on pp. 41, 42).

[195] K. Nishiya, J. Hasegawa, and T. Koike, "Dynamic state estimation including anomaly detection and identification for power systems," in *IEE Proceedings C-Generation, Transmission and Distribution*, IET, vol. 129, 1982, pp. 192–198 (cit. on p. 42).

[196] E. Handschin, "Real-time control of electric power systems," Elsevier Publishing Co., New York, NY, Tech. Rep., 1972 (cit. on p. 42).

[197] A. S. Debs and R. E. Larson, "A dynamic estimator for tracking the state of a power system," *IEEE Transactions on Power Apparatus and Systems*, no. 7, pp. 1670–1678, 1970 (cit. on p. 42).

[198] A. M. L. Da Silva, M. B. Do Coutto Filho, and J. M. C. Cantera, "An efficient dynamic state estimation algorithm including bad data processing," *IEEE transactions on Power Systems*, vol. 2, no. 4, pp. 1050–1058, 1987 (cit. on p. 42).

[199] W. Miller and J. Lewis, "Dynamic state estimation in power systems," *IEEE Transactions on automatic control*, vol. 16, no. 6, pp. 841–846, 1971 (cit. on p. 42).

[200] G Durgaprasad and S. S. Thakur, "Robust dynamic state estimation of power systems based on M-estimation and realistic modeling of system dynamics," *IEEE Transactions on Power Systems*, vol. 13, no. 4, pp. 1331–1336, 1998 (cit. on p. 42).

[201] J. J. Grainger, W. D. Stevenson, and G. W. Chang, *Power system analysis*. McGraw-Hill New York, 1994, vol. 621 (cit. on pp. 42, 47).

[202] A. A. Girgis, "A new Kalman filtering based digital distance relay," *IEEE Transactions on Power Apparatus and Systems*, no. 9, pp. 3471–3480, 1982 (cit. on p. 42).

[203] H. C. Wood, N. G. Johnson, and M. S. Sachdev, "Kalman filtering applied to power system measurements relaying," *IEEE Transactions on Power Apparatus and Systems*, no. 12, pp. 3565–3573, 1985 (cit. on p. 42).

[204] H. M. Beides and G. T. Heydt, "Dynamic state estimation of power system harmonics using Kalman filter methodology," *IEEE Transactions on Power Delivery*, vol. 6, no. 4, pp. 1663–1670, 1991 (cit. on p. 42).

[205] S. J. Julier and J. K. Uhlmann, "New extension of the Kalman filter to nonlinear systems," in *Signal processing, sensor fusion, and target recognition VI*, International Society for Optics and Photonics, vol. 3068, 1997, pp. 182–194 (cit. on p. 42).

[206] E. A. Blood, B. H. Krogh, and M. D. Ilic, "Electric power system static state estimation through Kalman filtering and load forecasting," in *Power and Energy Society General Meeting-Conversion and Delivery of Electrical Energy in the 21st Century, 2008 IEEE*, IEEE, 2008, pp. 1–6 (cit. on p. 42).

[207] C. Hernández and P. Maya-Ortiz, "Comparison between WLS and Kalman filter method for power system static state estimation," in *Smart Electric Distribution Systems and Technologies (EDST), 2015 International Symposium on*, IEEE, 2015, pp. 47–52 (cit. on p. 42).

[208] N. Gupta and R. Hauser, "Kalman filtering with equality and inequality state constraints," *arXiv preprint arXiv:0709.2791*, 2007 (cit. on p. 43).

[209] K. Li, "State estimation for power distribution system and measurement impacts," *IEEE Transactions on Power Systems*, vol. 11, no. 2, pp. 911–916, 1996 (cit. on p. 44).

[210] C. N. Lu, J. H. Teng, and W.-H. Liu, "Distribution system state estimation," *IEEE Transactions on Power systems*, vol. 10, no. 1, pp. 229–240, 1995 (cit. on p. 44).

[211] W.-M. Lin and J.-H. Teng, "Distribution fast decoupled state estimation by measurement pairing," *IEE Proceedings-Generation, Transmission and Distribution*, vol. 143, no. 1, pp. 43–48, 1996 (cit. on p. 44).

[212] M. E. Baran and A. W. Kelley, "A branch-current-based state estimation method for distribution systems," *IEEE transactions on power systems*, vol. 10, no. 1, pp. 483–491, 1995 (cit. on p. 44).

[213] H. Wang and N. N. Schulz, "A revised branch current-based distribution system state estimation algorithm and meter placement impact," *IEEE Transactions on Power Systems*, vol. 19, no. 1, pp. 207–213, 2004 (cit. on p. 44).

[214] A. K. Ghosh, D. L. Lubkeman, M. J. Downey, and R. H. Jones, "Distribution circuit state estimation using a probabilistic approach," *IEEE Transactions on Power Systems*, vol. 12, no. 1, pp. 45–51, 1997 (cit. on p. 45).

[215] D. L. Lubkeman, J. Zhang, A. K. Ghosh, and R. H. Jones, "Field results for a distribution circuit state estimator implementation," *IEEE Transactions on Power Delivery*, vol. 15, no. 1, pp. 399–406, 2000 (cit. on p. 45).

[216] M. K. Celik and W.-H. Liu, "A practical distribution state calculation algorithm," in *Power Engineering Society 1999 Winter Meeting, IEEE*, IEEE, vol. 1, 1999, pp. 442–447 (cit. on p. 45).

[217] I. Roytelman and S. M. Shahidehpour, "State estimation for electric power distribution systems in quasi real-time conditions," *IEEE Transactions on Power Delivery*, vol. 8, no. 4, pp. 2009–2015, 1993 (cit. on p. 45).

[218] R. D. Zimmerman, C. E. Murillo-Sánchez, R. J. Thomas, and Others, "MATPOWER: Steady-state operations, planning, and analysis tools for power systems research and education," *IEEE Transactions on power systems*, vol. 26, no. 1, pp. 12–19, 2011 (cit. on p. 46).

[219] D. Hewes, S. Altschaeffl, I. Boiarchuk, and R. Witzmann, "Development of a dynamic model of the European transmission system using publicly available data," in *Energy Conference (ENERGYCON), 2016 IEEE International*, IEEE, 2016, pp. 1–6 (cit. on p. 47).

[220] M. H. Kutner, C. Nachtsheim, and J. Neter, *Applied linear regression models*. McGraw-Hill/Irwin, 2004 (cit. on pp. 47, 48).

[221] T. I. R. E. A. IRENA, "The International Renewable Energy Agency: IRENA," Tech. Rep., 2016 (cit. on p. 48).

[222] N. energy policy, "Mini-Grids Information Portal," Tech. Rep., 2015 (cit. on p. 48).

[223] NEP, "National Energy Policy," Tech. Rep., 2015 (cit. on pp. 49, 50, 52).

[224] S. Lavalin and P. Brickenhoff, *Regional Power System Master Plan and Grid Code Study*, 2011 (cit. on p. 54).

[225] Japan International Cooperation Agency, "REVIEW OF POWER SYSTEM MASTER PLAN 2012," Tech. Rep., 2012. [Online]. Available: `http://open{\_}jicareport.jica.go.jp/pdf/12288502{\_}01.pdf` (cit. on p. 54).

[226] J. A. P. Lopes, N Hatziargyriou, J Mutale, P Djapic, and N Jenkins, "Integrating distributed generation into electric power systems: A review of drivers, challenges and opportunities," *Electric power systems research*, vol. 77, no. 9, pp. 1189–1203, 2007 (cit. on pp. 67, 143).

[227] F. Ding and B. Mather, "On Distributed PV Hosting Capacity Estimation, Sensitivity Study, and Improvement," *IEEE Transactions on Sustainable Energy*, 2017, ISSN: 19493029. DOI: `10.1109/TSTE.2016.2640239` (cit. on pp. 68, 94).

[228] AEEG, "Resolution ARG/elt 223/10, Monitoring the development of distributed generation in Italy during 2009 and analysis of the possible effects of distributed generation on the national electricity system," Tech. Rep. [Online]. Available: `http://www.autorita.energia.it/it/docs/10/223-10arg.htm` (cit. on p. 68).

[229] CEI 0-16 V2, "Interpretation Sheet F1: Reference technical rules for the connection of active and passive Users to HV and MV networks of electricity distribution Companies," Tech. Rep., 2009 (cit. on pp. 70, 95, 161).

[230] CENELEC, "Technical Standard EN 50160, Voltage characteristics of electricity supplied by public distribution systems," Tech. Rep., 2007 (cit. on pp. 75, 78).

[231] V. Allegranza, A. Ardito, E. De Berardinis, M. Delfanti, and L. L. Schiavo, "Assessment of short circuit power levels in HV and MV networks with respect to power quality," in *19th International Conference on Electricity Distribution (CIRED), Vienna*, 2007 (cit. on p. 75).

[232] CEI EN 50363, "Insulating, Sheathing and Covering Materials For Low Voltage Eneregt Cables," Tech. Rep. (cit. on p. 79).

[233] CEI-021, "Reference Technical Rules for Connecting Users to the Active and Passive LV Distribution Companies of Electricity," Milan, Tech. Rep., 2011 (cit. on pp. 95, 145).

[234] Satel-Light, *The european database of daylight and solar radiation.* (Cit. on p. 98).

[235] M. Moncecchi, "La Pianificazione Energetica Territoriale E L'Impatto Della GD Sulla Rete Di Distribuzione," Master Thesis, Politecnico di Milano, 2016 (cit. on p. 101).

[236] A. S. Vicente, "Laying the foundations for greener transport. TERM 2011: Transport indicators tracking progress towards environmental targets in Europe, EEA Report 7/2011," *European Environment Agency: Copenhagen, Denmark*, 2011 (cit. on p. 126).

[237] E. Commission, *Roadmap to a Single European Transport Area: Towards a Competitive and Resource Efficient Transport System: White Paper*. Publications Office of the European Union, 2011 (cit. on pp. 126, 127).

[238] G. Benetti, M. Delfanti, T. Facchinetti, D. Falabretti, and M. Merlo, "Real-time modeling and control of electric vehicles charging processes," *IEEE Transactions on Smart Grid*, vol. 6, no. 3, pp. 1375–1385, 2015 (cit. on p. 126).

[239] J. Dings, *How clean are Europe's cars? An analysis of carmaker progress towards EU CO2 targets in 2010*, 2011 (cit. on p. 126).

[240] J. A. P. Lopes, F. J. Soares, and P. M. R. Almeida, "Integration of electric vehicles in the electric power system," *Proceedings of the IEEE*, vol. 99, no. 1, pp. 168–183, 2011 (cit. on p. 126).

[241] O. Sundstrom and C. Binding, "Flexible charging optimization for electric vehicles considering distribution grid constraints," *IEEE Transactions on Smart Grid*, vol. 3, no. 1, pp. 26–37, 2012 (cit. on pp. 126, 130).

[242] K. De Craemer, S. Vandael, B. Claessens, and G. Deconinck, "An event-driven dual coordination mechanism for demand side management of PHEVs," *IEEE Transactions on Smart Grid*, vol. 5, no. 2, pp. 751–760, 2014 (cit. on pp. 126, 127).

[243] Y. He, B. Venkatesh, and L. Guan, "Optimal scheduling for charging and discharging of electric vehicles," *IEEE transactions on smart grid*, vol. 3, no. 3, pp. 1095–1105, 2012 (cit. on pp. 126, 127).

[244] E. Sortomme and M. A. El-Sharkawi, "Optimal scheduling of vehicle-to-grid energy and ancillary services," *IEEE Transactions on Smart Grid*, vol. 3, no. 1, pp. 351–359, 2012 (cit. on p. 126).

[245] A. T. Al-Awami and E. Sortomme, "Coordinating vehicle-to-grid services with energy trading," *IEEE Transactions on smart grid*, vol. 3, no. 1, pp. 453–462, 2012 (cit. on p. 126).

[246] J. Soares, H. Morais, T. Sousa, Z. Vale, and P. Faria, "Day-ahead resource scheduling including demand response for electric vehicles," *IEEE Transactions on Smart Grid*, vol. 4, no. 1, pp. 596–605, 2013 (cit. on pp. 127, 134).

[247] European Commision, "A strategy for smart sustainable and inclusive growth," Tech. Rep., 2010. [Online]. Available: `eur-lex.europa.eu` (cit. on p. 127).

[248] European Parliament and Council, "Directive 2009/33/CE, promotion of clean and energy-efficient road transport vehicles," Tech. Rep., 2009. [Online]. Available: `eur-lex.europa.eu` (cit. on p. 127).

[249] European Commission, "Cars 2020: for a strong competitive and sustainable European car industry," Tech. Rep., 2012. [Online]. Available: `europa.eu` (cit. on p. 128).

[250] European Automobile Manufactures Association, "ACEA position and recommendations for the standardization of the charging of electrically chargeable vehicles," Tech. Rep., 2012. [Online]. Available: `acea.be` (cit. on p. 128).

[251] EURELECTRIC, "Facilitating e-mobility: EURELECTRIC views on charging infrastructure," Tech. Rep., 2012. [Online]. Available: eurelectric.org (cit. on p. 128).

[252] EURELECTRIC, "Deploying publicly accessible charging infrastructure for electric vehicles: how to organize the market?" Tech. Rep., 2013. [Online]. Available: eurelectric.org (cit. on p. 128).

[253] Autorità di Regolazione per Energia Reti e Ambiente, "Decision ARG/elt 56/10, Disposizioni in materia di connessioni per l'alimentazione di pompe di calore a uso domestico e di veicoli elettrici," Tech. Rep., 2010. [Online]. Available: arera.it (cit. on p. 128).

[254] Autorità di Regolazione per Energia Reti e Ambiente, "Decision ARG/elt 242/10, Disposizioni speciali per l'erogazione dei servizi di trasmissione distribuzione e misura e del servizio di dispacciamento ai fini della sperimentazione dei sistemi di bassa tensione di ricarica pubblica dei veicoli elettrici," Tech. Rep., 2010. [Online]. Available: arera.it (cit. on p. 128).

[255] Autorità di Regolazione per Energia Reti e Ambiente, "ARG/elt 242/10, Decision ARG/elt 96/11, Selezione dei progetti piltota di ricarica pubblica di veicoli elettrici di cui alla deliberazione dell'Autorità per l'energia elettrica e il gas," Tech. Rep., 2011. [Online]. Available: arera.it (cit. on p. 128).

[256] European Parliament and Council, "Directive 2014/94/EU, Deployment of alternative fuels infrastructure," Tech. Rep., 2014. [Online]. Available: eur-lex.europa.eu (cit. on p. 128).

[257] Ministero delle Infrastrutture e dei Trasporti, "PNire, Piano Nazionale Infrastrutturale per la Ricarica dei veicoli alimentati ad energia Elettrica," Tech. Rep., 2016. [Online]. Available: governo.it (cit. on p. 129).

[258] Il Presidente della Repubblica e il Consiglio dei Ministri, "Decreto Legislativo 16 Dicembre 2016 n. 257," Tech. Rep., 2016. [Online]. Available: gazzettaufficiale.it (cit. on p. 129).

[259] G. E.G. E. Council Eur. Energy Reg. (CEER), "The Drive Towards Smart Grids: A Fact Sheet by the European Energy Regulators on How the Drive Towards Smarter Grids can Help Meet European Policy Objectives on Energy and Climate Change and Empower Customers," Tech. Rep., 2010 (cit. on p. 130).

[260] L. P. Fernandez, T. G. San Román, R. Cossent, C. M. Domingo, and P. Frias, "Assessment of the impact of plug-in electric vehicles on distribution networks," *network*, vol. 16, p. 21, 2011 (cit. on p. 130).

[261] S. Shafiee, M. Fotuhi-Firuzabad, and M. Rastegar, "Investigating the impacts of plug-in hybrid electric vehicles on power distribution systems," *IEEE Transactions on Smart Grid*, vol. 4, no. 3, pp. 1351–1360, 2013 (cit. on p. 130).

[262] M. Delfanti, D. Falabretti, M. Fiori, and M. Merlo, "Smart Grid on field application in the Italian framework: The AS SE. M. project," *Electric Power Systems Research*, vol. 120, pp. 56–69, 2015 (cit. on p. 134).

[263] A. Bonhomme, D. Cortinas, F. Boulanger, and J.-L. Fraisse, "A new voltage control system to facilitate the connection of dispersed generation to distribution networks," in *Electricity Distribution, 2001. Part 1: Contributions. CIRED. 16th International Conference and Exhibition on (IEE Conf. Publ No. 482)*, IET, vol. 4, 2001, 10–pp (cit. on p. 143).

[264] T. J. T. Hashim, A. Mohamed, and H. Shareef, "A review on voltage control methods for active distribution networks," *Electrical review*, vol. 6, pp. 304–312, 2012 (cit. on pp. 144, 145, 151).

[265] C. L. Masters, "Voltage rise: the big issue when connecting embedded generation to long 11 kV overhead lines," *Power engineering journal*, vol. 16, no. 1, pp. 5–12, 2002 (cit. on p. 144).

[266] K. Pandiaraj and B. Fox, "Novel voltage control for embedded generators in rural distribution networks," in *Power System Technology, 2000. Proceedings. PowerCon 2000. International Conference on*, IEEE, vol. 1, 2000, pp. 457–462 (cit. on p. 145).

[267] P. Kang and D Birtwhistle, "Condition assessment of power transformer on-load tap-changers using wavelet analysis," *IEEE Power Engineering Review*, vol. 21, no. 5, p. 64, 2001 (cit. on p. 145).

[268] T. Soares, R. J. Bessa, P. Pinson, and H. Morais, "Active distribution grid management based on robust AC optimal power flow," *IEEE Transactions on Smart Grid*, 2017 (cit. on p. 145).

[269] T. Sansawatt, L. F. Ochoa, and G. P. Harrison, "Integrating distributed generation using decentralised voltage regulation," in *Power and Energy Society General Meeting, 2010 IEEE*, IEEE, 2010, pp. 1–6 (cit. on pp. 145, 146).

[270] P. N. Vovos, A. E. Kiprakis, A. R. Wallace, and G. P. Harrison, "Centralized and distributed voltage control: Impact on distributed generation penetration," *IEEE Transactions on power systems*, vol. 22, no. 1, pp. 476–483, 2007 (cit. on p. 145).

[271] F. A. Viawan and D. Karlsson, "Coordinated voltage and reactive power control in the presence of distributed generation," in *Power and Energy Society General Meeting-Conversion and Delivery of Electrical Energy in the 21st Century, 2008 IEEE*, IEEE, 2008, pp. 1–6 (cit. on p. 145).

[272] S. K. Salman, F. Jiang, and W. J. S. Rogers, "Effects of wind power generators on the voltage control of utility distribution networks," in *Renewable Energy-Clean Power 2001, 1993., International Conference on*, IET, 1993, pp. 196–201 (cit. on pp. 145, 146).

[273] M. E. Baran and M.-Y. Hsu, "Volt/Var control at distribution substations," *IEEE Transactions on Power Systems*, vol. 14, no. 1, pp. 312–318, 1999 (cit. on p. 146).

[274] J. H. Harlow, "Transformer tap changing under load: a review of concepts and standards," in *Proc. 1993 64th Annual Engineering Conf.*, 1993, pp. 305–310 (cit. on p. 146).

[275] F. A. Viawan, A. Sannino, and J. Daalder, "Voltage control with on-load tap changers in medium voltage feeders in presence of distributed generation," *Electric power systems research*, vol. 77, no. 10, pp. 1314–1322, 2007 (cit. on p. 146).

[276] A. Kulmala, K. Maki, S. Repo, and P. Jarventausta, "Including active voltage level management in planning of distribution networks with distributed generation," in *PowerTech, 2009 IEEE Bucharest*, IEEE, 2009, pp. 1–6 (cit. on p. 146).

[277] K. Turitsyn, P. Sulc, S. Backhaus, and M. Chertkov, "Local control of reactive power by distributed photovoltaic generators," in *Smart Grid Communications (SmartGridComm), 2010 First IEEE International Conference on*, IEEE, 2010, pp. 79–84 (cit. on p. 146).

[278] T. Sansawatt, J. O'Donnell, L. F. Ochoa, and G. P. Harrison, "Decentralised voltage control for active distribution networks," in *Universities Power Engineering Conference (UPEC), 2009 Proceedings of the 44th International*, IEEE, 2009, pp. 1–5 (cit. on p. 146).

[279] D. Ranamuka, A. P. Agalgaonkar, and K. M. Muttaqi, "Examining the interactions between DG units and voltage regulating devices for effective voltage control in distribution systems," *IEEE Transactions on Industry Applications*, vol. 53, no. 2, pp. 1485–1496, 2017 (cit. on pp. 146, 147).

[280] J. W. Smith, W Sunderman, R Dugan, and B. Seal, "Smart inverter volt/var control functions for high penetration of PV on distribution systems," in *Power Systems Conference and Exposition (PSCE), 2011 IEEE/PES*, IEEE, 2011, pp. 1–6 (cit. on p. 146).

[281] E. Demirok, P. C. Gonzalez, K. H. B. Frederiksen, D. Sera, P. Rodriguez, and R. Teodorescu, "Local reactive power control methods for overvoltage prevention of distributed solar inverters in low-voltage grids," *IEEE Journal of Photovoltaics*, vol. 1, no. 2, pp. 174–182, 2011 (cit. on p. 146).

[282] C. M. Hird, H Leite, N Jenkins, and H Li, "Network voltage controller for distributed generation," *IEE Proceedings-Generation, Transmission and Distribution*, vol. 151, no. 2, pp. 150–156, 2004 (cit. on p. 149).

[283] M. E. Baran and I. M. El-Markabi, "A multiagent-based dispatching scheme for distributed generators for voltage support on distribution feeders," *IEEE Transactions on power systems*, vol. 22, no. 1, pp. 52–59, 2007 (cit. on p. 149).

[284] K. A. Alobeidli, M. H. Syed, M. S. El Moursi, and H. H. Zeineldin, "Novel Coordinated Voltage Control for Hybrid Micro-Grid With Islanding Capability.," *IEEE Trans. Smart Grid*, vol. 6, no. 3, pp. 1116–1127, 2015 (cit. on p. 149).

[285] H. Hatta and H. Kobayashi, "A study of centralized voltage control method for distribution system with distributed generation," in *19 th International Conference on Electricity Distribution (CIRED)*, 2007 (cit. on p. 149).

[286] F. Bignucolo, R. Caldon, and V. Prandoni, "Radial MV networks voltage regulation with distribution management system coordinated controller," *Electric power systems research*, vol. 78, no. 4, pp. 634–645, 2008 (cit. on p. 149).

[287] Q. Zhou and J. W. Bialek, "Generation curtailment to manage voltage constraints in distribution networks," *IET Generation, Transmission & Distribution*, vol. 1, no. 3, pp. 492–498, 2007 (cit. on p. 149).

[288] P. H. Nguyen, J. M. A. Myrzik, and W. L. Kling, "Coordination of voltage regulation in active networks," in *Transmission and Distribution Conference and Exposition, 2008. T&D. IEEE/PES*, IEEE, 2008, pp. 1–6 (cit. on p. 149).

[289] H. E. Farag, E. F. El-Saadany, and R. Seethapathy, "A two ways communication-based distributed control for voltage regulation in smart distribution feeders," *IEEE Transactions on Smart Grid*, vol. 3, no. 1, pp. 271–281, 2012 (cit. on p. 149).

[290] T. Senjyu, Y. Miyazato, A. Yona, N. Urasaki, and T. Funabashi, "Optimal distribution voltage control and coordination with distributed generation," *IEEE Transactions on power delivery*, vol. 23, no. 2, pp. 1236–1242, 2008 (cit. on p. 149).

[291] T. Niknam, A. M. Ranjbar, and A. R. Shirani, "Impact of distributed generation on volt/var control in distribution networks," in *Power Tech Conference Proceedings, 2003 IEEE Bologna*, IEEE, vol. 3, 2003, 7–pp (cit. on p. 149).

[292] A. G. Madureira and J. A. P. Lopes, "Coordinated voltage support in distribution networks with distributed generation and microgrids," *IET renewable Power generation*, vol. 3, no. 4, pp. 439–454, 2009 (cit. on p. 149).

[293] A. Kulmala, S. Repo, and P. Järventausta, "Coordinated voltage control in distribution networks including several distributed energy resources," *IEEE Transactions on Smart Grid*, vol. 5, no. 4, pp. 2010–2020, 2014 (cit. on p. 149).

[294] V. Galdi, A. Vaccaro, and D. Villacci, "Voltage regulation in MV networks with dispersed generations by a neural-based multiobjective methodology," *Electric Power Systems Research*, vol. 78, no. 5, pp. 785–793, 2008 (cit. on p. 149).

[295] K. K. Mehmood, S. U. Khan, S.-J. Lee, Z. M. Haider, M. K. Rafique, and C.-H. Kim, "A real-time optimal coordination scheme for the voltage regulation of a distribution network including an OLTC, capacitor banks, and multiple distributed energy resources," *International Journal of Electrical Power & Energy Systems*, vol. 94, pp. 1–14, 2018 (cit. on p. 149).

[296] D. Ranamuka, A. P. Agalgaonkar, and K. M. Muttaqi, "Online Coordinated Voltage Control in Distribution Systems Subjected to Structural Changes and DG Availability.," *IEEE Trans. Smart Grid*, vol. 7, no. 2, pp. 580–591, 2016 (cit. on p. 150).

[297] A. Angioni, A. Sadu, F. Ponci, A. Monti, D. Patel, F. Williams, D. della Giustina, and A. Dedè, "Coordinated voltage control in distribution grids with LTE based communication infrastructure," in *Environment and Electrical Engineering (EEEIC), 2015 IEEE 15th International Conference on*, IEEE, 2015, pp. 2090–2095 (cit. on p. 150).

[298] M. E. Elkhatib, R. El-Shatshat, and M. M. A. Salama, "Novel coordinated voltage control for smart distribution networks with DG," *IEEE transactions on smart grid*, vol. 2, no. 4, pp. 598–605, 2011 (cit. on p. 150).

[299] A. Berizzi, C. Bovo, M. Merlo, and M. Delfanti, "A ga approach to compare orpf objective functions including secondary voltage regulation," *Electric Power Systems Research*, vol. 84, no. 1, pp. 187–194, 2012 (cit. on p. 150).

[300] A. Berizzi, C. Bovo, C. Bruno, M. Delfanti, M. Merlo, and M. Pozzi, "ORPF procedures for voltage security in a market framework," in *Power Tech, 2005 IEEE Russia*, IEEE, 2005, pp. 1–7 (cit. on p. 150).

[301] D. Jakus, J. Vasilj, and P. Sarajcev, "Voltage control in MV distribution networks through coordinated control of tap changers and renewable energy sources," in *PowerTech, 2015 IEEE Eindhoven*, IEEE, 2015, pp. 1–6 (cit. on p. 150).

[302] S. Santoso, N. Saraf, and G. K. Venayagamoorthy, "Intelligent techniques for planning distributed generation systems," in *Power Engineering Society General Meeting, 2007. IEEE*, IEEE, 2007, pp. 1–4 (cit. on p. 150).

[303] S. Kawano, S. Yoshizawa, and Y. Hayashi, "Centralized voltage control method using voltage forecasting by JIT modeling in distribution networks," in *Transmission and Distribution Conference and Exposition (T&D), 2016 IEEE/PES*, IEEE, 2016, pp. 1–5 (cit. on p. 150).

[304] Z. Hu, X. Wang, H. Chen, and G. A. Taylor, "Volt/VAr control in distribution systems using a time-interval based approach," *IEE Proceedings-Generation, Transmission and Distribution*, vol. 150, no. 5, pp. 548–554, 2003 (cit. on p. 150).

[305] S. S. Alkaabi, H. H. Zeineldin, V. Khadkikar, and M. S. Elmoursi, "Dynamic analysis of OLTC and voltage regulator under active network management considering different load profiles," in *2017 IEEE Power & Energy Society Innovative Smart Grid Technologies Conference (ISGT)*, IEEE, 2017, pp. 1–5 (cit. on p. 150).

[306] J. Barr and R. Majumder, "Integration of Distributed Generation in the Volt/VAR Management System for Active Distribution Networks.," *IEEE Trans. Smart Grid*, vol. 6, no. 2, pp. 576–586, 2015 (cit. on p. 150).

[307] M. Chamana and B. H. Chowdhury, "Optimal Voltage Regulation of Distribution Networks With Cascaded Voltage Regulators in the Presence of High PV Penetration," *IEEE Transactions on Sustainable Energy*, vol. 9, no. 3, pp. 1427–1436, 2018 (cit. on p. 150).

[308] G. Cavraro and R. Carli, "Local and distributed voltage control algorithms in distribution network," *IEEE Transactions on Power Systems*, vol. 33, no. 2, pp. 1420–1430, 2017 (cit. on p. 151).

[309] B. Zhang, A. Y. S. Lam, A. D. Dominguez-Garcia, and D. Tse, "An optimal and distributed method for voltage regulation in power distribution systems," *IEEE Transactions on Power Systems*, vol. 30, no. 4, pp. 1714–1726, 2015 (cit. on p. 151).

[310] R. D. Zimmerman, C. E. Murillo-Sánchez, and R. J. Thomas, "MATPOWER's extensible optimal power flow architecture," in *Power & Energy Society General Meeting, 2009. PES'09. IEEE*, IEEE, 2009, pp. 1–7 (cit. on p. 157).

[311] *The MathWorks, Cluster analysis*. [Online]. Available: `https://es.mathworks.com/help/stats/examples/cluster-analysis.html` (cit. on p. 161).